



**HAL**  
open science

# Further Characterization of Recombinant Epoxide Hydrolase Kau2 Derived from Metagenomic DNA and Application in Biocatalytic Reactions

Wei Zhao

► **To cite this version:**

Wei Zhao. Further Characterization of Recombinant Epoxide Hydrolase Kau2 Derived from Metagenomic DNA and Application in Biocatalytic Reactions. Organic chemistry. Ecole Centrale Marseille, 2014. English. NNT : 2014ECDM0008 . tel-01128878

**HAL Id: tel-01128878**

**<https://theses.hal.science/tel-01128878>**

Submitted on 10 Mar 2015

**HAL** is a multi-disciplinary open access archive for the deposit and dissemination of scientific research documents, whether they are published or not. The documents may come from teaching and research institutions in France or abroad, or from public or private research centers.

L'archive ouverte pluridisciplinaire **HAL**, est destinée au dépôt et à la diffusion de documents scientifiques de niveau recherche, publiés ou non, émanant des établissements d'enseignement et de recherche français ou étrangers, des laboratoires publics ou privés.

ECOLE CENTRALE DE MARSEILLE & UNIVERSITE D'AIX-  
MARSEILLE

Identification N°:

**Further Characterization of Recombinant Epoxide Hydrolase  
Kau2 Derived from Metagenomic DNA and Application in  
Biocatalytic Reactions**

THESE

Présentée par

**Wei ZHAO**

Pour obtenir le grade de Docteur de l'Ecole de Centrale de Marseille

*Spécialité : chimie organique*

Institut des Sciences Moléculaires de Marseille (*iSm2*)-UMR 7313

Ecole Doctorale des Sciences Chimiques - ED 250

**Soutenue publiquement le 16 Octobre 2014 devant la commission d'examen composée de:**

Mme. Anne ZAPARUCHA	Professeur, Université d'Evry	Rapporteur
M. Bastien DOUMECHÉ	Maitre de Conférences, Université Lyon 1	Rapporteur
M. Michael KOTIK	Docteur, A.S. Czech Republic	Examinateur
M. Gilles IACAZIO	Professeur, Aix-Marseille Université	Directeur de thèse
M. Alain ARCHELAS	Directeur de Recherches, CNRS	Co-directeur de thèse

# Table of contents

<b>CHAPTER I. INTRODUCTION.....</b>	<b>4</b>
<b>CHAPTER II. EPOXIDE HYDROLASES AND THEIR APPLICATION IN ORGANIC SYNTHESIS .....</b>	<b>9</b>
II.1 INTRODUCTION .....	10
II.2 SOURCES AND REACTION MECHANISM OF EHS .....	12
II.2.1 Sources of EHs .....	12
II.2.2 Heterologous expression of EHs.....	13
II.2.3 Reaction mechanisms of EHs .....	14
II.3 MONO-FUNCTIONAL EPOXIDES AS CHIRAL BUILDING BLOCKS FOR THE SYNTHESIS OF BIOLOGICALLY ACTIVE COMPOUNDS.....	15
II.3.1 Mono-substituted aromatic epoxides .....	16
II.3.2 Di-substituted aromatic epoxides .....	25
II.3.3 Non aromatic epoxides.....	29
II.3.4 meso-Epoxides.....	38
II.4 PREPARATION OF VALUABLE CHIRAL BUILDING BLOCKS FOR THE SYNTHESIS OF BIOLOGICALLY ACTIVE COMPOUNDS STARTING FROM BI-FUNCTIONAL EPOXIDES.....	40
II.4.1 Halogenated epoxides.....	40
II.4.2 Epoxyamide.....	43
II.4.3 Protected epoxy-alcohols .....	44
II.4.4 Epoxy-ester.....	45
II.4.5 Epoxy-aldehyde .....	46
II.5 CONCLUSIONS.....	48
<b>CHAPTER III. RESULTS.....</b>	<b>56</b>
<b>III.1 INTRODUCTION OF KAU2-EH .....</b>	<b>57</b>
III.1.1 Cloning of Kau2-EH from metagenomic DNA and properties .....	57
III.1.2 Biocatalytic properties of Kau2-EH.....	58
III.1.3 Purposes of this PhD work.....	60
<b>III.2 MODELISATION STUDY OF KAU2-EH .....</b>	<b>62</b>
III.2.1 Introduction.....	62
III.2.2 Preparation of CDU and CIU.....	65
III.2.3 Determination of kinetic parameters of Kau2-EH.....	65
III.2.4 Determination of $K_i$ and CDU & CIU type of inhibition with Kau2-EH.....	67
III.2.5 Determination of $K_i$ and CDU & CIU type of inhibition of with potato EH.....	71
III.2.6 Summary .....	73
III.2.7 Conclusion .....	73
<b>III.3 BIOCONVERSION STUDIES.....</b>	<b>76</b>
III.3.1 Introduction.....	76
III.3.2 Chemical Synthesis .....	78
III.3.3 Kau2-EH production in fermentor.....	81
III.3.4 Bioconversion using Kau2-EH.....	81
III.3.5 Overall conclusion.....	122
<b>III.4 KINETIC STUDIES.....</b>	<b>125</b>
III.4.1 Introduction.....	125
III.4.2 Construction of Kau2-HisTag and mutants.....	126
III.4.3 Heterologous expression of Kau2-His <sub>6</sub> and the corresponding mutants.....	128
III.4.4 Purification of Kau2-His <sub>6</sub> and the corresponding mutants .....	129
III.4.5 Preparation of (SS)- and (RR)-TSO.....	131
III.4.6 Kinetic study.....	132
III.4.7 Conclusion .....	139
<b>CHAPTER IV. CONCLUSION.....</b>	<b>143</b>
<b>CHAPTER V. MATERIAL AND METHODS.....</b>	<b>147</b>
<b>V.1 GENERAL.....</b>	<b>149</b>
V.1.1 Reagents, solvents and chromatography .....	149
V.1.2 Buffer and culture media.....	149
<b>V.2 INSTRUMENTS.....</b>	<b>151</b>

V.2.1 Nuclear Magnetic Resonance (NMR).....	151
V.2.2 Gas chromatography (GC).....	151
V.2.3 High Pressure Liquid Chromatography (HPLC).....	151
V.2.4 5 L Fermentor.....	152
V.2.5 Chromatography.....	152
V.2.6 Others.....	152
<b>V.3 CHEMICAL SYNTHESIS</b> .....	153
V.3.1 Synthesis of <i>N</i> -cyclohexyl- <i>N'</i> -decylurea (CDU)-2.....	153
V.3.2 Synthesis of <i>N</i> -cyclohexyl- <i>N'</i> -(4-iodophenyl) urea (CIU)-3.....	153
V.3.3 Synthesis of <i>rac</i> - <i>trans</i> -methyl phenylglycidate 4.....	154
V.3.4 Synthesis of <i>rac</i> - <i>trans</i> -ethyl-3-phenylglycidate-5.....	155
V.3.5 Synthesis of <i>cis</i> and <i>trans</i> -2, 3-epoxy-3-phenylpropanenitrile 7 and 8.....	155
V.3.6 Synthesis of <i>rac</i> - <i>trans</i> -2,3-epoxy-3-phenyl-1-bromo propane-9 and <i>rac</i> - <i>trans</i> -2,3-epoxy-3-phenyl-1-chloro propane-10.....	156
V.3.7 Synthesis of <i>rac</i> - <i>cis</i> -methyl phenylglycidate-13.....	157
V.3.8 Chemical hydrolysis of <i>rac</i> - <i>trans</i> -methyl phenylglycidate-4.....	158
<b>V.4 KAU2-EH PRODUCTION</b> .....	158
V.4.1 Cells expressing <i>Kau2</i> -EH production in flask.....	158
V.4.2 Cells production in fermentor.....	158
V.4.3 Determination of EH activity.....	159
<b>V.5 MODELISATION STUDY OF KAU2-EH</b> .....	160
V.5.1 Determination of EH activities and kinetic parameters ( $K_m$ , $V_{max}$ ).....	160
V.5.2 Determination of $K_i$ and type of inhibition using CDU and <i>Kau2</i> -EH.....	160
V.5.3 Determination of $K_i$ and type of inhibition using CIU and <i>Kau2</i> -EH.....	160
V.5.4 Determination of $K_i$ and type of inhibition using CDU and Potato-EH.....	160
V.5.5 Determination of $K_i$ and the type of inhibitor of CIU with Potato EHs.....	161
<b>V.6 BIOCONVERSIONS</b> .....	161
V.6.1 Bioconversion of <i>rac</i> - <i>trans</i> -methyl-phenylglycidate-4.....	161
V.6.2 Bioconversion of <i>rac</i> - <i>trans</i> -ethyl-3-phenylglycidate-5.....	162
V.6.3 Bioconversion of <i>rac</i> -methyl- <i>trans</i> -3-(4-methoxyphenyl)-glycidate-6.....	163
V.6.4 Bioconversion of <i>rac</i> - <i>trans</i> -2,3-epoxy-3-phenylpropanenitrile-7.....	164
V.6.5 Bioconversion of <i>rac</i> - <i>cis</i> -2,3-epoxy-3-phenylpropanenitrile-8.....	165
V.6.6 Bioconversion of <i>rac</i> - <i>trans</i> -2,3-epoxy-3-phenylpropyl bromide 9.....	167
V.6.7 Bioconversion of <i>rac</i> - <i>trans</i> -2,3-epoxy-3-phenylpropyl-chloride 10.....	168
V.6.8 Bioconversion of <i>rac</i> - <i>trans</i> -stilbene oxide-11.....	170
V.6.9 Bioconversion of <i>cis</i> -stilbene oxide-12.....	171
<b>V.7 KINETIC STUDIES</b> .....	172
V.7.1 Protein purification.....	172

# Chapter I. Introduction

Catalytic asymmetric synthesis is an ever growing field in organic chemistry. Biocatalysis as well as asymmetric (metal-, organo-, Lewis acid-) catalysis have developed in the past decades to permit the access to enantiomerically enriched (or pure) chiral compounds in order to meet the rising needs for such molecules from both the academic and industrial world (Pamies and Bäckvall, 2003). Biocatalysis makes use of enzymes or whole cells possessing the desired enzyme(s), as catalysts for chemical transformations. Being composed of chiral amino acids of the L-series, proteins and thus enzymes are intrinsically chiral catalysts and particularly suited for catalytic asymmetric synthesis. Taking into account i) the vast chemistry developed by Nature based on enzyme catalysis, ii) the fact that gene coding enzymes could be easily heterologously overexpressed in various suitable microbial hosts (especially *E. coli*), iii) the exponential development of genetic and protein engineering and iv) the simplicity of operating conditions (ambient temperature, atmospheric pressure, neutral pH) highlighting the catalytic power of enzymes, the growing interest in Biocatalysis is thus fully explained, making this discipline an important part of today Chemistry (Clouthier and Pelletier, 2012; Davis and Boyer, 2001; Hudlicky and Reed, 2009; Liese and Villela Filho, 1999; Santacoloma *et al.*, 2010; Wandrey *et al.*, 2000; Wohlgemuth, 2010; Zaks, 2001; Zhao *et al.*, 2002).

Many of the various advantages shown by biocatalysis are listed below:

- Enzymes are generally highly chemo-, regio-, and enantio-selective catalysts
- Enzymes could present either narrow substrate specificity or large substrate promiscuity
- Enzymes could present either narrow product specificity or large product promiscuity
- Enzymes generally present high turnover numbers and very high acceleration rates
- Biocatalysis is in line with the 12 principles of green chemistry
- Biocatalytic reaction conditions are environmentally benign
- Enzymes and whole cells are non-toxic and largely biodegradable

A number of disadvantages have also been listed (see below) but some of them have been recently tackled through protein and genetic engineering:

- Enzymes are high cost catalysts

- Not all chemical reactions have a counterpart in Nature
- Not all enzymes are routinely available
- Some enzymes are poorly stable and prone to substrate/product inhibition
- Some enzymes require co-substrates and/or cofactors
- Enzymes have been designed to function in water as reaction solvent

When employed in asymmetric synthesis, enzymes could be used in a number of well-defined strategies depending on whether the initial substrate is chiral and used as a racemate or is prochiral. Beside the classical kinetic resolution of a racemate presenting the intrinsic limitation of a maximum theoretical yield of 50% in one pure enantiomer (Chen *et al.*, 1982), dynamic kinetic resolution (Pamies and Bäckvall, 2003) has been developed in order to achieve the total conversion of a racemate into a single pure product enantiomer (with thus a theoretical yield of 100%). The same ideal 100% yield in one optically pure product enantiomer is also achievable using prochiral substrates but in a desymmetrization process as long as the biocatalyst is totally selective. Finally and almost restricted to a special class of enzymes, *i.e.* epoxide hydrolases, enantioconvergent reactions could present the same important feature of transforming a racemate into a single enantiomerically pure product by acting with an opposite regioselectivity on the two enantiomers of the substrate leading to the same product enantiomer.

Actually hydrolases and ketoreductases are the most frequently used biocatalysts in academic and industrial organic synthesis (Nestl *et al.*, 2014). Within the former class of enzymes Epoxide Hydrolases (EHs, EC 3.3.2.9) is a very popular source of biocatalysts (Archelas and Furstoss, 1997; Archelas and Furstoss, 2001; Bala and Chimni, 2010; de Vries and Janssen, 2003; Kotik *et al.*, 2012; Orru and Faber, 1999; Steinreiber and Faber, 2001; Weijers and de Bont, 1999; Widersten *et al.*, 2010). Because they act on epoxides to generate diols, both type of compounds being of outstanding interest as chiral compounds, and because they are cofactor free, EHs have become, for more than twenty years now, one of the preeminent element of the biocatalytic toolbox available to organic chemists. Within this framework, the PhD work described in this dissertation was conducted in order to get insights about a newly discovered EH from a metagenomic analysis of a biofilter (Kotik, 2009; Kotik *et al.*, 2010) called Kau2. The enzyme proved to be particularly performant when *trans*- and *cis*-methyl styrene oxides were used as substrates. In the former case an highly enantioselective kinetic resolution was observed ( $E > 200$ ) and in the latter case an

enantioconvergent process occurred affording the corresponding diol with an excellent enantiomeric excess of more than 99% at 100% conversion (Kotik *et al.*, 2010).

After a first bibliographic chapter dedicated to previous described uses of EHs in bioconversion reactions, the results chapter will first describe studies devoted to the better understanding of Kau2-EH active site by inhibition and molecular modeling studies. The obtained results were used by M. Kotik to construct Kau2-EH variants that showed increased enantioconvergency toward *para*-chlorostyrene oxide. Then after Kau2-EH was tested as biocatalytic reactions involving various aromatic epoxides as substrates in order to reveal the (bio)catalytic potential of this enzyme. Finally kinetic studies (stopped-flow) were concluded using purified 6×His-tagged Kau2-EH and *trans*-stilbene oxide as substrate. A final chapter of conclusion will also highlight the possible developments that could be conducted following the present work on Kau2-EH.

## Reference:

- Archelas, A. and Furstoss (1997) Synthesis of enantiopure epoxides through biocatalytic approaches. *Annu. Rev. Microbiol.*, **51**, 491-525.
- Archelas, A. and Furstoss, R. (2001) Synthetic applications of epoxide hydrolases. *Curr. Opin. Chem. Biol.*, **5**, 112-119.
- Bala, N. and Chimni, S.S. (2010) Recent developments in the asymmetric hydrolytic ring opening of epoxides catalysed by microbial epoxide hydrolase. *Tetrahedron: Asymmetry*, **21**, 2879-2898.
- Chen, C.S., Fujimoto, Y., Girdaukas, G. and Sih, C.J. (1982) Quantitative analyses of biochemical kinetic resolutions of enantiomers. *J. Am. Chem. Soc.*, **104**, 7294-7299.
- Clouthier, C.M. and Pelletier, J.N. (2012) Expanding the organic toolbox: a guide to integrating biocatalysis in synthesis. *Chem. Soc. Rev.*, **41**, 1585-1605.
- Davis, B.G. and Boyer, V. (2001) Biocatalysis and enzymes in organic synthesis. *Nat. Prod. Rep.*, **18**, 618-640.
- de Vries, E.J. and Janssen, D.B. (2003) Biocatalytic conversion of epoxides. *Curr. Opin. Biotechnol.*, **14**, 414-420.
- Hudlicky, T. and Reed, J.W. (2009) Applications of biotransformations and biocatalysis to complexity generation in organic synthesis. *Chem. Soc. Rev.*, **38**, 3117-3132.
- Kotik, M. (2009) Novel genes retrieved from environmental DNA by polymerase chain reaction: current genome-walking techniques for future metagenome applications. *J. Biotechnol.*, **144**, 75-82.
- Kotik, M., Archelas, A. and Wohlgemuth, R. (2012) Epoxide hydrolases and their application in organic synthesis. *Curr. Org. Chem.*, **16**, 451-482.
- Kotik, M., Štěpánek, V., Grulich, M., Kyslík, P. and Archelas, A. (2010) Access to enantiopure aromatic epoxides and diols using epoxide hydrolases derived from total biofilter DNA. *J. Mol. Catal. B: Enzym.*, **65**, 41-48.
- Liese, A. and Villela Filho, M. (1999) Production of fine chemicals using biocatalysis. *Curr. Opin. Biotechnol.*, **10**, 595-603.
- Nestl, B.M., Hammer, S.C., Nebel, B.A. and Hauer, B. (2014) New Generation of Biocatalysts for Organic Synthesis. *Angew. Chem. Int. Ed.*, **53**, 3070-3095.
- Orru, R.V. and Faber, K. (1999) Stereoselectivities of microbial epoxide hydrolases. *Curr. Opin. Chem. Biol.*, **3**, 16-21.
- Pamies, O. and Bäckvall, J.-E. (2003) Combination of enzymes and metal catalysts. A powerful approach in asymmetric catalysis. *Chem. Rev.*, **103**, 3247-3262.
- Santacoloma, P.A., Sin, G.r., Gernaey, K.V. and Woodley, J.M. (2010) Multienzyme-catalyzed processes: next-generation biocatalysis. *Org. Process Res. Dev.*, **15**, 203-212.
- Steinreiber, A. and Faber, K. (2001) Microbial epoxide hydrolases for preparative biotransformations. *Curr. Opin. Biotechnol.*, **12**, 552-558.
- Wandrey, C., Liese, A. and Kihumbu, D. (2000) Industrial biocatalysis: past, present, and future. *Org. Process Res. Dev.*, **4**, 286-290.
- Weijers, C.A. and de Bont, J.A. (1999) Epoxide hydrolases from yeasts and other sources: versatile tools in biocatalysis. *J. Mol. Catal. B: Enzym.*, **6**, 199-214.
- Widersten, M., Gurell, A. and Lindberg, D. (2010) Structure–function relationships of epoxide hydrolases and their potential use in biocatalysis. *Biochim. Biophys. Acta, Gen. Subj.*, **1800**, 316-326.
- Wohlgemuth, R. (2010) Asymmetric biocatalysis with microbial enzymes and cells. *Curr. Opin. Microbiol.*, **13**, 283-292.
- Zaks, A. (2001) Industrial biocatalysis. *Curr. Opin. Chem. Biol.*, **5**, 130-136.
- Zhao, H., Chockalingam, K. and Chen, Z. (2002) Directed evolution of enzymes and pathways for industrial biocatalysis. *Curr. Opin. Biotechnol.*, **13**, 104-110.

## Chapter II. Epoxide hydrolases and their application in organic synthesis

## II.1 Introduction

Organic chemists have become interested in enzymes as catalysts due to their high efficiencies and specificities. Moreover, recent progress in molecular biology and enzyme-related research areas enabled and simplified the production and purification of recombinant enzymes in large quantities and their engineering towards tailor-made biocatalysts using straightforward mutagenesis and screening techniques. This is also true for epoxide hydrolases (EHs), as evidenced by the many published research papers about the synthetic applications of naturally occurring or engineered EHs.

EHs catalyze the opening of oxirane rings, generating a vicinal diol as the final product (**Figure 1**).

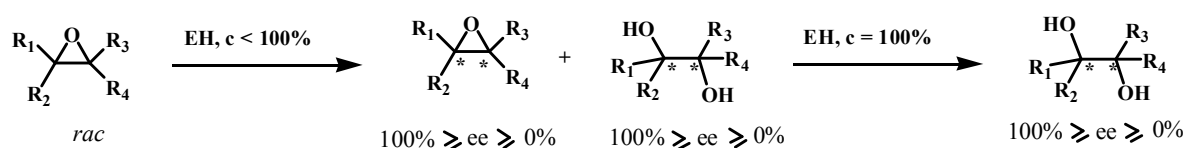


**Figure 1.** EH-catalyzed hydrolysis of a racemic epoxide, resulting in the formation of a vicinal diol with an enantiomeric excess of  $100\% \geq ee_p \geq 0\%$  at complete conversion ( $c = 100\%$ ) of the substrate. Depending on the EH-substrate interactions and consequently its substrate-related enantiomeric ratio or E-value (which characterizes the ability of the enzyme to discriminate between the two competing substrate enantiomers, Chen *et al.*, 1982), enantiopure epoxide is obtained at a specific degree of conversion within the range of  $50\% < c < 100\%$ . The kinetics of highly enantioselective EHs is characterized by a rapid hydrolysis of the preferred epoxide enantiomer, followed by a much slower hydrolysis of the remaining epoxide.

From a synthetic chemistry point of view, the most valuable EHs are those with either (1) high enantioselectivities or (2) a combination of low enantioselectivity with a high level of enantioconvergence. While the former generate enantiopure epoxides with a maximum yield of 50% in a kinetic resolution process, the latter produce ideally an enantiopure diol product with a theoretical yield of 100%. Thus, EHs provide convenient access to enantiopure epoxides or diols from racemic epoxides. Furthermore, the enantiopure diols can then be often chemically transformed back to the corresponding epoxides with no effect on the enantiomeric excess (ee). High values of enantioselectivity or enantioconvergence are a consequence of particular enzyme-substrate interactions, which can be modulated by specific reaction conditions or through the exchange of specific amino acids of the biocatalyst. The final stereochemical outcome of an EH-catalyzed reaction depends solely on the regioselectivity coefficients, which determine the absolute configuration and the ee of the diol

product when the reaction reaches 100% conversion. During the reaction, the oxirane ring of each enantiomer is often attacked at either carbon atom, resulting in a mixture of diol enantiomers (**Figure 2**).

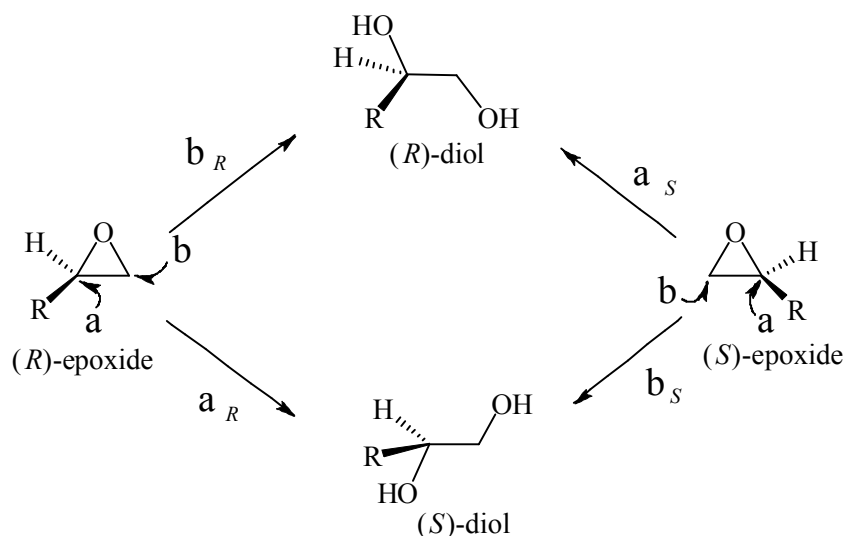


**Figure 2.** Attack at the oxirane ring can occur at either the terminal carbon atom, which results in a diol product with retained configuration ( $\beta$ -attack), or the carbon atom with the substituent R, resulting in a diol with an inverted configuration ( $\alpha$ -attack). The percentages of epoxide molecules following a particular reaction pathway are represented by the corresponding regioselectivity coefficients; the following relationships between the four regioselectivity coefficients are valid:  $\alpha_R + \beta_R = 100\%$ , and  $\alpha_S + \beta_S = 100\%$ .

The ideal enantioconvergent EH leads to deracemization of a racemic mixture of an epoxide and exhibits reversed regioselectivity for either substrate enantiomer, i.e.  $\alpha_S = 100\%$  and  $\alpha_R = 0\%$ , or  $\alpha_S = 0\%$  and  $\alpha_R = 100\%$ , affording an enantiomerically pure diol in a theoretical yield of 100%. However, enantioconvergence levels of above 90% (i.e.  $ee_p > 90\%$  at complete conversion of the substrate) are quite rare with wild-type EHs. EHs can also be used to de-racemize *meso* epoxides and in this case the ee of the formed diol keeps constant during the entire reaction. The resulting ee is here again fixed by the four regioselectivity coefficients. In the ideal case the diol product is obtained in 100% ee and 100% yield.

The scope of this chapter is to provide a comprehensive overview of the most interesting applications of EHs for the generation of enantiopure epoxides or diols, which are valuable chiral building blocks and key intermediates for the synthesis of various natural products or pharmacologically active compounds.

## II.2 Sources and reaction mechanism of EHs

### II.2.1 Sources of EHs

EHs have been found in many prokaryotic and eukaryotic organisms, including bacteria, fungi, yeast, plants, insects, fish and mammals (**Figure 3**). The physiological role of EHs appears to be manifold; they are involved in the detoxification of potentially harmful, naturally occurring or anthropogenic epoxides (Decker *et al.*, 2009), in lipid metabolism in plants and animals (Newman *et al.*, 2005; Morisseau, 2013), and in the metabolism of juvenile hormones in insects (Newman *et al.*, 2005). Recently, a new role of EHs in the biosynthesis of two antibiotics has been established in two *Streptomyces* strains (Lin *et al.*, 2006; Lin *et al.*, 2010). The substrates of EHs are structurally very diverse, representing a broad range of metabolites and xenobiotics. The substrate specificity of individual EHs appears to be diverse as well, being in many cases broad, but occasionally limited to a few available epoxidic compounds (Elfström and Widersten, 2005; van Loo *et al.*, 2006; Kotik *et al.*, 2009). Sources of novel EHs are not limited to known (micro-) organisms. Metagenomic or environmental DNA (eDNA), *i.e.* the total microbial DNA of a microcosm such as a small soil or groundwater sample, can serve as a source of novel EHs without the need to isolate and cultivate the microorganisms. PCR-based amplification of EH gene fragments in conjunction with genome-walking techniques (Kotik, 2009) have been used to retrieve entire genes encoding  $\alpha/\beta$ -hydrolase fold EHs directly from the metagenomic DNA (Kotik *et al.*, 2009; Kotik *et al.*, 2010). Moreover, activity screening of recombinant clones containing fragments of eDNA and hybridization to EH-specific target sequences led to the discovery of novel eDNA-derived EHs with considerable potential for biotransformations (Zhao *et al.*, 2004).

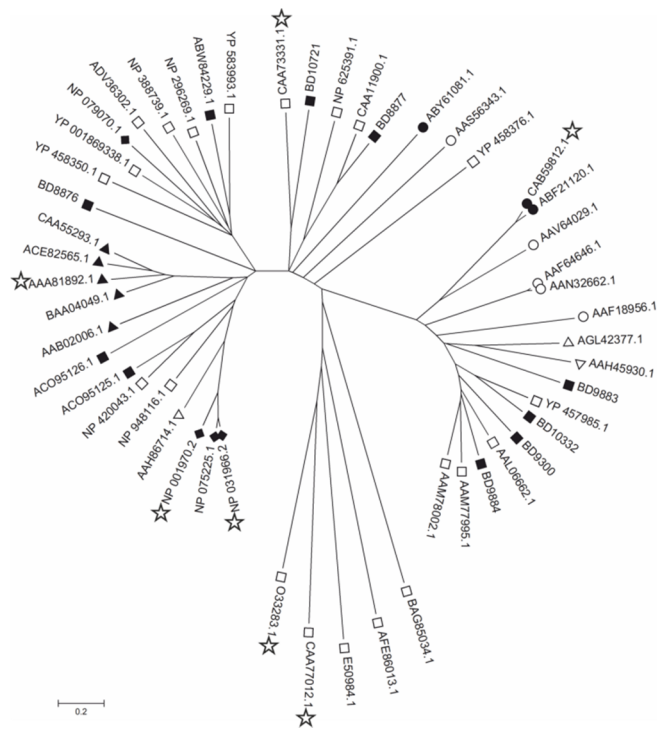


**Figure 3.** Phylogenetic relationships among protein sequences encoding EHs with confirmed activities. Each sequence is represented by its GenBank accession number; for sequences and further data regarding EHs with codes starting with BD, see Zhao *et al.*, 2004. The data set includes sequences of mammalian EHs (◆), plant EHs (▲), fish EHs (▽), insect EHs (△), yeast EHs (○), fungal EHs (●), bacterial EHs (□), and eDNA-derived EHs (■). A star represents an EH with a determined X-ray protein structure: human EH (NP\_001970), murine EH (NP\_031966), potato EH (AAA81892), a bacterial EH from *Agrobacterium radiobacter* AD1 (CAA73331), a fungal EH from *Aspergillus niger* LCP 521 (CAB59812), and two bacterial EHs which are not members of the  $\alpha/\beta$ -hydrolase fold superfamily (CAA77012 and O33283). The bootstrap consensus tree was inferred from 1000 replicates. The evolutionary distances were computed using the Poisson correction method. The bar represents 0.2 amino acid substitutions per site.

## II.2.2 Heterologous expression of EHs

Most EH expression systems were based on *Escherichia coli* as a host; however, heterologous expression of EHs was also established in mammalian cells (Grant *et al.*, 1993), the baculovirus system with *Spodoptera frugiperda* and *Trichoplusia ni* insect cell lines (Kamita *et al.*, 2013), in the yeast strains *Pichia pastoris*, *Saccharomyces cerevisiae* and *Yarrowia lipolytica* (Kim *et al.*, 2006; Labuschagne and Albertyn, 2007; Botes *et al.*, 2008), and in *Aspergillus niger* NW 219 (originally published as *A. niger* NW171; Naundorf *et al.*, 2009). The latter heterologous host offered the possibility to use a low-cost culture medium with inexpensive corn steep liquor as the main component. Further, *E. coli* RE3 as the

recombinant host enabled EH production in a minimal growth medium with inexpensive sucrose as the sole carbon source (Grulich *et al.*, 2011). Co-expression of molecular chaperones together with the optimization of culture conditions resulted in lower levels of inclusion bodies in the recombinant strain *E. coli* BL21(DE3) when overexpressing the EH from *Rhodotorula glutinis* (Visser *et al.*, 2003).

### II.2.3 Reaction mechanisms of EHs

A large fraction of EHs belongs to the  $\alpha/\beta$ -hydrolase fold superfamily, which contains – besides EHs – other structurally related hydrolytic enzymes with a characteristic arrangement of  $\alpha$ -helices and  $\beta$ -sheets: esterases, haloalkane dehalogenases, lipases, amidases, and some more (Heikinheimo *et al.*, 1999; Lenfant *et al.*, 2013). It appears that all EHs of the  $\alpha/\beta$ -hydrolase fold superfamily share a common three-step reaction mechanism, which involves the action of the active site-located catalytic triad (Asp-His-Glu/Asp), two tyrosine residues and a water molecule (**Figure 4**). In a first step, the carboxylic acid of aspartate attacks an oxirane carbon of the bound epoxide substrate, resulting in a transiently formed ester intermediate. Two conserved tyrosines assist in this step of catalysis, polarizing the epoxide ring by hydrogen bonding with the oxirane oxygen. The second step of the reaction mechanism, which is often rate-limiting, is characterized by the hydrolysis of the ester intermediate, catalyzed by an activated water molecule; the amino acid pair His-Glu/Asp of the catalytic triad is responsible for this activation. In the third and final step the formed diol product is released, leaving behind the restored catalytic triad of the enzyme.

Some EHs are not members of the  $\alpha/\beta$ -hydrolase fold superfamily, as shown for the limonene-1,2-epoxide hydrolase from *Rhodococcus erythropolis* (Arand *et al.*, 2003) and the EH from *Mycobacterium tuberculosis* (Johansson *et al.*, 2005). These two enzymes, which are dimers, have similar overall structures, each subunit consisting of a curved six-stranded  $\beta$ -sheet and four helices. The active site is located in a deep pocket with an Asp-Arg-Asp catalytic triad at its bottom. In contrast to the above-mentioned catalytic mechanism of  $\alpha/\beta$ -hydrolase fold EHs, a single-step push-pull mechanism has been proposed, which includes the activation of a water molecule by hydrogen bonding, resulting in a nucleophilic attack at the epoxide ring; at the same time, the epoxide is polarized and thereby activated by making available a proton to the oxirane oxygen (acid catalysis) (**Figure 5**).

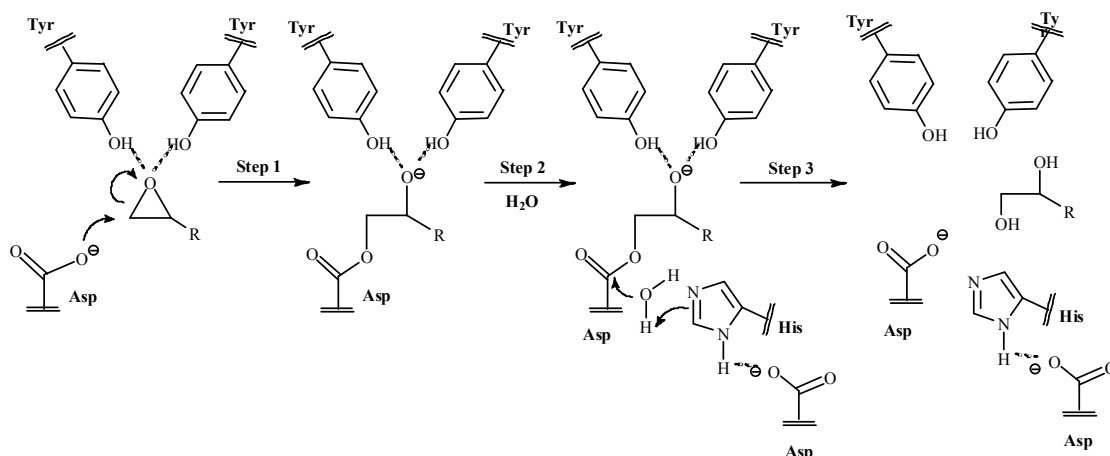


**Figure 4.** Proposed catalytic mechanism of EHs which are members of the  $\alpha/\beta$ -hydrolase fold superfamily.

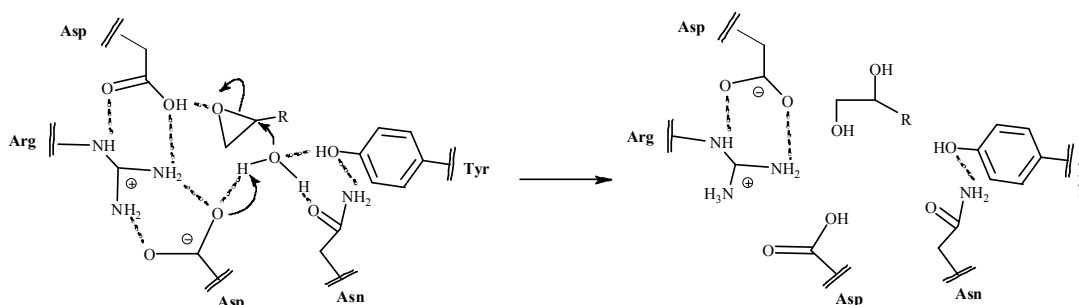


**Figure 5.** Proposed catalytic mechanism of the limonene-1,2-epoxide hydrolase from *Rhodococcus erythropolis* and the EH from *Mycobacterium tuberculosis*. The catalytic water molecule is activated by the formation of hydrogen bonds involving aspartic acid, asparagine and tyrosine residues. At the same time, polarization and activation of the oxirane ring is achieved by hydrogen bonding with the oxirane oxygen involving another aspartic acid residue.

### II.3 Mono-functional epoxides as chiral building blocks for the synthesis of biologically active compounds

Mono-functional epoxides are the simplest EH substrates and some of them, such as styrene oxide and derivatives thereof, are routinely used as standard substrates for EH activity measurements. Even within such a simple class of compounds it is possible to distinguish between, for example, mono-, di- and tri-substituted epoxides, aromatic and non-aromatic epoxides, and *meso* epoxides. The following reflects such a subdivision of epoxides and may

assist in finding the right enzyme for as yet not studied epoxides just by structure comparison with already described substrates of EHs.

### II.3.1 Mono-substituted aromatic epoxides

#### II.3.1.1 Styrene oxide

Both enantiomers of styrene oxide (SO) and phenyl-1,2-ethanediol are common chiral aromatic molecular building blocks for the synthesis of pharmaceuticals and other specialty chemicals. In the last decades a substantial amount of work has been dedicated to the enantioselective biohydrolysis of SO, the reason probably being the commercial availability of SO and the corresponding diol in both racemic and enantiopure forms. In 1993 Furstoss and co-workers described the first preparative access to both enantiomers of SO by enantioselective hydrolysis of the racemate using cells of two fungal strains that were enantiocomplementary, i.e. enantioselectively hydrolyzed either of the two SO enantiomers (Pedragosa-Moreau *et al.*, 1993; Pedragosa-Moreau *et al.*, 1995). In addition, it was observed that the hydrolysis of racemic SO using cells of *Aspergillus niger* LCP 521 proceeded with retention of configuration at the chiral center, generating the (*R*)-diol and leaving behind the (*S*)-epoxide as the residual compound. On the other hand, hydrolysis of SO using cells of *Beauveria sulfurescens* ATCC 7159 resulted in the formation of the (*R*)-diol from the (*S*)-epoxide by inversion of configuration, leaving behind the unreacted (*R*)-epoxide. These findings were used for a biohydrolysis reaction in the presence of both molds, resulting in the first enantioconvergent bi-enzymatic process for the production of (*R*)-phenyl-1,2-ethanediol in high yield (92%) and with an ee as high as 89% (**Figure 6**).

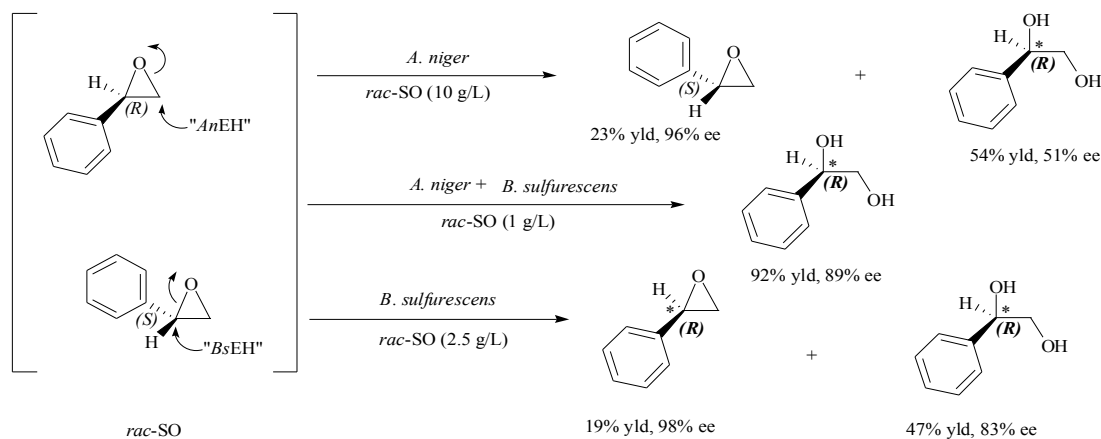


**Figure 6.** Biohydrolytic kinetic resolution of racemic styrene oxide (*rac*-SO) catalyzed by *Aspergillus niger* LCP 521 (*AnEH*) and/or *Beauveria sulfurescens* ATCC 7159 (*BsEH*). Using both fungi together led to an enantioconvergent production of (*R*)-phenyl-1,2-ethanediol.

More recently, this bi-enzymatic enantioconvergent strategy was applied for the preparation of the same (*R*)-diol compound in a higher ee, using different combinations of EHs. For example, by mixing two purified EHs, a wild-type EH from *S. tuberosum* and an evolved EH from *A. radiobacter* AD1, SO was rapidly converted to the corresponding (*R*)-diol in 98% ee and 100% yield (Cao *et al.*, 2006). However, this process had to be carried out at a low substrate concentration of 5 mM due to product inhibition of the *S. tuberosum* EH. Moreover, a mixture of recombinant whole cells harboring the EH-encoding genes from *A. niger* LK and *C. crescentus* was also used in a preparative-scale batch reaction for the enantioconvergent hydrolysis of 1.2 g of racemic SO at a concentration of 33 mM. 1.3 g of (*R*)-phenyl-1,2-ethanediol with an enantiopurity of 91% was obtained with an overall yield of 95%. Substrate concentrations exceeding 50 mM could not be used due to product inhibition of the bacterial EH (Hwang *et al.*, 2008b). A similar approach was described later in which the *A. niger* LK EH was replaced by an EH mutant from *Mugil cephalus*, a marine fish (Min and Lee, 2012). After optimization of the reaction conditions, (*R*)-phenyl-1,2-ethanediol was obtained in 90% ee and 95% yield from 50 mM racemic styrene oxide. Shen and co-workers isolated two bacterial EHs (SgcF and NcsF<sub>2</sub>), which are involved in the biosynthesis of enediynes, antitumor antibiotics produced by *Streptomyces globisporus* and *Streptomyces carzinostaticus*. Using SO as a substrate mimic, SgcF and NcsF<sub>2</sub> were shown to be enantiocomplementary, leading to the formation of (*R*)-phenyl-1,2-ethanediol in 99% ee and 87% yield from racemic SO (14 mM) when used together in the reaction mixture (Lin *et al.*,

2010). An interesting enantioconvergent process with whole cells of *Aspergillus tubingensis* TF1 was recently described (Duarah *et al.*, 2013). (*R*)-phenyl-1,2-ethanediol was isolated from the reaction mixture in 97% ee after 45 min, reaching >99% conversion of racemic SO (8.75 mM). Although a single enzyme was claimed to be responsible for this process, the possibility of two enantiocomplementary EHs with opposite regioselectivity being present in the microorganism cannot be ruled out from the described data.

Although a great number of wild-type EHs was found to kinetically resolve racemic SO, to the best of our knowledge no EH showed a very high enantioselectivity level. Nevertheless, several kinetic resolutions at high SO concentrations have been described using EHs from yeast, bacteria and plants in the last decade. For example, (*S*)-SO with 98% ee was obtained in 41% yield from racemic SO at a very high concentration of 1.8 M using a *Pichia pastoris* strain overexpressing the EH from *Rhodotorula glutinis*. Such a high substrate concentration in the reaction mixture called for optimized reaction conditions, *i.e.* the reaction was taking place at 4° C in the presence of 40% (v/v) Tween 20 and 5% (v/v) glycerol (Yoo *et al.*, 2008). Biomass of *Achromobacter* sp. MTCC 5605, which was isolated from a petroleum-contaminated sludge sample, enabled the hydrolytic kinetic resolution of racemic SO at a high concentration of 0.5 M using a biphasic reaction system composed of isooctane and buffer. Under these conditions, an enantiomeric ratio of 64 was determined; the remaining (*S*)-SO (42% yield) and the formed (*R*)-phenyl-1,2-ethanediol were isolated in > 99 and 65% ee, respectively (Kamal *et al.*, 2013). It is worth mentioning that an improvement of the enantioselectivity was obtained after covalent immobilization of the multimeric EH from *A. niger* LCP 521 onto Eupergit C which was partially modified with ethylene diamine (Eupergit C/EDA), resulting in an E-value of 56 instead of 25 (Mateo *et al.*, 2003).

### II.3.1.2 Chlorostyrene oxide

(*R*)-*para*- and (*R*)-*meta*-chlorostyrene oxides are important building blocks for the synthesis of various biologically active molecules. Indeed, these compounds are, for example, essential chiral intermediates for the production of Eliprodil (Pabel *et al.*, 2000), an effective NMDA receptor antagonist, and various  $\beta$ -3-adrenergic receptor agonists such as SR 58611A or AJ-9677 (Harada *et al.*, 2003). Numerous biohydrolytic kinetic resolutions have been described in the literature with the purpose of preparing these chiral synthons in enantiopure form. However, it is well known that one of the general drawbacks of including a resolution step in a chemical synthesis is its intrinsic 50% yield limitation. This is the reason why

various enantioconvergent processes with the aim of approaching the ideal situation of “100% yield and 100% ee” have been elaborated.

As far as *para*-chlorostyrene oxide (*p*-ClSO) is concerned, enzymatic extracts of overexpressed EHs from *A. niger* LCP 521 (*AnEH*) and *S. tuberosum* (*StEH*) were shown to efficiently resolve this racemic epoxide (E-values of 100 at 0 °C). The enantiocomplementarity of these two enantioselective EHs enabled the preparation of both enantiomers of *p*-ClSO, the (*R*)-*p*ClSO and (*S*)-*p*ClSO being preferentially hydrolyzed by the *AnEH* and the *StEH*, respectively. The absolute configuration of the formed diol was determined to be *R* in both cases. Preparative-scale resolutions were performed at very high substrate concentrations of 306 g/L and 30.6 g/L using respectively *AnEH* and *StEH* as the biocatalysts (Manoj *et al.*, 2001). Similar results were also obtained in a repeated batch reaction with both enzymes immobilized onto DEAE-cellulose by ionic adsorption (Karboune *et al.*, 2005b).

Based on the complementary enantio- and regioselectivities of these two EHs, an enantioconvergent production of (*R*)-*para*-chlorophenyl-1,2-ethanediol from *rac-p*-ClSO was established using a sequential bi-enzymatic strategy. Thus, a preparative-scale experiment was carried out at a substrate concentration of 30.6 g/L using first the *StEH* followed by the *AnEH*. The (*R*)-diol was obtained with an overall yield as high as 93% and 96% ee (**Figure 7**) (Manoj *et al.*, 2001).

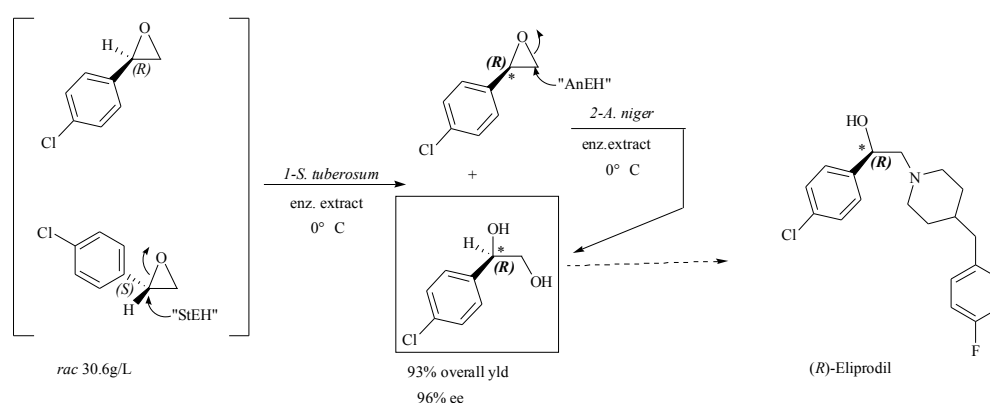


**Figure 7.** Enantioconvergent bihydrolytic transformation of *para*-chlorostyrene oxide using a bi-enzymatic process. The sequential use of *Solanum tuberosum* and *Aspergillus niger* EHs as biocatalysts led to the formation of enantiopure (*R*)-*para*-chlorophenyl-1,2-diol, a chiral building block for the synthesis of (*R*)-Eliprodil.

Unfortunately, the substrate concentration had to be decreased by a factor of 10 in this bi-enzymatic process, compared to a single-enzyme resolution process with *AnEH*, to diminish the inhibitory effect of the formed diol on the *StEH* activity. Later, a repeated batch experiment using these two EHs, separately immobilized onto DEAE-cellulose, was also described (Karboune *et al.*, 2005a). More recently, other teams reported a similar strategy using two EHs. A sequential bi-enzymatic hydrolysis of *p*-CISO was described by Lee *et al.* (Min and Lee, 2012), using a heterologously expressed EH from *Caulobacter crescentus* and an EH mutant from *Mugil cephalus*. The combined use of whole cells overexpressing these two EHs enabled the production of (*R*)-*para*-chlorophenyl-1,2-ethanediol with 92% enantiopurity and 71% yield, starting from 17 g/L of *rac-p*-CISO. In a previous paper, the same authors described an enantioconvergent process which was based on a mono-enzymatic approach using the EH from *C. crescentus* (Hwang *et al.*, 2008a). This EH was shown to have opposite enantioselectivity and regioselectivity toward either enantiomer of *rac-p*-CISO, which led to the almost exclusive formation of the (*R*)-diol. With the enantioselectivity being not too high (*E*-value = 30), a preparative-scale biohydrolysis at a substrate concentration of 16.8 g/L resulted in the formation of (*R*)-*para*-chlorophenyl-1,2-ethanediol with 98% ee and 78% overall yield. Kotik *et al.* have described the first example of regioselectivity engineering in EHs by directed evolution starting from a non-enantioconvergent enzyme (Kotik *et al.*, 2011). The substrate binding cavity of the EH from *A. niger* M200 was redesigned to generate an enantioconvergent biocatalyst by guiding the point of nucleophilic attack to the benzylic oxirane position of the bound (*S*)-enantiomer. After nine amino acid exchanges, the final enzyme variant transformed racemic *p*-CISO to the (*R*)-diol with an ee of 70.5%. These authors reported in the same article a sequential bi-enzymatic reaction using the wild-type EH from *A. niger* M200 and its evolved variant, resulting in the formation of the (*R*)-diol with an ee-value of 88%. More recently, Kotik and co-workers reported that an EH (named Kau2), whose gene was isolated from a biofilter-derived metagenome, exhibited an opposite regioselectivity for the two enantiomers of *p*-CISO, which enabled them to obtain (*R*)-*para*-chlorophenyl-1,2-ethanediol in 84% ee at 100% conversion (Kotik *et al.*, 2010).

An enantioconvergent preparative-scale production of (*R*)-*meta*-chlorophenyl-1,2-ethanediol was described by Furstoss and co-workers using the EH from *Solanum tuberosum* (Monterde *et al.*, 2004). The enzyme exhibited a low enantioselectivity (*E*-value of 6) in conjunction with an opposite regioselectivity for each enantiomer of *m*-CISO, which are ideal conditions for an enantioconvergent process. Starting from *rac-m*-CISO, nine cycles of a repeated batch experiment in a stirred reactor at 10 g/L of substrate concentration furnished

the (*R*)-diol with an ee-value of 97% and an 88% overall yield. Very recently, Li and co-workers have studied the biohydrolysis of numerous epoxides (including *meso* compounds) using the EH from *Sphingomonas* sp. HXN-200 overexpressed in *E. coli* (*SpEH*) (Wu *et al.*, 2013). This EH with an E-value of 41 was shown to be more enantioselective than any other known EH for the hydrolysis of *rac-m*-ClSO. Interestingly, *SpEH* reacted preferentially with the (*R*)-epoxide, forming the (*R*)-diol and leaving behind the (*S*)-*m*-ClSO, which is a useful chiral building block for the preparation of an IGF-1R kinase inhibitor (Witmann *et al.*, 2005). A gram-scale kinetic resolution of *rac-m*-ClSO was performed in a two-phase system (buffer/*n*-hexane) at 15 g/L of substrate with resting *SpEH*-containing cells. Enantiopure (*S*)-*m*-ClSO was obtained in 37.9% yield.

### II.3.1.3 Nitrostyrene oxide

(*R*)-*para*-nitrostyrene oxide (*p*-NSO) is the key chiral synthon for the synthesis of Nifenalol, a compound showing  $\beta$ -blocking activity and used in the treatment of hypertensive diseases (Murmman *et al.*, 1967). This epoxide, which is mostly insoluble in water, has been resolved with good enantioselectivity by fungal, bacterial and yeast EHs (**Table 1**).

**Table 1.** Selected kinetic resolutions of *rac-p*-nitrostyrene oxide.

Source of EH	Notes	E-value	Substrate conc. (mM)	Abs. Conf. Residual epoxide/ Formed diol	References
<i>Aspergillus niger</i> LCP 521	Enzymatic extract	48	330	<i>S/R</i>	Morisseau <i>et al.</i> , 1997
<i>Agrobacterium radiobacter</i> AD1	Purified enzyme	65	3	<i>S/R</i>	Spelberg <i>et al.</i> , 2002
<i>Agrobacterium radiobacter</i> AD1, variant Y215F		>200	3	<i>S/R</i>	Rink <i>et al.</i> , 2000
<i>Agrobacterium radiobacter</i> AD1, variant S7	Error-prone PCR and DNA shuffling; cell-free extract or purified EH	>200	2	<i>S/R</i>	van Loo <i>et al.</i> , 2004
<i>Aspergillus niger</i> GBCF 79 (recombinant strain)	Enzymatic extract, EH immobilized onto silica gel, co-solvent: 20% DMSO	85	4.5	<i>S/R</i>	Petri <i>et al.</i> , 2005
<i>Aspergillus niger</i> M200	Purified enzyme	>100	8	<i>S/R</i>	Kotik and Kyslik, 2006
Kau2 (metagenome)	Crude extract, EH overexpressed in <i>E. coli</i> Whole cells, EH overexpressed in <i>Y. lipolytica</i>	80	3.5	<i>R/R</i>	Kotik <i>et al.</i> , 2010
Kau8 (metagenome)		65	3.5	<i>S/R</i>	
Oxy-4		>100	500	<i>S/R</i>	Pienaar <i>et al.</i> , 2008 Botes <i>et al.</i> , 2007c
Oxy-10		>100	500	<i>R/R</i>	
<i>Bacillus megaterium</i> ECU1001	Crude extract, EH overexpressed in <i>E. coli</i>	>200	20	<i>R/-</i>	Zhao <i>et al.</i> , 2013

The first examples were described with whole cells of the fungi *A. niger* LCP 521 and *Beauveria sulfurescens* ATCC7159 (Pedragosa-Moreau *et al.*, 1996c). One year later, a cell-

free extract from *A. niger* LCP 521 was used as a biocatalyst (Morisseau *et al.*, 1997). To improve the solubility of *p*-NSO in the reaction mixture 20% of a miscible solvent (DMSO or DMF) were added. Under these experimental conditions, the hydrolysis was relatively enantioselective (*E*-value = 48) and could be performed at a high substrate concentration of 54 g/L (330 mM) to produce (*S*)-*p*-NSO (99% ee; 49% yield). Later, high enantioselectivity with an *E*-value of >100 at 10 °C was also determined with another EH present in the strain *Aspergillus niger* M200, which was isolated from industrial biofilters (Kotik *et al.*, 2005; Kotik and Kyslik, 2006). Starting from the wild-type EH from *Agrobacterium radiobacter* AD1 with an *E*-value of 65 (Spelberg *et al.*, 2002), a substantial improvement of the enantioselectivity was obtained by error-prone PCR and DNA shuffling, reaching an *E*-value >200 (Rink *et al.*, 2000; van Loo *et al.*, 2004). Interestingly, a very high enantioselectivity (*E*-value >200) together with a reversed (*S*)-enantioselectivity was observed for the EH from *Bacillus megaterium* ECU1001, retaining the useful (*R*)-*p*-NSO for the direct synthesis of (*R*)-Nifenalol (Zhao *et al.*, 2011). More recently, EHs exhibiting opposite enantioselectivity toward the two antipodes of *p*-NSO were also described. Two of them, Kau2 and Kau8, were isolated from biofilter-derived metagenomes (Kotik *et al.*, 2010), and two others, oxy-4 and oxy-10, from yeast (Pienaar *et al.*, 2008). It should be noticed that the remaining epoxides of Kau2- and Oxy-10-mediated kinetic resolutions were determined to be (*R*)-*p*-NSO, which is the correct enantiomer for the synthesis of (*R*)-Nifenalol.

A one-pot chemo-enzymatic enantioconvergent process for the production of (*R*)-*p*-NSO was described by Furstoss *et al.* in 1997 (Pedragosa-Moreau *et al.*, 1997). The strategy was based on the sequential hydrolysis of the (*R*)-epoxide using an enzymatic extract of *An*EH followed by an acid-catalysed hydrolysis of the remaining (*S*)-epoxide (**Figure 8**).

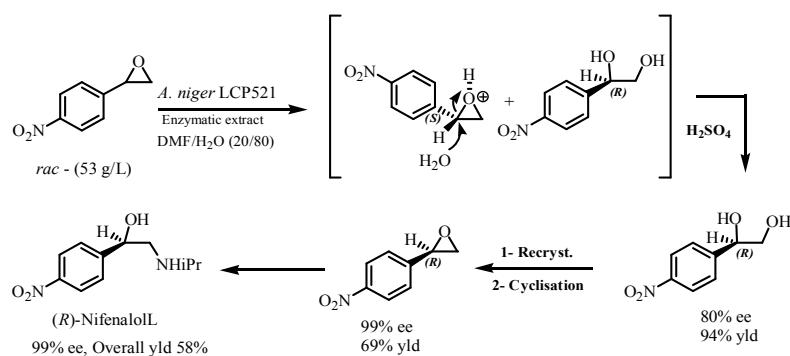


**Figure 8.** Enantioconvergent synthesis of the  $\beta$ -blocker (*R*)-Nifenalol using a combined chemoenzymatic approach.

A 330 mM (54 g/L) solution of *p*-NSO was hydrolysed within 6 h to furnish the (*S*)-epoxide in 49% yield and 99% ee. Then, the controlled acid hydrolysis of the reaction mixture yielded the (*R*)-diol (80% ee) as a result of steric inversion upon acid hydrolysis of the unreacted (*S*)-epoxide. After recrystallisation, the (*R*)-diol could be easily recycled to the epoxide and transformed into (*R*)-Nifenalol. Interestingly, Botes *et al.* (Pienaar *et al.*, 2008; Botes *et al.*, 2007c) described the enantioconvergent production of the (*R*)-diol in one pot at a high substrate concentration using the combined action the Oxy-4 and Oxy-10 biocatalysts (bi-enzymatic-process).

### II.3.1.4 Trifluomethylstyrene oxide

Enantiocontrolled synthesis of fluorinated organic compounds has gained tremendous impetus over the recent years because it is well known that the presence of fluorine atoms in a molecule can have dramatic effects on its biological activity (Soloshonok, 1999). In this context, the kinetic resolution of a specific trifluoro-methyl-substituted aromatic epoxide family was studied using a recombinant EH from *A. niger* LCP 521, and the productivity of the biotransformation process was evaluated (Deregnaucourt *et al.*, 2007). A two liquid-liquid phase methodology with an appropriate co-solvent (isooctane, 10 to 35% (v/v)) and optimized operational conditions led to a very efficient and cost-effective resolution process. The best results (high E-value, high TON and TOF) were obtained in the case of *para*-substituted CF<sub>3</sub>-, OCF<sub>3</sub>- and SCF<sub>3</sub>-derivatives. For example, resolution of (4-trifluoromethoxyphenyl)-oxirane could be performed at 250 g/L, resulting in the residual (*S*)-epoxide and the formed (*R*)-diol in good yields and very high enantiomeric excess (**Figure 9**).

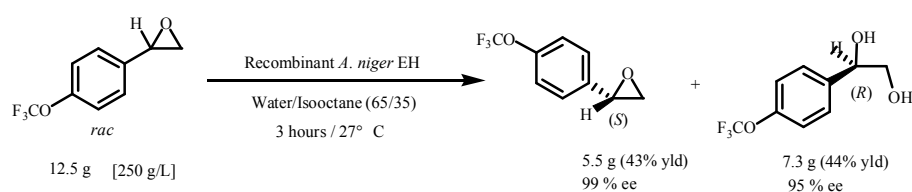


**Figure 9.** Preparative scale synthesis of enantiopure (4-trifluoromethoxyphenyl)-oxirane using a partially purified recombinant EH from *Aspergillus niger* LCP 521 as a biocatalyst.

### II.3.1.5 Pyridyl oxirane

Enantiopure 2-, 3- and 4-pyridyloxirane are key-building blocks for the synthesis of several biologically active compounds, such as  $\beta$ -adrenergic receptor agonists or antiobesity drugs (Mathvink *et al.*, 1999; Devries *et al.*, 1998; Fisher *et al.*, 1996). Up to now, none of these products could be obtained in a satisfactory enantiopure form using the most effective heavy metal-containing catalysts (Jacobsen epoxidation, Jacobsen HKR or Sharpless dihydroxylation). Interestingly, the recombinant EH from *A. niger* LCP 521 exhibited a rather high enantioselectivity toward all three substrates with E-values of 96, 27 and 47, respectively, hydrolyzing preferentially the (*R*)-enantiomer and thus enabling the recovery of the slowly reacting (*S*)-epoxide. Unfortunately, it was shown that the E-value decreased with increasing substrate concentration. Nevertheless, the preparative-scale synthesis of each pyridyloxirane could be performed at about 10 g/L substrate concentration, which enabled these three target compounds to be obtained in nearly enantiopure form (Genzel *et al.*, 2001a). In the same year, it was shown that a Tyr215Phe mutation in the EH from *Agrobacterium radiobacter* AD1 resulted in an enzyme variant that could efficiently resolve 2-pyridyloxirane (E-value = 55) at a substrate concentration as high as 127 mM (15.5 g/L) (**Figure 10**) (Genzel *et al.*, 2001b).

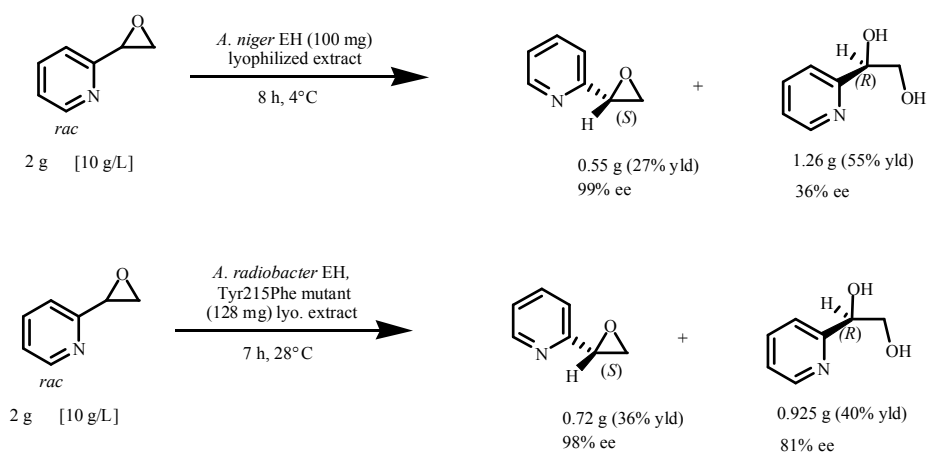


**Figure 10.** Preparative kinetic resolution of 2-pyridyloxirane with EHs from *A. niger* and *A. radiobacter* AD1 (mutant Tyr215Phe).

## II.3.2 Di-substituted aromatic epoxides

### II.3.2.1 *p*-Bromo-, *p*-isobutyl- and *p*-trifluoromethyl- $\alpha$ -methyl styrene oxide

To overcome the problem of low solubility of aromatic epoxides in the water phase, Furstoss and collaborators studied in 1998 enzymatic resolutions at high substrate concentration without adding organic solvents (Cleij *et al.*, 1998). They showed that at a high concentration of 80 g/L of *para*-bromo-  $\alpha$ -methyl styrene oxide a biphasic system was formed with the epoxide constituting one phase by itself. This enabled a good kinetic resolution of the aromatic epoxide using an EH-containing extract from *A. niger* LCP 521 as a biocatalyst. Under these experimental conditions, the residual epoxide was found to be of (*S*) configuration, whereas the formed product was the corresponding (*R*)-diol. Surprisingly, the use of this procedure led to a dramatic enhancement in the enantioselectivity with the E-value increasing from 20 at low substrate concentration (1.7 g/L) to 260 at 80 g/L (**Figure 11**).

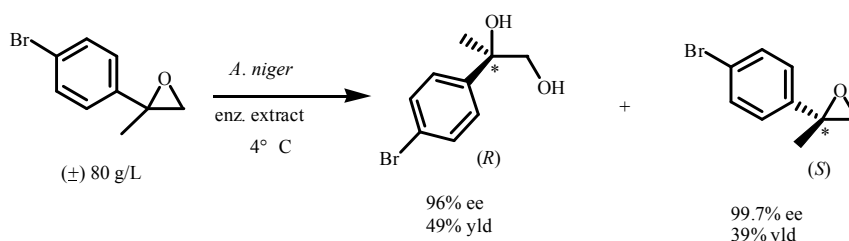


**Figure 11.** Kinetic hydrolytic resolution at high substrate concentration of *para*-bromo-  $\alpha$ -methyl styrene oxide using an enzymatic extract of *A. niger* LCP 521.

One year later, the same authors studied the biohydrolysis of seven differently substituted-methylstyrene oxide derivatives, including the *para*-bromo-methyl styrene oxide, using 10 different EHs (Cleij *et al.*, 1999). The best results were obtained with the EH from *A. niger* LCP 521; however, the E-values were relatively moderate. A four-step synthesis of (*S*)-Ibuprofen, a non-steroidal anti-inflammatory drug, was performed to illustrate the synthetic potential of EHs. The strategy was to achieve the enantioselective hydrolysis of *rac*-4-isobutyl- $\alpha$ -methylstyrene oxide using the EH from *A. niger*, which has been shown to specifically hydrolyse the undesired (*R*)-enantiomer, and to further transform the enantiopure residual (*S*)-epoxide into (*S*)-Ibuprofen using classical chemical synthesis. As in the case of the *para*-bromo derivative, the biohydrolysis was performed at a high substrate concentration

of 50 g/L, leading to a biphasic process, and at a low reaction temperature of 4 °C to enhance enzyme stability and decrease the spontaneous hydrolysis of the substrate. Following this strategy, the overall yield of (*S*)-Ibuprofen was only 27%. Recycling of the formed diol via chemical racemization substantially improved the process yield. Indeed, treatment of the formed diol with HBr/AcOH and subsequent cyclization of the bromhydrin intermediate under basic conditions afforded racemic 4-isobutyl-methylstyrene oxide in 80% yield, which could thus be resubmitted to the enzymatic resolution step. Under these conditions, the overall yield increased from 27 to 47% (**Figure 12**).

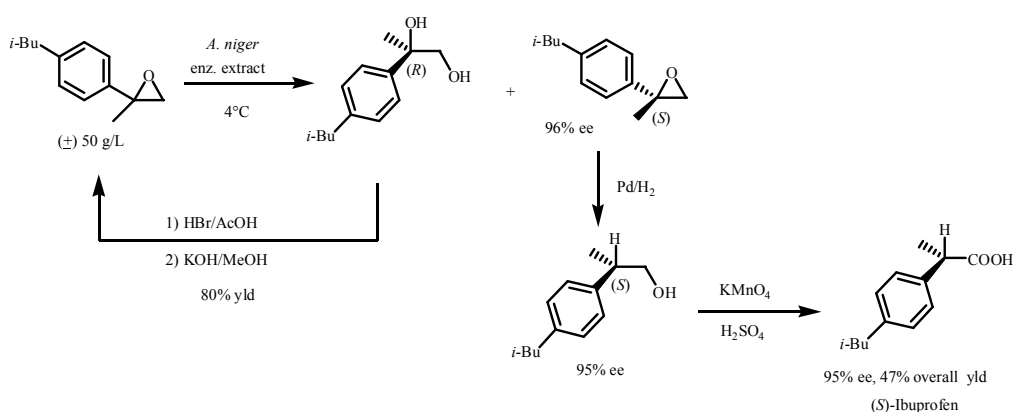


**Figure 12.** Preparative-scale resolution of *rac*-4-isobutyl- $\alpha$ -methylstyrene oxide using an enzymatic extract of *A. niger* LCP 521. A four step enantioconvergent procedure enabled the synthesis of (*S*)-Ibuprofen.

Ten years later, Furstoss's group confirmed the high kinetic resolving power of the EH from *A. niger* LCP 521 by showing that the enzyme could also be used for the efficient resolution of *para*-trifluoromethyl- $\alpha$ -methyl styrene oxide (Deregnacourt *et al.*, 2007). Indeed, the preparative-scale biohydrolysis at 100 g/L could be performed in a short reaction time in a biphasic reaction medium containing water-organic solvent. Isooctane (25% v/v) was added to the reactor to obtain a good substrate emulsion, leading to an optimal transfer of the substrate from the organic phase to the water phase. Under these experimental conditions, a loading of 25 g of racemic epoxide resulted in the formation of 10.5 g (42% yield) of (*S*)-epoxide (99.7% ee) and 13.4 g (78.5% yield) of (*R*)-diol (78.5% ee) (**Figure 13**).

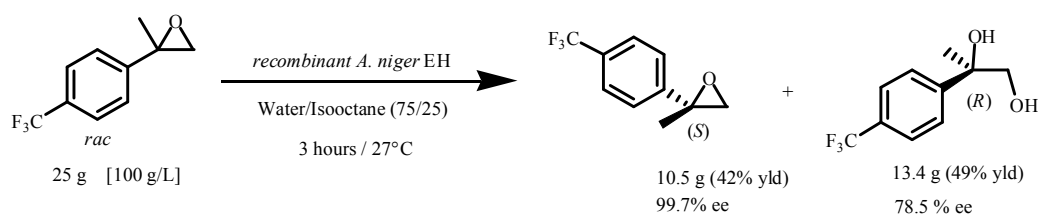


**Figure 13.** Preparative-scale synthesis of enantiopure *para*-trifluoromethyl- $\alpha$ -methyl styrene oxide using a partially purified recombinant EH from *Aspergillus niger* LCP 521 as biocatalyst.

### II.3.2.2 *cis*- and *trans*- $\beta$ -methylstyrene oxide

Enantiopure form of *trans*- $\beta$ -methylstyrene oxide has been used as a building block for the synthesis of a potential cocaine abuse therapeutic agent and an anti-obesity drug (Hsin *et al.*, 2003; Lin *et al.*, 2006). Very satisfactory resolutions of *trans*- $\beta$ -methylstyrene oxide were achieved with a metagenome-derived EH (termed Kau2) (Kotik *et al.*, 2010) and EHs from fungi, e.g. *Beauveria sulfurescens* (Pedragosa *et al.*, 1996b), and yeasts *Rhodotorula glutinis* CIMW147 (Weijers, 1997), *Rhodotorula glutinis* UOFS Y-0123 (Lotter *et al.*, 2004), and *Rotoruloides mucoides* UOFSY-0471 (Botes *et al.*, 2007a). A comparison of all the described results leads to the conclusion that the hydrolysis of *trans*- $\beta$ -methylstyrene oxide proceeded with a similar enantioselectivity and stereochemistry. Indeed, in all cases the (1*S*,2*S*)-epoxide was preferentially hydrolysed to the (1*R*,2*S*)-*erythro*-diol, indicating that the enzymatic attack occurred at the benzylic position. The best result was achieved in a preparative-scale reaction at 80 g/L of substrate concentration, using freeze-dried *E. coli* RE3 cells harbouring the plasmid pSEKau2 for expression of the EH Kau2. Both (1*R*,2*R*)-epoxide and the corresponding (1*R*,2*S*)-diol were isolated in high enantiomeric excess (>99%) and good yield (>45%), corresponding to a very high enantioselectivity (E-value >200) (**Figure 14**).

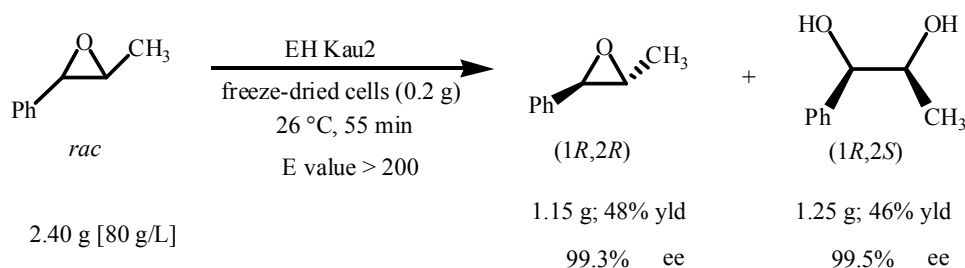


**Figure 14.** Preparative-scale kinetic resolution of racemic *trans*- $\beta$ -methylstyrene oxide using the Kau2-EH at high substrate concentration.

In contrast to these results, Chiappe *et al.* (Chiappe *et al.*, 2004) reported that the reaction catalyzed by the EH from cress was partially stereoconvergent, furnishing the corresponding (1*S*,2*R*)-*erythro*-1-phenylpropane-1,2-diol as the main product. Using pure enantiomers as starting epoxides, it was determined that the formal nucleophilic attack of water occurred exclusively at C1 in the case of (1*R*,2*R*)-epoxide, while the same enzyme was practically non-selective for the same carbon atom of its antipode.

As far as *cis*- $\beta$ -methylstyrene oxide is concerned, very few EHs with the ability to hydrolyze this compound have been described. Three similar and interesting enantioconvergent processes were described using fungal EHs from *Beauveria sulfurescens* ATCC7159 (Pedragosa-Moreau *et al.*, 1996b), *Aspergillus terreus* (Moussou *et al.*, 1998b), and the metagenome-derived Kau2-EH (Kotik *et al.*, 2010). Indeed, it was observed that the two antipodes were hydrolyzed with a low enantioselectivity (E-value = 10) and an opposite regioselectivity, leading to the formation of the same (1*R*,2*R*)-diol in almost optically pure form and nearly quantitative yield (**Figure 15**). It should be noticed that the modification of the stereochemistry (*trans* to *cis*) of the starting epoxide resulted in a significant decrease of the reaction rate.

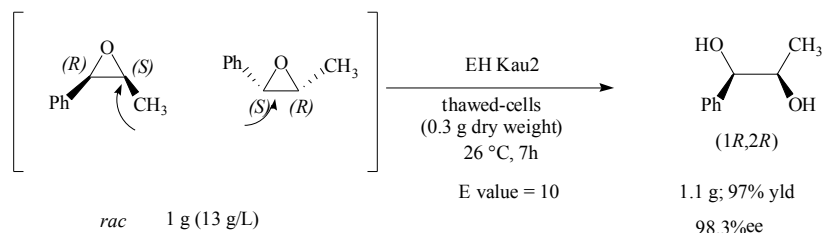


**Figure 15.** Preparative enantioconvergent biohydrolysis of racemic *cis*- $\beta$ -methylstyrene oxide using the Kau2-EH.

### II.3.2.3 Indene oxide

Chiral (1*S*,2*R*)-indene oxide is a valuable precursor for the synthesis of the side chain of the HIV protease inhibitor MK 639, which was developed by Merck Research Laboratories. Several teams searched for EHs capable of catalyzing the kinetic resolution of racemic indene oxide. Selected strains of bacteria (Hwang *et al.*, 2006), yeast (Weijers, 1997) and fungi (Zhang *et al.*, 1995; Pedragosa-Moreau *et al.*, 1996a) were shown to be useful for the preparation of the two antipodes of indene oxide (**Figure 16**). However, low

enantioselectivity of the implied EHs and instability of indene oxide in water resulted in low yields when attempting to reach 100% ee of the residual epoxide.

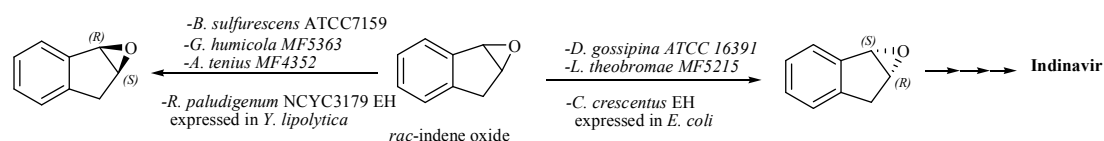


**Figure 16.** Biohydrolytic kinetic resolution of racemic indene oxide. Access to (1*S*,2*R*)- or (1*R*,2*S*)-indene oxide as a function of the biocatalyst used.

Recently, kinetic resolution performed at high substrate concentration was described in a patent by Botes *et al.* (Botes *et al.*, 2007a) using a recombinant yeast EH. Indeed, a preparative-scale biohydrolysis at 264 g/L (2 M) substrate concentration was performed using whole cells of a recombinant *Yarrowia lipolytica* strain expressing the EH from the yeast *Rhodospiridium paludigenum* NCYC 3179. In this process, crystalline indene oxide powder (26.4 g) was directly added to 100 mL of phosphate buffer which contained thawed whole cells (13.5 g wet weight). After 150 minutes at 25 °C, the resolution process was complete and 8.5 g (32% yield) of residual enantiopure (1*R*,2*S*)-indene oxide were isolated. Unfortunately, the recovered (1*R*,2*S*)-indene oxide exhibited the wrong stereochemistry for the synthesis of Indinavir.

### II.3.3 Non aromatic epoxides

#### II.3.3.1 Mono-substituted alkyl epoxides

Highly enantioselective EHs toward mono-aliphatic terminal oxiranes were detected in some species of specific yeast genera such as *Rhodotorula* sp. and *Rhodospiridium* sp. (Botes *et al.*, 1998; Botes *et al.*, 1999). Although enantiomeric distinction of these highly flexible molecules is believed to be a difficult task for the enzyme, high E-values of >100 were reported in several cases. All enantioselective EHs reacted preferentially with the (*R*)-epoxide, forming (*R*)-diols and leaving behind the (*S*)-epoxide. Using whole cells of *Rhodotorula araucariae* CBS 6031 or *Rhodospiridium toruloides* CBS 0349 it was possible to perform a preparative-scale hydrolysis of racemic 1,2-epoxyoctane at a 500 mM substrate concentration (Figure 17).

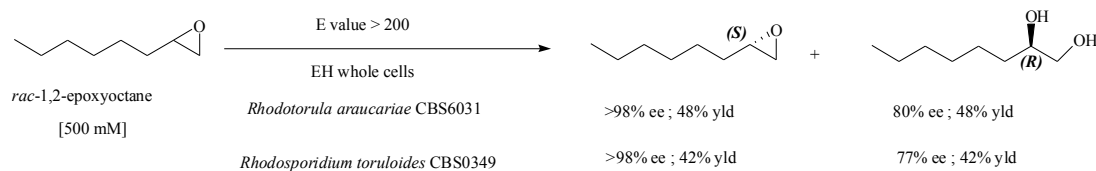


**Figure 17.** Kinetic resolution of 1,2-epoxyoctane at high substrate concentration with two yeast EHs.

### II.3.3.2 Glycidyl ether and derivatives thereof

Biohydrolytic kinetic resolutions of alkyl and aryl glycidyl ethers, which are important building blocks for the production of various bioactive compounds, have been extensively investigated using EHs from bacteria, yeast and filamentous fungi. Concerning phenyl glycidyl ether (PGE) and various derivatives thereof, interesting results were obtained with the EH from *Bacillus megaterium* ECU1001. In contrast to the majority of other EHs, this enzyme exhibited an unusual (*R*)-enantioselectivity for PGE, retaining the useful (*S*)-PGE for the synthesis of  $\beta$ -blocker compounds; it also exhibited the highest enantioselectivity ( $E = 58$ ) among all known wild-type EHs (Zhao *et al.*, 2011). In addition, it was observed that introducing a methyl substituent at the phenyl ring of PGE had a pronounced influence on the enantioselectivity of the hydrolysis reaction. As a general trend, the  $E$ -value increased as the substituent was shifted from the *para* ( $E = 11$ ) to the *meta* position ( $E = 19$ ), with the *ortho* position exhibiting the highest  $E$ -value of more than 200. It appears that wild-type EHs are not very efficient catalysts for the preparation of (*R*)-PGE, the best results were obtained with the EHs from *Agrobacterium radiobacter* ( $E$ -value = 12) (Spelberg *et al.*, 1998), *Trichosporon loubierii* ( $E$ -value = 20) (Xu *et al.*, 2004), and a *Rhodobacterales* species ( $E$ -value = 38) (Woo *et al.*, 2010). However, as described at the beginning of this review, molecular engineering techniques can be used to improve enzymatic properties such as enantioselectivity or enantioconvergence. For example, starting from the wild-type EH from *A. niger* LCP 521, which catalyzes the kinetic resolution of PGE with quite low enantioselectivity ( $E$ -value = 4.6), Reetz and collaborators generated by directed evolution the highly enantioselective variant LW202, which exhibited an  $E$ -value of 115 (Reetz *et al.*, 2009). Interestingly, in all cases involving other monosubstituted epoxides such as substituted glycidyl ethers or alkyl and aromatic epoxides, a substantial increase in  $E$ -value of the

evolved EH compared to the wild-type EH was observed as well, leading to Reetz's conclusion: "The traditional credo in directed evolution, 'You get what you screen for', can be extended by the corollary 'You may get more than what you originally screened for'". Two years later, Reetz and collaborators managed to improve the expression efficiency and enantioselectivity of the LW202 EH variant by laboratory evolution again (Reetz and Zheng, 2011). The strategy was to focus first on expression and then improve the enantioselectivity. The expression of the generated mutant EH222 was 50 times higher than that of the wild-type *AnEH*, and a very high enantiomeric ratio (E-value = 160) in favor of the (*S*)-diol was detected (**Figure 18**).

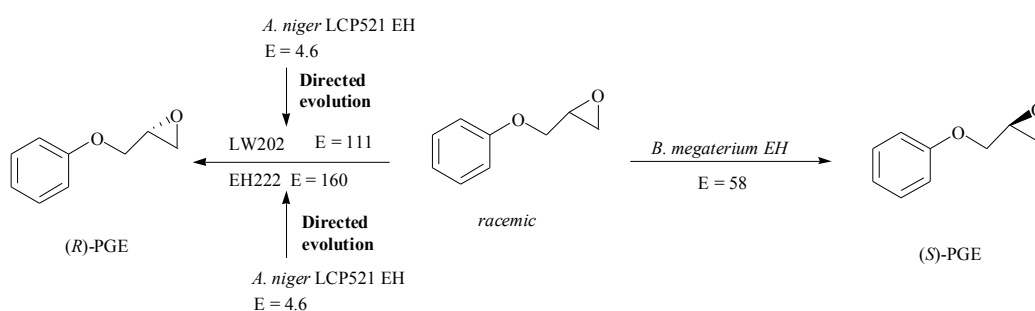


**Figure 18.** Biohydrolytic kinetic resolutions of racemic-PGE. Use of enantiocomplementary wild-type and evolved mutant EHs for the preparation of two antipodes of PGE.

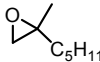
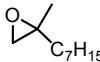
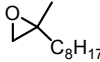
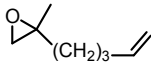
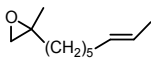
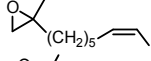
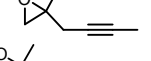
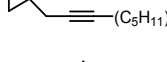
Kotik *et al.* screened 270 microbial isolates from biofilters and petroleum-contaminated bioremediation sites for enantioselective EHs using *tert*-butyl glycidyl ether, benzyl glycidyl ether and allyl glycidyl ether as substrates. The best results were obtained with the most substituted ether, *tert*-glycidyl ether, for which a moderate enantioselective EH activity (E-value = 30) was found in a fungal isolate identified as an *Aspergillus niger* species (Kotik *et al.*, 2005). Under optimized biotransformation conditions which included a low reaction temperature of 5 °C, a low substrate concentration of 5 mM and a high biocatalyst concentration, the enantiomeric ratio could be increased to 100, and enantiopure (*R*)-*tert*-butyl glycidyl ether and (*S*)-3-butoxy-1,2-propanediol were isolated as residual epoxide and formed diol.

### II.3.3.3 Di-substituted alkyl epoxides

#### II.3.3.3.1 *gem*-disubstituted oxiranes

*gem*-disubstituted oxiranes bearing linear alkyl, alkenyl, alkynyl or benzyl substituents were enantioselectively hydrolyzed by EHs of the following bacterial genera: *Rhodococcus*, *Mycobacterium*, *Nocardia*, *Methylobacterium*, and *Arthrobacter*. Only EHs reacting with the (*S*)-enantiomer have been found so far, forming the (*S*)-diol (**Table 2**). Using these results, Faber and co-workers developed chemo-enzymatic approaches for deracemization of several *gem*-disubstituted oxiranes (**Table 2**, entries 1, 5, 9, 10). Enantioselective biohydrolysis of the (*S*)-epoxide proceeded with retention of configuration, resulting in the formation of the corresponding (*S*)-1,2-diol. In a subsequent step, acid-catalyzed hydrolysis of the residual (*R*)-epoxide took place exclusively at the substituted oxirane atom with complete inversion of configuration, yielding the same (*S*)-1,2-diol. The combination of both reaction steps resulted in the generation of the (*S*)-1,2-diol in enantiopure form and in almost quantitative yield (**Figure 19**). Valuable illustrations of these enantioconvergent processes are the synthesis of natural compounds such as Frontalin (**Table 2**, entry 5), Fridamycin (**Table 2**, entry 9) and Mevanolactone (**Table 2**, entry 10).

**Table 2.** Selected kinetic resolutions of some *gem*-disubstituted alkyl epoxides.

Entry	Substrate	Source of EH	<i>E</i> -value	Subs. conc.	Abs. Conf. <sup>a</sup>	References
1		<i>Rhodococcus ruber</i> DSM 43338 <i>Nocardia</i> H8, TB1 and EH1	>200	20 g/L	<i>R/S</i>	Osprian <i>et al.</i> , 1997; Orru <i>et al.</i> , 1998a
2		<i>Rhodococcus</i> sp. NCIMB 11216	126	2.5 g/L	<i>R/S</i>	Wandel <i>et al.</i> , 1995
3		<i>Rhodococcus</i> sp. NCIMB 11216 <i>Arthrobacter</i> sp. DSM 312	>200 172	5 g/L	<i>R/S</i>	Osprian <i>et al.</i> , 2000
4		<i>Rhodococcus</i> sp. NCIMB 11216	>200	2.5 g/L	<i>R/S</i>	Wandel <i>et al.</i> , 1995
5		<i>Nocardia</i> EH1	>200	20 g/L	<i>R/S</i>	Orru <i>et al.</i> , 1998a Kroutil <i>et al.</i> , 1997b
6		<i>Rhodococcus</i> sp. NCIMB 11216	125	5 g/L	<i>R/S</i>	Osprian <i>et al.</i> , 2000
7		<i>Rhodococcus</i> sp. NCIMB 11216	142	5 g/L	<i>R/S</i>	Osprian <i>et al.</i> , 2000
8		<i>Rhodococcus</i> sp. NCIMB 11216	>200	5 g/L	<i>R/S</i>	Osprian <i>et al.</i> , 2000
9		<i>Methylobacterium</i> sp. FCC 031	>200	10 g/L	<i>R/S</i>	Ueberbacher <i>et al.</i> , 2005
10		<i>Nocardia</i> EH1	123	40 g/L	<i>R/S</i>	Orru <i>et al.</i> , 1998b

<sup>a</sup> Absolute configuration of the remaining epoxide and the formed diol, respectively.

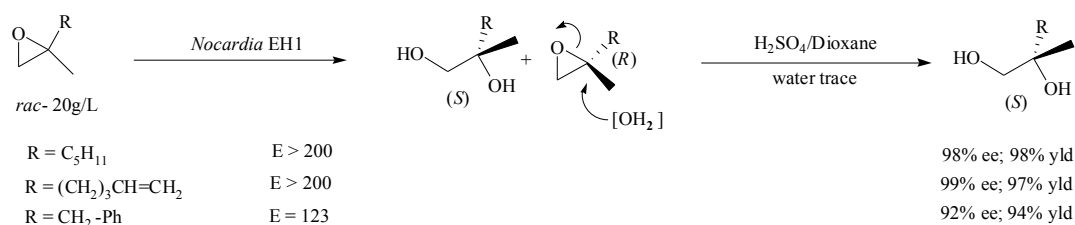


**Figure 19.** Chemoenzymatic deracemization of *rac*-gem-disubstituted oxiranes.

The kinetic resolution of a range of methyl-substituted 1-oxaspiro[2,5]octanes was investigated by Weijers *et al.* in 2005 using a yeast EH from *Rhodotorula glutinis* (Weijers *et al.*, 2005). It was observed that the positioning of substituents close to the spiroepoxide carbon atom resulted in a decreased reaction rate but increased enantioselectivity. The best enantioselectivity with an E-value >100 was obtained for O-axial or O-equatorial 4-methyl-1-oxaspiro[2,5]octane (**Figure 20**).

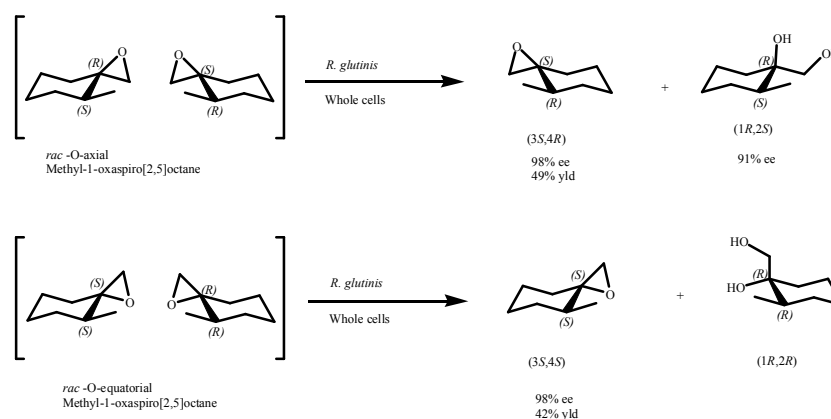


**Figure 20.** Kinetic resolution of O-axial or O-equatorial 4-methyl-1-oxaspiro[2,5]octane by *Rhodotorula glutinis* EH.

The first deracemisation of a *trans*-divinyl spiroepoxide, a strategic key building block of 11-heterosteroids, was described in 2007 using two enantiocomplementary microbial EHs as biocatalysts (Bottalla *et al.*, 2007). One enzyme was the partially purified recombinant EH from *A. niger* LCP 521 (*AnEH*), the other enzyme, the so-called ‘Limonene EH’ (LEH), was isolated from the bacterium *Rhodococcus erythropolis*. The residual (*R,R*)-spiroepoxide (from the *AnEH*-mediated reaction) and the residual (*S,S*)-spiroepoxide (using LEH) were isolated

in nearly enantiopure forms (99% ee). However, because of the moderate E-values of around 20 in both kinetic resolutions, the respective reaction yields did not exceed 26%. A process-improving strategy enabled transformation of the formed enantiomerically enriched diols of opposite absolute configuration, *i.e.* (*S,S*)-spirodiol and (*R,R*)-spirodiol, back to the corresponding epoxides, which were then submitted to a second enzymatic resolution cycle using the enantiocomplementary enzyme (*i.e.* the LEH for (*S,S*)-spiroepoxide or the *AnEH* for (*R,R*)-spiroepoxide). In conclusion, both enantiomers of the substrate could be obtained in high enantiomeric purity (99%) and a reasonable yield of 50% (**Figure 21**).

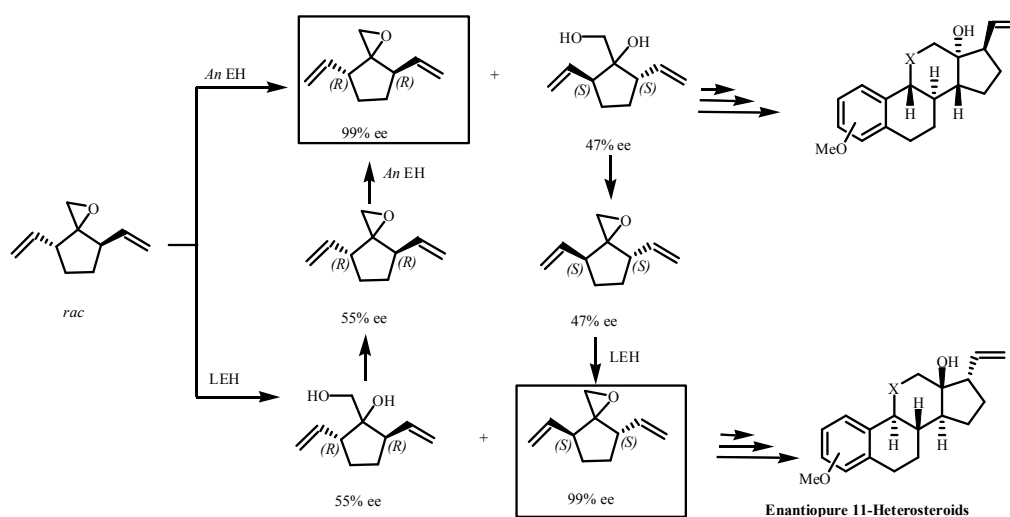


**Figure 21.** Preparative hydrolytic resolution of *trans*-divinyl spiroepoxide using *AnEH* and LEH as biocatalysts, enabling the synthesis of enantiopure 11-heterosteroids.

### II.3.3.3.2 *cis*- and *trans*-disubstituted epoxides

2,3-disubstituted aliphatic oxiranes have been reported to be hydrolyzed by EHs from fungi (Moussou *et al.*, 1998a), yeast and bacteria. The most interesting results were observed with yeast and bacterial EHs. As far as kinetic resolution is concerned, it was shown by Weijers (Weijers, 1997) that *Rhodotorula glutinis* catalyzed the enantioselective hydrolysis of *cis*-2,3- and *trans*-2,3-epoxypentane, resulting in residual (*2R*)-epoxides with yields that approached the theoretical maximum of 50%. More interestingly, biocatalytic transformations of racemic 2,3-disubstituted oxiranes to vicinal diols with high ees at complete conversion were obtained using bacterial EHs. Satisfactory results were described for the first time by Faber's group after a screening of 18 strains. Lyophilized biomass of *Nocardia* EH1 proved to

be the best biocatalyst, leading to almost deracemization of racemic *cis*-2,3-epoxy-heptane at a concentration of 16 g/L, thus producing the corresponding (*R,R*)-diol in 79% overall yield and 91% ee in gram-scale amounts (**Figure 22**) (Kroutil *et al.*, 1997a).

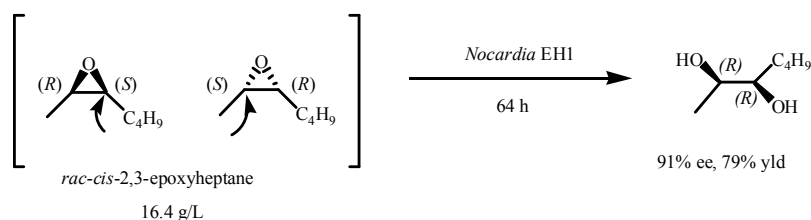


**Figure 22.** Deracemization of *rac-cis*-2,3-epoxyheptane via enantioconvergent biohydrolysis using *Nocardia* EH1 leading to the formation of an (*R,R*)-diol.

It was shown by  $^{18}\text{O}$ -labelling that the hydrolysis of both enantiomers occurred with opposite regioselectivity via attack at the (*S*)-configured oxirane carbon atom with concomitant inversion of the configuration for both enantiomers. It is worth mentioning that, although the *trans*-isomers were easily hydrolyzed by all the tested strains, no enantioconvergent hydrolysis occurred. Based on these results, the same group developed several preparative syntheses of natural products such as antitumor agents (two stereoisomers of Panaxytriol (Mayer *et al.*, 2002b)), (+)-Pestalotin (Mayer *et al.*, 2002a), and a constituent of Jamaican rum (Mayer *et al.*, 2002a).

Recently, Reetz and co-workers reported on a laboratory evolution experiment with the *A. niger* LCP 521 EH. Several EH variants were isolated that accepted *trans*-2-benzyl-3-methyloxirane as a substrate, in contrast to the wild-type EH, which was found to be inactive. Two variants exhibited high enantioselectivity (E-value >200) towards this epoxide (Reetz *et al.*, 2008). Later, using the same substrate, enantioconvergence was detected with one of these selected mutants, *i.e.* enantiopure (*2R,3S*)-diol at a high conversion ratio of 92% was formed. Directed evolution with this mutant identified second-generation mutants showing higher reaction rates while maintaining the enantioconvergence (Reetz *et al.*, 2010).

### II.3.3.4 Tri-substituted epoxides

One of the first examples of biohydrolytic kinetic resolution of tri-substituted epoxides was the synthesis of both enantiomers of Bower's compound, which is a potent analogue of the insect juvenile hormone (Archelas *et al.*, 1993). The enantioselective biohydrolysis of the

racemic Bower's compound using whole cells of *Aspergillus niger* LCP 521 as a biocatalyst resulted in the formation of the corresponding (6*S*)-diol in 48% yield and 70% ee (**Figure 23**). The remaining (6*S*)-epoxide (96% ee) was isolated in 36% yield, and starting from this pure enantiomer its antipode was easily prepared by chemical means in two steps. Interestingly, it was shown that the (6*R*)-enantiomer was 10 times more active against the yellow meal worm *Tenebrio molitor* than its antipode.

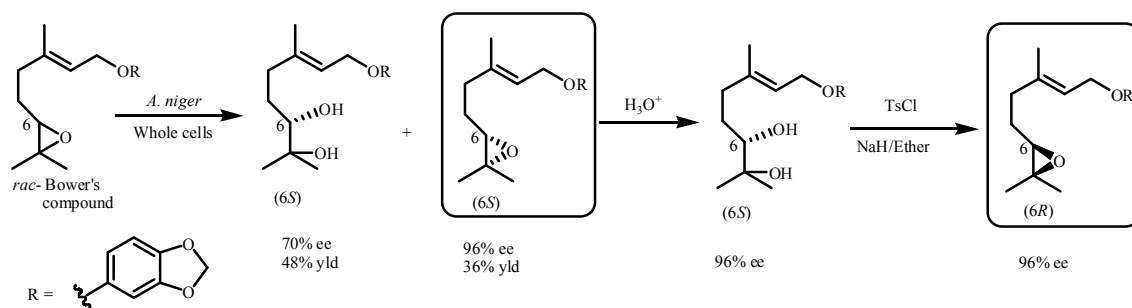


**Figure 23.** Synthesis of both enantiomers of Bower's compound using whole cells of *A. niger* LCP 521 as biocatalyst.

In 1996 Archer *et al.* reported a highly enantioselective chemoenzymic resolution of *rac*-1-methyl-1,2-epoxycyclohexane using whole cells of *Corynebacterium* C12, giving rise to the (1*R*,2*S*)-epoxide in > 99% ee (30% yield) and the (1*S*,2*S*)-diol in 92% ee (42% yield) (Archer *et al.*, 1996). Further, an additional efficient chemoenzymatic deracemization process was run in tandem using the EH from *Corynebacterium* C12 and perchloric acid for the acid-catalyzed ring opening of the residual epoxide (**Figure 24**).

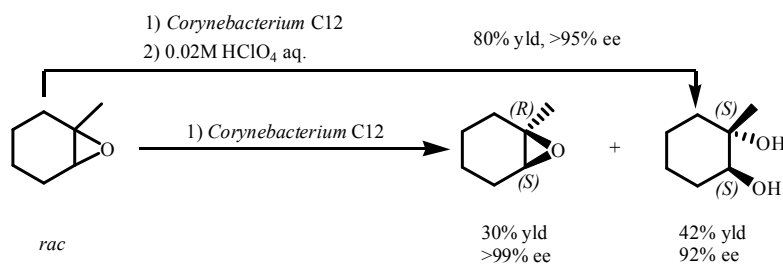


**Figure 24.** Chemoenzymic resolution and deracemization of *rac*-1-methyl-1,2-epoxycyclohexane using whole cells of *Corynebacterium* C12.

Although enantioconvergent biohydrolysis of trisubstituted epoxides seemed rather unlikely due to their steric bulkiness, Faber's group succeeded in finding several bacterial strains that could perform such a reaction. The biohydrolysis of three racemic trialkyl epoxides at 5–6 g/L using lyophilized cells of *Rhodococcus* and *Mycobacterium* sp. resulted in the formation of the corresponding (*R*)-diols with enantiopurities exceeding 80% ee (**Figure 25**) (Steinreiber *et al.*, 2001d).

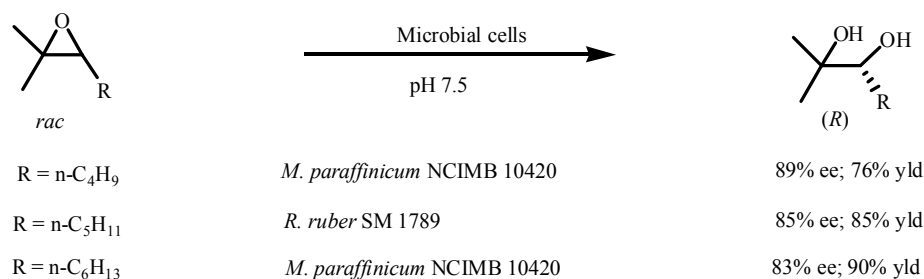


**Figure 25.** Deracemization of three *rac*-trialkyl oxiranes via enantioconvergent biohydrolysis using whole cells of *Mycobacterium paraffinicum* and *Rhodococcus ruber*.

Using lyophilized cells of *Rhodococcus ruber* DSM 44540, Faber and co-workers described the synthesis of two enantiomerically pure diastereoisomers of the bark beetle pheromone Pityol (Steinreiber *et al.*, 2001a). Their approach was based on a diastereoconvergent biohydrolysis of a mixture of (*3RS,6S*)- or (*3RS,6R*)-6-bromo-2-methyl-2-heptene oxide diastereomers, which were obtained respectively from (*R*)- and (*S*)-Sulcatol after bromination and epoxidation of the double bond. As exemplified below, the (*3RS,6R*)-6-bromo-2-methyl-2-heptene oxide mixture of diastereomers afforded upon EH catalysis the corresponding (*3R,6S*)-bromo-diol, which was formed as the sole intermediate. Due to the presence of a bromine atom in the molecule, this intermediate underwent spontaneous ring-closure affording (*2R,5R*)-Pityol in 54% yield and 98% ee after separation of the formed minor (*2S,5R*) diastereomer (12% yield) (**Figure 26**).

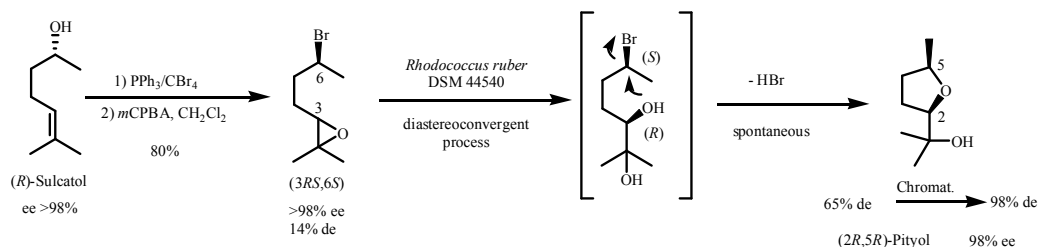


**Figure 26.** Synthesis of the pheromone (2R,5R)-Pityol via a diastereoconvergent biohydrolysis using *Rhodococcus ruber* DSM 44540 EH as biocatalyst.

The same group used the EH from *Rhodococcus ruber* for the preparative biohydrolysis of two trisubstituted epoxides bearing an olefinic side chain with one or two double bonds. The formed corresponding diols enabled them to prepare natural compounds such as (R)-Myrcenediol and a beer-aroma constituent (Steinreiber *et al.*, 2001c).

### II.3.4 meso-Epoxides

Interestingly, desymmetrization of *meso*-epoxides can produce optically enriched vicinal (*R,R*)- or (*S,S*)-diols in 100% theoretical yield through a stereoselective attack at only one carbon atom of the oxirane. It is worth mentioning that the enantiopurity of the formed diol does not change with reaction time or conversion ratio. Desymmetrizations of *meso*-epoxides by microbial biotransformations are scarce. For example, EHs from the yeast *R. glutinis* ATCC 201718 (Weijers, 1997) and from the bacterium *Sphingomonas* sp. HXN-200 (Chang *et al.*, 2003b) have been used to stereoselectively hydrolyse cyclohexene oxide to the corresponding (*R,R*)-diols with enantiomeric excesses of 90% and 87%, respectively. It should be also mentioned that Botes and co-workers described in a patent various yeast strains that were able to produce optically active vicinal diols from *meso*-epoxides (Botes *et al.*, 2007b). Recombinant *Yarrowia lipolytica* cells expressing exogenous yeast EHs enabled them to obtain (*R,R*)-vicinal diols in high enantiomeric excess starting from *meso*-epoxides such as *cis*-epoxybutane and cyclopentene oxide.

An interesting desymmetrization of a *meso*-bis-epoxide was recently described by Faber and co-workers (Ueberbacher *et al.*, 2009). EHs from various sources (bacteria, fungi and plants) were found to catalyze the transformation of 6,7:9,10-bis(epoxy)pentadecane by hydrolysis/cyclisation cascades leading to different tetrahydrofuran derivatives with excellent de and ee values (**Figure 27**).

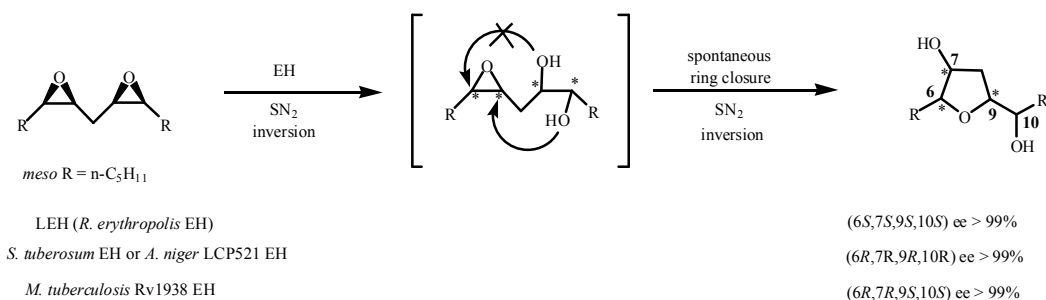


**Figure 27.** Stereochemical courses of EH-catalyzed hydrolysis/cyclisation cascades of 6,7:9,10-bis(epoxy)pentadecane to yield tetrahydrofuran derivatives.

The reaction pathway was initiated by EH-catalyzed hydrolysis of an oxirane moiety followed by spontaneous ring-closure of the epoxy-diol intermediate. Based on these results, the authors suggested that the formation of tetrahydrofuran moieties found in numerous natural products such as acetogenins proceeds through a nucleophilic cascade mechanism starting from bis-epoxide without involvement of a ‘cyclase’.

Besides classical screening the following strategies were used for the discovery or generation of EHs capable of desymmetrization of *meso*-epoxides. The first was based on high-throughput screening of DNA libraries which were generated from environmental samples. Using this approach, 50 novel microbial EHs have been discovered and among these 11 were able to desymmetrize not only cyclic *meso*-epoxides (cyclopentyl and cyclohexyl epoxides) but also bulky internal epoxides such as *cis*-stilbene oxide with various substituents including dipyrindyl analogues (**Figure 28**) (Zhao *et al.* 2004).

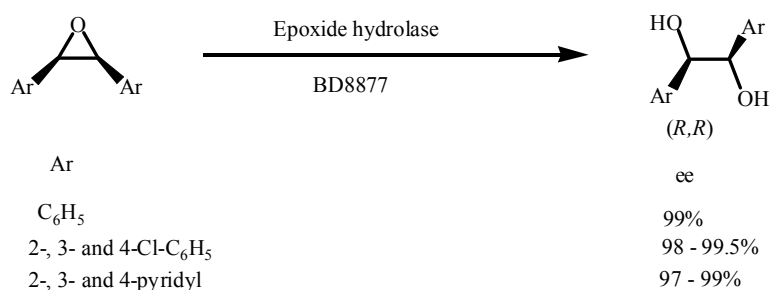


**Figure 28.** Desymmetrization of aryl *meso*-epoxides with BD887 obtained from DNA libraries of environmental samples.

The second strategy comprised a screening of genomic databases for the presence of EH-encoding genes (van Loo *et al.*, 2006). Five recombinant EHs were found to be active toward *meso*-epoxides such as cyclohexene oxide and *cis*-2,3-epoxybutane. Finally, Reetz and co-workers applied an iterative saturation mutagenesis strategy to the limonene EH (LEH) from *Rhodococcus erythropolis* DCL 14 and obtained three LEH variants (H150, H173, H178) that catalyzed the desymmetrization of cyclic *meso*-epoxides and *cis*-1,2-homo-disubstituted *meso*-epoxides with stereoselective formation of either the (*R,R*)- or the (*S,S*)-diol on an optional basis (Zheng *et al.*, 2010).

Very recently, Li and co-workers described the gram-scale preparative desymmetrization of cyclohexene oxide, cyclopentene oxide and N-benzyloxycarbonyl-3,4-epoxypyrrolidine using the EH from *Sphingomonas* sp. HXN-200 expressed in the recombinant host *E. coli* (SpEH) (Wu *et al.*, 2013). Desymmetrization of 10 g of cyclohexene oxide (500 mM substrate concentration) with resting cells of *E. coli* (SpEH) (10g cdw/L ) afforded 10.3 g (89% isolated yield) of (1*R*,2*R*)-1,2-cyclohexanediol in 86% ee. Desymmetrization of the two other *meso*-epoxides (200 mM substrate concentration) afforded (1*R*,2*R*)-1,2-cyclopentanediol in 87% ee and 70.4% isolated yield and (3*R*,4*R*)-N-benzyloxycarbonyl-3,4-dihydroxypyrrolidine in 93% ee and 94.1% isolated yield, respectively.

## II.4 Preparation of valuable chiral building blocks for the synthesis of biologically active compounds starting from bi-functional epoxides

### II.4.1 Halogenated epoxides

#### II.4.1.1 Alkyl Chloro-epoxide

##### II.4.1.1.1 Epichlorohydrine

Bi-functional small molecules are particularly useful synthons which give access to various valuable biologically active products. A typical example is epichlorohydrin, which has been used (Kasai *et al.*, 1998) for the synthesis of – among others – the nutritional supplement L-Carnitine, the  $\beta$ -adrenergic blocking agent (*S*)-atenolol, (+)-Trehazolin, which is a potent inhibitor of glycosidases, and the beetle pheromone (*S*)-Ipsenol. Both (*S*)- and (*R*)-epichlorohydrin have been obtained in optically or nearly optically pure form through the kinetic resolution of the racemate at high to very high substrate concentrations using the

purified EH from *Agrobacterium radiobacter* overexpressed in *E. coli* (Jin *et al.*, 2013b) (**Figure 29**) or the purified EH from *Agromyces mediolanus* (Xue *et al.*, 2014) (**Figure 30**). In the former case, the highest concentrations of racemic epichlorohydrin called for a biphasic system with 40% cyclohexane.

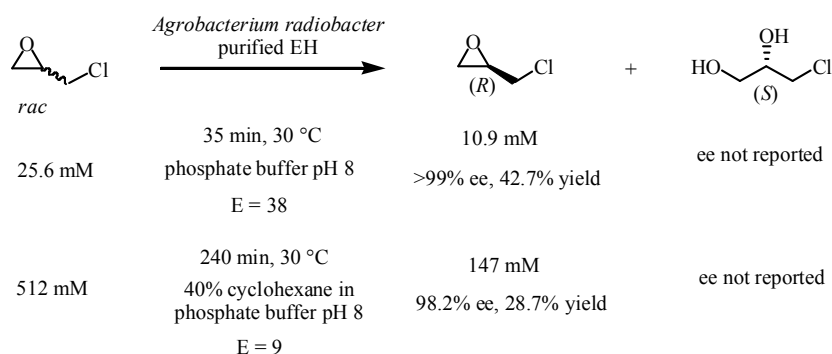


**Figure 29.** Kinetic resolution of racemic epichlorohydrin using purified EH from *Agrobacterium radiobacter* leading to the formation of enantiomerically pure (*R*)-epichlorohydrin.

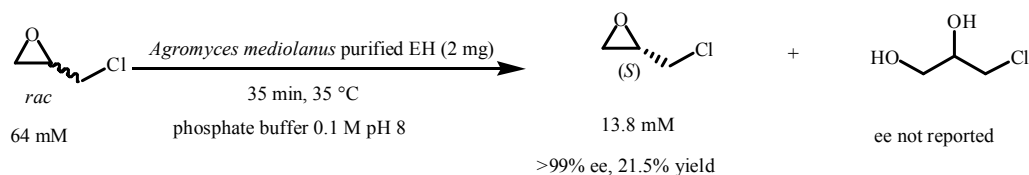


**Figure 30.** Kinetic resolution of racemic epichlorohydrin using the purified EH from *Agromyces mediolanus* leading to the formation of enantiomerically pure (*S*)-epichlorohydrin.

#### II.4.1.1.2 Aromatic chloro-epoxide

Furstoss and collaborators have shown that the partially purified recombinant EH from *A. niger* LCP 521 efficiently catalyzes the kinetic resolution of 1-chloro-2-(2,4-difluorophenyl)-2,3-epoxypropane at a very high substrate concentration of 500 g/L using a biphasic process (Montfort *et al.*, 2004a). The unreacted (*S*)-chloro-epoxide and the formed (*R*)-chloro-diol were obtained in nearly enantiopure form and nearly quantitative yield. Due to the fact that the formed (*R*)-chloro-diol was easily chemically transformed into the (*S*)-chloro-epoxide, an enantioconvergent process could be set up. Using the difference in chemical

reactivity between the oxirane ring and the chlorine substituent, it was possible to use this enantiopure chloro-epoxide as a building block for the synthesis of D0870, a triazole drug derivative known to display efficient activity against human fungal infections (**Figure 31**). Such an enantioselective hydrolysis was also performed with the corresponding epoxy-triazole compound at 50 g/L (Montfort *et al.*, 2004b).

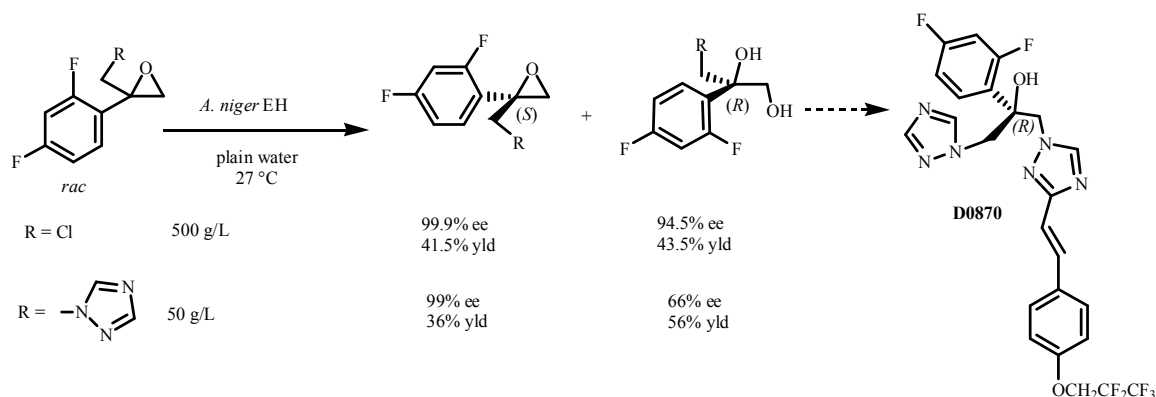


**Figure 31.** Preparative hydrolytic resolution of *rac*-1-chloro- and 1-triazole-2(2,4-difluorophenyl)-2,3-epoxypropane using *AnEH* as biocatalyst. The latter compound is a useful building block for the synthesis of enantiopure D0870.

#### II.4.1.2 Bromo-epoxide

*Yarrowia lipolytica* has been established as a heterologous host for EH overexpression in the company Oxyrane Ltd. (Pienaar *et al.*, 2008). The origin of some EHs which were used in various biotransformation reactions was released in different patents (Botes *et al.*, 2005; Botes *et al.*, 2007a; Botes *et al.*, 2008). The following biotransformation reaction was performed with the *Y. lipolytica* Oxy-9 strain, which overexpressed an EH whose origin was not released. Thus, racemic 4-bromo-1,2-epoxybutane (60 g) was kinetically resolved with five grams of wet cells in 40 mL of 0.1 M phosphate buffer at pH 7.5 (Pienaar *et al.*, 2008). The reaction was stopped after 90 minutes, and after extraction and purification (*S*)-4-bromo-1,2-epoxybutane was obtained in 26% yield and 98.6% ee (**Figure 32**). The residual epoxide was then easily transformed into a hydroxy pyrrolidine derivative, which was used as a chiral synthon for the synthesis of the calcium antagonist Barnidipine (Li *et al.*, 2001).

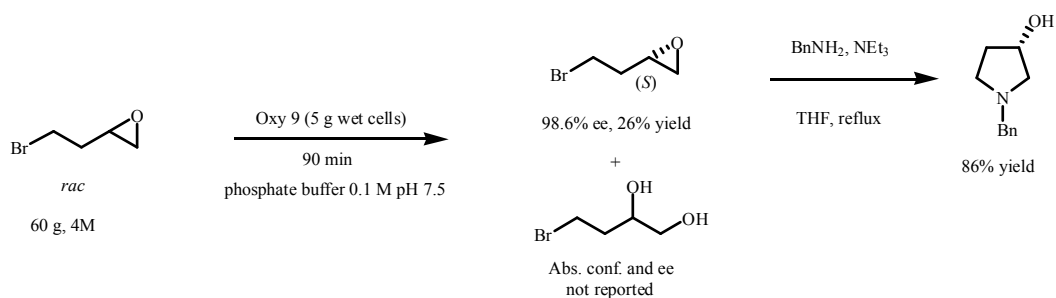


**Figure 32.** Kinetic resolution of racemic 4-bromo-1,2-epoxybutane using purified Oxy-9 EH and its use in the synthesis of (*S*)-*N*-benzyl-3-hydroxypyrrolidine.

## II.4.2 Epoxyamide

Using another EH overexpressed in *Y. lipolytica* (Oxy-10), the kinetic resolution of an epoxyamide was performed at 50% conversion, resulting in the optically pure residual (*R,R*)-epoxide and the formed *threo*-diol with yields of 32 and 22%, respectively (Pienaar *et al.*, 2008) (**Figure 33**). The remaining (*R,R*)-epoxide is of synthetic interest, because it is used for the synthesis of the  $\alpha$ -mannosidase inhibitor (–)-Swainsonine.

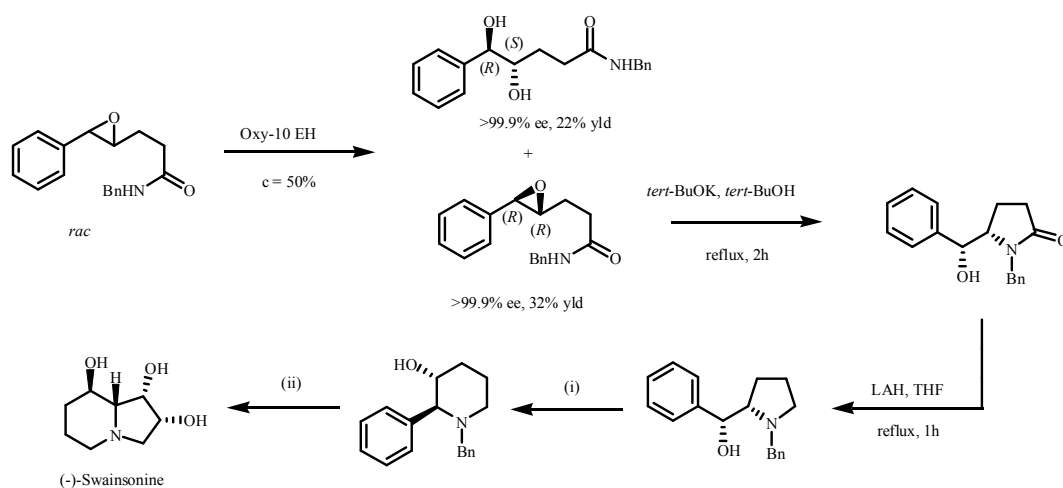


**Figure 33.** Kinetic resolution of racemic epoxyamide using purified Oxy-10 EH and its application to the synthesis of (*S*)-*N*-benzyl-3-hydroxypyrrolidine en route to (–)-Swainsonine. (i) See Calvez *et al.*, 1998; (ii) See Haddad *et al.*, 2001 and Ferreira *et al.*, 1997.

### II.4.3 Protected epoxy-alcohols

With yet another overexpressed EH in *Y. lipolytica* (Oxy-3) (*S*)-4-acetoxy-buten-1,2-oxide was obtained in 20% yield and 97.8% ee starting from the racemate. The (*S*)-epoxide is easily converted to (*S*)-3-hydroxytetrahydrofuran (**Figure 34**), a compound used for the synthesis of the HIV protease inhibitors Amprenavir and Fosamprenavir (Honda *et al.*, 2004).

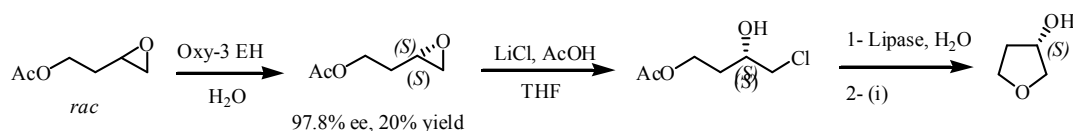


**Figure 34.** Chemo-enzymatic access to (*S*)-3-hydroxytetrahydrofuran. (i) See Yuasa *et al.*, 1997; 79%

Another protected epoxy-alcohol, *rac*-2-methylglycidyl benzyl ether, has been the subject of numerous investigations. Two types of EHs proved to be useful: those from various *Rhodococcus* strains (Steinreiber *et al.*, 2001b; Fuchs *et al.*, 2009; Hellstrom *et al.*, 2001; Simeó and Faber, 2006) and the one from *Bacillus subtilis* (Fujino *et al.*, 2007; Shimizu *et al.*, 2010). Both types of EHs exhibited the same enantioselectivity, generating the (*R*)-diol and leaving behind the unreacted (*R*)-epoxide (see note below), and were used for the enantioconvergent access to the highly enantio-enriched (*R*)-diol (**Figure 35**).

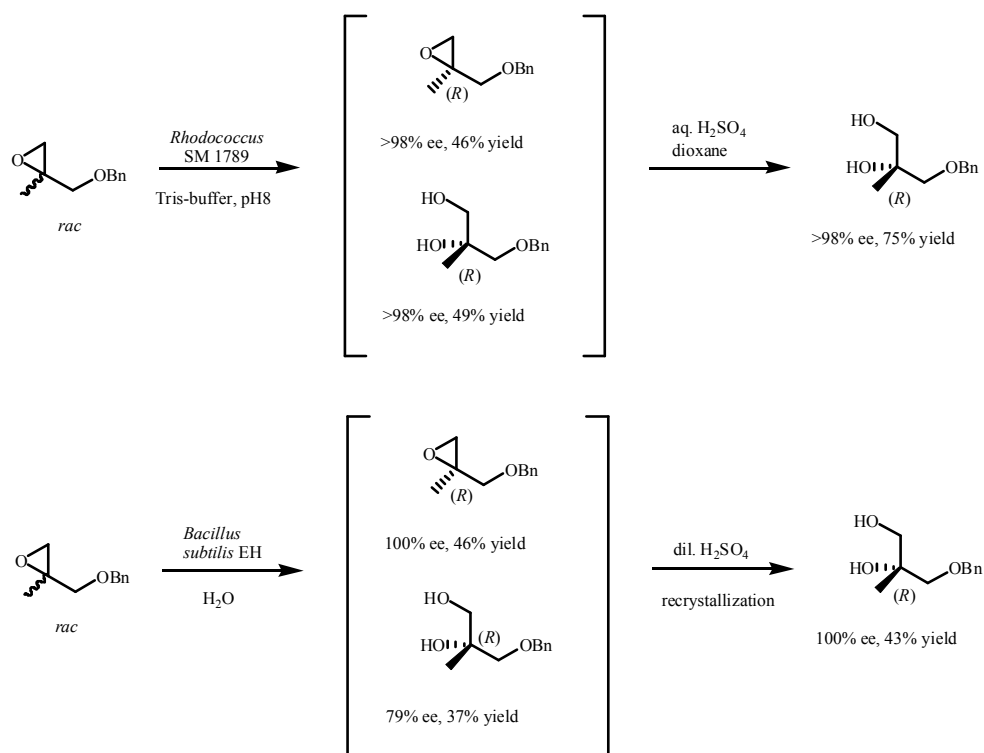


**Figure 35.** Enantioconvergent chemo-enzymatic access to (*R*)-3-benzyloxy-2-methylpropane-1,2-diol.

Enantiopure (*R*)-3-benzyloxy-2-methylpropane-1,2-diol was the starting material for the synthesis of (*R*)-Bicalutamide, a synthetic antiandrogen (Fujino *et al.*, 2007). The same (*R*)-diol was used as the starting material for the bio-assisted synthesis of the intermediate (*R*)-3-hydroxy-3-methyl-5-hexanoic acid *p*-methoxybenzyl ester, which was then used in the synthesis of Taurospongins A (Fujino and Sugai, 2008), a natural product inhibiting DNA polymerase  $\beta$  and HIV reverse transcriptase.

#### II.4.4 Epoxy-ester

As a result of a screening for microorganisms with high EH activities using enrichment cultures with alkenes as the sole carbon source, Choi *et al.* isolated a bacterial strain which was identified as *Acinetobacter baumannii* and showed high selectivity in the kinetic resolution of ethyl-3,4-epoxybutyrate (Choi *et al.*, 2008). Using wet cells of *Acinetobacter baumannii* ethyl-3,4-epoxybutyrate was kinetically resolved at a concentration of 60 mM, affording after 2 hours of reaction (*R*)-ethyl-3,4-epoxybutyrate (ee >99%) in 46%

yield and (*S*)-ethyl-3,4-dihydroxybutyrate (ee = 80%) in 49% yield (**Figure 36**). The unreacted (*R*)-epoxide is a valuable intermediate that can be used in the synthesis of (*R*)-GABOB, (*R*)-Carnitine, the anti-cancer agent Lobatamide C and the statin Lipitor<sup>®</sup>.

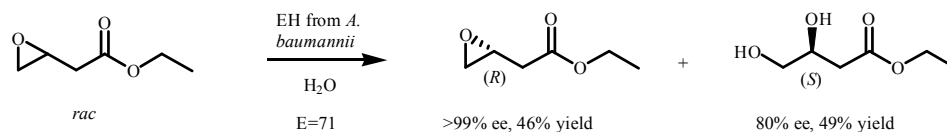


**Figure 36.** Kinetic resolution of *rac*-ethyl-3,4-epoxybutyrate by *Acinetobacter baumannii*.

Other bi-functional epoxy-esters such as some *trans*-(+/-)-3-phenyl glycidates have been studied as substrates for EH-mediated reactions (Devi *et al.*, 2008) to obtain the useful chiral synthons (*2S,3R*)-3-phenyl glycidate or (*2S,3R*)-*O*-methoxy-3-phenyl glycidate, which can be used to access the Taxol side chain or Diltiazem, respectively (**Figure 37**).

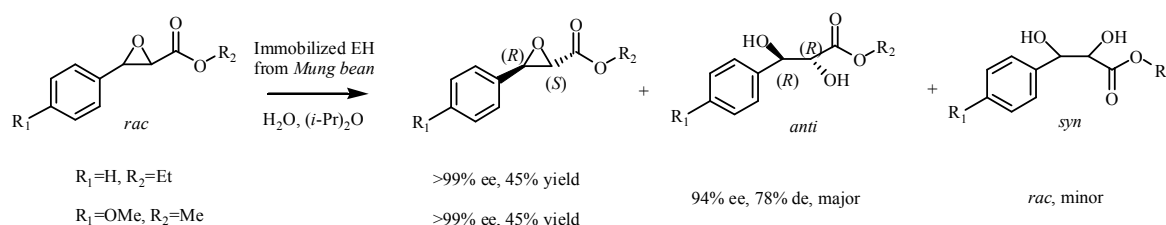


**Figure 37.** Kinetic resolution of two *trans*-(+/-)-3-phenyl glycidates by immobilized Mung bean EH.

The EH from Mung bean was immobilized in a gelatin gel for this kinetic resolution, and di-isopropyl ether was used as an immiscible organic co-solvent to minimize spontaneous hydrolysis of the substrates. In both cases the (*2S,3R*)-glycidate ester was obtained in 45% yield (90% of the theoretical value) and very high enantiomeric purity (>99%).

#### II.4.5 Epoxy-aldehyde

Glycidyl acetal derivatives, *i.e.* C3 chiral building blocks bearing one stereogenic centre and two different and chemically differentiable functions (such as protected aldehyde and epoxide) located on a short carbon skeleton, are of particular interest due their high chemical versatility. Five enantiopure glycidyl acetal derivatives were prepared by using the

partially purified recombinant EH from *Aspergillus niger* LCP 521 as a biocatalyst (Doumèche *et al.*, 2006). All the epoxides of (*R*) absolute configuration were prepared in high enantiomeric excess (ee >99%), whereas the formed diols were of (*S*) absolute configuration and showed moderate to excellent ees (45–97%) (**Figure 38**).

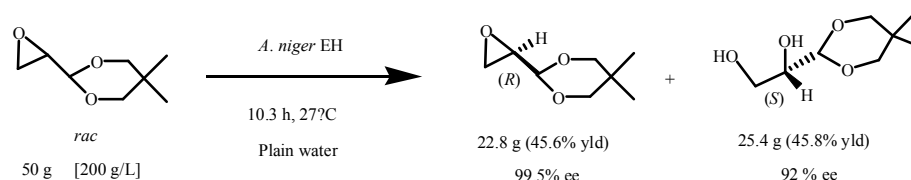


**Figure 38.** Gram scale and high substrate concentration preparation of enantiopure glycidaldehyde 2,2-dimethyltrimethylene acetal using partially purified recombinant EH from *Aspergillus niger* LCP 521 as biocatalyst.

The E-values were shown to be modest to excellent, depending on the structure of the acetal moiety. The best results were obtained when the protecting group was a cyclic acetal (E-value of 126) and a diisopropyl acetal (E-value > 200). As a proof-of-principle a 50-g scale resolution of glycidaldehyde 2,2-dimethyltrimethylene acetal was performed at 200 g/L, leading to 22.8 g of residual (*R*)-epoxide (ee >98%) and 25.4 g of the formed (*S*)-diol (ee = 92%). It is worthwhile to note that this enzymatic transformation was performed as a biphasic process using solely demineralised water as a solvent.

With the aim to explore the metabolism of fructose, Boltes and co-workers synthesized 4-deoxy-D-fructose 6-phosphate in four steps, which included two enzymatic reactions (Guérard *et al.*, 1999) starting from racemic 1,1-diethoxy-3,4-epoxybutane (**Figure 39**).

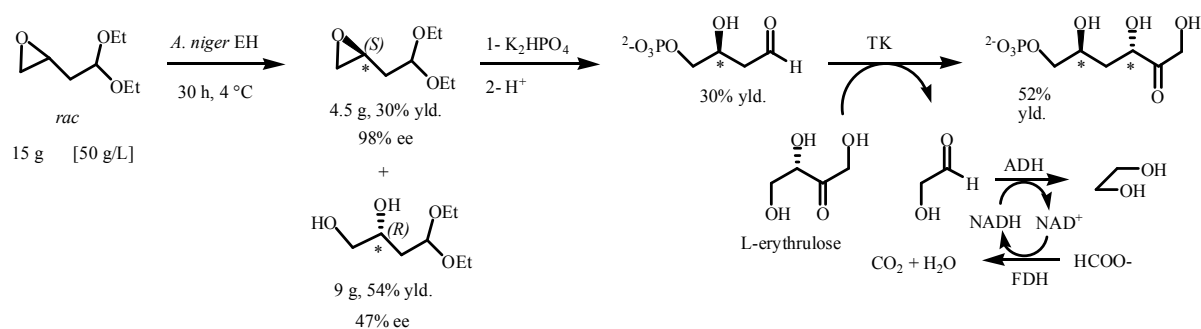


**Figure 39.** Synthesis of enantiopure 4-deoxy-D-fructose 6-phosphate using two enzymatic steps.

In the first step, optically pure (3*S*)-1,1-diethoxy-3,4-epoxybutane was obtained using an EH-catalysed kinetic resolution. After a screening of several fungal strains, the best results were obtained with the *Aspergillus niger* LCP 521 EH. Although the enantioselectivity was only moderate (E-value of 15), a large-scale resolution with 15 g of substrate at 50 g/L enabled generation of 4.5 g of the (*S*)-residual epoxide in high enantiomeric excess (98% ee). Opening of the epoxide with inorganic phosphate followed by deprotection of the acetal moiety in acidic conditions which led to the formation of enantiopure (*S*)-2-hydroxy 4-oxobutyl 1-phosphate. In the last step, the transketolase-catalysed reaction of this enantiomer with L-erythrulose enabled the stereochemical control of the second asymmetric center of the formed enantiopure 4-deoxy-D-fructose 6-phosphate. Recycling of the NADH cofactor, required for shifting the equilibrium of the transketolase-mediated reaction towards the formation of 4-deoxy-D-fructose-6-phosphate by removing the formed glycoaldehyde, was achieved with formate dehydrogenase

## II.5 Conclusions

For more than twenty years EHs have proved to be outstanding biocatalysts in a large number of applications in fine chemistry. This success is largely due to the fact that EHs are robust enzymes which do not need any cofactors for catalysis. Furthermore, although these enzymes catalyse a hydrolytic reaction, they are tolerant to both water-miscible and water-immiscible organic solvents. From a practical point of view, this allows to increase the used substrate concentration and consequently, in a lot of cases, it enables the alleviation of one of the main drawbacks in using EHs, *i.e.* substrate and product inhibition. Indeed, the presence of a water-immiscible solvent limits the substrate and product concentration in the aqueous phase, which consequently limits enzyme inhibition to a large extent. Another interesting property of EHs is their relatively large substrate spectrum as exemplified in this review. Even trisubstituted epoxides could act as substrates for some EHs. Numerous types of biocatalytic reactions have been performed with EHs; this should arouse the interest of many organic chemists in these catalysts in the near future. Beside the classical kinetic resolution of a racemate with its intrinsic limitation of a 50% maximum theoretical yield in both residual epoxide and formed diol, EHs can also be used in stereoselective desymmetrization of *meso*-epoxides or in the enantioconvergent hydrolysis of racemic epoxides, both processes offering the possibility to generate enantiopure diol products in theoretically 100% yield. The latter case is a characteristic of EHs and is the result of the intrinsic capacity of some of these

enzymes to react with either of the two oxirane carbon atoms in an enantiomer-dependent fashion, resulting in the same diol enantiomer at complete conversion of the racemic substrate. Such a situation is also encountered in classical kinetic resolutions when the remaining epoxide is chemically transformed (under acidic conditions for example) into the same enantiomer of the enzymatically formed diol product, or when two enantiocomplementary enzymes are used together.

The development of molecular biology tools has had a great impact on many aspects of biocatalysis. Numerous chemistry labs are now familiar with gene cloning and protein overexpression techniques, which offer the possibility to obtain as-yet uncharacterized enzymes. Especially, screening complex samples of high biodiversity for a specific activity can uncover enzymes with novel properties in terms of activity, substrate range and stereo-, regio- and chemoselectivity. As a consequence, recombinant hosts such as *Escherichia coli* or yeast overexpressing EHs are now routinely used in biotransformation reactions as a powerful alternative to naturally occurring EH-containing microorganisms. The high attainable level of overexpression enables extremely high substrate concentrations to be used, in conjunction with significantly shorter reaction times. Consequently, the time-consuming preparation of purified or partially purified enzymes is no longer a prerequisite for high enzymatic activities. Site-directed mutagenesis and laboratory evolution (error-prone PCR, DNA shuffling and iterative saturation mutagenesis) further offer the possibility to modify existing enzymes in order to improve one or more enzyme characteristics. Such tailor-made catalysts can now be developed to fulfil specific needs of the chemical industry. Another emerging area (although not described here) is the use of multienzyme-based transformations to perform several consecutive reactions in one pot (Chang *et al.*, 2003a; Xu *et al.*, 2009; Wu *et al.*, 2014; Jin *et al.*, 2013a). Combining epoxide-generating enzymes with EHs in a single process or host can considerably reduce the complexity of biotransformation processes. In conclusion, EHs are extremely useful enzymes in organic synthesis due to their ease of use, robustness, ubiquity, and applicability and will probably continue to be a field of intense research in the near future, both from an applied and fundamental point of view.

## References:

- Arand, M., Hallberg, B.M., Zou, J., Bergfors, T., Oesch, F., van der Werf, M.J., de Bont, J.A.M., Jones, T.A. and Mowbray, S.L. (2003) Structure of *Rhodococcus erythropolis* limonene-1,2-epoxide hydrolase reveals a novel active site. *EMBO J.*, **22**, 2583–2592.
- Archelas, A., Delbecq, J.P. and Furstoss, R. (1993) Microbiological transformations.30. Enantioselective hydrolysis of racemic epoxides : the synthesis of enantiopure insect juvenile hormone analogs (Bower's compound). *Tetrahedron: Asymmetry*, **4**, 2445-2446.
- Archer, I.V.J., Leak, D.J. and Widdowson D.A. (1996) Chemoenzymatic resolution and deracemisation of ( $\pm$ )-1-methyl-1,2-epoxycyclohexane: the synthesis of (1-*S*,2-*S*)-1-methylcyclohexane-1,2-diol. *Tetrahedron Lett.*, **37**, 8819–8822.
- Botes, A.L., Steenkamp, J.A., Weijers, C.A.G.M. and van Dyk, M.S. (1998) Biocatalytic resolution of 1,2-epoxyoctane using resting cells of different yeast strains with novel epoxide hydrolase activities. *Biotechnol. Lett.*, **20**, 421–426.
- Botes, A.L., Weijers, C.A.G.M., Botes, P.J. and van Dyk, M.S. (1999) Enantioselectivities of yeast epoxide hydrolases for 1,2-epoxides. *Tetrahedron-Asymmetry*, **10**, 3327–3336.
- Botes, A.L., Lotter, J., Labuschagne, M. and Mitra, R.K. (2005) Methods for the preparation of optically active epoxides and vicinal diols from styrene epoxides using enantioselective epoxide hydrolases derived from yeasts. WO Pat. 100569 A2 (CSIR, Oct. 27, 2005).
- Botes, A.L., Labuschagne, M., Roth, R., Mitra, R.K., Lotter, J., Abrahams, N., Simpson, C. and Van der Westhuizen, C. (2007a) Methods for obtaining optically active epoxides and diols from 2,3-disubstituted and 2,3-trisubstituted epoxides. WO Pat. 069079 A2 (CSIR, June 21, 2007).
- Botes, A.L., Lotter, J. and Labuschagne, M. (2007b) Methods of obtaining optically active epoxides and vicinal diols from meso-epoxides. U.S. Pat. 0275448 A1 (CSIR, Nov. 29, 2007)
- Botes, A.L., Mitra, R. and Plenaar, D. (2007c) Epoxide Hydrolases: Process Applications *Innov. Pharma Technol.*, 90-92.
- Botes, A.L., Labuschagne, M., Roth, R., Mitra, R.K., Lotter, J., Laloo, R., Ramduth, D., Rohitlall, N., Simpson, C. and Van Zyl, P. (2008) Recombinant yeasts for synthesizing epoxide hydrolases. U.S. Pat. 0171359 A1 (Oxyrane (UK) Ltd, Jul. 17, 2008).
- Bottalla, A.L., Ibrahim-Ouali, M., Santelli, M., Furstoss, R. and Archelas, A. (2007) Epoxide hydrolase-catalyzed kinetic resolution of a spiroepoxide, a key building block of various 11-heterosteroids. *Adv. Synth. Catal.*, **349**, 1102–1110.
- Calvez, O., Chiaroni, A. and Langlois, N. (1998) Enantioselective synthesis of 2,3-disubstituted piperidines from (*S*)-methylpyroglutamate. *Tet. Lett.* **39**, 9447-9450.
- Cao, L, Lee, J., Chen, W. and Wood, T.K. (2006) Enantioconvergent production of (*R*)-1-phenyl-1,2-ethanediol from styrene oxide by combining the *Solanum tuberosum* and an evolved *Agrobacterium radiobacter* AD1 epoxide hydrolases. *Biotech. Bioeng.*, **94**, 522–529.
- Chang, D., Heringa, M.F., Witholt, B. and Li, Z. (2003a) Enantioselective trans dihydroxylation of nonactivated C-C double bonds of aliphatic heterocycles with *Sphingomonas* sp. HXN-200. *J. Org. Chem.*, **68**, 8599-8606.
- Chang, D., Wang, Z., Heringa M.F., Wirthner, R., Witholt, B. and Li, Z. (2003b) Highly enantioselective hydrolysis of alicyclic meso-epoxides with a bacterial epoxide hydrolase from *Sphingomonas* sp. HXN-200: simple synthesis of alicyclic vicinal trans-diols. *Chem. Commun.*, 960–961.
- Chen, C.-S., Fujimoto, Y., Girdaukas, G. and Sih, C.J. (1982) Quantitative analyses of biochemical kinetic resolutions of enantiomers. *J. Am. Chem. Soc.*, **104**, 7294–7299.
- Chiappe, C., Leandri, E., Lucchesi, S., Pieraccini, D., Hammock, B.D. and Morisseau, C. (2004) Biocatalysis in ionic liquids: the stereoconvergent hydrolysis of trans- $\beta$ -methylstyrene oxide catalyzed by soluble epoxide hydrolase. *J. Mol. Catal. B: Enzym.*, **27**, 243–248.
- Choi, W.J., Pua, S.M., Tan, L.L. and Ng, S.S. (2008) Production of (*R*)-ethyl-3,4-epoxybutyrate by newly isolated *Acinetobacter baumannii* containing epoxide hydrolase. *Appl. Microbiol. Biotechnol.* **79**, 61-67.
- Cleij, M., Archelas, A. and Furstoss, R. (1998) Microbiological transformations. Part 42: a two-liquid-phase preparative scale process for an epoxide hydrolase catalysed resolution of *para*-bromo- $\alpha$ -methyl styrene oxide. Occurrence of a surprising enantioselectivity enhancement. *Tetrahedron:Asymmetry*, **9**, 1839–1842.
- Cleij, M., Archelas, A. and Furstoss, R. (1999) Microbial transformations 43. Epoxide hydrolase as tools for the synthesis of enantiopure alpha-methylstyrene oxides: a new and efficient synthesis of (*S*)-Ibuprofen. *J. Org. Chem.*, **64**, 5029–5035.
- Decker, M., Arand, M. And Cronin, A. (2009) Mammalian epoxide hydrolases in xenobiotic metabolism and signalling *Arch. Toxicol.*, **83**, 297–318.

Deregnacourt, J., Archelas, A., Barbirato, F., Paris, J-M. and Furstoss, R. (2007) Enzymatic Transformations 63. High-Concentration Two Liquid-Liquid Phase *Aspergillus niger* Epoxide Hydrolase-Catalysed Resolution: Application to Trifluoromethyl-Substituted Aromatic Epoxides. *Adv. Synth. Catal.*, **349**, 1405-1417.

Devi, A.V., Lahari, C., Swarnalatha, L. and Fadnavis, N.W. (2008) Gelozymes in organic synthesis. Part IV: Resolution of glycidate esters with crude Mung bean *Phaseolus radiatus*) epoxide hydrolase immobilized in gelatin matrix. *Tetrahedron: Asymmetry* **19**, 1139-1144.

Devries, K. M., Dow, R. L. and Wright, S. W. (1998) Procédé de preparation de pyridines substituées WO Pat. 021184 A1 (May 22, 1998).

Doumèche, B., Archelas, A. and Furstoss, R. (2006) Enzymatic transformations 62. Preparative scale synthesis of enantiopure glycidylacetals using an *A. niger* epoxide hydrolase catalysed kinetic resolution. *Adv. Synth. Catal.*, **348**, 1948-1957.

Duarah, A., Goswami, A., Bora, T.C., Talukdar, M. and Gogoi, B.K. (2013) Enantioconvergent bihydrolysis of racemic styrene oxide to *R*-phenyl-1,2-ethanediol by a newly isolated filamentous fungus *Aspergillus tubingensis* TF1 *Appl. Biochem. Biotechnol.*, **170**, 1965-1973.

Elfström, L.T. and Widersten, M. (2005) The *Saccharomyces cerevisiae* ORF YNR064c protein has characteristics of an 'orphaned' epoxide hydrolase. *BBA-Proteins Proteomics*, **1748**, 213-221.

Ferreira, F., Greck, C. and Genêt, J.P. (1997) Stereocontrolled syntheses of *trans*-3-hydroxypipercolic acids and application to (-)-Swainsonine. *Bull. Soc. Chim. Fr.* **134**, 615-621.

Fisher, M. H., Naylor, E. M., Ok, D., Weber, A. E., Shih, T. and Ok, H. (1996) Substituted sulfonamides as selective  $\beta_3$  agonists for the treatment of diabetes and obesity US Pat. 5561142 A (Merck&Co, Inc., Oct.1, 1996).

Fuchs, M., Simeo, Y., Ueberbacher, B.T., Mautner, B., Netscher, T. and Faber, K. (2009) Enantiocomplementary Chemoenzymatic Asymmetric Synthesis of (*R*)- and (*S*)-Chromanemethanol. *Eur. J. Org. Chem.* **6**, 833-840.

Fujino, A. and Sugai, T. (2008) Chemoenzymatic approach to enantiomerically pure (*R*)-3-hydroxy-3-methyl-4-pentenoic acid ester and its application to a formal total synthesis of taurospongine A. *Adv. Synth. Catal.* **350**, 1712-1716.

Fujino, A., Asano, M., Yamaguchi, H., Shirasaka, N., Sakoda, A., Ikunaka, M., Obata, R., Nishiyama S. and Sugai, T. (2007) *Bacillus subtilis* epoxide hydrolase-catalyzed preparation of enantiopure 2-methylpropane-1,2,3-triol monobenzyl ether and its application to expeditious synthesis of (*R*)-bicalutamide. *Tetrahedron Lett.*, **48**, 979-983.

Genzel, Y., Archelas, A., Broxterman, Q.B., Schulze, B. and Furstoss, R. Microbiological transformations. 47. A step toward a green chemistry preparation of enantiopure (*S*)-2-, -3-, and -4-pyridyloxirane via an epoxide hydrolase catalysed kinetic resolution. (2001a) *J. Org. Chem.*, **66**, 538-543.

Genzel, Y., Archelas, A., Lutje, J.F.H., Janssen, D.B. and Furstoss, R. (2001b) Microbiological transformations. Part 48: Enantioselective bihydrolysis of 2-,3- and 4-pyridyloxirane at high substrate concentration using the *Agrobacterium radiobacter* AD1 epoxide hydrolase and its Tyr215Phe mutant. *Tetrahedron*, **57**, 2775-2779.

Grant, D.F., Storms, D.H. and Hammock, B.D. (1993) Molecular cloning and expression of murine liver epoxide hydrolase. *J. Biol. Chem.*, **268**, 17628-17633.

Grulich, M., Maršálek, J., Kyslík, P., Štěpánek, V. and Kotik, M. (2011) Production, enrichment and immobilization of a metagenome-derived epoxide hydrolase. *Process Biochem.*, **46**, 526-532.

Guérard, C., Alphan, V., Archelas, A., Demuynck, C., Hecquet, L., Furstoss, R. and Bolte, J. (1999) Transketolase-Mediated synthesis of 4-deoxy-D-fructose 6-phosphate by epoxide hydrolase-catalysed resolution of 1,1-diethoxy-3,4-epoxybutane. *Eur. J. Org. Chem.*, 3399-3402.

Haddad, M. and Larchevêque, M. (2001) An alternative stereoselective synthesis of *trans*-(2*R*,3*R*)-3-hydroxypipercolic acid. *Tet. Lett.* **42**, 5223-5225.

Harada, H., Hirokawa, Y., Suzuki, K., Hiyama, Y., Oue, M., Kawashima, H., Yoshida, N., Furutani, Y. and Kato, S. (2003) Novel and potent human and rat  $\beta_3$ -Adrenergic receptor agonists containing substituted 3-indolylalkylamines. *Bioorg. Med. Chem. Lett.*, **13**, 1301-1305.

Heikinheimo P., Goldman A., Jeffries C. and Ollis D.L. (1999) Of barn owls and bankers: a lush variety of  $\alpha/\beta$  hydrolases. *Structure*, **7**, R141-R146.

Hellstrom, H., Steinreiber, A., Mayer, S.F. and Faber, K. (2001) Bacterial epoxide hydrolase-catalyzed resolution of a 2,2-disubstituted oxirane: optimization and upscaling. *Biotech. Lett.* **23**, 169-173.

Honda, Y., Katayama, S., Kojima, M., Suzuki, T., Kishibata, N. and Izawa, K. (2004) New approaches to the industrial synthesis of HIV protease inhibitors. *Org. Biomol. Chem.*, **2**, 2061-2070.

Hsin, L-W., Prisinzano, T., Wilkerson, C.R., Dersch, C.M., Horel, R., Jacobson, A.E., Rothman, R.B. and Rice, K.C. (2003) Synthesis and dopamine transporter affinity of chiral 1-[2-[bis(4-fluorophenyl)methoxy]ethyl]-4-(2-hydroxypropyl)piperazines as potential cocaine abuse therapeutic agents. *Bioorg. Med. Chem. Lett.*, **13**, 553-556.

Hwang, S., Hyun, H., Lee, B., Park, Y., Lee, E.Y. and Choi, C. (2006) Purification and Characterization of a Recombinant *Caulobacter crescentus* Epoxide Hydrolase *Biotech. Bioprocess Bioeng.*, **11**, 282-287.

- Hwang, S., Choi, C.Y. and Lee, E.Y. (2008a) Enantioconvergent bioconversion of *p*-chlorostyrene oxide to (*R*)-*p*-chlorophenyl-1,2-ethandiol by the bacterial epoxide hydrolase of *Caulobacter crescentus*. *Biotechnol. Lett.*, **30**, 1219-1225.
- Hwang, S., Choi, C.Y. and Lee, E.Y. (2008b) One-pot biotransformation of racemic styrene oxide into (*R*)-1,2-phenylethanediol by two recombinant microbial epoxide hydrolases. *Biotech. Bioprocess Eng.*, **13**, 453-457.
- Jin, H.-X., Liu, Z.-Q., Hu, Z.-C. and Zheng, Y.-G. (2013a) Production of (*R*)-epichlorohydrin from 1,3-dichloro-2-propanol by two-step biocatalysis using haloalcohol dehalogenase and epoxide hydrolase in two-phase system. *Biochem. Eng. J.*, **74**, 1-7.
- Jin, H.-X., Liu, Z.-Q., Hu, Z.-C. and Zheng, Y.-G. (2013b) Biosynthesis of (*R*)-epichlorohydrin at high substrate concentration by kinetic resolution of racemic epichlorohydrin with a recombinant epoxide hydrolase *Eng. Life Sci.* **13**, 385-392.
- Johansson, P., Unge, T., Cronin, A., Arand, M., Bergfors, T., Jones, T.A. and Mowbray, S.L. (2005) Structure of an atypical epoxide hydrolase from *Mycobacterium tuberculosis* gives insights into its function. *J. Mol. Biol.*, **351**, 1048-1056.
- Kamal, A., Khanna, R., Kumar, C.G., Shaik, A.B. and Kumar, M.S. (2013) A novel bacterial strain of *Achromobacter* sp. MTCC 5605 and a highly enantioselective epoxide hydrolase isolated therefrom. WO Pat. 030851 A1 (March 7, Council of Scientific & Industrial Research).
- Kamita, S.G., Oshita, G.H., Wang, P., Morisseau, C., Hammock, B.D., Nandety, R.S. and Falk, B.W. (2013) Characterization of Hovi-mEH1, a microsomal epoxide hydrolase from the glassy-winged sharpshooter *Homalodisca vitripennis*. *Arch. Insect Biochem. Physiol.*, **83**, 171-179.
- Karboune, S., Archelas, A., Furstoss, R. and Baratti, J. (2005a) Immobilization of the *Solanum tuberosum* epoxide hydrolase and its application in an enantioconvergent process. *Biocatal. Biotransform.*, **23**, 397-405.
- Karboune, S., Archelas, A., Furstoss, R., Baratti, J. (2005b) Immobilization of epoxide hydrolase from *Aspergillus niger* onto DEAE-cellulose: enzymatic properties and application for the enantioselective resolution of a racemic epoxide. *J. Mol. Catal. B: Enzym.*, **32**, 175-183.
- Kasai, N., Suzuki, T. and Furukawa, Y. (1998) Chiral C3 epoxides and halohydrins: Their preparation and synthetic application *J. Mol. Catal. B: Enzymatic* **4**, 237-252.
- Kim, H.S., Lee, S.J. and Lee, E.Y. (2006) Development and characterization of recombinant whole-cell biocatalysts expressing epoxide hydrolase from *Rhodotorula glutinis* for enantioselective resolution of racemic epoxides. *J. Mol. Catal. B: Enzym.*, **43**, 2-8.
- Kotik, M., Brichac, J. and Kyslik, P. (2005) Novel microbial epoxide hydrolases for bihydrolysis of glycidyl derivatives. *J. Biotechnol.*, **120**, 364-375.
- Kotik, M. and Kyslik, P. (2006) Purification and characterisation of a novel enantioselective epoxide hydrolase from *Aspergillus niger* M200. *Biochem. Biophys. Acta*, **1760**, 245-252.
- Kotik, M. (2009) Novel genes retrieved from environmental DNA by polymerase chain reaction: Current genome-walking techniques for future metagenome applications. *J. Biotechnol.*, **144**, 75-82.
- Kotik, M., Štěpánek, V., Marešová, H., Kyslík, P. and Archelas, A. (2009) Environmental DNA as a source of a novel epoxide hydrolase reacting with aliphatic terminal epoxides. *J. Mol. Catal. B: Enzym.*, **56**, 288-293.
- Kotik, M., Štěpánek, V., Grulich, M., Kyslík, P. and Archelas, A. (2010) Access to enantiopure aromatic epoxides and diols using epoxide hydrolases derived from total biofilter DNA. *J. Mol. Catal. B: Enzym.*, **65**, 41-48.
- Kotik, M., Archelas, A., Faměrova, V., Oubrechtova, P. and Křen, V. (2011) Laboratory evolution of an epoxide hydrolase – Towards an enantioconvergent biocatalyst. *J. Biotechnol.*, **156**, 1-10.
- Kroutil, W., Mischitz, M. and Faber, K. (1997a) Deracemisation of (±)-2,3-disubstituted oxiranes via biocatalytic hydrolysis using bacterial epoxide hydrolases: kinetics of an enantioconvergent process. *J. Chem. Soc. Perkin Trans 1*, 3629-3636.
- Kroutil, W., Osprian, I., Mischitz, M. and Faber, K. (1997b) Chemoenzymatic synthesis of (*S*)-(-)-Frontalin using bacterial epoxide hydrolases. *Synthesis*, 156-158.
- Labuschagne, M. and Albertyn, J. (2007) Cloning of an epoxide hydrolase-encoding gene from *Rhodotorula mucilaginosa* and functional expression in *Yarrowia lipolytica*. *Yeast*, **24**, 69-78.
- Lenfant, N., Hotelier, T., Velluet, E., Bourne, Y., Marchot, P. and Chatonnet, A. (2013) ESTHER, the database of the  $\alpha/\beta$ -hydrolase fold superfamily of proteins: tools to explore diversity of functions *Nucleic Acids Research.*, **41**, D423-D429.
- Li Z., Feiten, H.-J., Chang, D., Duetz, W.A., van Beilen, J.B. and Witholt, B. (2001) Preparation of (*R*)- and (*S*)-*N*-protected 3-hydroxypyrrolidines by hydroxylation with *Sphingomonas* sp. HXN-200, a highly active, region- and stereoselective, and easy to handle biocatalyst. *J. Org. Chem.* **66**, 8424-8430.
- Lin, L.S., Lanza, T.J. Jr., Jewell, J.P., Liu, P., Shah, S.K., Qi, H., Tong, X., Wang, J., Xu, S.S., Fong, T.M., Shen, C-P., Lao, J., Xiao, J.C., Shearman, L.P., Stribling, D.S., Rosko, K., Strack, A., Marsh, D.J., Feng, Y., Kumar, S., Sumuel, K., Yin, W., Van der Ploeg, L.H.T., Goulet, M.T. and Hagmann, W.K. (2006) Discovery of N-[(1*S*,2*S*)-3-(4-chlorophenyl)-2-(3-cyanophenyl)-1-methylpropyl]-2-methyl-2-[5-(trifluoro-methyl)pyridin-2-yl]oxy

propanamide (MK-0364), a novel, acyclic cannabinoid-1 receptor inverse agonist for the treatment of obesity. *J. Med. Chem.*, **49**, 7584–7587.

Lin, S., Horsman, G.P. and Shen, B. (2010) Characterization of the epoxide hydrolase NcsF2 from the neocarzinostatin biosynthetic gene cluster. *Org. Lett.*, **12**, 3816–3819.

Lotter, J., Botes, A.L., van Dyk, M.S. and Breytenbach, J.C. (2004) Hydrolytic kinetic resolution of the enantiomers of the structural isomers trans-1-phenylpropene oxide and (2,3-epoxypropyl)benzene by yeast epoxide hydrolase. *Biotech. Lett.*, **15**, 1197-1200.

Manoj, K.M., Archelas, A., Baratti, J. and Furstoss, R. Microbiological transformations. Part 45. A green chemistry preparative scale synthesis of enantiopure building blocks of Eliprodil: elaboration of a high substrate concentration epoxide hydrolase-catalyzed hydrolytic kinetic resolution process. (2001) *Tetrahedron*, **57**, 695-701.

Mateo, C., Archelas, A., Fernandez-Lafuente, R., Guisan, J.M. and Furstoss, R. (2003) Enzymatic transformations. Immobilized *A. niger* epoxide hydrolase as a novel biocatalytic tool for repeated-batch hydrolytic kinetic resolution of epoxides. *Org. Biomol. Chem.*, **1**, 2739–2743.

Mathvink, R. J., Barritta, A. M., Candelore, M. R., Cascieri, M. A., Deng, L., Tota, L., Strader, C. D., Wyvratt, M. J., Fisher, M. H. and Weber, A. E. (1999) *Bioorg. Med. Chem. Lett.*, **9**, 1869-1874.

Mayer, S.F., Steinreiber, A., Goriup, M., Saf, R. and Faber, K. (2002a) Chemoenzymatic asymmetric total syntheses of a constituent of Jamaican rum and of (+)-Pestalotin using an enantioconvergent enzyme-triggered cascade reaction. *Tetrahedron:Asymmetry*, **13**, 523-528.

Mayer, S.F., Steinreiber, A., Orru, R.V.A. and Faber, K. (2002b) Chemoenzymatic asymmetric total synthesis of antitumor agents (3*R*,9*R*,10*R*)- and (3*S*,9*R*,10*R*)-Panaxytriol and (*R*)- and (*S*)-Falcarinol from *Panax ginseng* using an enantioconvergent enzyme-triggered cascade reaction. *J. Org. Chem.*, **67**, 9115–9121.

Min, J.Y. and Lee, E.Y. (2012) Biosynthesis of (*R*)-1,2-phenylethanediol and (*R*)-4-chloro-1,2-phenylethanediol by using two recombinant cells expressing enantiocomplementary epoxide hydrolases *J. Ind. Eng.*, **18**, 160-164.

Monfort, N., Archelas, A. and Furstoss, R. (2004a) Enzymatic transformations. Part 55: Highly productive epoxide hydrolase catalysed resolution of an azole antifungal key synthon. *Tetrahedron*, **60**, 601–605.

Monfort, N., Archelas, A. and Furstoss, R. (2004b) Unpublished results.

Monterde, M.I., Lombard, M., Archelas, A., Cronin, A., Arand, M. and Furstoss, R. (2004) Enzymatic transformations. Part 58: Enantioconvergent bihydrolysis of styrene oxide derivatives catalysed by the *Solanum tuberosum* epoxide hydrolase. *Tetrahedron:Asymmetry*, **15**, 2801–2805.

Morisseau C. (2013) Role of epoxide hydrolases in lipid metabolism. *Biochimie*, **95**, 91–95.

Morisseau, C., Nellaiah, H., Archelas, A., Furstoss, R. and Baratti, J.C. (1997) Asymmetric hydrolysis of racemic *para*-nitrostyrene oxide using an epoxide hydrolase preparation from *Aspergillus niger*. *Enzyme Microb. Technol.*, **20**, 446-452.

Moussou P., Archelas A. and Furstoss R. (1998a) Microbiological transformations 40. Use of fungal epoxide hydrolases for the synthesis of enantiopure alkyl epoxides. *Tetrahedron*, **54**, 1563-1572.

Moussou, P., Archelas, A., Baratti, J. and Furstoss, R. (1998b) Microbiological transformations. Part 39: determination of the regioselectivity occurring during oxirane ring opening by epoxide hydrolases: a theoretical analysis and a new method for its determination. *Tetrahedron: Asymmetry*, **9**, 1539-1547.

Murmann, W., Rumore, G. and Gamba, A. (1967) Pharmacological properties of 1-(4'-nitrophenyl)-2-isopropylamino-ethanol (INPEA), a new beta-adrenergic receptor antagonist. V. Effects of the optical isomers D(minus) and L(plus) INPEA on heart rate, oxygen consumption and body temperature and on the cardiac and metabolic effects of adrenaline and noradrenaline in urethane-anesthetized rats. *Boll. Chim. Farm.*, **106**, 251-268.

Naundorf, A., Melzer, G., Archelas, A., Furstoss, R. and Wohlgemuth, R. (2009) Influence of pH on the expression of a recombinant epoxide hydrolase in *Aspergillus niger*. *Biotechnol. J.*, **4**, 756–765.

Newman, J.W., Morisseau, C. and Hammock, B.D. (2005) Epoxide hydrolases: their roles and interactions with lipid metabolism. *Progress in Lipid Research*, **44**, 1–51

Orru, R.V.A., Mayer, S.F., Kroutil, W. and Faber, K. (1998a) Chemoenzymatic deracemization of (+)-2,2-disubstituted oxiranes. *Tetrahedron*, **54**, 859-874.

Orru, R.V.A., Osprian, I., Kroutil, W. and Faber, K. (1998b) An Efficient Large-Scale Synthesis of (*R*)-(-)-Mevalonolactone Using Simple Biological and Chemical Catalysts. *Synthesis*, 1259-1263.

Osprian, I., Kroutil, W., Mischitz, M. and Faber, K. (1997) Biocatalytic resolution of 2-methyl-2-(aryl)alkyloxiranes using novel bacterial epoxide hydrolases. *Tetrahedron-Asymmetry*, **18**, 65–71.

Osprian, I., Stampfer, W. and Faber, K. (2000) Selectivity enhancement of epoxide hydrolase catalyzed resolution of 2,2-disubstituted oxiranes by substrate modification. *J. Chem. Soc. Perkin Trans. 1*, 3779–3785.

Pabel, J., Hofner, G. and Wanner, K.T. (2000) *Bioorg. Med. Chem. Lett.*, **10**, 1377–1380.

Pedragosa-Moreau, S., Archelas, A. and Furstoss, R. (1993) Microbiological transformations. 28. Enantiocomplementary epoxide hydrolyses as a preparative access to both enantiomers of styrene oxide. *J. Org. Chem.*, **58**, 5533-5536.

Pedragosa-Moreau, S., Archelas, A. and Furstoss R. (1995) Preparative access to both enantiomers of styrene oxide by hydrolysis of the racemate using *Aspergillus niger* or *Beauveria sulfurescens*. In "Preparative Biotransformation", Wiley & Sons, Ltd, **1**, 18.1-18.7.

Pedragosa-Moreau, S., Archelas, A. and Furstoss, R. (1996a) Microbiological transformations. 31: Synthesis of enantiopure epoxides and vicinal diols using fungal epoxide hydrolase mediated hydrolysis. *Tetrahedron Lett.*, **37**, 3319–3322.

Pedragosa-Moreau, S., Archelas, A. and Furstoss, R. (1996b) Microbial transformations 32: use of epoxide hydrolase mediated biotransformation as a way to enantiopure epoxides and vicinal diols: application to substituted styrene oxide derivatives. *Tetrahedron*, **52**, 4593-4606.

Pedragosa-Moreau, S., Morisseau, C., Zylber, J., Archelas, A., Baratti, J. and Furstoss, R. (1996c) Microbiological transformations. 33. Fungal epoxide hydrolases applied to the synthesis of enantiopure para-substituted styrene oxides. A mechanistic approach. *J. Org. Chem.*, **61**, 7402-7407.

Pedragosa-Moreau, S., Morisseau, C., Baratti, J., Zylber, J., Archelas, A. and Furstoss, R. (1997) Microbiological transformations 37. An enantioconvergent synthesis of the  $\beta$ -blocker  $\alpha$ -Nifénalol using a combined chemoenzymatic approach. *Tetrahedron*, **53**, 9707-9714.

Petri, A., Marconcini, P. and Salvadori, P. (2005) Efficient immobilization of epoxide hydrolase onto silica gel and use in the enantioselective hydrolysis of racemic *para*-nitrostyrene oxide. *J. Mol. Catal. B: Enzym.*, **32**, 219–224.

Pienaar, D.P., Mitra, R.K., van Deventer, T.I. and Botes, A.L. (2008) Synthesis of a variety of optically active hydroxylated heterocyclic compounds using epoxide hydrolase technology. *Tetrahedron Lett.*, **49**, 6752-6755.

Reetz, M.T. and Zheng, H. (2011) Manipulating the expression rate and enantioselectivity of an epoxide hydrolase by using directed evolution. *ChemBioChem*, **12**, 1529–1535.

Reetz, M.T., Kahakeaw, D. and Lohmer, R. (2008) Addressing the numbers problem in directed evolution. *ChemBioChem*, **9**, 1797–1804.

Reetz, M.T., Bocola, M., Wang, L-W., Sanchis, J., Cronin, A., Arand, M, Zou, J., Archelas, A., Bottalla, A-L., Naworyta, A. and Mowbray, S.L. (2009) Directed Evolution of an Enantioselective Epoxide Hydrolase: Uncovering the Source of Enantioselectivity at Each Evolutionary Stage. *J. Am. Chem. Soc.*, **131**, 7334-7343.

Reetz, M.T., Prasad, S., Carballeira, J.D., Gumulya, Y. and Bocola, M. (2010) Iterative saturation mutagenesis accelerates laboratory evolution of enzyme stereoselectivity: rigorous comparison with traditional methods. *J. Am. Chem. Soc.*, **132**, 9144–9152.

Rink, R., Kingma, J., Spelberg, H. L. and Janssen, D. (2000) Tyrosine residues serve as proton donor in the catalytic mechanism of epoxide hydrolase from *Agrobacterium radiobacter*. *Biochem.*, **39**, 5600-5613.

Shimizu, K.I, Sakamoto, M., Hamada, M., Higashi, T., Sugai, T. and Shoji, M. (2010) The scope and limitation of the regio- and enantioselective hydrolysis of aliphatic epoxides using *Bacillus subtilis* epoxide hydrolase, and exploration toward chirally differentiated tris(hydroxymethyl)methanol. *Tetrahedron: Asymmetry* **21**, 2043-2049.

Simeó, Y. and Faber, K. (2006) Selectivity enhancement of enantio- and stereo-complementary epoxide hydrolases and chemo-enzymatic deracemization of ( $\pm$ )-2-methylglycidyl benzyl ether. *Tetrahedron: Asymmetry* **17**, 402-409.

Soloshonok, V.A. (1999) EnantioControlled Synthesis of Fluoro-organic Compounds: Stereochemical Challenges and Biomedical Targets, Wiley, Chichester.

Spelberg, J.H.L., Rink, R., Kellogg, R.M. and Janssen, D.B. (1998) Enantioselectivity of a recombinant epoxide hydrolase from *Agrobacterium radiobacter*. *Tetrahedron: Asymmetry*, **9**, 459-466.

Spelberg, J.H.L., Rink, R., Archelas, A., Furstoss, R. and Janssen, D. (2002) Biocatalytic potential of the epoxide hydrolase from *Agrobacterium radiobacter* AD1 and a mutant with enhanced enantioselectivity. *Adv. Synth. Catal.*, **344**, 980-985.

Steinreiber, A., Edegger K., Mayer, S.F. and Faber K. (2001a) Enantio- and diastereo-convergent synthesis of (2*R*,5*R*)- and (2*R*,5*S*)-Pityol through enzyme-triggered ring closure. *Tetrahedron: Asymmetry*, **12**, 2067-2071.

Steinreiber, A., Hellstrom, H., Mayer S.F., Orru, R.V.A. and Faber, K. (2001b) Chemo-enzymatic enantioconvergent synthesis of C4-building blocks containing a fully substituted chiral carbon center using bacterial epoxide hydrolases *Synlett* 111-113.

Steinreiber, A., Mayer, S.F. and Faber, K. (2001c) Asymmetric Total Synthesis of a Beer-Aroma Constituent Based on Enantioconvergent Biocatalytic Hydrolysis of Trisubstituted Epoxides *Synthesis*, **13**, 2035-2039.

Steinreiber, A., Mayer, S.F., Saf, R. and Faber, K. (2001d) Biocatalytic asymmetric enantioconvergent hydrolysis of trisubstituted oxiranes. *Tetrahedron: Asymmetry*, **12**, 1519–1528.

Ueberbacher, B.J., Osprian, I., Mayer, S.F. and Faber, K. (2005) A chemoenzymatic, enantioconvergent, asymmetric total synthesis of (*R*)-Fridamycin E. *Eur. J. Org. Chem.*, 1266–1270.

Ueberbacher, B.T., Oberdorfer, G., Gruber, K. and Faber, K. (2009) Epoxide-hydrolase-initiated hydrolysis/rearrangement cascade of a methylene-interrupted bis-epoxide yields chiral THF moieties without involvement of a "cyclase". *ChemBioChem*, **10**, 1697–1704.

- van Loo, B., Kingma, J., Arand, M., Wubbolts, M.G. and Janssen, D.B. (2006) Diversity and biocatalytic potential of epoxide hydrolases identified by genome analysis. *Appl. Environ. Microbiol.*, **72**, 2905–2917.
- van Loo, B., Lutje Spelberg, J.H., Kingma, J., Sonke, T., Wubbolts, M.G. and Janssen, D.B. (2004) Directed evolution of epoxide hydrolase from *A. radiobacter* toward higher enantioselectivity by error-prone PCR and DNA shuffling. *Chem. Biol.*, **11**, 981–990.
- Visser, H., de Oliveira Villela Filho, M., Liese, A., Weijers, C.A.G.M. and Verdoes, J.C. (2003) Construction and characterisation of a genetically engineered *Escherichia coli* strain for the epoxide hydrolase-catalysed kinetic resolution of epoxides. *Biocatal. Biotransform.*, **21**, 33–40.
- Wandel, U., Mischitz, M., Kroutil, W. and Faber, K. (1995) Highly selective asymmetric hydrolysis of 2,2-disubstituted epoxides using lyophilized cells of *Rhodococcus* sp. NCIMB 11216. *J. Chem. Soc. Perkin Trans. 1*, 735–736.
- Weijers, C.A.G.M. (1997) Enantioselective hydrolysis of aryl, alicyclic and aliphatic epoxides by *Rhodotorula glutinis*. *Tetrahedron:Asymmetry*, **8**, 639–647.
- Weijers, C.A.G.M., Meeuwse, P., Herpers, R.L.J.M., Franssen, M.C.R. and Sudhoelter, E.J.R. (2005) Stereoselectivity and Substrate Specificity in the Kinetic Resolution of Methyl-Substituted 1-Oxaspiro[2.5]octanes by *Rhodotorula glutinis* Epoxide Hydrolase. *J. Org. Chem.*, **70**, 6639–6646.
- Wittman, M., Carboni, J., Attar, R., Balasubramanian, B., Balimane, P., Brassil, P., Beaulieu, F., Chang, C., Clarke, W., Dell, J., Eummer, J., Frennesson, D., Gottardis, M., Greer, A., Hansel, S., Hurlburt, W., Jacobson, B., Krishnananthan, S., Lee, F.Y., Li, A., Lin, T.-A., Liu, P., Ouellet, C., Sang, X., Saulnier, M.G., Stoffan, K., Sun, Y., Velaparthy, U., Wong, H., Zang, Z., Zimmermann, K., Zoeckler, M. and Vyas, D. (2005) Discovery of a 1H-benzoimidazol-2-yl)-1H-pyridin-2-one (BMS-536924) inhibitor of insulin-like growth factor I receptor kinase with in vivo antitumor activity. *J. Med. Chem.*, **48**, 5639–5643.
- Woo, J-H., Kang, J-H., Hwang, H-O., Cho, J-C., Kim, S-J. and Kang, S.G. (2010) Biocatalytic resolution of glycidyl phenyl ether using a novel epoxide hydrolase from a marine bacterium, *Rhodobacteriales bacterium* HTCC2654. *J. Biosci. Bioeng.*, **109**, 539-544.
- Wu, S., Li, A., Chin, Y.S. and Li, Z. (2013) Enantioselective Hydrolysis of Racemic and Meso-Epoxides with Recombinant *Escherichia coli* expressing Epoxide Hydrolase from *Sphingomonas* sp. HXN-200: Preparation of Epoxides and vicinal Diols in High ee and High Concentration *ACS Catalysis*, **3**, 752-759.
- Wu, S., Chen, Y., Xu, Y., Li, A., Xu, Q., Glieder, A. and Li, Z. (2014) Enantioselective trans-dihydroxylation of aryl olefins by cascade biocatalysis with recombinant *Escherichia coli* coexpressing monooxygenase and epoxide hydrolase. *ACS Catal.* **4**, 409-420.
- Xu, Y., Xu, J-H., Pan, J. and Tang, Y-F. (2004) Biocatalytic resolution of glycidyl aryl ethers by *Trichosporon loubierii* : cell/substrate ratio influences the optical purity of (*R*)-epoxides. *Biotechnol. Lett.*, **26**, 1217-1221.
- Xu, Y., Jia, X., Panke, S. and Li, Z. (2009) Asymmetric dihydroxylation of aryl olefins by sequential enantioselective epoxidation and regioselective hydrolysis with tandem biocatalysts. *Chem. Commun.*, 1481-1483.
- Xue, Feng, Liu, Z-Q., Zou, S-P., Wan, N-W., Zhu, W-Y., Zhu, Q. and Zheng, Y-G. (2014) A novel enantioselective epoxide hydrolase from *Agromyces mediolanus* ZJB120203: Cloning, characterization and application *Process Biochem.* **49**, 409-417.
- Yoo, S.S., Park, S. and Lee, E.Y. (2008) Enantioselective resolution of racemic styrene oxide at high concentration using recombinant *Pichia pastoris* expressing epoxide hydrolase of *Rhodotorula glutinis* in the presence of surfactant and glycerol. *Biotech. Lett.*, **30**, 1807-1810.
- Yuasa, Y. and Tsuruta, H. (1997) Practical Syntheses of (*S*)-4-Hydroxytetrahydrofuran-2-one, (*S*)-3-Hydroxytetrahydrofuran and Their (*R*)-Enantiomers *Liebigs Ann. Recl.*, **9**, 1877-1879.
- Zhang, J., Reddy, J., Roberge, C., Senanayake, C., Greasham, R. and Chartrain, M. (1995) Chiral bio-resolution of racemic indene oxide by fungal epoxide hydrolases. *J. Ferment. Bioeng.*, **80**, 244–246.
- Zhao, J., Chu, Y-Y., Li, A-T., Ju, X., Kong, X-D., Pan, J., Tang, Y. and Xu, J-H. (2011) An Unusual (*R*)-Selective Epoxide Hydrolase with High Activity for Facile Preparation of enantiopure Glycidyl Ethers. *Adv. Synth. Catal.*, **353**, 1510-1518.
- Zhao, L., Han, B., Huang, Z., Miller, M., Huang, H., Malashock, D.S., Zhu, Z., Milan, A., Robertson, D.E., Weiner, D.P. and Burk, M.J. (2004) Epoxide hydrolase-catalyzed enantioselective synthesis of chiral 1,2-diols via desymmetrization of meso-epoxides. *J. Am. Chem. Soc.*, **126**, 11156–11157.
- Zheng, H., Kahakeaw, D., Acevedo, J.P. and Reetz, M. (2010) Directed evolution of enantioconvergence: the case of an epoxide hydrolase-catalyzed reaction of a racemic epoxide. *ChemCatChem*, **2**, 958–961.

## Chapter III. Results

## III.1 Introduction of Kau2-EH

In an effort to characterize and develop new EHs with potentially interesting characteristics, Kotik *et al.* have focused on metagenomic DNA (or environmental DNA, eDNA) to retrieve gene coding for such enzymes (Kotik *et al.*, 2009). Indeed it is known that the vast majority of microorganisms are currently not cultivable and thus a vast part of the associated biodiversity is not directly available. A convenient way to nevertheless get access to this biodiversity is to test whether recovered eDNA possesses homologous sequences to already known genes coding enzyme of interest. In order to do so different techniques have been developed (Kotik, 2009). One of them makes use of degenerate consensus sequences followed by genome walking in order to get access to the full genetic sequence of interest.

### III.1.1 Cloning of Kau2-EH from metagenomic DNA and properties

The total DNA from a biofilter used to purify styrene containing off-gas was first extracted (Kotik *et al.*, 2010). Thereafter, two of three already described EH consensus sequences (HGW/FP and GG/HDWG; (Van Loo *et al.*, 2006)) were used to design EH specific degenerated primers. From the total DNA and using these primers, amplified gene fragments of approximately 240 bp were obtained and then sequenced. The total eDNA was digested with Sau3AI restriction enzyme and linker DNA were ligated to the eDNA restriction fragments in order to perform genome-walking. To this end, linker DNA primers and EH degenerated or specific primers were used. After three steps of genome walking the full length EH gene was known allowing specific primers for the flanking regions to be designed. The full-length gene was then PCR amplified using initial eDNA as template. The amplicon was then ligated (after XbaI digestion) in the expression vector pSE420. The so-called *eph-k2* gene was sequenced and corresponding Kau2-EH overexpressed in *E. coli* RE3 cells. The *eph-k2* gene encoded a 339 amino-acid protein of 38.2 kDa that is the most closest to putative bacterial EHs from *Bradyrhizobium* sp. ORS278 and *Bradyrhizobium* sp. BTAi1 with 73% identity from both (BLASTP search). The amino acid sequence contained the three following consensus sequences characterized of EHs (HGWP, GHDWG and GYGAT). The Kau2-EH encoding gene was intron free and thus of probable bacterial origin. Kau2-EH thus belong to the bacterial EH family related to EHs of higher organisms (Barth *et al.*, 2004). Kau2-EH was overexpressed in *E. coli* RE3 at approximately 20% of the total soluble proteins and partially purified to account 35% of total protein after ammonium sulfate precipitation

(Kotik *et al.*, 2010). The partially purified Kau2-EH proved to be optimally active at pH 7.5 and 40 °C. A classical Michaelis-Menten behavior was noted with both enantiomers of 1,2-epoxyoctane-**A** ( $K_{mR}$ =6.9 mM,  $K_{mS}$ =4.4 mM,  $V_{maxR}$ =13.4 mmol/min/mg and  $V_{maxS}$ =7.9 mmol/min/mg for *R* and *S* enantiomers respectively) while a sigmoid behavior was observed when each benzyl glycidyl ether-**B** enantiomers were used.

### III.1.2 Biocatalytic properties of Kau2-EH

In order to broadly decipher the potential interest of Kau2-EH in biocatalytic reactions, the enzyme was tested over 13 epoxides (Kotik *et al.*, 2010) (**Figure 40**).

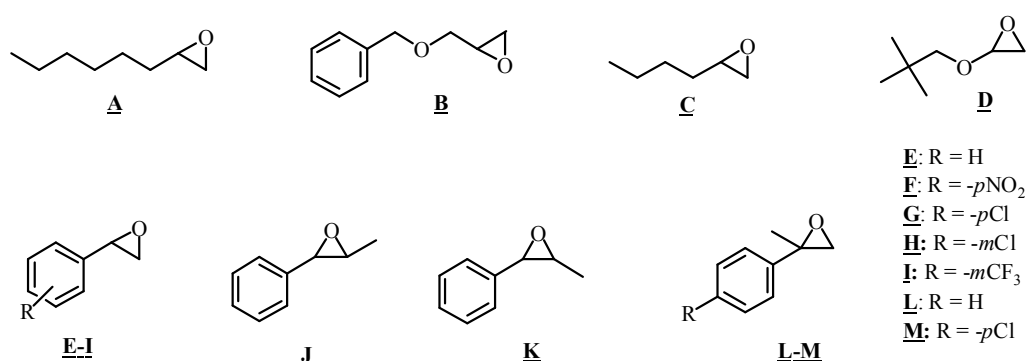


**Figure 40.** Various epoxide racemates tested as substrates of Kau2-EH.

The obtained results are listed in **Table 3**.

**Table 3.** Biohydrolytic reactions catalyzed by Kau2-EH using substrates **A-M**.

Substrates	Residual epoxide	Formed diol	E	ee diol at 100%
<i>rac-A</i>	<i>S</i>	<i>R</i>	1.1	not reported
<i>rac-B</i>	<i>S</i>	<i>S</i>	1.1	not reported
<i>rac-C</i>	<i>S</i>	<i>R</i>	1.3	50
<i>rac-D</i>	<i>S</i>	<i>S</i>	1.0	14
<i>rac-E</i>	<i>R</i>	<i>R</i>	65	77
<i>rac-F</i>	<i>R</i>	<i>R</i>	80	87
<i>rac-G</i>	<i>R</i>	<i>R</i>	35	85
<i>rac-H</i>	<i>R</i>	<i>R</i>	17	91
<i>rac-I</i>	<i>R</i>	<i>R</i>	2.4	82
<i>rac-J</i>	1 <i>R</i> ,2 <i>R</i>	1 <i>R</i> ,2 <i>S</i>	>200	79
<i>rac-K</i>	1 <i>R</i> ,2 <i>S</i>	1 <i>R</i> ,2 <i>R</i>	10	>99
<i>rac-L</i>	<i>R</i>	<i>S</i>	2.3	41
<i>rac-M</i>	<i>R</i>	<i>S</i>	6	50

From the above results it clearly appeared that the best results were obtained with mono and 1,2-disubstituted aromatic epoxides with E-values ranging from 35 to more than 200 when *meta*-substituted aromatic rings were excluded. In all cases more or less enantioconvergent reactions were encountered with one case showing nearly perfect enantioconvergency. Indeed when compound **K** was used, the ee of the diol *at completion* reached more than 99%. In order to further sustained the usefulness of Kau2-EH for synthetic applications a preparative scale transformation of both *rac-J* and *rac-K* was conducted on the 2.4 g and 1 g scale respectively (80 g/L or 600 mM and 13 g/L or 97 mM respectively, (Kotik *et al.*, 2010) (**Figure 41**).

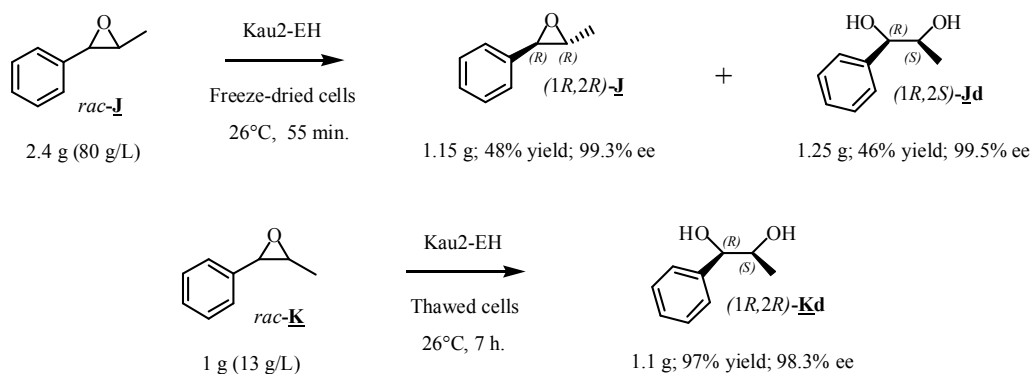


**Figure 41.** Preparative biohydrolysis of *trans*-methylstyrene oxide-**J** and *cis*-methylstyrene oxide-**M** using Kau2-EH.

When *rac*-**J** was used for biohydrolysis, a nearly perfect kinetic resolution was obtained with ees of both residual epoxide and formed diol over 99% within one hour. Furthermore both compounds were recovered in very high yields in a reaction where the starting epoxide concentration was very high (80 g/L). When *rac*-**K** was used the biohydrolysis was confirmed to be enantioconvergent, leading to the corresponding **Kd** in nearly quantitative yield and very high ees (>98%). The *cis*-epoxide-**K** was clearly a worse substrate than the *trans*-epoxide-**J** since both starting substrate concentration (13 g/L) and reaction time (7 h) were less interesting. Nevertheless the enantioconvergent bio-hydrolysis of **K** catalyzed by Kau2-EH is of outstanding interest because the experimental yield and ees of the formed diol approached the theoretical yield of 100% for an enantiopure product awaited for a perfect enantioconvergent reaction.

### III.1.3 Purposes of this PhD work

In order to build on the previously obtained results described above, the work described in the following was conducted in part to better understand Kau2-EH from a biochemical point of view. This was done to get valuable information about the active site of the enzyme in order to eventually be able to modify it by directed mutagenesis in order to develop tailor-made biocatalysts. In a first part modelling of Kau2-EH active site was undertaken with the help of comparative inhibition studies involving potato- and murine-EHS. In a second step and taking into account the fact that Kau2-EH looked to be a promising biocatalyst for kinetic resolution or enantioconvergent transformation of aromatic epoxides, we have explored the chemical space that can be reached with such an enzyme and focused

especially on bifunctional 1,2-disubstituted aromatic epoxides as potential chiral synthons. Finally a more detailed kinetic analysis of pure Kau2-EH was undertaken by stopped-flow experiments with the aim to get access to fundamental kinetic constants using *trans*-stilbene oxide as substrate.

## III.2 Modelisation Study of Kau2-EH

### III.2.1 Introduction

As described previously Kau2-EH showed broad substrate specificity and in some cases could be used to carry out high enantioselective or enantioconvergent processes (Kotik *et al.*, 2010). Unfortunately, such nice results could not be obtained for all the tested epoxides. For example, if Kau2-EH showed high activity against *para*-chlorostyrene oxide (*p*ClISO) as substrate, the level of enantioconvergency was not perfect, the enantiomeric excess of the formed (*R*)-*para*-chlorophenylethane-1,2-diol being only of 84 % at 100% conversion ratio. (Figure 42). Knowing that this enantiomer is a key building block in the synthesis of Eliprodil, a neuroprotective agent, a strong motivation to improve this biocatalyst further to higher degrees of enantioconvergence was established.

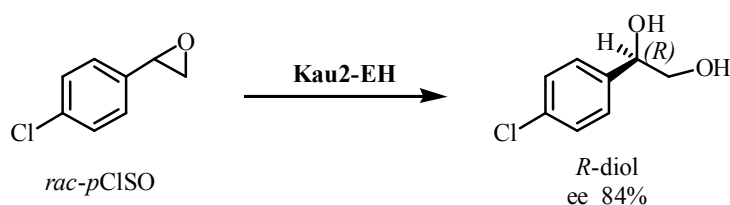


**Figure 42.** Hydrolysis of *rac*-*para*-chlorostyrene oxide using wild-type Kau2-EH.

It is now well established that directed evolution strategy can be used to improve the properties of a target enzyme. In theory, directed evolution is a method used in protein engineering that mimics the process of natural selection to evolve proteins toward a user-defined goal (Otten and Quax, 2005). The replacement of residues located in the active site or in the access substrate tunnel can also lead to significant beneficial effects, such as improved activities and increased enantioselectivity (Pavlova *et al.*, 2009). Combining the randomisation of such amino acids by saturation mutagenesis and using the selected clones of the first round of mutagenesis as template for the second round at different randomization site was shown to be an interesting strategy to improve the specificity of a biocatalyst (Bershtein and Tawfik, 2008; Reetz, 2004). However, to perform such a study the knowledge of the 3D protein structure is essential to use as a guide for the determination of the selected sites within the substrate binding cavity.

Lacking an X-ray structure, homology models of Kau2-EH were constructed based on an existing homologous protein whose crystal structure has been solved. The homology models allowed us to target sites for saturation mutagenesis experiments. Sequence alignments of Kau2-EH (**Table 4**) with sequences of  $\alpha/\beta$ -hydrolase fold EHs (see **Annexe 1**), whose structures have been solved revealed that three of them share a moderate similarity over the entire Kau2-EH sequence: the potato, the human and the murine EHs with sequence identities of 32, 35 and 37%, respectively (See **Table 5**).

**Table 4.** FASTA sequence of Kau2-EH.

1	mapammdmpp	lqyanvngir	mgfyeagpkt	dtpplvlchg	wpeiafswrh	qikalsetgl
61	rviapdqrgy	gatdrpepve	aydienltad	lvglldhlni	dkaifvghdw	ggfivwqmpl
121	rhpsrvagvi	gvntphtprt	atdpiellrq	rygdhlyiaq	fqhpsrepdr	ifadnvektf
181	dffmrkmpmq	kqpsaadana	gppaaglgas	pklmnafpqm	vagydgkldp	rekilspeem
241	kvfvdtfrgs	gftgginwyr	nmtrnwesa	hidhtvrtps	lmimaesdsv	lppsacdgme
301	qivpdlekyl	vrnsghtqg	eqpdevsaki	lewrrrrfg		

**Table 5.** Sequences identity between Kau2-EH and the other three EHs.

EH source	Sequences (Genbank entries)	Identity (Id.), positive aa (Pos.)	PDB-file/ref.
<i>Kau2-EH</i>	ACO95125 total: 339 aa	-	-
<i>Solanum tuberosum</i> (potato)	AAA81892 total: 321 aa	32% Id., 50% Pos. between aa 16-336 of Kau2-EH and aa 11-320 of <i>S.t.</i> EH	2CJP (Mowbray <i>et al.</i> , 2006)
<i>Homo sapiens</i>	AAA02756 total: 554 aa	35% Id., 52% Pos. between aa 19-333 of Kau2-EH and aa 248-540 of <i>H.s.</i> EH	1S8O (Gomez <i>et al.</i> , 2004)
<i>Mus musculus</i> (murine)	AAA37555 Total: 554 aa	37% Id., 52% Pos. between aa 13-333 of Kau2-EH and aa 239-540 of <i>M.m.</i> EH	1CQZ (Argiriadi <i>et al.</i> , 1999)

One should note in these alignments a low-homology stretch of approximately 45 amino acids that very likely represents the cap loop. We built three homology models of Kau2-EH using the crystal structures of these three EHs as templates (structural homology models of Kau2-EH were generated using SWISS-MODEL, an automated modeling server, using the default settings). The three generated homology models were found to have similar folds; a comparison of the models revealed r.m.s. deviations of 3.7–5.3 Å for 324 C $\alpha$  atoms, with the potato EH-derived model being structurally most different. Significant differences between the model tertiary structures are evident in some short loop regions and in a long unstructured segment, the cap loop, which connects helix 4 and 5 of the cap domain (**Figure**

**43** and **Table 6**). This domain consists of 6 helices and bears the two conserved tyrosine residues which hydrogen bond with the epoxide oxygen.

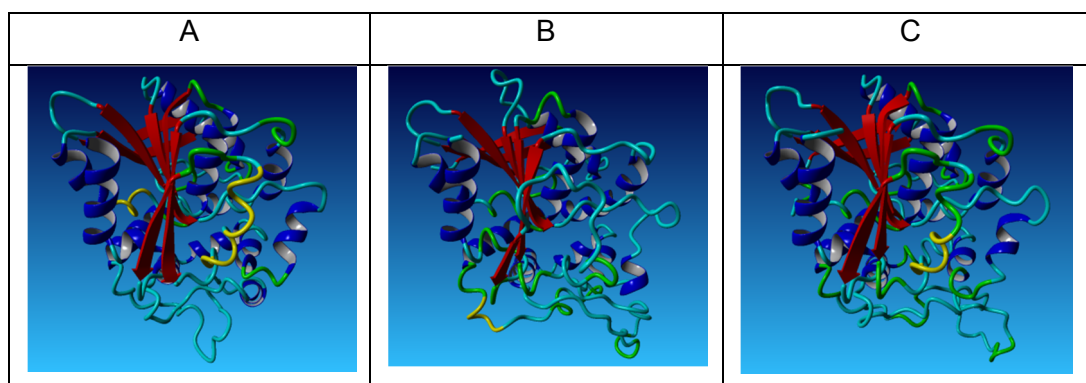


**Figure 43.** Three homology models of Kau2-EH based on the crystal structures of the murine (A), potato (B) and human EH (C). The models were built using SWISS-MODEL.

**Table 6.** Comparison between the three Kau2-EH homology models, which were generated using the crystal structures of the murine, potato or human EH as a template; indicated are the r.m.s. deviations for the C $\alpha$  atoms of the residues 12–335 and the segments with the most significant spatial differences between the model tertiary structures.

Template of Kau2-EH homology model	Potato EH	Human EH
murine EH	5.3 Å; Asp-74–Glu-80, Leu-95–Asp-101, Pro-187–Leu-235 <sup>a</sup>	3.7 Å; Asn-199–Tyr-224 <sup>a</sup>
potato EH	–	5.1 Å; Arg-185–Glu-232 <sup>a</sup> , Leu-291–Lys-308

<sup>a</sup> This segment forms part of the cap loop, which comprises the residues Lys-186–Ser-236;

Based on these results the best model would correspond to the use of the crystal structure of murine EH as template. However, some parts of the model may be more reliable than others and since we were particularly interested in the active site of the protein, we decided to substantiate these computational results by the study of two inhibitor compounds, N-cyclohexyl-N'-decylurea (CDU) and N-cyclohexyl-N'-(4-iodophenyl) urea (CIU), which were previously shown to act as potent competitive inhibitors of murine sEH (**Table 7**) (Argiriadi *et al.*, 2000). Therefore, using Kau2-EH and *Solanum tuberosum* EHs as targets we have carried out a complete inhibition study in order to compare the inhibition constants of these two inhibitors for these three EHs.

**Table 7.** Inhibition of CDU and CIU with murine EH.

	CDU	CIU
murine EH	competitive inhibition $K_i = 6.3 \text{ nM}$	competitive inhibition $K_i = 17 \text{ nM}$

Modelisation study of Kau2-EH was divided into 4 major parts:

- 1) Preparation of inhibitors CDU and CIU.
- 2) Determination of kinetic parameters of Kau2-EH using (*S*)-*p*-chlorostyrene oxide as substrate.
- 3) Inhibition study of CDU and CIU with Kau2-EH.
- 4) Inhibition study of CDU and CIU with potato EHs.

### III.2.2 Preparation of CDU and CIU

Specific enzyme inhibitors are important research tools to understand the catalytic mechanism of an enzyme and pathologies that may be associated with dysfunctions of this enzyme. Two alkylurea inhibitors were investigated, CDU and CIU (**Figure 44**), the binding of this two inhibitors to epoxide hydrolase clarified mechanistic inferences and implicated the active site Tyrosines in substrate activation. The two same inhibitors were used in our study, and were synthesized as described in the literature (Argiriadi *et al.*, 2000)(see **V. 3. 1** and **V. 3. 2**).

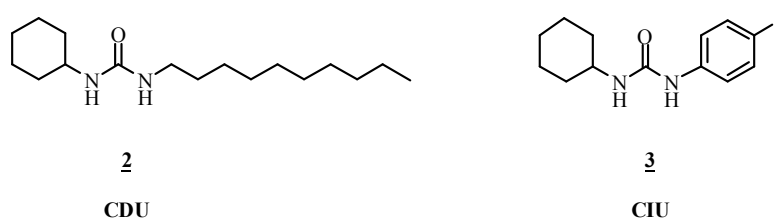


**Figure 44.** Structure of CDU and CIU.

### III.2.3 Determination of kinetic parameters of Kau2-EH

To determine the inhibition constants of CDU and CIU against Kau2-EH and potato EH, it was necessary to use an epoxide as a reference substrate. Our choice was to use the

*p*ClISO and more specifically the (*S*)-enantiomer that corresponds to the enantiomer showing the higher activity (**Figure 45**) (Kotik *et al.*, 2010).

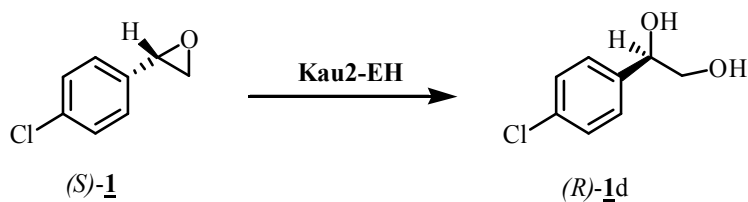


**Figure 45.** Hydrolysis of *rac*-**1** using Kau2-EH.

The EH activity of the whole cells over expressing Kau2-EH was determined by HPLC (see V. 4. 3) using (*S*)-*p*ClISO ((*S*)-**1**) as substrate. Kinetic parameters were determined using a nonlinear regression program (**Figure 46**). Experimental data were fitted to Michaelis-Menten equation.

$$v = \frac{d[P]}{d[t]} = \frac{V_{\max}[S]}{K_m + [S]}$$

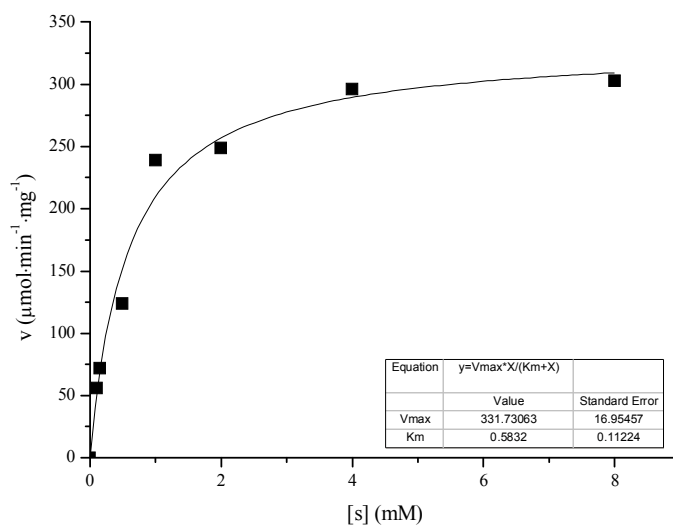


**Figure 46.** Relationship between enzyme activity and substrate concentration.

According to **Figure 46**, the Michaelis constant  $K_m$  is  $583 \mu\text{M}$ , representing the substrate concentration at which the reaction rate is half of  $V_{\text{max}}$ , and the  $V_{\text{max}}$  is  $332 \mu\text{mol}\cdot\text{min}^{-1}\cdot\text{mg}^{-1}$  of cells (dry weight).

### III.2.4 Determination of $K_i$ and CDU & CIU type of inhibition with Kau2-EH

The methods to determine the inhibition constant  $K_i$  and the type of inhibition (competitive, uncompetitive and no competitive) were previously described in literature (Cornish-Bowden, 1974; Cortes *et al.*, 2001).  $V^{-1}$  and  $S\cdot V^{-1}$  are plotted against inhibitor concentration  $I$ , at two or more values of substrate concentration  $S$ . For each  $S$  value, a straight line should be obtained. From these curves the value of  $K_i$  and type of inhibition can be determined. (**Figure 47**)

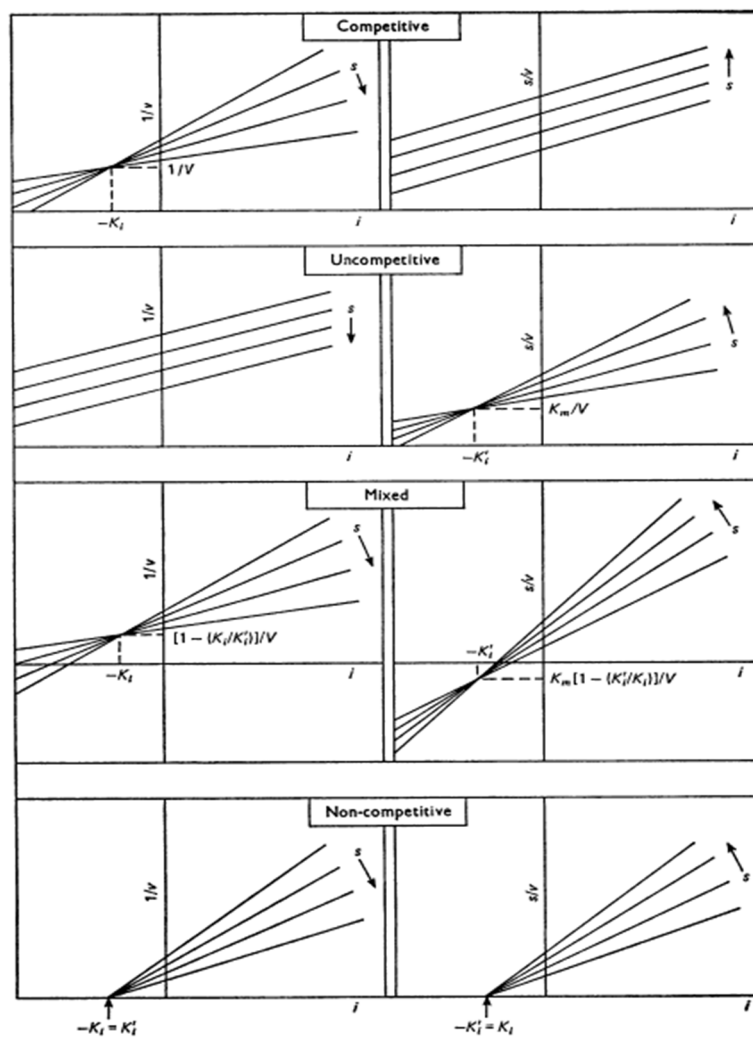


**Figure 47.** Characteristic plots for the common inhibition types (Cortes *et al.*, 2001).

### III.2.4.1. Determination of $K_i$ and CDU type of inhibition with Kau2-EH

Enzymatic reactions were carried out at 27 °C in phosphate buffer containing (*S*)-*p*ClSO ((*S*)-**1**) with inhibitor (CDU) (concentration range 30~120 nM). For the detailed protocol and HPLC analysis conditions see V.2.3 and V.5.2.

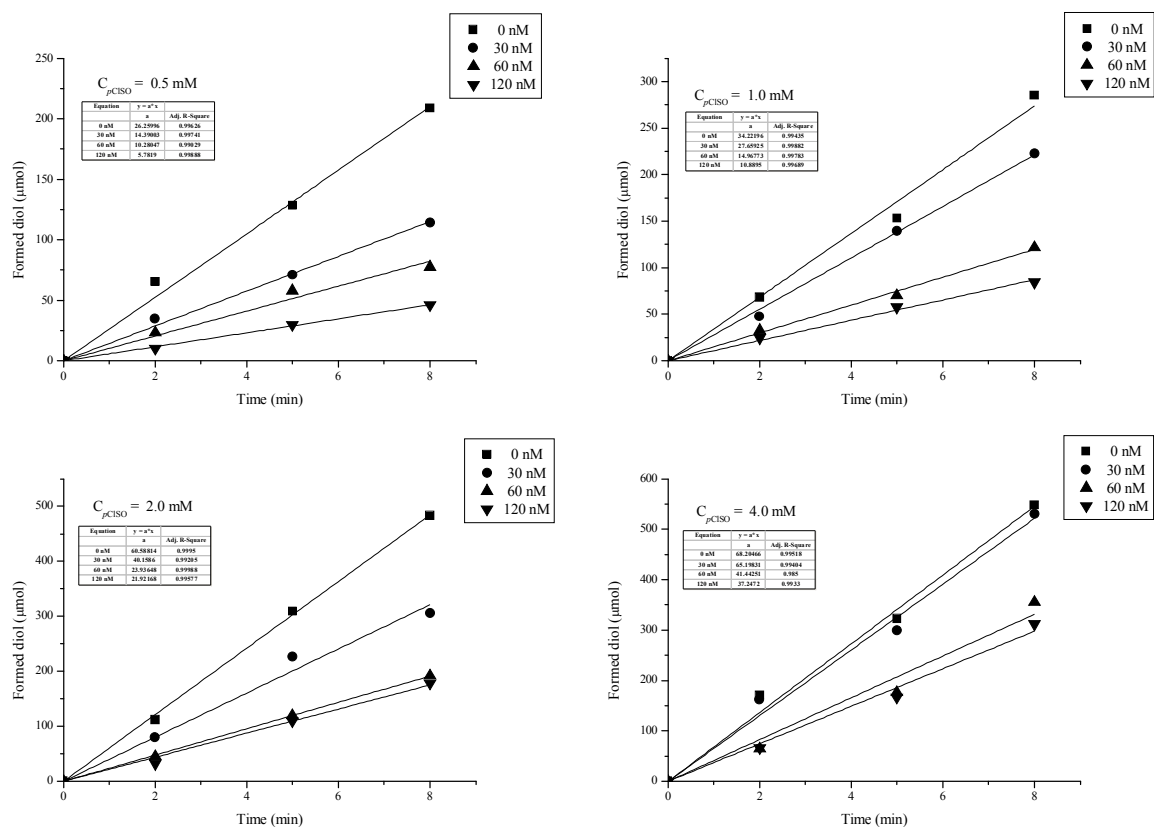


**Figure 48.** Effect of various concentrations of CDU inhibitor on EH activity at different substrate concentrations.

From **Figure 48**, the variation activities (slopes) obtained at each substrate concentration for various CDU concentrations were determined and reported in **Table 8**.

**Table 8.** Values of  $V^{-1}$  and  $S \cdot V^{-1}$  determined for various CDU inhibitor concentrations at different substrate concentrations during Kau2-EH catalyzed biohydrolysis of (*S*)-*p*CISO.

CDU	$C_{pCISO} = 0.5 \text{ mM}$	$C_{pCISO} = 1.0 \text{ mM}$	$C_{pCISO} = 2.0 \text{ mM}$	$C_{pCISO} = 4.0 \text{ mM}$
<b>I</b>	<b><math>V^{-1}</math></b>	<b><math>V^{-1}</math></b>	<b><math>V^{-1}</math></b>	<b><math>V^{-1}</math></b>
<b>(nM)</b>	<b>(<math>\text{mg} \cdot \text{min} \cdot \text{mmol}^{-1}</math>)</b>			
0	7.6	5.8	3.3	2.9
30	13.8	7.2	5.0	3.1
60	19.5	13.4	8.4	4.8
120	34.6	19.0	9.14	5.4
<b>I</b>	<b><math>S \cdot V^{-1}</math></b>	<b><math>S \cdot V^{-1}</math></b>	<b><math>S \cdot V^{-1}</math></b>	<b><math>S \cdot V^{-1}</math></b>
<b>(nM)</b>	<b>(<math>\text{mg} \cdot \text{min} \cdot \text{L}^{-1}</math>)</b>			
0	3.9	5.8	6.64	11.7
30	6.9	7.2	10.0	12.3
60	9.8	13.4	16.7	19.3
120	17.3	18.9	18.3	21.6

The plots of  $V^{-1}$  and  $S \cdot V^{-1}$  against inhibitor concentration **I** for the several **S** values are reported in **Figure 49**. Analysis of these plots clearly showed that CDU was a *competitive inhibitor* with an inhibition constant  $K_i$  of 24 nM. In competitive inhibition, the substrate and inhibitor cannot bind to the enzyme active site at same time but are in competition to access the active site. Interestingly, competitive inhibitors are often similar in structure to the true enzyme substrate.  $K_i$  reflects the strength of the interaction between the enzyme and the inhibitor. A small  $K_i$  value reflects tight binding of an inhibitor to an enzyme, whereas a larger  $K_i$  value reflects weaker binding. The low  $K_i$  value of 24 nM for CDU on Kau2-EH means that CDU is a good inhibitor and binds tightly in the active site (**Figure 49**).

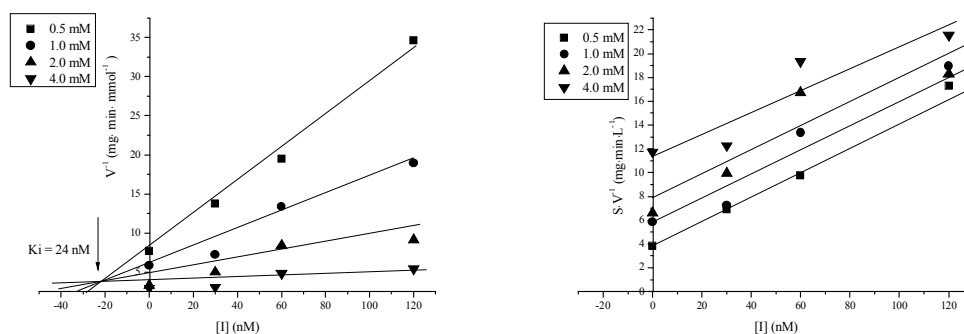


**Figure 49.** Determination of inhibition constant for CDU and type of inhibition using Kau2-EH.

### III.2.4.2. Determination of $K_i$ and CIU type of inhibition with Kau2-EH

The same protocol was used as previously described for CDU inhibitor. The results are reported in **Table 9**.

**Table 9.** Values of  $V^{-1}$  and  $S \cdot V^{-1}$  determined for various CIU inhibitor concentrations at different substrate concentrations during Kau2-EH catalyzed biohydrolysis of (*S*)-*p*CISO.

CIU	$C_{pCISO} = 0.5 \text{ mM}$	$C_{pCISO} = 1.0 \text{ mM}$	$C_{pCISO} = 2.0 \text{ mM}$	$C_{pCISO} = 3.0 \text{ mM}$
<b>I</b>	<b><math>V^{-1}</math></b>	<b><math>V^{-1}</math></b>	<b><math>V^{-1}</math></b>	<b><math>V^{-1}</math></b>
<b>(nM)</b>	<b>(<math>\text{mg} \cdot \text{min} \cdot \text{mmol}^{-1}</math>)</b>			
0	3.3	3.4	3.1	2.7
120	5.5	3.6	3.3	3.6
240	6.7	4.1	4.4	3.7
360	7.5	5.4	4.6	3.7
<b>I</b>	<b><math>S \cdot V^{-1}</math></b>	<b><math>S \cdot V^{-1}</math></b>	<b><math>S \cdot V^{-1}</math></b>	<b><math>S \cdot V^{-1}</math></b>
<b>(nM)</b>	<b>(<math>\text{mg} \cdot \text{min} \cdot \text{L}^{-1}</math>)</b>			
0	1.6	3.4	6.16	8.1
120	2.7	3.6	6.6	10.7
240	3.4	4.16	8.76	11.2
360	3.8	5.46	9.16	11.2

The plots of  $V^{-1}$  and  $S \cdot V^{-1}$  against inhibitor concentration **I** for the several **S** values are reported in **Figure 50**. Analysis of these plots clearly shows that CIU is a *competitive inhibitor* as CDU, but with a larger inhibition constant  $K_i$  of 80 nM.

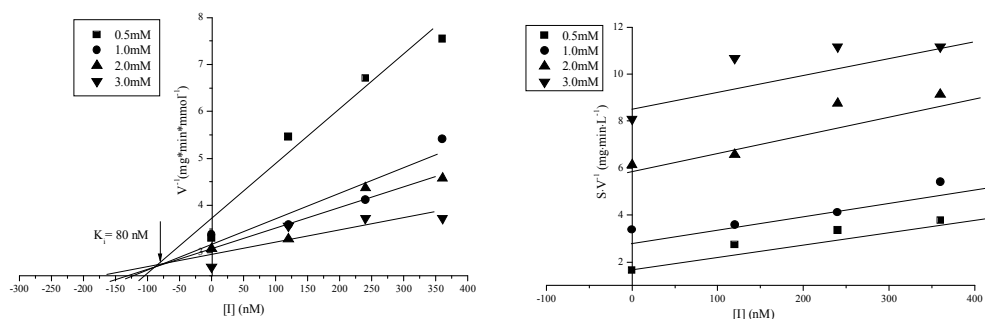


**Figure 50.** Determination of inhibition constant for CIU and type of inhibition using Kau2-EH.

In conclusion CDU and CIU were proved to be both competitive and tight-binding inhibitors of Kau2-EH.

### III.2.5 Determination of $K_i$ and CDU & CIU type of inhibition of with potato EH

A crude enzymatic extract of the potato EH was used in this study. The lyophilized powder obtained by overexpression of potato EH in *E. coli* BL21 (DE3), was available in our laboratory and was used without further purification. Enzymatic reactions were incubated at 27 °C in phosphate buffer containing 0.5 mM, 1.0 mM or 3.0 mM of (*S*)-*p*ClISO ((*S*)-**1**). The concentration range of CDU used for inhibition study was from 1000 to 1500 nM. At lower concentrations, such as 500 nM, no decrease of the reaction rate could be quantified. For the detailed protocol and HPLC analysis conditions see **V.2.3**.

The same protocol was used as previously described for CDU and CIU inhibition of Kau2-EH. The results are reported in **Table 10** and **Figure 51** and in **Table 11** and **Figure 52** for CDU and CIU respectively.

**Table 10.** Values of  $V^{-1}$  and  $S \cdot V^{-1}$  determined for various CDU inhibitor concentrations at different substrate concentrations during potato EH catalyzed biohydrolysis of (*S*)-*p*ClISO.

CDU	$C_{pClISO} = 0.5 \text{ mM}$	$C_{pClISO} = 1.0 \text{ mM}$	$C_{pClISO} = 3.0 \text{ mM}$
<b>I</b>	<b><math>V^{-1}</math></b>	<b><math>V^{-1}</math></b>	<b><math>V^{-1}</math></b>
<b>(nM)</b>	<b>(<math>\text{mg} \cdot \text{min} \cdot \text{mmol}^{-1}</math>)</b>	<b>(<math>\text{mg} \cdot \text{min} \cdot \text{mmol}^{-1}</math>)</b>	<b>(<math>\text{mg} \cdot \text{min} \cdot \text{mmol}^{-1}</math>)</b>
0	6.3	4.8	4.5
1000	9.8	7.2	4.8
1250	10.8	8.1	6.0
1500	12.0	7.9	6.7
<b>I</b>	<b><math>S \cdot V^{-1}</math></b>	<b><math>S \cdot V^{-1}</math></b>	<b><math>S \cdot V^{-1}</math></b>
<b>(nM)</b>	<b>(<math>\text{mg} \cdot \text{min} \cdot \text{L}^{-1}</math>)</b>	<b>(<math>\text{mg} \cdot \text{min} \cdot \text{L}^{-1}</math>)</b>	<b>(<math>\text{mg} \cdot \text{min} \cdot \text{L}^{-1}</math>)</b>
0	3.2	4.8	13.4
1000	4.9	7.2	14.4
1250	5.4	8.1	18.0
1500	6.0	7.9	20.1

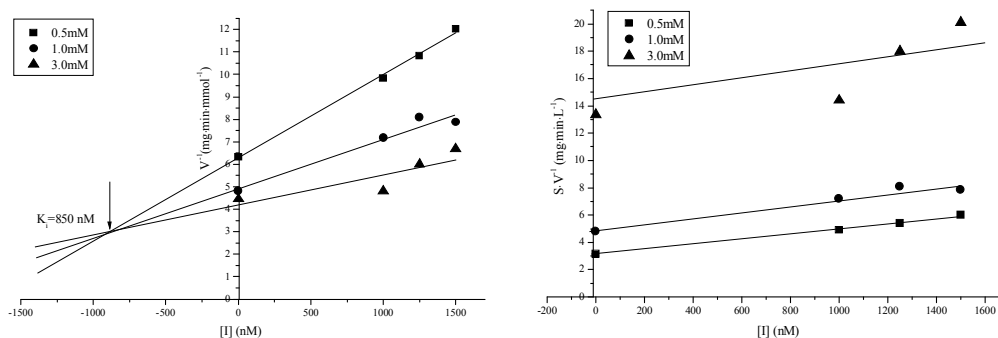


**Figure 51.** Determination of inhibition constant for CDU and type of inhibition using potato EH.

The results from **Figure 51** show that type of inhibition CDU using potato EHs is still competitive inhibition, but the inhibition constant  $K_i$  is about 850 nM, forty times higher than CDU with Kau2-EH. Therefore, it can be concluded that there is a very weaker binding of CDU with potato EHs than with Kau2-EH.

**Table 11.** Values of  $V^{-1}$  and  $S \cdot V^{-1}$  determined for various CIU inhibitor concentrations at different substrate concentrations during potato EH catalyzed biohydrolysis of (*S*)-*p*ClSO.

CIU	$C_{pClSO} = 0.5 \text{ mM}$	$C_{pClSO} = 1.0 \text{ mM}$	$C_{pClSO} = 2.0 \text{ mM}$
<b>I</b>	<b><math>V^{-1}</math></b>	<b><math>V^{-1}</math></b>	<b><math>V^{-1}</math></b>
<b>(nM)</b>	<b>(<math>\text{mg} \cdot \text{min} \cdot \text{mmol}^{-1}</math>)</b>	<b>(<math>\text{mg} \cdot \text{min} \cdot \text{mmol}^{-1}</math>)</b>	<b>(<math>\text{mg} \cdot \text{min} \cdot \text{mmol}^{-1}</math>)</b>
0	7.0	5.8	4.9
1500	10.1	8.8	6.6
2000	13.1	10.2	6.8
3000	14.2	10.4	6.4
<b>I</b>	<b><math>S \cdot V^{-1}</math></b>	<b><math>S \cdot V^{-1}</math></b>	<b><math>S \cdot V^{-1}</math></b>
<b>(nM)</b>	<b>(<math>\text{mg} \cdot \text{min} \cdot \text{L}^{-1}</math>)</b>	<b>(<math>\text{mg} \cdot \text{min} \cdot \text{L}^{-1}</math>)</b>	<b>(<math>\text{mg} \cdot \text{min} \cdot \text{L}^{-1}</math>)</b>
0	3.5	5.8	9.8
1500	5.1	8.8	13.2
2000	6.6	10.2	13.6
3000	7.1	10.4	12.9

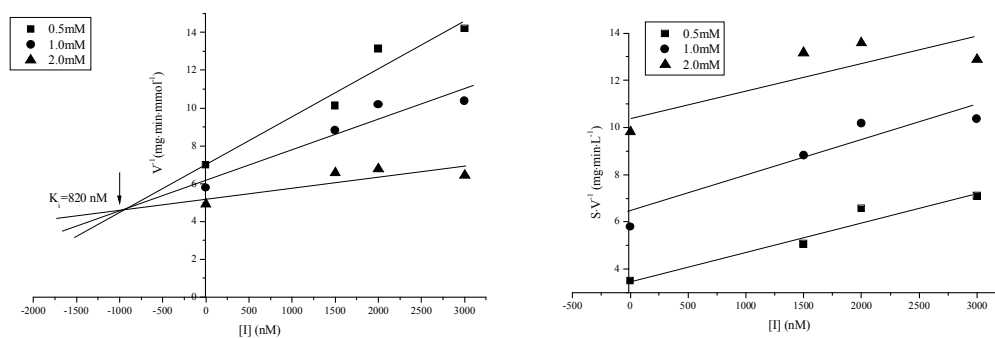


**Figure 52.** Determination of inhibition constant for CIU and type of inhibition using potato EH.

Similar results were obtained for CIU with potato EH as for CDU. The inhibition type of CIU with potato EH is still competitive, but the inhibition constant  $K_i$  (820 nM) is 16 times higher than the one of CIU towards Kau2-EH.

### III.2.6 Summary

The inhibition constants previously described for murine EH and the results obtained during this study are reported in **Table 12**.

**Table 12.** Inhibitions of CDU and CIU with murine, Kau2 and potato EHs.

	CDU	CIU
murine	competitive inhibition $K_i = 6.3$ nM	competitive inhibition $K_i = 17$ nM
Kau2-EH	competitive inhibition $K_i = 24$ nM	competitive inhibition $K_i = 80$ nM
potato EHs	competitive inhibition $K_i = 850$ nM	competitive inhibition $K_i = 820$ nM

### III.2.7 Conclusion

The purpose of this inhibition study was to select the appropriate homology model of Kau2-EH based on sequence alignment. To substantiate these computational results, two inhibitor compounds were synthesized, CDU and CIU, which were previously shown to act as potent competitive inhibitors of murine sEH with inhibition constants  $K_i$  of 6.3 and 17 nM, respectively. The behaviour of these two inhibitors was investigated using Kau2-EH and potato EHs as target. Based on the above obtained results, using Kau2-EH as a target, we determined a competitive inhibition mechanism for both CDU and CIU with  $K_i$  values of 24

and 80 nM, respectively. A second inhibition study, using the potato EH, revealed weak binding of CDU and CIU with inhibition constants exceeding 800 nM. Taking the sequence alignment and inhibition data together, the murine EH-based homology model was chosen as a guide for selecting appropriate randomization sites (**Figure 53**).

Based on this structural model, the Kau2-EH has a long L-shaped tunnel, with both ends accessible to the solvent and catalytic residues located at the bend of the “L” (**Figure. 54**), as was found in the X-ray structure of the murine EH.

The directed evolution study of Kau2-EH was performed by M. Kotik in Prague using the homology model based on X-ray structure of murine EH as a guide for saturation mutagenesis experiments, targeted at specific residues within the large substrate binding pocket. During the molecular evolution process, several enzyme variants with enhanced enantioconvergence and/or higher enantioselectivity towards *rac-p*ClSO were found. Five amino acid substitutions (W110L, F113L, F161Y, P193G and V290W) were sufficient to increase the degree of enantioconvergence from 84.2% for the wild-type enzyme to 93.0% for the final evolved EH variant, enabling the production of the chiral building block (*R*)-*para*-chlorophenylethane-1,2-diol with an enantiomeric excess of 93.0% at complete conversion of the racemic epoxide. It appears thus that the metagenome-derived Kau2-EH is amenable to the redesign of its enantioselectivity and regioselectivity properties by directed evolution using a homology model as a guide. This work has been published recently (Kotik *et al.*, 2013).

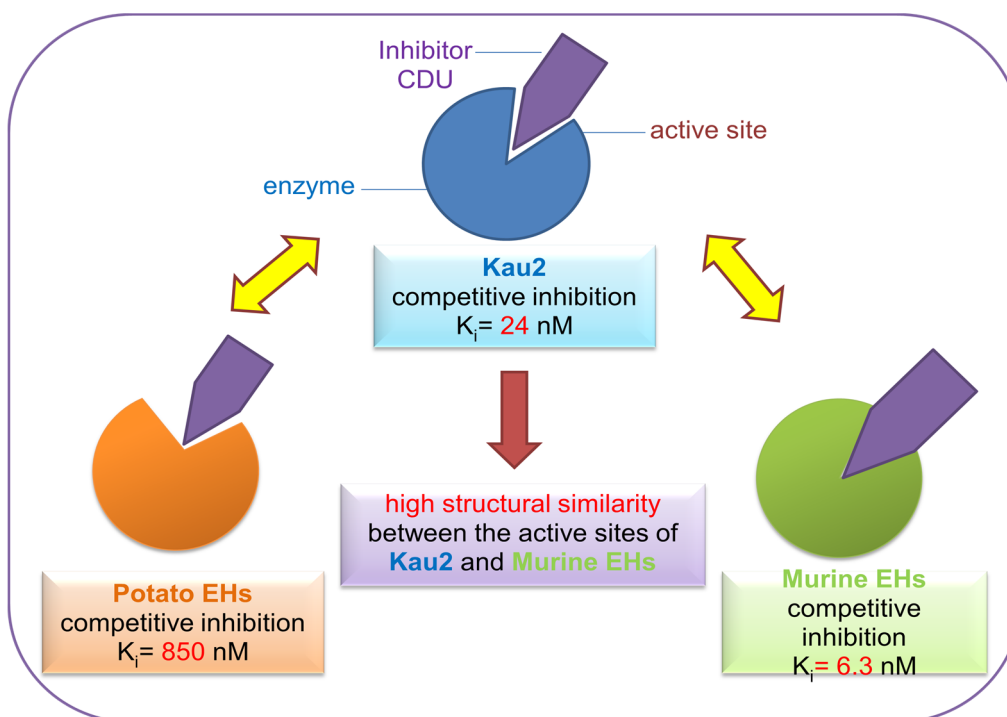


**Figure 53.** Comparison of CDU inhibition acting on murine, potato and Kau2-EHs.

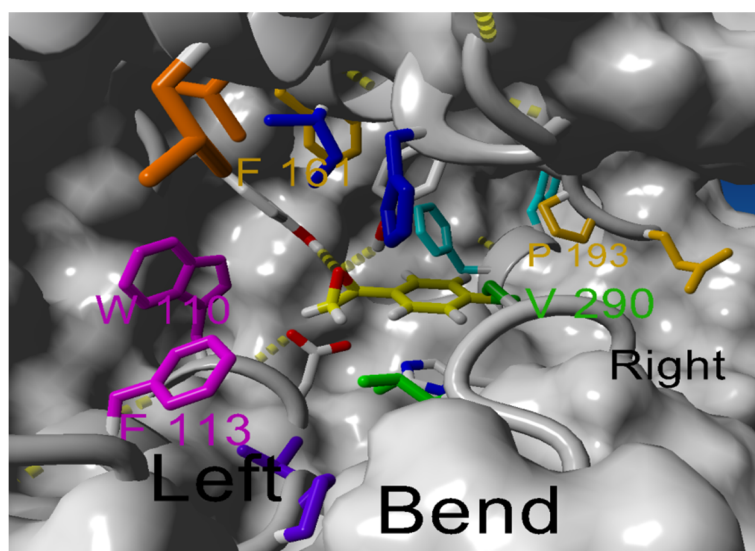


**Figure 54.** Substrate binding pocket of Kau2-EH homology model based on X-ray structure of murine EH. The *(S)*-*p*-chlorostyrene oxide (in yellow) is represented after docking (Autodock 4.0 software) in the active site of Kau2-EH. The catalytic nucleophile Asp-109, the oxirane-polarizing tyrosines Tyr-157 and Tyr-259, and the general base His-316 are depicted in grey stick representation. Important residues of sites that were randomized during the directed evolution are depicted in color.

## III.3 Bioconversion Studies

### III.3.1 Introduction

The production of enantiopure compounds has become more and more important because of the increasing needs for manufacturing chiral drugs as single stereoisomers (Dehli and Gotor, 2002). Epoxide hydrolases (EHs) are very efficient biocatalysts that are able to catalyze enantioselective and regioselective hydrolysis of epoxides (Archelas and Furstoss, 1997; Steinreiber and Faber, 2001; Yudin, 2006). This versatility make them very useful in order to prepare enantiopure epoxides and diols, compounds that are highly valuable chiral synthons used in numerous synthesis of biologically actives molecules (Archelas and Furstoss, 1998). The aim of the bioconversion studies described in this chapter was to explore the possibility of using Kau2-EH as a biocatalyst for the synthesis of very useful chiral compounds starting from various aromatic epoxides as substrates. Indeed Kau2-EH proved recently to be of interest for the kinetic resolution and enantioconvergent deracemization of respectively *trans*- and *cis*-methyl styrene oxide (Kotik *et al.*, 2010) Indeed the enzyme exhibited a E value of more than 200 in the former case and proved to be enantioconvergent in the latter case affording i) (1*R*,2*R*)-*trans*-methyl styrene oxide in 99.3% ee and 48% yield as well as (1*R*,2*S*)-1-phenyl-2,3-dihydroxy propane in 99.5% ee and 46% yield and ii) (1*R*,2*R*)-1-phenyl-2,3-dihydroxy propane in 98.3% ee and 97% yield respectively (**Figure 55**).

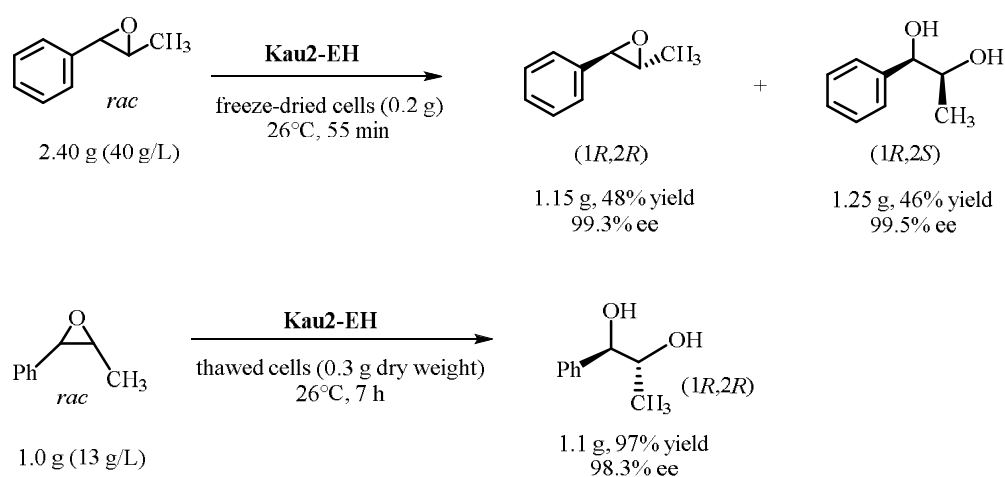


**Figure 55.** Preparative kinetic resolution of *trans*-methyl styrene oxide and enantioconvergent deracemization of *cis*-methyl styrene oxide using Kau2-EH as catalyst (Kotik *et al.*, 2010).

In order to further explore the chemical space to be reached with such an enzyme, we tested various aromatic racemic epoxides as Kau2-EH substrates, some of them being of potential synthetic interest as they could be used in the synthesis of highly relevant biologically active compounds such as Taxol, Diltiazem, Clausenamide, Cytosazole, Leiocarpin C and Gonodiol. Indeed some of the tested substrates were bi-functional expanding thus their synthetic utility. We described here the kinetic resolution of methyl-phenyl-glycidate-**4**, ethyl-phenyl-glycidate-**5**, methyl-*p*-methoxy-phenyl-glycidate-**6**, *cis*- and *trans*-cyano-phenyl-glycidate -**7** and -**8**, *trans*-bromomethyl-styrene-oxide-**9**, *trans*-chloromethyl-styrene-oxide-**10** and *trans*-stilbene-oxide-**11** as well as the desymmetrization of *cis*-stilbene-oxide-**12** using lyophilized cells of *E. coli* overexpressing Kau2-EH as biocatalyst.

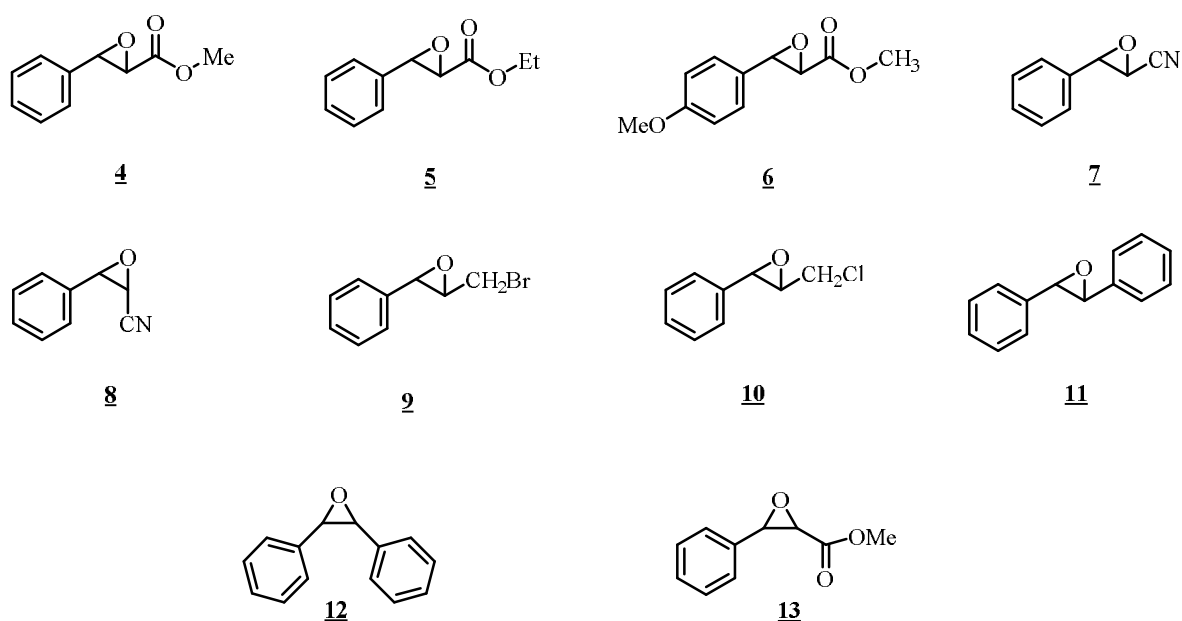


**Figure 56.** Aromatic epoxides tested as potential substrates of Kau2-EH as catalyst.

In the following the chemical synthesis of some racemic epoxides as potential Kau2-EH substrates will be first described, then how the biocatalyst Kau2-EH was obtained and thereafter the bioconversion reactions will be described each, first on the analytical scale then on the preparative scale.

### III.3.2 Chemical Synthesis

The racemic epoxides **4**, **5**, **7**, **8**, **9**, **10** and **13** were obtained by chemical synthesis. The other epoxides **6**, **11**, and **12** were commercial products.

#### III.3.2.1 Synthesis of *rac-trans*-ethyl-3-phenylglycidate-**5** and of *rac-trans*-methyl-3-phenylglycidate-**4**

The synthesis of *rac*-**5** was carried out as described previously (Saikia *et al.*, 2010) (**Figure 57**). In a first step 10 g of Chloroamine-T and 2 mL of bromine were mixed in water yielding a yellow precipitate. After washing and drying 10.54 g of Dibromoamine-T (91% yield) were recovered as a yellow solid. In a second step and starting from 5.5 mmol of *trans*-Methyl-cinnamate and 11 mmol of Dibromoamine-T an intermediate bromohydrin is formed in aqueous acetonitrile in 10 minutes. Thereafter, the cyclisation to the desired epoxide is performed by adding 7.5 mmol K<sub>2</sub>CO<sub>3</sub> and leaving the reaction stirred at room temperature for 45 minutes. In that case the yield in expected epoxide was only 13% as compared to 70 % in the original publication. In order to improve this yield we first added 5 times more potassium carbonate as originally described, raising the yield of *rac*-**5** to 51.6%. A further improvement was obtained by leaving the cyclisation reaction overnight instead of 45 minutes. A yield of 77.7% was thus obtained affording 0.82 g of *rac-trans*-ethyl phenylglycidate-**5** something judged sufficient to our purpose. The optimization of this reaction is reported in **Table 13**.

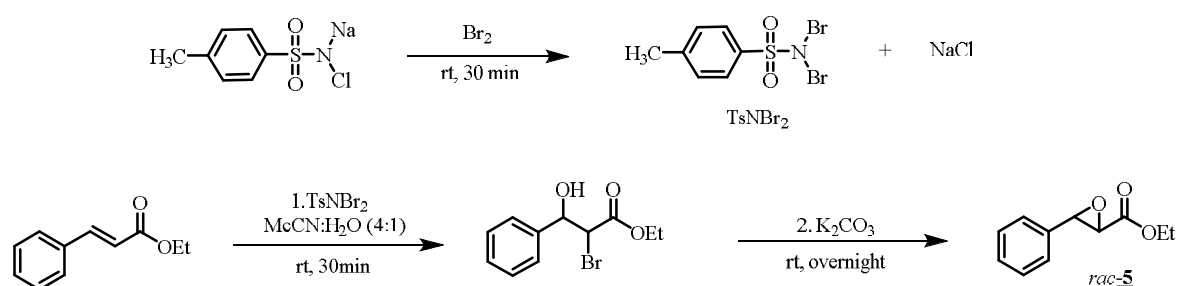


**Figure 57.** Synthesis of *rac*-**5**.

**Table 13.** Comparison of the different conditions used for the synthesis of *rac-5*.

Reaction	Reaction time (first step)	Reaction time (second step)	<i>trans</i> -Ethyl-cinnamate	K <sub>2</sub> CO <sub>3</sub>	Yield ( <i>rac-5</i> )
1	10 min	45 min	5.5 mmol	7.5 mmol	13.3%
2	10 min	45 min	5.5 mmol	37.5 mmol	51.6%
3	10 min	Overnight	5.5 mmol	37.5 mmol	77.7%

The synthesis of *rac-4* was performed similarly to the optimized one of *rac-5* described above (**Figure 58**). After purification, 0.81g of *rac-trans*-methyl-phenylglycidate-**4** was obtained in 82% yield as a colourless liquid. The epoxide was stored at -20 °C.

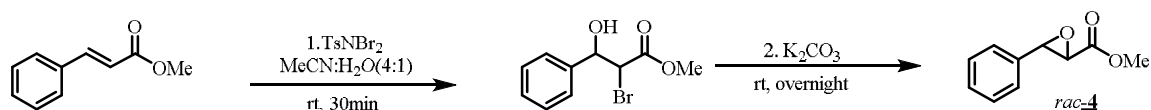


**Figure 58.** Synthesis of *rac-4*.

### Summary

The preparation of the two *rac*-epoxides-**4** and -**5** following a previously described procedure and adapted to our targets, was achieved. Some practical improvements were realized in order to reach reasonable overall yields:

- 1) The added quantity of K<sub>2</sub>CO<sub>3</sub> was crucial to attain a high overall yield. Putting 5 times more K<sub>2</sub>CO<sub>3</sub>, largely increase the yield in epoxide.
- 2) The second step should be longer in order to form more epoxide. Changing the reaction time from 45 min to overnight allowed the yield to increase from 51.6% to 77.7%.

### III.3.2.2 Synthesis of *cis*- and *trans*-2,3-epoxy-3-phenylpropanenitrile-**7** and -**8**

The synthesis of *rac-7* and -**8** was carried out as described previously (Mhamdi *et al.*, 2011) (**Figure 59**).

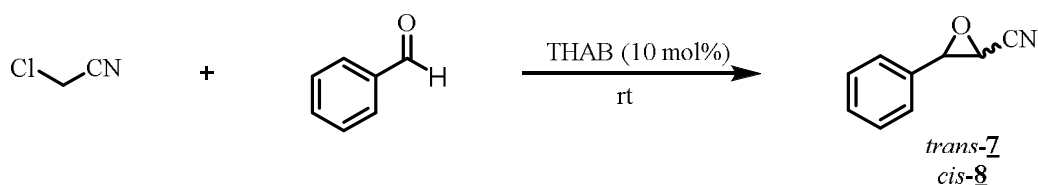


**Figure 59.** Synthesis of *rac*-7 and 8.

The Darzens reaction of  $\alpha$ -chloroacetonitrile using tetrahexylammonium bromide (THAB) as the phase transfer catalyst was carried out by starting from benzaldehyde (380 mg, 3.0 mmol), chloroacetonitrile (450 mg, 6.0 mmol) and KOH (400 mg, 7.2 mmol) in Tetrahydrofuran (15 mL). After 22 h, the products were purified by flash chromatography affording 0.09 g of *trans*-epoxide-7 as a colourless liquid in 22.5% yield and 0.16 g of *cis*-epoxide-8 as a white solid in 39.6% yield.

### III.3.2.3 Synthesis of *rac-trans*-2-Bromomethyl-3-phenyloxirane 9 and *rac-trans*-2,3-epoxy-3-phenyl-1-chloro propane-10

The synthesis of *rac*-9 and *rac*-10 were carried out as described in the following (**Figure 60**) using *meta*-Chloro-peroxybenzoic acid (*m*CPBA) as the epoxidation agent.

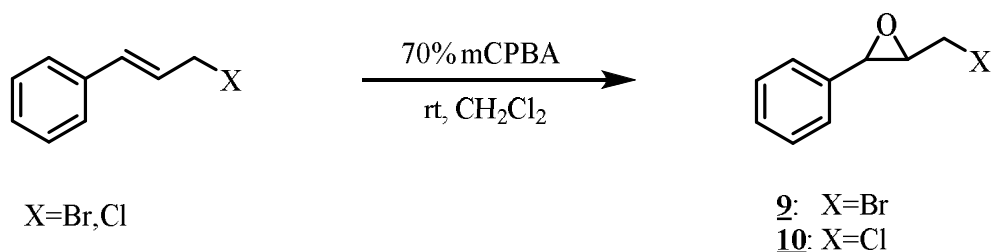


**Figure 60.** Synthesis of *rac*-9 and *rac*-10.

A mixture of *m*CPBA (8.5 mmol) and cinnamyl bromide (571 mg, 2.9 mmol) was reacted at 25 °C for 17 h. After purification, 0.302 g of *rac-trans*-2-bromomethyl-3-phenyloxirane-9 was obtained in 48.9% yield as a yellow liquid. The same conditions were used for the synthesis of *rac-trans*-2,3-epoxy-3-phenyl-1-chloro-propane-10. After purification, 0.275 g *rac*-10 was obtained in 52.1% yield as a colourless liquid.

### III.3.2.4 Synthesis of *rac-cis*-methyl-phenylglycidate-13

The synthesis of *rac*-13 was carried out as described previously (Svoboda *et al.*, 1988) (Figure 61) and is based on the easy transformation of *cis*-2,3-epoxy-3-phenylpropanenitrile-8 into the corresponding methyl ester-13.

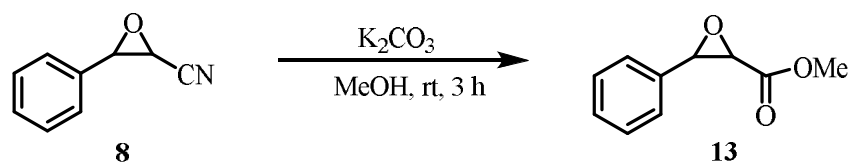


Figure 61. Synthesis of *rac*-13.

A mixture of *cis*-2,3-epoxy-3-phenylpropanenitrile-8 (0.302 g, 2 mmol), dry potassium carbonate (0.289 g, 2.0 mmol) and distilled methanol (10 mL) was stirred at room temperature for 3 hours. The crude product was purified by flash chromatography affording 0.287 g of *rac-cis*-methyl-phenylglycidate-13 (80.1% yield) as a colourless liquid.

### III.3.3 Kau2-EH production in fermentor

Kau2-EH was obtained as previously described by Kotik (Grulich *et al.*, 2011) in *E. coli* (DE3) Star. The overexpressions were carried out in Flasks and in Fermentor. The obtained cells were stored in the fridge as a lyophilized powder. From all these experiments several stock of lyophilized cells, showing different activity, were use along this work. (See V.4)

### III.3.4 Bioconversion using Kau2-EH

#### III.3.4.1 Bioconversion of *rac-trans*-methyl-phenylglycidate-4

The *rac-trans*-methyl-phenylglycidate-4 is an interesting easily accessible bi-functional compound bearing both an epoxide and a methyl ester functionality allowing thus further transformation. Indeed one of its enantiomer has been used in the synthesis of the side chain of Taxol<sup>TM</sup>. Paclitaxel (Taxol<sup>TM</sup>), an anti-microtubule agent isolated from the bark of

*Taxus brevifolia*, has recently attracted much attention because of its efficacy in the treatment of various types of cancer (McGuire *et al.*, 1989; Rowinsky *et al.*, 1990).

The enantiopure epoxide *trans*-2*S*,3*R*-methyl-phenyl-glycidate (that could arise from the enantioselective hydrolysis of the corresponding racemate through EH catalysis) was used to synthesize the side chain of Paclitaxel (Taxol™) (Figure 62) (Hamamoto *et al.*, 2000).

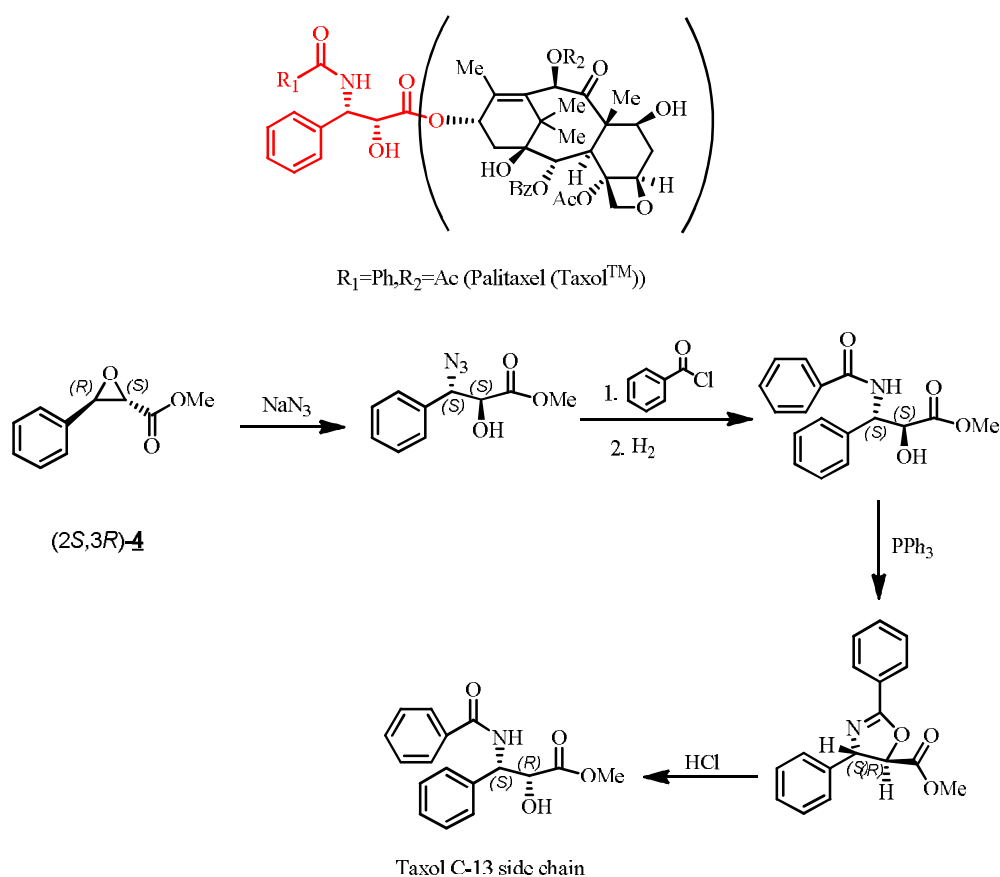


**Figure 62.** Structure of Paclitaxel (Taxol™) and synthesis of its side chain using *trans*-2*S*,3*R*-methyl phenyl glycidate (Afon'kin *et al.*, 2012).

Clausenamide, as a racemate, was isolated from the leaves of *Clausena lansium* (Lour) Skeels (Yang *et al.*, 1987). Its chemical structure contained four asymmetric carbons and thus eight pairs of enantiomers. A pair of them, whose absolute configurations were 3*S*, 4*R*, 5*R*, 6*S* and 3*R*, 4*S*, 5*S*, 6*R*, were named (-)-Clausenamide and (+)-Clausenamide, respectively. Pharmacological studies revealed that (+)-Clausenamide was a distomer, whereas (-)-Clausenamide was an active eutomer with great potential for treatment of Alzheimer's disease (Zhu *et al.*, 2004). The enantiopure epoxide *trans*-2*S*,3*R*-methyl-phenyl-glycidate-**4** could be

use as starting material for the chemical enantioselective synthesis of (-)-Clausenamide (Zheng *et al.*, 2006) (**Figure 63**).

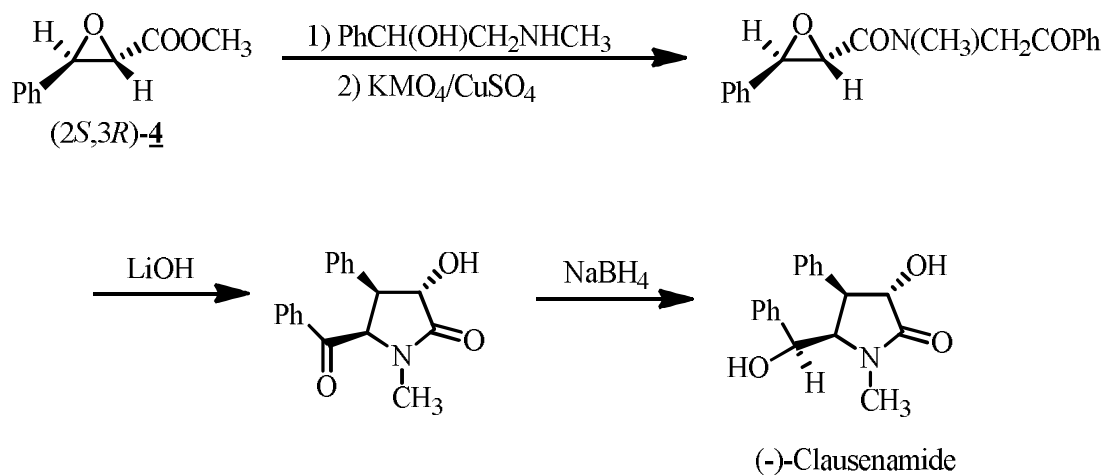
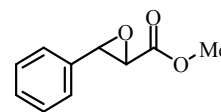


**Figure 63.** Synthesis of (-)-Clausenamide using *trans*-2*S*,3*R*-methyl-phenyl-glycidate-**4** (Zheng *et al.*, 2006).

#### III.3.4.1.1 Analytical scale study of *Kau2-EH* catalysed bio-hydrolysis of *rac-trans*-methyl-phenylglycidate-**4**

In order to meet industrial desirability, there are some major requirements for EH biotransformation to be achieved: high enantioselectivity, acceptable activity, high substrate concentration and process stability. In order to test these requirements the analytical scale bioconversion of *rac*-**4** was explored focusing on the following points:



**4**

- 1) Study of enzyme stability under the used reaction conditions.
- 2) Optimization of reaction conditions, like substrate and biocatalyst concentrations, nature and concentration of used co-solvent.
- 3) Conducting the bio-hydrolysis at high substrate concentration, exploring the possible inhibitory effects of substrate and product.

#### III.3.4.1.2 Stability of *Kau2-EH* under the used reaction conditions

A preliminary set of reaction conditions was chosen to conduct Kau2-EH catalysed reaction:

- Solvent: phosphate buffer (pH 7.0, 50 mM)
- Co-solvent: isooctane 10%
- Temperature: 27 °C
- Magnetic stirring: 1200 rpm
- *rac*-**4** concentration: 25 g/L
- Kau2-EH concentration: 50 g/L (780 U/mg)

In order to test stability, the enzyme was either incubated 1 h under the defined reaction conditions before substrate addition or directly incubated in presence of substrate. The reaction was followed by chiral GC, analysing the ee of the remaining epoxide during the time course of the biocatalyzed reaction (**Figure 64**) (**Annexe 2**).

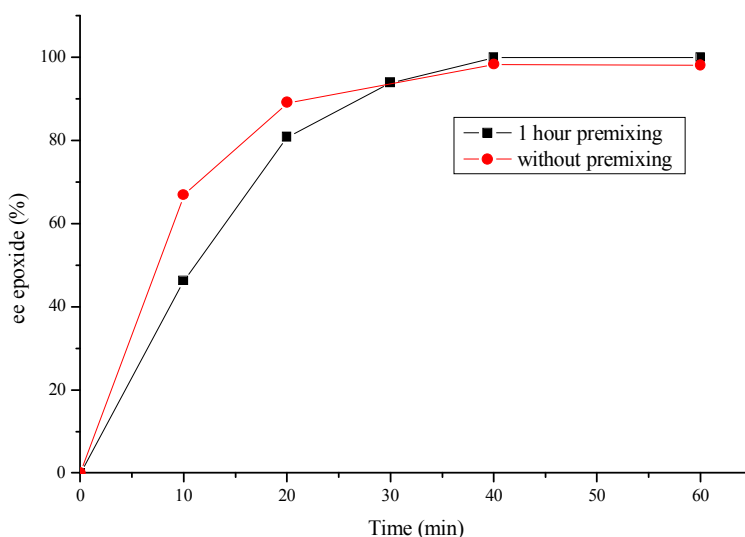


**Figure 64.** Evolution of the ees of the remaining epoxide-**4** during stability test of Kau2-EH.

From this result, it appears that Kau2-EH is stable under the tested reaction conditions. Indeed an ee of nearly 100% is obtained after 40 minutes for epoxide-**4** in both cases.

### ***III.3.4.1.3 Optimization of the reaction conditions***

Many examples of valuable asymmetric hydrolysis of racemic epoxides using EHs have been described. However a general limitation of EH-catalyzed hydrolysis is that

numerous epoxide substrates are poorly water-soluble limiting thus their availability to the active site of the biocatalyst. Typically, the solubility of epoxides such as styrene oxide is less than 5 g/L at 30 °C. The use of a biphasic system is a well-established tool for bioconversion reaction and especially those involving EHs (Wubbolts *et al.*, 1996). In that case both substrate solubility and stability problems found in water-based reaction media could be overcome by using an organic solvent as the second phase. Selection of a suitable organic solvent is thus a key factor to be tested as well as the volume ratio between the two non-miscible phases.

Isooctane, ethyl acetate and di-isopropyl ether were tested as immiscible co-solvents at 10% concentration (v/v). The enzymatic reactions were carried out using Kau2-EH at a concentration of 100 g/L when *rac*-**4** concentration was set at 50 g/L. As previously described, the reaction was followed by chiral GC, analysing the ee of the remaining epoxide during the time course of the biocatalyzed reaction (**Figure 65**).

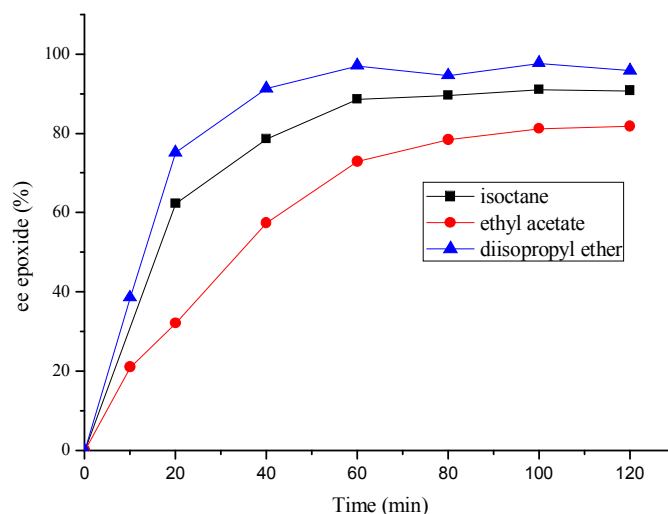


**Figure 65.** Evolution of the ees of the remaining epoxide-**4** as influenced by different types of co-solvent during the Kau2-EH catalyzed kinetic resolution of *rac*-**4**.

From the above results the use of di-isopropyl ether was a better choice since higher ees were obtained than for isooctane and ethyl acetate.

Based on the above results, different concentrations of di-isopropyl ether were tested in the range 10% to 30% (**Figure 66**), the concentrations of Kau2-EH and *rac*-**4** being

unchanged.

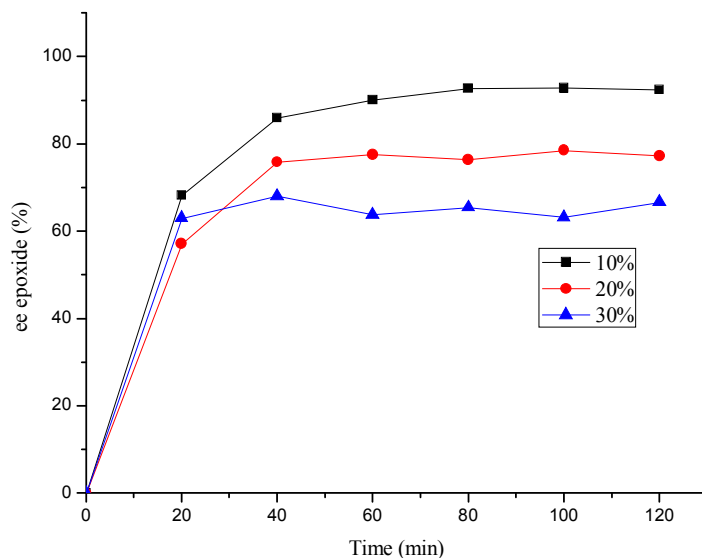


**Figure 66.** Evolution of the ees of the remaining epoxide-4 as influence by various di-isopropyl ether concentrations (10-30%, v/v) during the Kau2-EH catalyzed kinetic resolution of *rac*-4.

According to **Figure 66**, the highest is the co-solvent concentration, the lowest is the ee of the remaining epoxide. At 30% di-isopropyl ether concentration the highest reached ee was around 65% while at 10% concentration the achieved ee was 92%. In order to have a balance between solubility of substrate in the reaction system and decrease activity at high organic solvent concentration, 10% di-isopropyl ether was used in the following.

#### ***III.3.4.1.4 Analytical scale bio-hydrolysis of *rac*-4 at various substrate concentrations using Kau2-EH***

Whatever the design catalytic process, a key to success is the ability to conduct the reaction of interest at the highest possible substrate concentration using the lowest quantity of catalyst in the shortest period of time in order to access the highest possible volumetric productivity. In a first series of experiment we tested concentrations of *rac*-4 in the 1-75 g/L range and adapt the Kau2-EH concentration (1667 U/mg) in order to try to reach an ee of more than 99% for the remaining epoxide in one hour.

In the series of experiments described below (10% di-isopropyl ether (v/v), 27 °C), the evolution of the ees of the remaining epoxide-4 was followed by chiral GC over a two hour

period of time using two times more Kau2-EH than substrate on a mass basis (m/m). It was found that the ees of the remaining epoxide reached very high values (more than 99%) within one hour at substrate concentrations up to 25 g/L and that for substrate concentrations of 50 and 75 g/L the ees of the remaining epoxide levelled at 95% and 65% respectively (**Figure 67**).

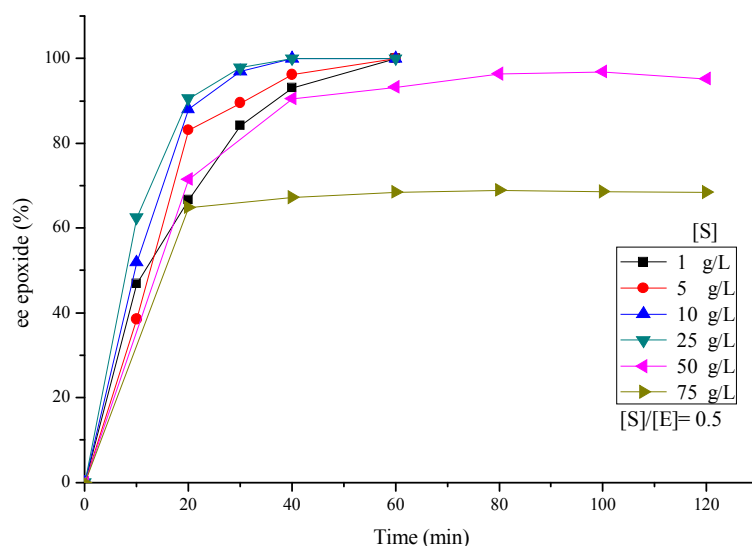


**Figure 67.** Evolution of the ees of the remaining epoxide-**4** during the Kau2-EH catalyzed kinetic resolution of *rac*-**4** at different substrate concentration [S] (1-75 g/L), the ratio of [S]/[E] was 0.5.

It should be noted that the ee-value of the formed diol was over 99% for all experiments (**Annexe 2**) and that addition of fresh biocatalyst did not increase the ee of remaining epoxide-**4** at 50 and 75 g/L substrate concentration (data not shown). According to the results described in **Figure 67** we were pleased to note that for substrate concentrations up to 25 g/L, Kau2-EH displayed nearly perfect kinetic resolution of *rac*-**4**. Indeed the ee-values of both remaining epoxide and formed diol reached more than 99% within one hour. For substrate concentrations higher than 25 g/L, we can notice a clear decrease of the ees of the remaining epoxide upon increasing substrate concentration.

At this point there are two different hypotheses that can be proposed to explain this feature observed at high substrate concentrations.

- 1) *The formed diol during bio-hydrolysis was an inhibitor.*
- 2) *The used enzyme concentration (over 50 g/L) is detrimental to the reaction.*

In order to answer these two questions further experiments were conducted.

### 1) Is the formed diol an inhibitor of the reaction?

At high *rac*-**4** substrate concentrations, the formed diol concentration also reached high titre and could thus have an inhibitory effect on the bio-hydrolysis of *rac*-**4**. If true, this phenomenon arose for diol concentrations higher than 25 g/L since when the bio-hydrolysis is carried out at 50 g/L of *rac*-**4**, the ees of the remaining epoxide blocked at 95%. Therefore we ran the bio-hydrolysis of *rac*-**4** at 5 and 25 g/L substrate concentration using Kau2-EH at 10 or 50 g/L respectively in the presence or absence of 25 g/L of the enantiomerically pure diol-**4d** formed in the normal bioconversion of *rac*-**4** using Kau2-EH, and added at the start of bio-hydrolysis.

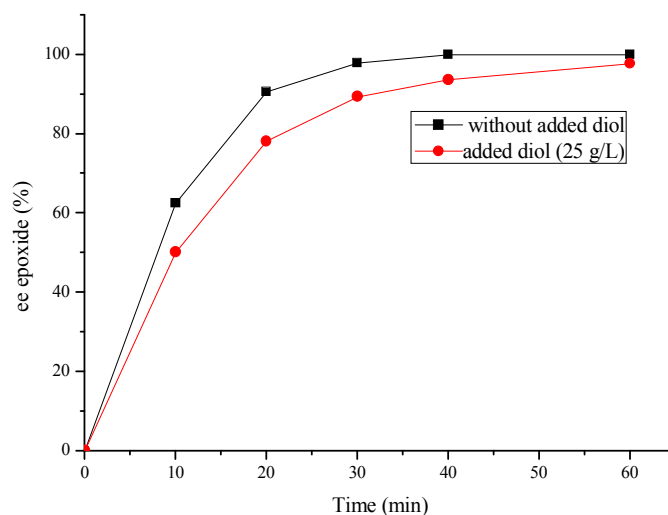


**Figure 68.** Evolution of the ees of the remaining epoxide-**4** during the Kau2-EH catalyzed kinetic resolution of *rac*-**4** (25 g/L) in absence or in presence of diol-**4d** (25 g/L).

From the reported results (**Table 14** and **Figure 68**), the addition of 25 g/L diol-**4d** at the beginning of the reaction did not influence dramatically the course of the reaction. A slight decrease of the final ee was observed for the remaining epoxide (97.3% instead of >99%) at substrate concentration of 25 g/L in the presence of 25 g/L diol-**4d**. Analysis of the results described in **Table 14** and **Figure 68** do not allow getting a clear picture of the

observed phenomenon. It should be notice that in this case, the diol-**4d** is exogenously added in the reaction mixture and thus we probably did not match exactly what was really happening within the cells. Indeed much higher diol quantities could accumulate in the cells under turnover conditions, something that the exogenous addition of diol could probably not reproduce perfectly. From the above experiments no clear conclusion could be drawn about an inhibitory effect of diol-**4d**.

**Table 14.** Kau2-EH bio-hydrolysis of *rac-4* at two substrate concentrations (5 and 25 g/L) in absence or presence of 25 g/L diol-**4d**.

Reaction	Concentration of <i>rac-4</i> (g/L)	Concentration of Kau2-EH (g/L)	Concentration of diol- <b>4d</b> (g/L)	ee% of the remaining epoxide (at 60min)	ee% of the formed diol (at 60min)
1	5	10	0	>99%	>99%
2	5	10	25	>99%	>99%
3	25	50	0	>99%	>99%
4	25	50	25	97.3%	>99%

## 2) What is the influence of the substrate-over-enzyme ratio (S/E)?

In order to explain the observed decrease in final epoxide ees at high substrate concentrations, we then tested the initial substrate-over-enzyme ratio (S/E) on the evolution of the ees of the remaining epoxide during biocatalysis. In order to do so, we conducted the kinetic resolution of *rac-4* at a fixed concentration of 50 g/L by varying the enzyme concentration in order to test S/E ratio ranging from 1 to 0.33.

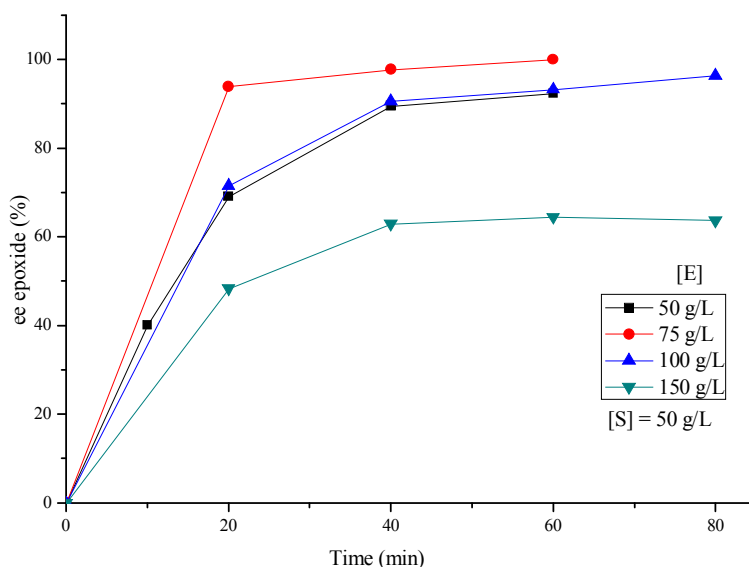


**Figure 69.** Evolution of the ees of the remaining epoxide-**4** during the Kau2-EH catalyzed kinetic resolution of *rac*-**4** at a fixed substrate concentration of 50 g/L and varying S/E ratio ranging from 1 to 0.33.

**Table 15.** Biohydrolysis of *rac*-**4** (50 g/L) with Kau2-EH at different S/E ratio.

Reaction	Concentration of <i>rac</i> - <b>4</b> (g/L)	Concentration of Kau2-EH (g/L)	Substrate-over-enzyme ratio (S/E) <sup>a</sup>	ee% of the remaining epoxide (at 60 min)	ee% of the formed diol (at 60 min)
1	50	50	1	92.3%	>99%
2	50	75	0.67	>99%	>99%
3	50	100	0.5	96.3%	>99%
4	50	150	0.33	63.7%	>99%

<sup>a</sup> Substrate-over-enzyme ratio (S/E): substrate concentration (g/L) divided by the enzyme concentration (lyophilized whole cells, g/L).

As shown in **Table 15** and **Figure 69**, the S/E ratio had a considerable effect on the ees of the remaining epoxide. Counterintuitively the highest the biocatalyst concentration, the worst were the ees of the remaining epoxide. This result could eventually be explained by the formation of a sticky phase within the reaction vessel probably due to the simultaneous presence of high cell concentration and of an organic solvent. For the used 50 g/L concentration of epoxide-**4** there was clearly an optimum in the biocatalyst concentration since for an S/E ratio of 0.67 an ee of more than 99% for the remaining epoxide could be

reached. Thus a sufficient quantity of biocatalyst should be present in the reaction but not too much in order to reach the expected more than 99% ee for the remaining epoxide.

Another experiment run at 75 g/L of epoxide-**4** and an S/E ratio ranging from 0.375 to 0.75 did not provide much more information except than in this case the ees of the remaining epoxide could not reach >99% (**Table 16** and **Figure 70**).

**Table 16.** Kau2-EH catalyzer biohydrolysis of *rac*-**4** (70 g/L) at different S/E ratio.

Reaction	Concentration of <i>rac</i> - <b>4</b> (g/L)	Concentration of Kau2-EH (g/L)	Substrate-over-enzyme ratio (S/E) <sup>a</sup>	ee% of the remaining epoxide (at 60 min)	ee% of the formed diol (at 60 min)
1	75	100	0.75	76.4%	100%
2	75	150	0.5	68.4%	100%
3	75	200	0.375	60.5%	100%

<sup>a</sup> Substrate-over-enzyme ratio (S/E): substrate concentration (g/L) divided by the enzyme concentration (lyophilized whole cells, g/L).

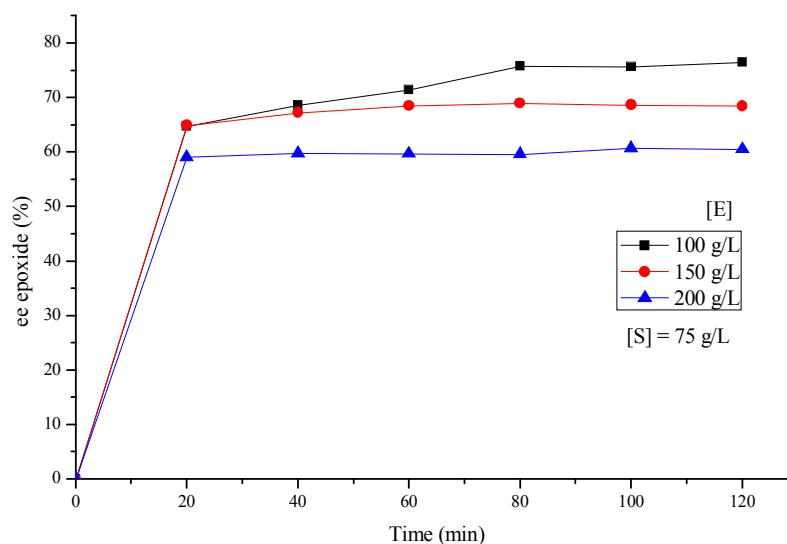


**Figure 70.** Evolution of the ees of the remaining epoxide during the bio-hydrolysis of *rac*-**4** (75 g/L) using Kau2-EH at different substrate-over-enzyme ratio.

These combined results do not give a clear answer to the impossibility to reach both very high substrate concentrations (> 50 g/L) and nearly perfect kinetic resolution for *rac*-**4**

when using Kau2-EH as biocatalyst. It should be remembered that adding fresh cells to the reaction, when the ees of the remaining epoxide had levelled, did not allow the reaction to go further nor to increase epoxide ees. It should be also mentioned that, the highest were both concentrations of epoxide and biocatalyst, the quickest the ees of the remaining epoxide levelled. From the previous experiments it has been shown that it was possible to use a 50 g/L concentration for substrate *rac*-**4**, with an S/E ratio of 0.67 and still performed a nearly perfect kinetic resolution. Thus in order to perform the reaction on a higher scale, to isolate sufficient quantities of both remaining epoxide and formed diol and to determine their absolute configurations, the reaction was conducted on a preparative scale.

#### III.3.4.1.5 Preparative kinetic resolution of *rac*-**4** at 50 g·L<sup>-1</sup> on the 1 g scale

Using the optimized conditions described above, the kinetic resolution of *rac*-**4** was conducted on a 1 g preparative scale for 80 minutes (**Figure 71**), affording after extraction and purification (2*S*,3*R*)-**4** in 49% isolated yield (490 mg, ee>99%) and (2*R*,3*R*)-**4d** in 46.8% isolated yield (520 mg, ee>99%).

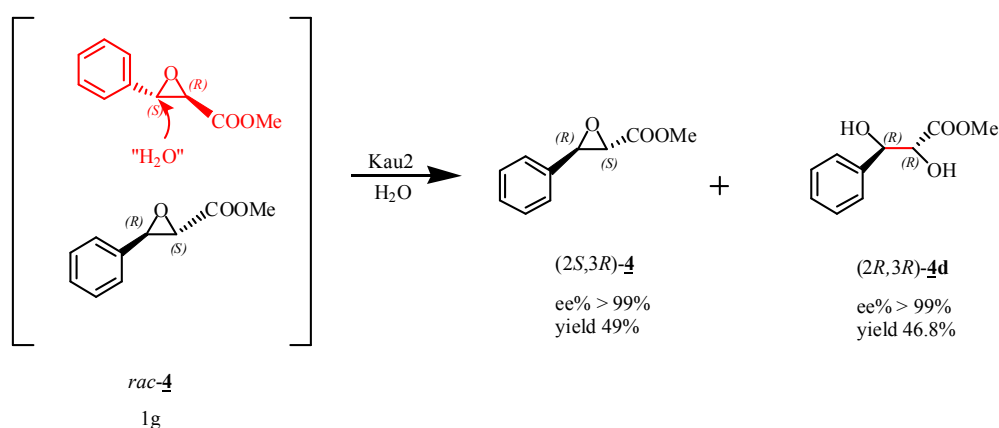


**Figure 71.** Preparative scale (1 g) bio-hydrolysis of *rac*-**4** using Kau2-EH.

Absolute configurations have been determined through comparison of available optical rotations found in the literature (**Table 17**).

**Table 17** Optical rotations and absolute configurations of isolated products obtained from preparative scale bio-hydrolysis of *rac*-**4**.

Compound	Abs. conf./ee/[ $\alpha$ ] <sub>D</sub> <sup>a</sup>	Abs. conf./ee/[ $\alpha$ ] <sub>D</sub> <sup>b</sup>	Reference
<b>4</b>	(2 <i>S</i> ,3 <i>R</i> )/99% [ $\alpha$ ] <sub>D</sub> <sup>15</sup> = + 171.9° (c=1.0,CHCl <sub>3</sub> )	(2 <i>S</i> ,3 <i>R</i> )/99% [ $\alpha$ ] <sub>D</sub> <sup>15</sup> = +170.9° (c=1.3,CHCl <sub>3</sub> )	(Zheng <i>et al.</i> , 2006)
<b>4d</b>	(2 <i>R</i> ,3 <i>R</i> )/99% [ $\alpha$ ] <sub>D</sub> <sup>22</sup> = - 44° (c=0.48,CHCl <sub>3</sub> )	(2 <i>R</i> ,3 <i>R</i> )/99% [ $\alpha$ ] <sub>D</sub> <sup>22</sup> = - 41.3° (c=0.48,CHCl <sub>3</sub> )	(Matthews <i>et al.</i> , 1990)

<sup>a</sup> Absolute configuration of the compounds obtained from Kau2-EH catalysed bioconversion.

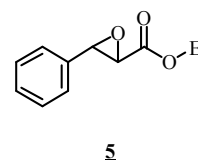
<sup>b</sup> Absolute configuration and optical rotation of the same compounds retrieved from literature.

As a conclusion of this chapter, it could be stressed that Kau2-EH is an extremely well suited catalyst in order to perform the kinetic resolution of *rac*-**4** since both remaining epoxide and formed diol were obtained nearly optically pure and in excellent yield at a very interesting substrate concentration of 50 g/L. These results compared particularly well to a recent study (Wei *et al.*, 2014). Indeed using *rac*-**4** in the presence *Galactomyces geotrichum* ZJUTZQ200 whole cells allowed the retention of (2*R*,3*S*)-**4** in 98.6% ee at 62.5 conversion leading to an E-value of 19 instead of a nearly infinite E-value in our case.

It should be noted that when tested in the same conditions as for *rac*-*trans*-**4**, the *rac*-*cis*-methyl phenyl glycidate **13** was not substrate of Kau2-EH to the contrary of its *rac*-*trans* counterpart *rac*-**4**.

### III.3.4.2 Bioconversion of *rac*-*trans*-ethyl 3-phenylglycidate **5**

In order to get some more structural information about the size of accepted substrates in the binding pocket of Kau2-EH, the ethyl ester of phenyl glycidate-**5** was tested using the optimized conditions defined for the methyl ester-**4**. It should be noted that **5** could behave as **4** as a chiral synthon for the synthesis of Taxol side chain or (-)-Clausenamide.



The objectives of this study were the following:

- 1) Analytical scale bio-hydrolysis of *rac*-**5** at various concentrations using Kau2-EH.
- 2) Optimization of reaction conditions at high substrate concentrations.
- 3) Conducting a preparative scale reaction.

### III.3.4.2.1 Analytical scale study of Kau2-EH catalysed bio-hydrolysis of *rac-trans*-ethyl-phenylglycidate-**5**

The evolution of the ees of the remaining epoxide-**5** was followed in a time dependant manner for increasing substrate concentrations of *rac*-**5** (1 to 50 g/L) by using a two times higher Kau2-EH concentration (1667 U/mg) (**Figure 72**).

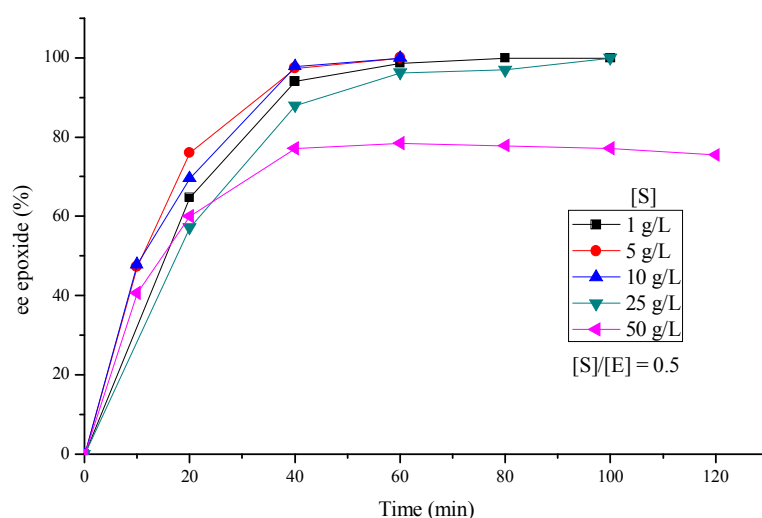


**Figure 72.** Evolution of the ees of the remaining epoxide during the bio-hydrolysis of *rac*-**5** at different substrate concentrations (1-50 g/L) using Kau2-EH.

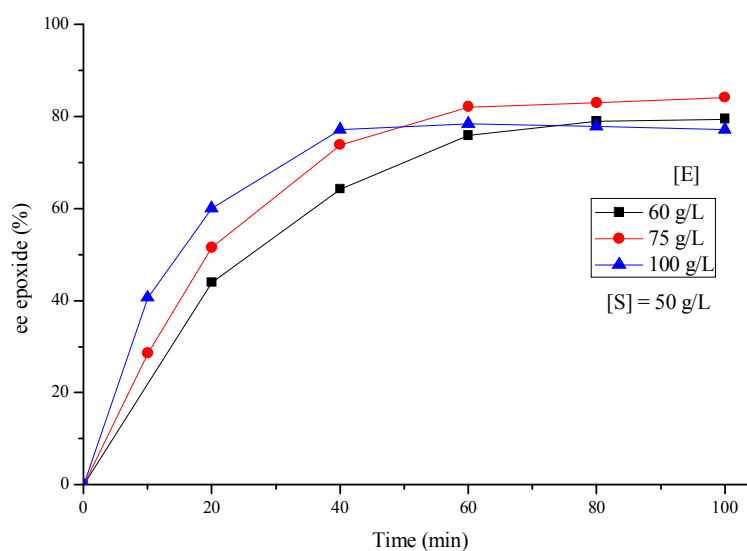
Essentially the same results were obtained up to 10 g/L substrate concentration (ees of remaining epoxide-**5** and formed diol-**5d** over 99% at 50% conversion). At 25 g/L substrate concentration, epoxide ee reached over 99% while diol ee was around 96% during the whole experiment. At higher 50 g/L substrate concentration the ee of (2*S*,3*R*)-**5** could not exceeded 78% while diol ees kept constant during the whole reaction at 96%.

From the above results the highest substrate concentration allowing a more than 99% ee to be reached for the remaining epoxide was 25 g/L. In order to increase this concentration for preparative purposes we then tested the same reaction at 50 g/L substrate concentration by varying the S/E ratio in order to improve the achievable remaining epoxide ee by diminishing the enzyme concentration (**Table 18** and **Figure 73**).

**Table 18.** Kau2-EH catalyzed biohydrolysis of *rac*-**5** at different substrate-over-enzyme ratio.

Reaction	Concentration of <i>rac</i> - <b>5</b> (g/L)	Concentration of Kau2-EH (g/L)	Substrate-over-enzyme ratio (S/E) <sup>a</sup>	ee% of the remaining epoxide (at 60 min)	ee% of the formed diol (at 60 min)
1	50	100	0.5	77.5%	96.3%
2	50	75	0.67	84.1%	95.3%
3	50	60	0.83	79.5%	98.3%

<sup>a</sup> Substrate-over-enzyme ratio (S/E): substrate concentration (g/L) divided by the enzyme concentration (lyophilized whole cells, g/L).

**Figure 73.** Evolution of the ees of the remaining epoxide during the Kau2-EH catalyzed biohydrolysis of *rac*-**5** (50 g/L) at different substrate-over-enzyme ratio.

From the above results and whatever the S/E ratio, it appeared that using Kau2-EH in order to catalyse the kinetic resolution of *rac*-**5** at 50 g/L did not permit to reach 100% ee for the remaining epoxide. The best result was obtained for an S/E ratio of 0.67 with a final 84% ee for remaining epoxide-**5**.

#### III.3.4.2.2 Preparative kinetic resolution of *rac*-**5** at 25 g·L<sup>-1</sup> on the 1 g scale

According to the conclusion of analytical scale bioconversions, the ethyl-glycidate ester-**5** was found to be somewhat less interesting than its methyl ester counterpart using Kau2-EH as biocatalyst. Nevertheless a preparative reaction conducted on the 1 g scale at 25 g/L of *rac*-**5** allowed the isolation after 100 minutes of the remaining epoxide (*2S,3R*)-**5** in 46.8% isolated yield (468mg) and >99% ee and formed diol (*2R,3R*)-**5d** in 47% isolated yield (490mg) and 94% ee (**Figure 74**). Absolute configuration for (*2S,3R*)-**5** have been determined through comparison of available optical rotations found in the literature ( $[\alpha]_{20}^D = +152$  (c = 1.0, CHCl<sub>3</sub>) (Caban *et al.*, 1995)) and the one experimentally determined in this work ( $[\alpha]_{25}^D = +154.7$  (c = 1.0, CHCl<sub>3</sub>)). Absolute configuration for (*2R,3R*)-**5d** have been determined through comparison of the elution order of (*2S,3S*)-**5d** (first eluted) and (*2R,3R*)-**5d** (second eluted) on Chiralpak AD-H column (Daicel) (Devi *et al.*, 2008) (**Annexe 3**).

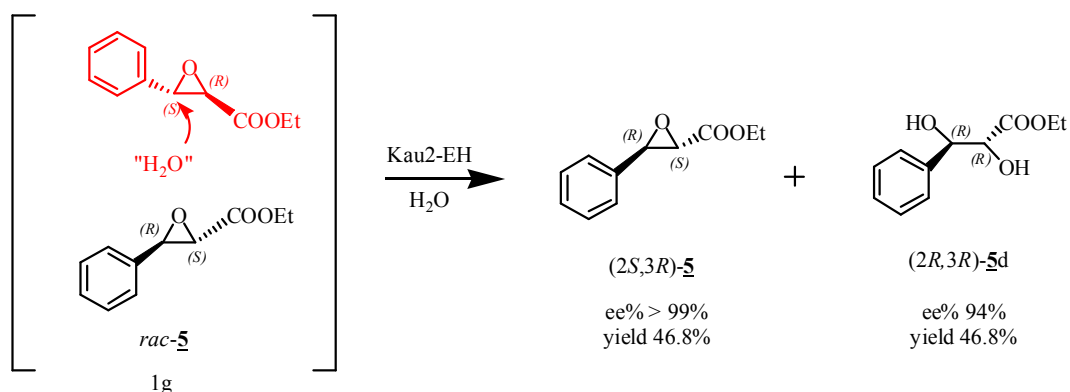


**Figure 74.** Preparative scale (1 g) Kau2-EH catalysed bio-hydrolysis of *rac*-**5**.

It could be seen from **Figure 75** that the ee of the formed diol is constant all along the reaction being equal to 94%.

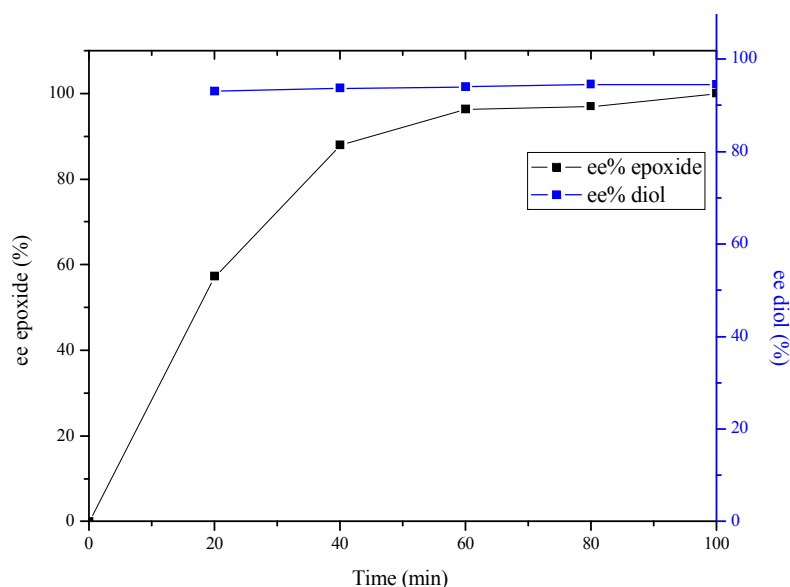


**Figure 75** Evolution of ees of both remaining epoxide and formed diol during the preparative Kau2-EH (50 g/L) catalyzed bio-hydrolysis of *rac*-**5** (25 g/L) on the 1 g scale.

**Table 19.** Optical rotations and absolute configurations of isolated products from preparative scale bio-hydrolysis of *rac*-**5**.

Compound	Abs. conf./ee/ $[\alpha]_D^a$	Abs. conf./ee/ $[\alpha]_D^b$	Reference
<b>5</b>	(2 <i>S</i> ,3 <i>R</i> )/99% $[\alpha]_D^{25} = +154.7^\circ$ ( $c=1.0$ , CHCl <sub>3</sub> )	(2 <i>S</i> ,3 <i>R</i> )/99% $[\alpha]_D^{20} = +152.0^\circ$ ( $c=1.3$ , CHCl <sub>3</sub> )	(Cabon <i>et al.</i> , 1995)
<b>5d</b>	(2 <i>R</i> ,3 <i>R</i> )/94%/ $[\alpha]_D^{25} = -37.5^\circ$ ( $c=1.0$ , CHCl <sub>3</sub> )	not reported	

<sup>a</sup> Absolute configuration of the compounds obtained from Kau2-EH catalysed bioconversion.

<sup>b</sup> Absolute configuration and optical rotation of the same compounds retrieved from literature.

Albeit the ethyl ester-**5** was less interesting than its methyl ester-**4** counterpart, Kau2-EH is equally efficient (Devi *et al.*, 2008) or compared favorably well (Li *et al.*, 2003; Wei *et al.*, 2014) to former EHs used in the kinetic resolution of *rac*-**5**. In the first case essentially the same results as described above have been reported for a gelozyme preparation of *Phaseolus radatus* (Mung bean) EH acting on *rac*-**5** (remaining epoxide (2*S*,3*R*)-**5** obtained in 45% isolated yield and ee>99%, formed diol (2*R*,3*R*)-**5d**, 94% ee, 78% yield). For the two latter cases, the more interesting remaining epoxide (2*R*,3*S*)-**5** was obtained either in 95% ee and 26% yield using whole cells of *Pseudomonas sp.* BZS21 (Li *et al.*, 2003) or in more than 99% ee and 37.1% yield using whole cells of *Galactomyces geotrichum* ZJUTZQ200 (Wei *et al.*, 2014).

### III.3.4.3 Bioconversion of *rac*-Methyl-*trans*3-(4-methoxyphenyl)-glycidate-**6**

(2*R*,3*S*)-Methyl-*trans*3-(4-methoxyphenyl)-glycidate-**6** is recognized as a key intermediate for the synthesis of Diltiazem, one of the most potent known calcium antagonists that has been widely used in the world for over 20 years for the treatment of cardiovascular diseases (Adger *et al.*, 1997; Gentile *et al.*, 1992; Seki *et al.*, 2001) (Figure 76).

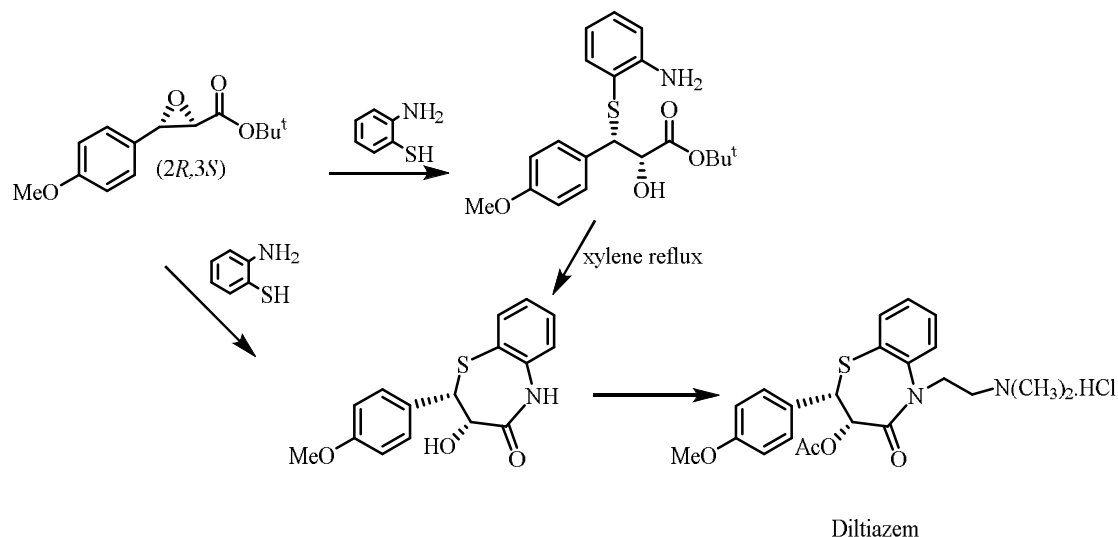
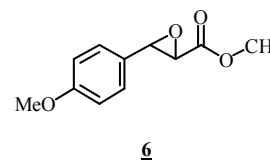


Figure 76. Synthesis of Diltiazem using *tert*-butyl-(2*R*,3*S*)-*trans*3-(4-methoxyphenyl)-glycidate-**6**.

Furthermore each enantiomer of **6** as well as the corresponding diols could be used for the synthesis of all stereoisomers of isocytosaxone, the structural isomer of the cytokine modulator of microbial origin (+)-Cytosaxone as described starting from methyl (2*S*,3*R*)-*p*-methoxy-phenyl-glycidate-**6** (Hameršak *et al.*, 2003) (Figure 77).

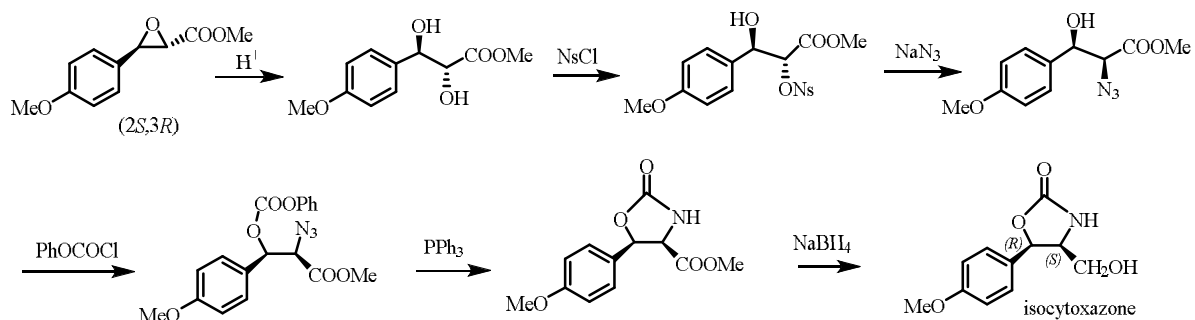


Figure 77. Synthesis of isocytosaxone using methyl (2*S*,3*R*)-*trans*3-(4-methoxyphenyl) glycidate-**6**.

Thus, the access to enantiomerically pure **6** is a synthetic challenge. Due to the close structural relationship existing between **4** and **6** we were interested to test *rac*-**6** as a potential Kau2-EH substrate.

The objectives of this study were the following:

- 1) *Optimization of the reaction medium.*
- 2) *Analytical scale bio-hydrolysis of *rac*-**6** at various concentrations using Kau2-EH.*
- 3) *Conducting a preparative scale reaction.*

#### **III.3.4.3.1 Optimization of the reaction medium**

Due to its *p*-methoxy substituent, **6** proved to be prompt to chemical hydrolysis during the time course of the biocatalytic reaction. This was detrimental to both final yields in remaining epoxide as well as ees of the formed diol. In order to minimize this chemical hydrolysis, the effect of the pH of the buffer phase (7, 7.5, 8, 8.5), of the temperature of the reaction (17 °C, 23 °C, 27 °C) and the percentage of non-miscible organic co-solvent (methyl *tert*-butyl ether, MTBE, 0, 20 or 40%) used were thoroughly tested.

#### **III.3.4.3.2 Chemical stability of *rac*-**6** at different pHs**

The chemical hydrolysis of *rac*-**6** was first followed by HPLC using 4-methoxybenzyl alcohol as standard, during one hour according to the pH medium (**Table 20**).

**Table 20.** Stability of *rac*-**6** at different Na-Phosphate buffer pHs.

pH <sup>a</sup>	spontaneous conversion of the epoxide % <sup>b</sup>
7.0	22.8
7.5	3.2
8.0	2.9
8.5	0.6

<sup>a</sup> 50 mM Na-phosphate buffer.

<sup>b</sup> Starting concentration of *rac*-**6** was 5 g/L, reaction time was 60 min, temperature was set at 23 °C.

From **Table 20** it is easily concluded that rising the pH from 7 to 8.5 dramatically reduce the chemical spontaneous hydrolysis of *rac*-**6** from 22.8% to 0.6% conversion. It appears that a pH of 8.5 is an appropriate value to conduct bio-hydrolysis of *rac*-**6**.

### III.3.4.3.3 Chemical stability of *rac-6* at different reaction temperatures

Then the chemical hydrolysis of *rac-6* was studied using the same analytical method, but according to the reaction temperature in the range of 17-27 °C during one hour (**Table 21**).

**Table 21.** Stability of *rac-6* at different reaction temperatures.

Temperature <sup>a</sup> (°C)	conversion of the epoxide % <sup>b</sup>
17	0.5
23	0.6
27	3.7

<sup>a</sup> 50 mM Na-phosphate buffer pH 8.5.

<sup>b</sup> Starting concentration of *rac-6* was 5 g/L, the reaction time was 60 min.

From **Table 21** it appears that the lower the reaction temperature, the better is the stability of *rac-6* in aqueous phase, as could be anticipated. Also the difference between 17 and 23 °C is tenuous, it was decided to select a reaction temperature of 17 °C for bioconversion reactions.

### III.3.4.3.4 Chemical stability of *rac-6* at different concentration of MTBE

Another mean to protect a water sensitive compound is to use immiscible organic solvent in order to create a phase where the sensitive compound will partition preferentially. We tested MTBE as an organic solvent at 20 and 40% (v/v) and compared the obtained results in the absence of solvent.

**Table 22.** Stability of *rac-6* under different MTBE concentrations.

MTBE <sup>a</sup> (%)	conversion of the epoxide % <sup>b</sup>
0	11.9
20	9.9
40	2.5

<sup>a</sup> 50 mM Na-phosphate buffer pH 7.0.

<sup>b</sup> Starting concentration of *rac-6* was 5 g/L, the reaction time was 60 min, temperature was set at 20 °C.

According to **Table 22** the use of 40 % (v/v) MTBE has a dramatic effect on the stability of *rac-6*. It was thus decided to use a 40% (v/v) MTBE for the biocatalytic reaction. In summary the following conditions have been determined in order to conduct the bio-

hydrolysis of *rac*-**6** catalyzed by Kau2-EH: temperature 17 °C, 50 mM Na-phosphate buffer pH 8.5, presence of 40 % (v/v) MTBE.

### III.3.4.3.5 Biohydrolysis of *rac*-**6** at different substrate concentrations with Kau2-EH.

The evolution of the ees of both the remaining epoxide and formed diol was followed in a time dependant depending on increasing *rac*-**6** concentrations (1 to 40 g/L) by using a two times higher Kau2-EH concentration (1667 U/mg) (**Figure 78** and **79**).

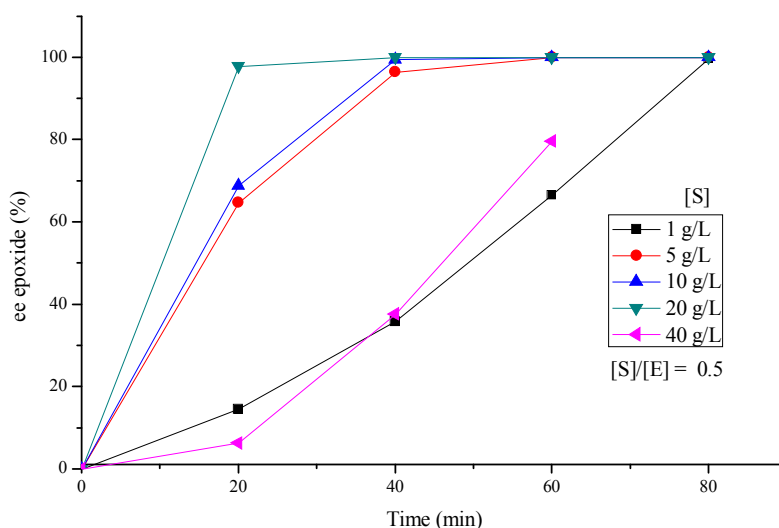


**Figure 78.** Evolution of the ees of the remaining epoxide during Kau2-EH catalyzed bio-hydrolysis of *rac*-**6** at different concentrations (1-40 g/L).

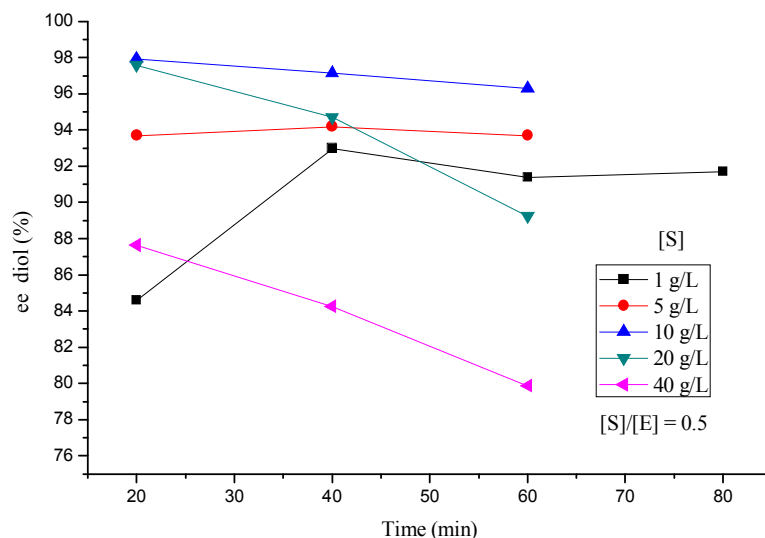


**Figure 79.** Evolution of the ees of the formed diol during Kau2-EH catalyzed bio-hydrolysis of *rac-6* at different substrate concentrations (1-40 g/L).

From **Figure 78**, it appears that an epoxide ee of more than 99% could be reached up to a substrate concentration of 40 g/L of *rac-6* with a two times more Kau2-EH concentration in the presence of 40% (vol/vol) MTBE at 17 °C. At *rac-6* concentration of 1 and 40 g/L the reaction should be prolonged to 80 minutes, instead of 60 minutes in the other cases, in order to reach an ee-value for the epoxide of more than 99%. From **Figure 79**, it could be seen that for the lowest substrate concentrations (1 to 10 g/L) the ees of the formed diol are quite constant during the reaction the best results being obtained at 10 g/L substrate concentration (97% ee). As the reaction proceeded, the diol ees were falling quite quickly at higher substrate concentrations (20 and 40 g/L).

At this point we wonder if a change in the S/E ratio could shorten the reaction times at high substrate concentration in order to minimize chemical hydrolysis leading thus to higher ees for the formed diol. From **Table 23**, it can be observed that at *rac-6* concentration of 40 g/L an increase in the S/E ratio from 0.5 to 0.57 allowed both to get a nearly enantiomerically pure epoxide in one hour and to limit the chemical hydrolysis, the ees of the formed diol rising from 74.1% to 83.4%.

**Table 23.** Biohydrolysis of *rac*-**6** with Kau2-EH at different substrate-over-enzyme ratio.

Reaction	Concentration of <i>rac</i> - <b>6</b> (g/L)	Concentration of Kau2-EH (g/L)	Substrate over enzyme ratio (S/E) <sup>a</sup>	ee% of the remaining epoxide (at 60 min)	ee% of the formed diol (at 60 min)
1	40	80	0.5	79.6%	74.1%
2	40	70	0.57	100%	83.4%

<sup>a</sup> Substrate over enzyme ratio (S/E): substrate concentration (g/L) divided by the enzyme concentration (lyophilized whole cells, g/L).

In summary and due to the instability of *rac*-**6** in aqueous solution, the bio-hydrolysis of *rac*-**6** at 40 g/L should be better performed at 17 °C, using 50 mM Na-phosphate buffer pH 8.5 in the presence of 40 % (vol/vol) MTBE and with an S/E ratio of 0.57. These conditions were used in the following.

#### ***III.3.4.3.6 Preparative kinetic resolution of *rac*-**6** at 40 g·L<sup>-1</sup> on the 1 g scale***

A preparative scale reaction was conducted involving 1 g (40 g/L) of *rac*-**6** (**Figure 80**). The latter was transformed by lyophilized Kau2-EH (70 g/L) affording in one hour remaining epoxide (*2S,3R*)-**6** in 40% isolated yield (400mg) and >99% ee and formed diol (*2R,3R*)-**6d** in 46% isolated yield (510mg) and 88% ee (**Figure 80** and **Figure 81**). Absolute configurations have been determined through comparison of available optical rotations found in the literature for (*2S,3R*)-**6** ( $[\alpha]_{\text{D}}^{24} = -205$  (c = 1.0, MeOH) (Imashiro and Seki, 2004)) and (*2R,3R*)-**6d** ( $[\alpha]_{\text{D}}^{18} = -43.9$  (c = 1, CHCl<sub>3</sub>) (Matthews *et al.*, 1990)) and the ones experimentally determined in this work  $[\alpha]_{\text{D}}^{24} = +190.7$  (c = 1.0, MeOH) and  $[\alpha]_{\text{D}}^{18} = -39.2$  (c = 1.0, CHCl<sub>3</sub>) respectively (**Table 24**).

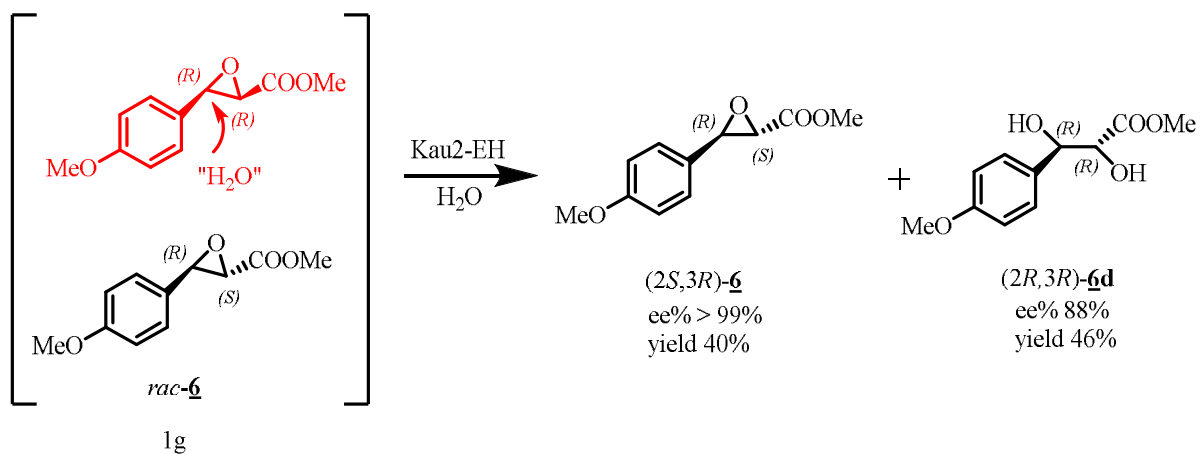


**Figure 80.** Preparative scale (1 g) bio-hydrolysis of *rac-6* using Kau2-EH.

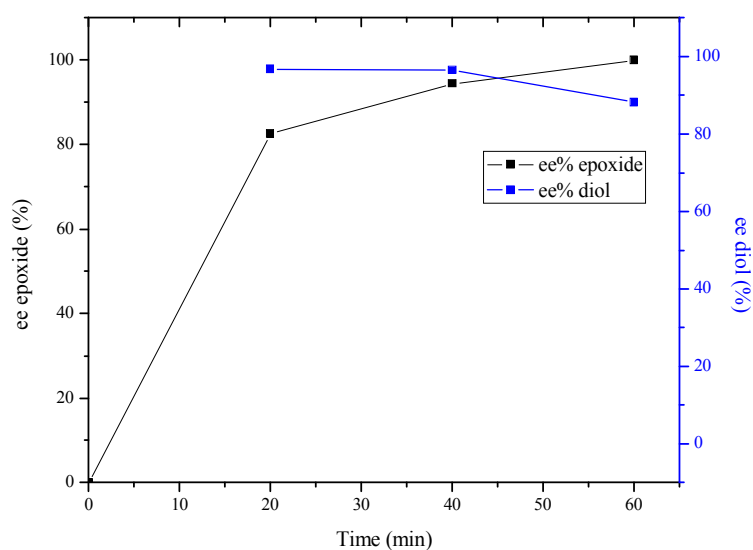


**Figure 81.** Evolution of the ees of both remaining epoxide and formed diol during the Kau2-EH (70 g/L) catalyzed preparative bio-hydrolysis of *rac-6* (40 g/L) on the 1 g scale.

**Table 24.** Optical rotations and absolute configurations of isolated products obtained from preparative scale bio-hydrolysis of *rac-6*.

Compound	Abs. conf./ee/[ $\alpha$ ] <sub>D</sub> <sup>a</sup>	Abs. conf./ee/[ $\alpha$ ] <sub>D</sub> <sup>b</sup>	Reference
$\underline{\mathbf{6}}$	(2 <i>S</i> ,3 <i>R</i> )/99% [ $\alpha$ ] <sub>D</sub> <sup>24</sup> =+190.7° (c=1.0, Methanol)	(2 <i>R</i> ,3 <i>S</i> )/99% [ $\alpha$ ] <sub>D</sub> <sup>24</sup> = -205° (c=1.0, Methanol)	(Imashiro and Seki, 2004)
$\underline{\mathbf{6d}}$	(2 <i>R</i> ,3 <i>R</i> )/84% [ $\alpha$ ] <sub>D</sub> <sup>18</sup> = -39.2° (c=1.0, CHCl <sub>3</sub> )	(2 <i>R</i> ,3 <i>S</i> )/99% [ $\alpha$ ] <sub>D</sub> <sup>18</sup> = -43.9° (c=1.08, CHCl <sub>3</sub> )	(Matthews <i>et al.</i> , 1990)

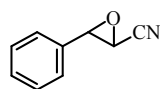
<sup>a</sup> Absolute configuration of the compounds obtained from Kau2-EH catalyzed bioconversion.

<sup>b</sup> Absolute configuration and optical rotation of the same compounds retrieved from literature.

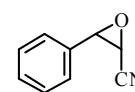
In line with the results obtained for glycidate **4** and **5**, the residual (2*S*,3*R*)-**6** is not the suitable enantiomer to conduct Diltiazem synthesis but could be used in the synthesis of one enantiomer of each *cis*- and *trans*-epicytozaxone (Hameršak *et al.*, 2003). When compared to previously reported kinetic resolutions of *rac*-**6** (Devi *et al.*, 2008; Wei *et al.*, 2014) Kau2-EH proved to be a better catalyst. Indeed using whole cells of *Galactomyces geotrichum* ZJUTZQ200, a E-value of only 3 was determined (Wei *et al.*, 2014) while using a gelozyme preparation of *Phaseolus radatus* (Mung bean) EH if remaining (2*S*,3*R*)-**6** epoxide was obtained in 45% yield and more than 99% ee, the formed diol-**6d** was racemic in this case.

#### III.3.4.4 Bioconversion of *trans*- and *cis*-2,3-epoxy-3-phenylpropanenitrile-**7** and -**8**

Following the good to excellent results obtained with phenylglycidate derivatives **4**, **5** and **6**, we decided to test whether other functionalities such as the cyano one could replace the ester functionality used previously.



**7**



**8**

Due to the chosen mode of synthesis, both *trans*-cyano-**7** and *cis*-cyano-**8** epoxides were obtained and easily chromatographically separated giving thus the possibility to test both compounds as substrates of Kau2-EH.

The objectives of this study were the following:

- 1) *Analytical scale bio-hydrolysis of rac-7 and rac-8 at various concentrations using Kau2-EH.*
- 2) *Conducting a preparative scale reaction.*

##### III.3.4.4.1 Analytical scale study of Kau2-EH catalyzed bio-hydrolysis of *rac-trans*-2,3-epoxy-3-phenylpropanenitrile-**7**

The *trans*-cyano derivative **7** was tested in the concentration range of 1 to 75 g/L and proved to be an excellent substrate (**Figure 82**). The use of *E. coli* cells showing higher Kau2-EH specific activity (2743 U/mg) than previous one (1667 U/mg) allowed to decrease the S/E ratio to 1.33 (m/m) and 20% MTBE was used to ensure the presence of a biphasic system. In the tested conditions both residual epoxide **7** and formed diol **7d** were obtained in more than 99% ee in 40 minutes for all tested concentrations except 1 and 75 g/L (**Figure 82**) (**Annexe**

5). In the former case the slow mass transfer of the substrate to the aqueous phase is probably the limiting factor preventing the ee from reaching >99% in less than one hour and in the latter case the high cell content, leading to a sticky reaction mixture, could slow down the transformation thus limiting the accessible ee of remaining 7 to 75%.

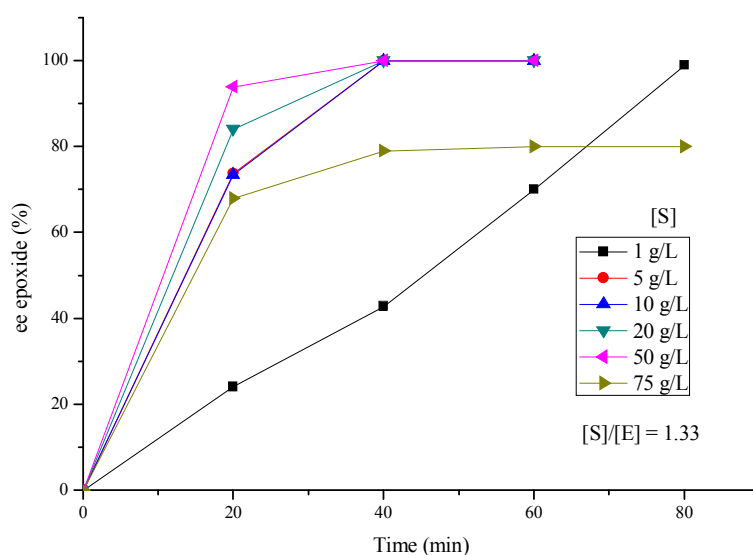


**Figure 82.** Evolution of the ees of the remaining epoxide during the Kau2-EH catalyzed biohydrolysis of *rac*-7 at different concentrations (1-75 g/L).

Once again, there was an impossibility to access more than 99% ee for the remaining epoxide beyond a certain substrate concentration (50 g/L in this case). Nevertheless we were pleased to note that Kau2-EH is able to accept other functionality than ester one, while keeping its very high degree of selectivity on compounds structurally related to phenylglycidates.

#### ***III.3.4.4.2 Preparative kinetic resolution of *rac*-7 at 50 g·L<sup>-1</sup> on the 1 g scale.***

According to the conclusion of the analytical scale bioconversions, it was decided to carry out a preparative kinetic resolution of *rac*-7 at a concentration of 50 g/L using Kau2-EH (37.5 g/L) on the 1 g scale (**Figure 83**).

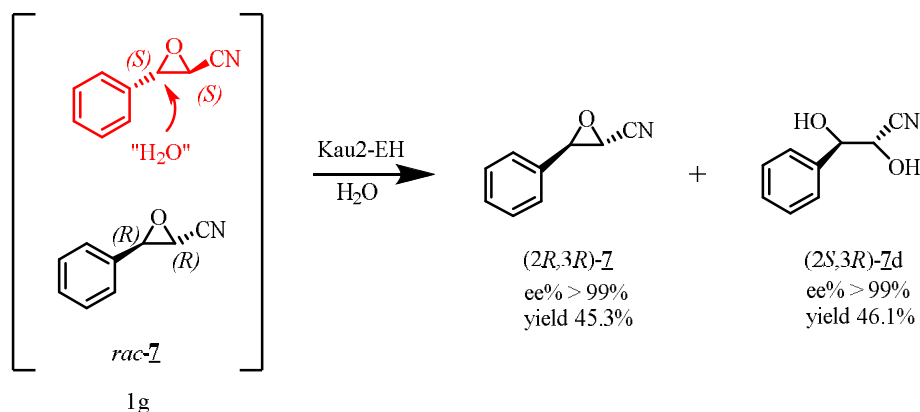


**Figure 83.** Preparative scale (1 g) Kau2-EH catalysed bio-hydrolysis of *rac*-**7**.

A preparative reaction ran at 50 g/L of *rac*-**7** (1 g) afforded after 80 minutes of reaction both residual epoxide (*2R,3R*)-**7** and formed diol (*2S,3R*)-**7d** with ees of more than 99% (**Annexe 5**) in respectively 45% (453 mg) and 46% (520 mg) isolated yield. Absolute configuration for (*2R,3R*)-**7** have been determined through comparison of available optical rotation found in the literature (for (*2R,3R*)-**7** with an ee = 29%,  $[\alpha]_{\text{D}}^{25} = + 24.3$  (c = 0.86, EtOH) (Zagozda and Plenkiewicz, 2008)) and the one experimentally determined in this work ( $[\alpha]_{\text{D}}^{20} = + 150.8$  (c = 1.1, EtOH)). In order to determine the absolute configuration of the formed diol-**7d**, it was first transformed to its acetonide which proved to be of *cis*-configuration ( $^1\text{H}$  NMR) and then to the corresponding *syn*-methyl-ester-diol-**4d** according to a previously described method (Effenberger *et al.*, 1991)(**Figure 84**). It should be noted that during the overnight reflux an epimerization of the *cis*-acetonide occurred on carbon-2. Such an epimerization did not occurred starting from a *trans*-acetonide (*vide infra*)(Effenberger *et al.*, 1991).

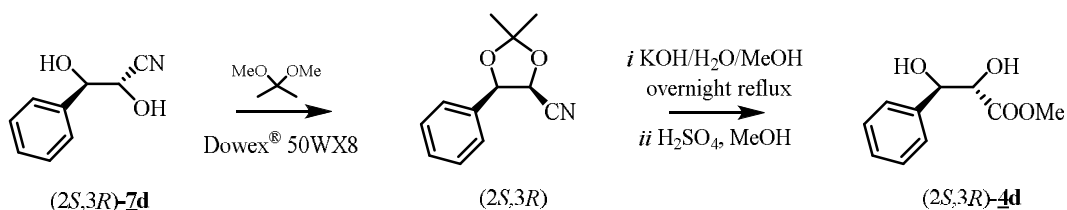


**Figure 84.** Absolute configuration determination of the formed diol (*2S,3R*)-**7d**.

The optical rotation of the formed diol-**4d** ( $[\alpha]_{\text{D}}^{20} = - 12.7$  (c = 0.71,  $\text{CH}_2\text{Cl}_2$ ) was compared to the one found in literature for (*2S,3R*)-*syn*-methyl-ester-diol-**4d** ( $[\alpha]_{\text{D}}^{20} = - 16.2$

( $c = 0.69$ ,  $\text{CH}_2\text{Cl}_2$ ) establishing thus the same absolute configuration for the obtained methyl-ester-diol-**4d** and thus the  $2S,3R$  configuration for the biocatalytically formed cyano-diol-**7d** (Figure 84).

#### III.3.4.4.3 Analytical scale study of Kau2-EH catalyzed bio-hydrolysis of *rac-cis-2,3-epoxy-3-phenylpropanenitrile-8*

In a previous paper (Kotik *et al.*, 2010), it was demonstrated that *cis*-1-methyl- styrene was a substrate of Kau2-EH and that it displayed enantioconvergent transformation leading to the corresponding  $1R,2R$  diol in 97% isolated yield and 98.3% ee (see Figure 55). As *cis*-methyl-phenyl-glycidate-**13** was not substrate of Kau2-EH, we were pleased to note that closely related *rac-cis*-2,3-epoxy-3-phenyl-propane-nitrile-**8** was indeed substrate of Kau2-EH (2757 U/mg) but underwent kinetic resolution instead of the expected enantioconvergent process. In that case the S/E ratio was 1 and 20% MTBE was used to ensure the presence of a biphasic system. Once again the kinetic resolution was almost perfect for substrate concentrations ranging from 1 to 25 g/L, both residual epoxide and formed diol being recovered essentially optically pure after 1 hour (Annexe 6)(Figure 85). For higher concentration (50 g/L) the reaction stopped after the ee of the remaining epoxide reached 77% (Figure 85), the obtained diol being nearly optically pure (data not shown).

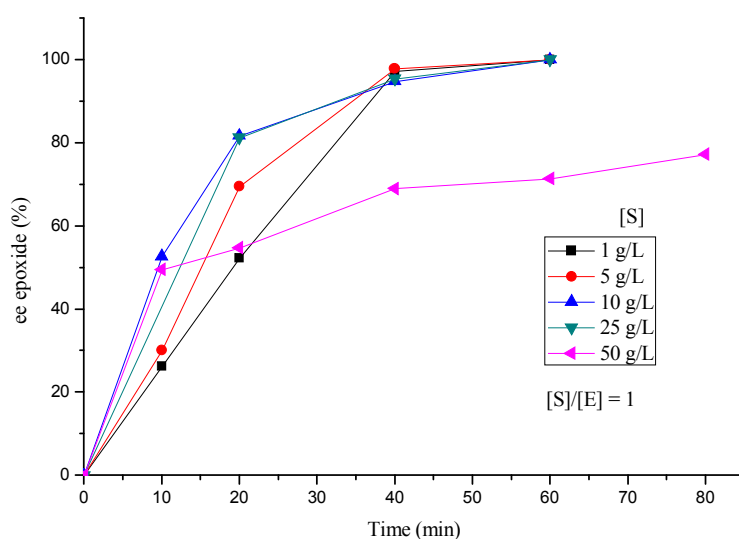


**Figure 85.** Evolution of the ees of the remaining epoxide during Kau2-EH catalyzed bio-hydrolysis of *rac-8* at different concentrations (1-50 g/L).

When the substrate concentration was 50 g/L, there are slight differences of enantioselectivity at different substrate over enzyme ratio. In line with previous results we tested a higher S/E ratio of 0.5 instead of 1.

**Table 25.** Bio-hydrolysis of *rac*-**8** with Kau2-EH at different substrate-over-enzyme ratio.

Reaction	Concentration of <i>rac</i> - <b>8</b> (g/L)	Concentration of Kau2-EH (g/L)	Substrate over enzyme ratio (S/E) <sup>a</sup>	ee% of the remaining epoxide (at 60 min)	ee% of the formed diol (at 60 min)
1	50	50	1	71.3%	100%
2	50	100	0.5	93%	100%

<sup>a</sup> Substrate over enzyme ratio (S/E): substrate concentration (g/L) divided by the enzyme concentration (lyophilized whole cells, g/L).

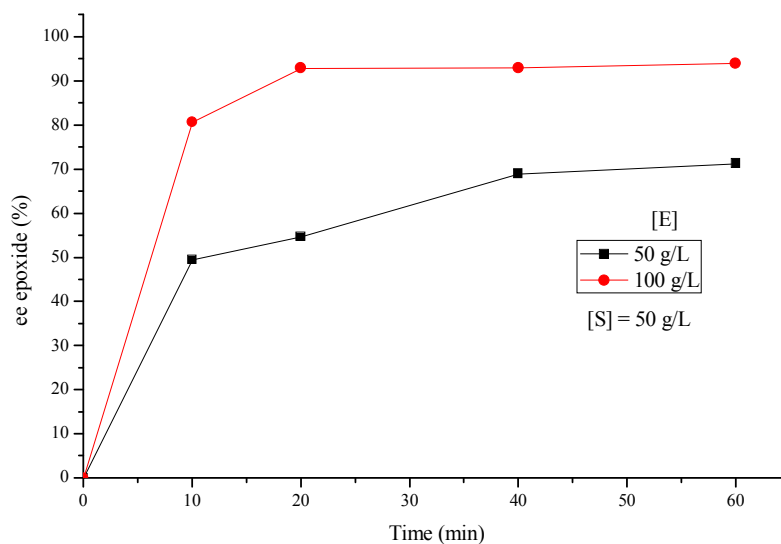


**Figure 86.** Biohydrolysis of *rac*-**8** (50 g/L) catalyzed by Kau2-EH at different substrate-over-enzyme ratio.

According to **Table 25** and **Figure 86** this modification lead to a better result, the ee after 1 h reaction was 93.3 % instead of 73%.

#### **III.3.4.4 Preparative kinetic resolution of *rac*-**8** at 25 g·L<sup>-1</sup> on the 1 g scale**

From the above results we thus choose to conduct a preparative kinetic resolution of *rac*-**8** at 25 g·L<sup>-1</sup> on the 1 g scale.

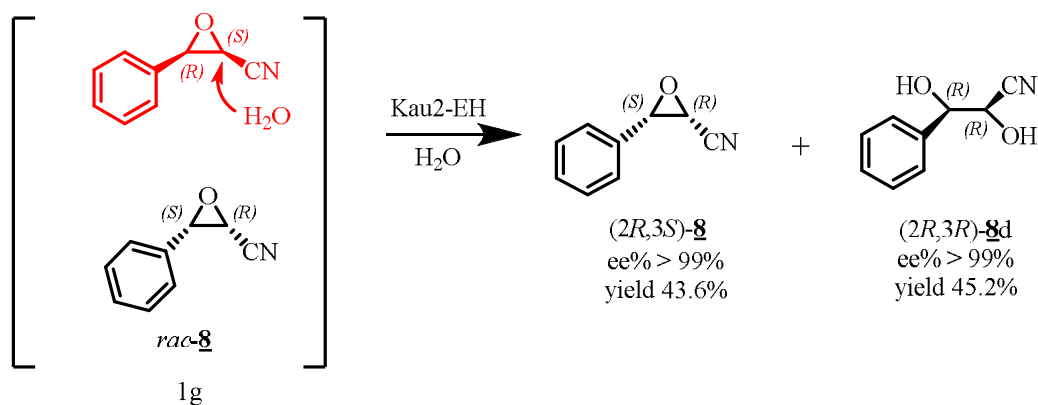


**Figure 87.** Preparative scale (1 g) bio-hydrolysis of *rac*-**8** using Kau2-EH.

After 80 minutes reaction time and silica gel purification, residual (2*R*,3*S*)-**8** and formed (2*R*,3*R*)-**8d** were obtained nearly optically pure (ee>99%) in 43.6% (436 mg) and 45.2% (510 mg) isolated yield respectively. The (2*S*,3*R*) absolute configuration of residual epoxide **8** was determined after transformation of the latter to its *cis*-methyl-ester counterpart (**Figure 88**)(Svoboda *et al.*, 1988).

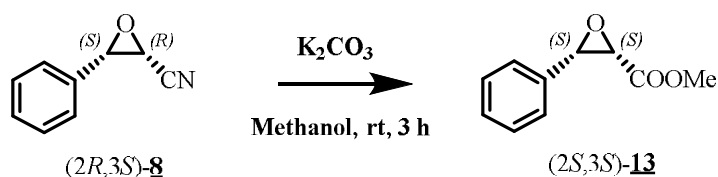


**Figure 88.** Chemical transformation of (2*R*,3*S*)-**8** into (2*S*,3*S*)-**13** (Svoboda *et al.*, 1988).

Then after chiral HPLC analysis (Chiralpak AD-H column) performed on formed **13** and using previously obtained *rac*-**13** as reference, revealed according to literature (Hoover *et al.*, 2006) that the obtained optically pure **13** correspond to the second peak of the racemic mixture and was thus of the (2*S*,3*S*) absolute configuration. This attribution then easily permitted to assess the absolute configuration of biocatalytically obtained remaining cyano-epoxide-**8** as being (2*R*,3*S*). It should be noted that when compared to previously tested substrates, *cis*-cyano-epoxide-**8** is the only one not to be attacked on the benzylic carbon but instead on carbon 2. In order to determine the absolute configuration of the formed diol-**8d**,

the same method described above for diol-**7d** was used. Formed diol-**8d** was first transformed to its acetonide which proved to be of *trans*-configuration ( $^1\text{H}$  NMR) and then to the corresponding *syn*-methyl-ester-diol-**4d** (Effenberger *et al.*, 1991)(**Figure 89**).

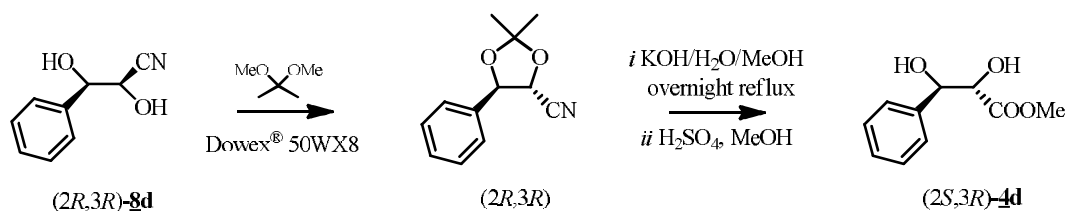


**Figure 89.** Absolute configuration determination of the formed diol  $(2R,3R)\text{-8d}$ .

The optical rotation of the formed diol-**4d** ( $[\alpha]_{\text{D}}^{20} = -14.7$  ( $c = 0.73$ ,  $\text{CH}_2\text{Cl}_2$ )) was compared to the one found in literature for  $(2S,3R)\text{-syn}$ -methyl-ester-diol-**4d** ( $[\alpha]_{\text{D}}^{20} = -16.2$  ( $c = 0.69$ ,  $\text{CH}_2\text{Cl}_2$ )) establishing thus the same absolute configuration for the obtained methyl-ester-diol-**4d** and thus the  $2R,3R$  configuration for the biocatalytically formed cyano-diol-**8d** (**Figure 89**). It should be noted that, when compared to previously tested substrates, *cis*-cyano-epoxide-**8** is the only one not to be attacked on the benzylic carbon but instead on carbon 2. Indeed the only possibility to generate both epoxide  $(2R,3S)\text{-8}$  and diol  $(2R,3R)\text{-8d}$  is to consider an attack on this carbon (**Figure 90**).

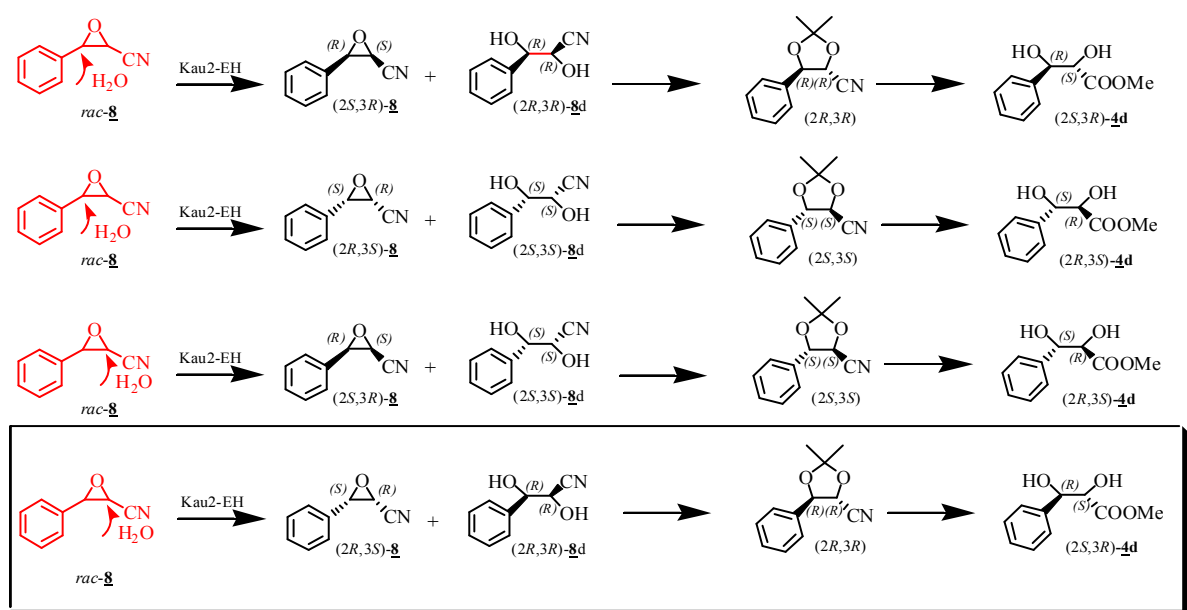


**Figure 90.** The four possible combination of remaining epoxides and formed products arising from Kau2-EH catalyzed bio-hydrolysis of *rac*-**8**.



Furthermore when obtained, the diol-**9d** and -**10d** could easily be transformed under basic conditions (with retention of stereochemistry) to get access to the terminal epoxide-**14** (**Figure 92**) useful in the synthesis of natural and biologically active compounds (Kumar *et al.*, 2012; Palin *et al.*, 2005) (**Figure 93**).

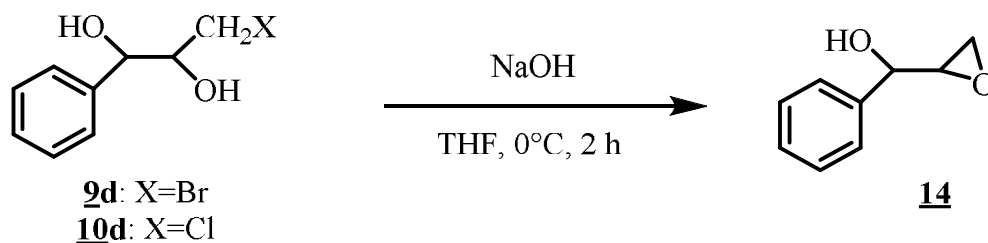


**Figure 92.** Synthesis of 1-Phenyl-glycidol-**14** using diol-**9d** and -**10d**.

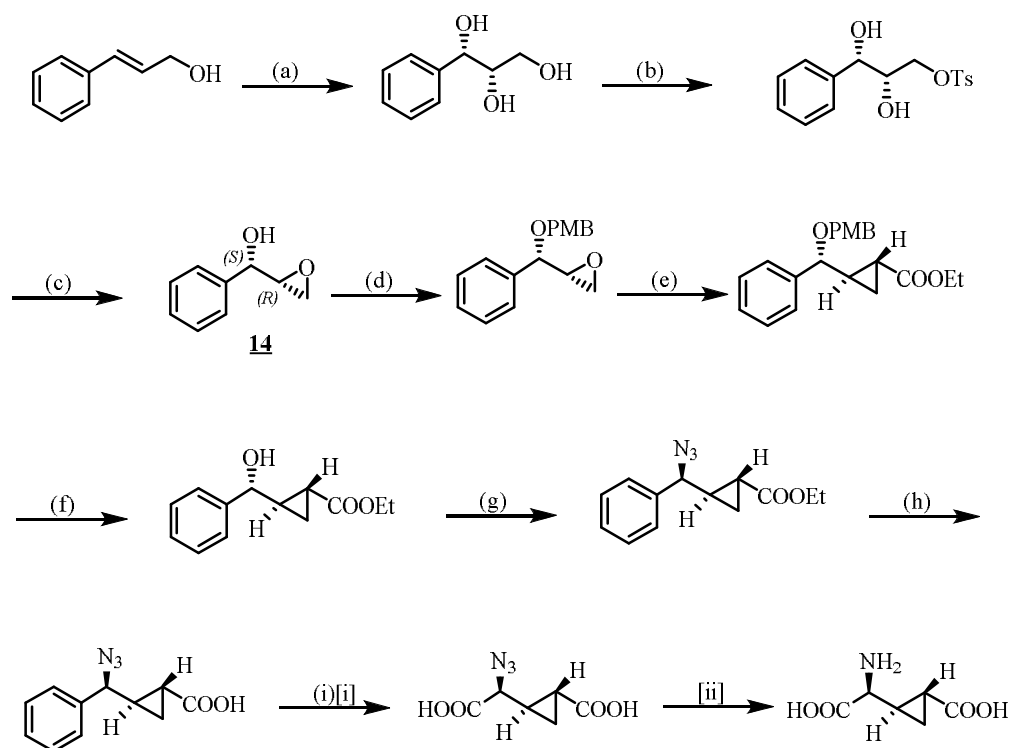


**Figure 93.** Synthesis of L-(-)-CCG-II using terminal epoxide-**14** (Kumar *et al.*, 2012).

It should be noted that when tested at a concentration of 25 g/L both bromo-**9** and chloro-**10** epoxide behaved similarly when exposed to Kau2-EH hydrolysis, **9** being

transformed slightly quicker than the corresponding chloro epoxide. Thus in the following only the analytical scale results obtained with bromo-epoxide-**9** are reported.

The objectives of this study were the following:

- 1) Analytical scale bio-hydrolysis of *rac*-**9** at various concentrations using Kau2-EH.
- 2) Conducting a preparative scale reaction with both *rac*-**9** and *rac*-**10**.

#### III.3.4.5.1 Analytical scale study of Kau2-EH catalysed bio-hydrolysis of *rac*-*trans*-2,3-epoxy-3-phenyl-1-bromo propane-**9**.

Using an S/E ratio of 2.5 from 1 to 75 g/L of **9** with 20% MTBE, a nearly perfect kinetic resolution was observed in each cases affording epoxide-**9** and diol-**9d** with ees reaching more than 99% after 80 minutes reaction time, except at 75 g/L of **9** where the ees reached 96% and then levelled off (**Figure 94**). These results proved that *rac*-**9** was an excellent substrate for Kau2-EH.

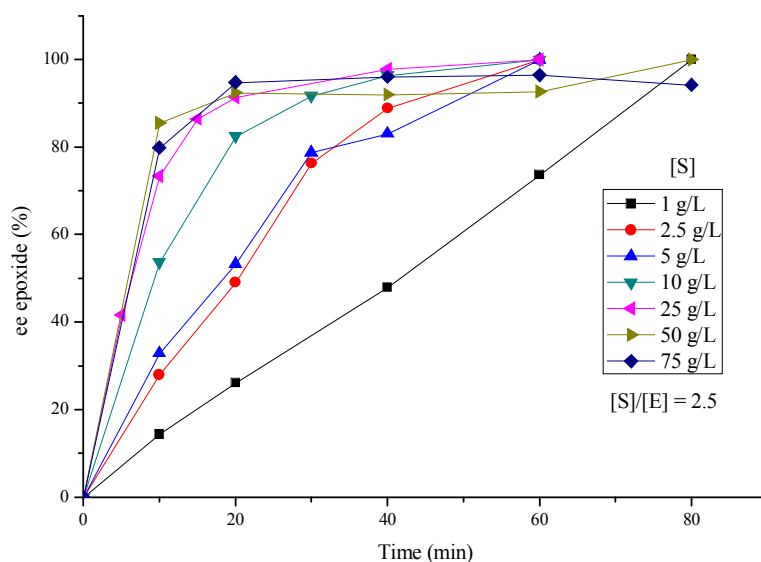


**Figure 94.** Evolution of the ees of the remaining epoxide during Kau2-EH catalyzed bio-hydrolysis of *rac*-**9** at different concentrations (1-75 g/L).

As the ee of the remaining epoxide at 75 g/L substrate concentration was quite high (94%) when the reaction stopped, we tested whether two smaller S/E ratio (1.25 and 1.85)

could improve the reaction allowing a more than 99% ee to be reached. According to **Table 26** this modification lead to a very nice result since after 1 h reaction the ee of the formed epoxide reached >99%.

**Table 26.** Kau2-EH catalyzed bio-hydrolysis of *rac*-**2** at different substrate-over-enzyme ratio.

Reaction	Concentration of <i>rac</i> - <b>2</b> (g/L)	Concentration of Kau2-EH (g/L)	Substrate-over-enzyme ratio (S/E) <sup>a</sup>	ee% of the remaining epoxide (at 60 min)	ee% of the formed diol (at 60 min)
1	75	40	1.85	96%	>99%
2	75	60	1.25	>99%	>99%

<sup>a</sup> Substrate over-enzyme-ratio (S/E): substrate concentration (g/L) divided by the enzyme concentration (lyophilized whole cells, g/L).

### III.3.4.5.2 Preparative kinetic resolution of *rac*-**2** and *rac*-**10** on the 1 g scale

When run on a preparative scale (1 g of *rac*-**2**, 75 g/L) in the presence of 0.8 g of biocatalyst (60 g/L), the reaction afforded optically pure (2*S*,3*R*)-**2** and (2*R*,3*R*)-**2d** in 44% (441 mg) and 48% (530 mg) isolated yields, respectively (**Figure 95**).

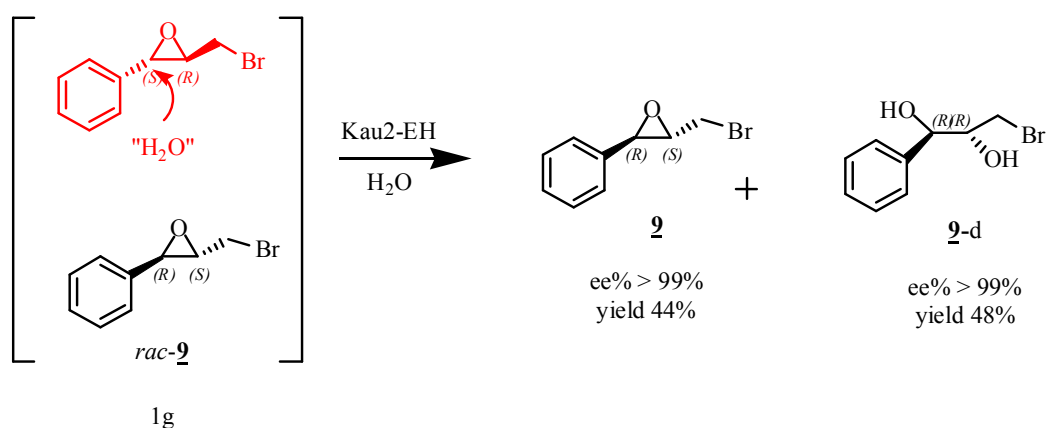


**Figure 95.** Preparative scale (1 g) Kau2-EH catalysed bio-hydrolysis of *rac*-**2**.

The similar preparative scale reaction performed on the chloro-epoxide-**10** (1 g of **10**, 50 g/L; 0.5 g of biocatalyst (2011 U/mg), 25 g/L), afforded optically pure (2*S*,3*R*)-**10** (43% isolated yield, 430 mg) and (2*R*,3*R*)-**10d** (44.5% isolated yield, 490 mg)(**Figure 96**).

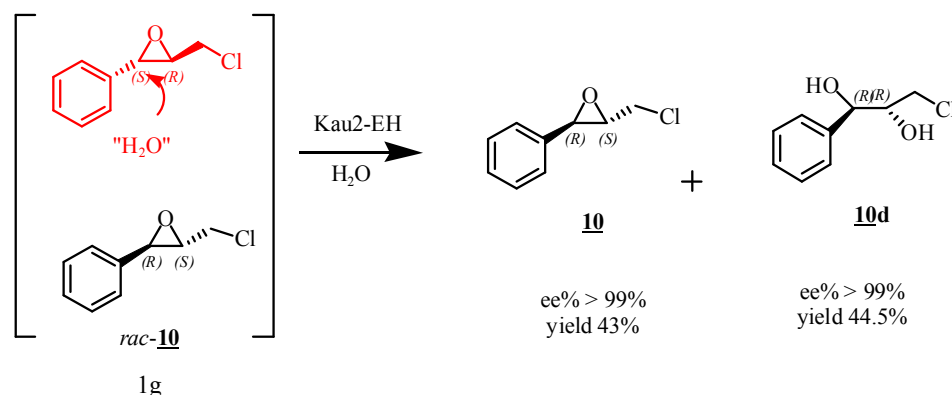


**Figure 96.** Preparative scale (1 g) Kau2-EH catalysed bio-hydrolysis of *rac*-**10**.

The absolute configuration of (2*S*,3*R*)-**10** has been determined through comparison of available optical rotation found in the literature (for (2*S*,3*R*)-**10**,  $[\alpha]_D^{25} = +21.4$  ( $c = 0.6$ ,  $\text{CHCl}_3$ ), (Wang and Shi, 1997)) and the one experimentally determined in this work ( $[\alpha]_D^{20} = +20$  ( $c = 0.6$ ,  $\text{CHCl}_3$ )). The absolute configuration of the remaining bromo-epoxide-**9** was assigned as (2*S*,3*R*) by analogy with the one of the chloro-epoxide-**10** assuming that both compounds react identically during Kau2-EH hydrolysis. This equivalent behavior was supported by the fact that the formed bromo-diol-**9d** and chloro-diol-**10d** possessed the same absolute configuration. Indeed both diols were cyclized under basic conditions to the corresponding epoxy-alcohol-**14** (Jobson *et al.*, 2009) (**Figure 97**). Epoxy-alcohol-**14** absolute configuration was established in both cases as 1*R*,2*S* through comparison of available optical rotation found in the literature (for (1*R*,2*S*)-**14**,  $[\alpha]_D^{25} = -100.2$  ( $c = 2.31$ ,  $\text{CHCl}_3$ ), (Palazón *et al.*, 1986)) and the one experimentally determined in this work ( $[\alpha]_D^{25} = -100$  ( $c = 2.74$ ,  $\text{CHCl}_3$ ) and  $[\alpha]_D^{25} = -104$  ( $c = 2.74$ ,  $\text{CHCl}_3$ )) for epoxy alcohol-**14** arising from chloro- and bromo-diol respectively.

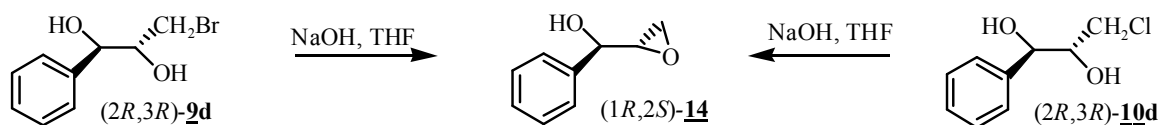


**Figure 97.** Cyclisation of formed diols **9d** and **10d** to epoxy-alcohol **14**.

**Table 27.** Optical rotations and absolute configurations of isolated products from the preparative scale bio-hydrolysis of *rac*-**9** and **10**.

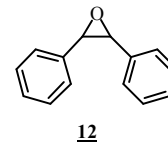
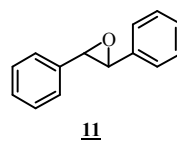
Compound	Abs. conf./ee/[ $\alpha$ ] <sub>D</sub> <sup>a</sup>	Abs. conf./ee/[ $\alpha$ ] <sub>D</sub> <sup>b</sup>	Reference
<b>9</b>	(2 <i>S</i> ,3 <i>R</i> )/99% [ $\alpha$ ] <sub>D</sub> <sup>24</sup> = +11.3° (c=1.0, CHCl <sub>3</sub> )	Not reported	
<b>9d</b>	(2 <i>R</i> ,3 <i>R</i> )/99% [ $\alpha$ ] <sub>D</sub> <sup>24</sup> = -8.5° (c=1.0, CHCl <sub>3</sub> )	Not reported	
<b>10</b>	(2 <i>S</i> ,3 <i>R</i> )/99% [ $\alpha$ ] <sub>D</sub> <sup>25</sup> = +20° (c=0.6, CHCl <sub>3</sub> )	(2 <i>S</i> ,3 <i>R</i> )/99% [ $\alpha$ ] <sub>D</sub> <sup>25</sup> = +21.4° (c=0.6, CHCl <sub>3</sub> )	(Wang and Shi, 1997)
<b>10d</b>	(2 <i>S</i> ,3 <i>R</i> )/99% [ $\alpha$ ] <sub>D</sub> <sup>25</sup> = -4.6° (c=1.0, Ethanol)	Not reported	
<b>14</b>	(1 <i>S</i> ,2 <i>R</i> )/99% [ $\alpha$ ] <sub>D</sub> <sup>25</sup> = -100° (c=2.74, CHCl <sub>3</sub> )	(1 <i>S</i> ,2 <i>R</i> )/99% [ $\alpha$ ] <sub>D</sub> <sup>25</sup> = -100.2° (c=2.31, CHCl <sub>3</sub> )	(Palazón <i>et al.</i> , 1986)

<sup>a</sup> Absolute configuration of the compounds obtained from Kau2-EH catalysed bioconversion.

<sup>b</sup> Absolute configuration and optical rotation of the same compounds retrieved from literature.

### III.3.4.6 Bioconversion of *rac*-**trans**-stilbene-oxide-**11** and *meso*-**cis**-stilbene-oxide-**12**

In order to further explore the chemical space to be reached with Kau2-EH catalyzed reactions, sterically more demanding epoxides such as *trans*-stilbene-oxide-



**11** and *cis*-stilbene-oxide-**12** were tested. Although these epoxides are not bi-functional they are of large interest since they could give a good idea of which type of substrates could be accepted by Kau2-EH active site.

The objectives of this study were the following:

- 1) Analytical scale bio-hydrolysis of *rac*-**11** and *meso*-**12** at various concentrations using Kau2-EH.
- 2) Conducting a preparative scale reaction with both *rac*-**11** and *meso*-**12**.

### III.3.4.6.1 Analytical scale study of Kau2-EH catalysed bio-hydrolysis of *rac-trans-stilbene-oxide-11*

As could be anticipated, the sterically challenging *trans*-stilbene oxide-**11** is a poorer substrate of Kau2-EH than previously tested ones. Indeed enantiomerically pure unreacted epoxide was obtained only after 24-48 hours of reaction rather than after around 1h for previous substrates. Excepted for substrate concentration of 1 g/L where the ees of the remaining epoxide reaches only 93% after 105 h, higher substrate concentrations (5, 10 and 25 g/L) allowed to get enantiomerically pure remaining epoxide after 24 h of reaction (**Figure 98**). At the higher 50 g/L substrate concentration an enantiomerically pure remaining epoxide was obtained but only after 40 h of reaction. In all cases 20% MTBE was used as an immiscible organic phase and the S/E ratio was 0.5, the specific activity of the enzyme being 2757 U/mg.

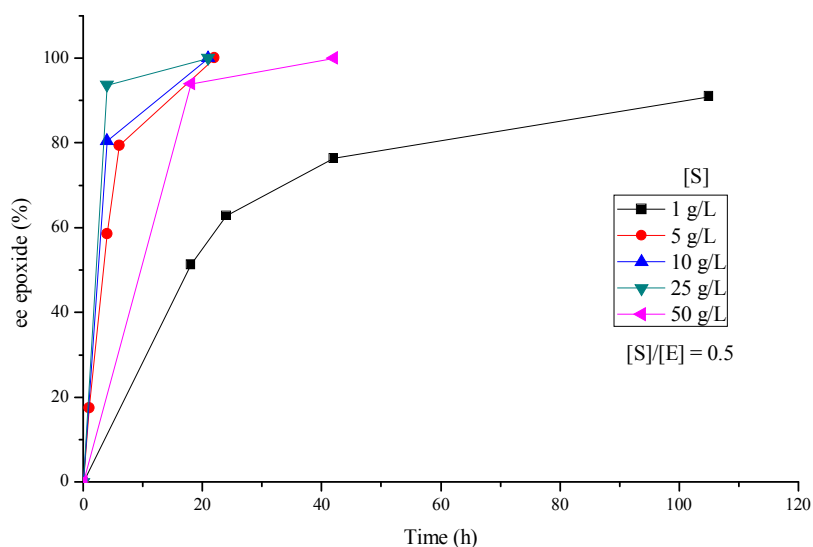


**Figure 98.** Evolution of the ees of the remaining epoxide during Kau2-EH bio-hydrolysis of *rac-11* at different concentrations (1-50 g/L).

The *meso* form of the diol-**11d** was obtained as well as the (1*R*,2*R*)-**11** remaining epoxide whose absolute configuration have been determined through comparison of available optical rotation found in the literature (for (1*R*,2*R*)-**11**,  $[\alpha]_D^{20} = + 357$  ( $c = 0.59$ , Benzene))

(Berti *et al.*, 1965)) and the one experimentally determined in this work ( $[\alpha]_D^{20} = +348$  (c = 0.59, Benzene)).

### III.3.4.6.2 Preparative kinetic resolution of *rac*-**11** at 50 g·L<sup>-1</sup> on the 1 g scale

When run on a preparative scale (1 g of **11**, 50 g/L) for 5h at 27 °C using a biocatalyst concentration of 100 g/L, the reaction afforded the remaining epoxide (1*R*,2*R*)-**11** with an ee of 99% in 45% isolated yield (450 mg) and the *meso*-diol-**11d** in 46% isolated yield (510mg) (**Figure 99**).

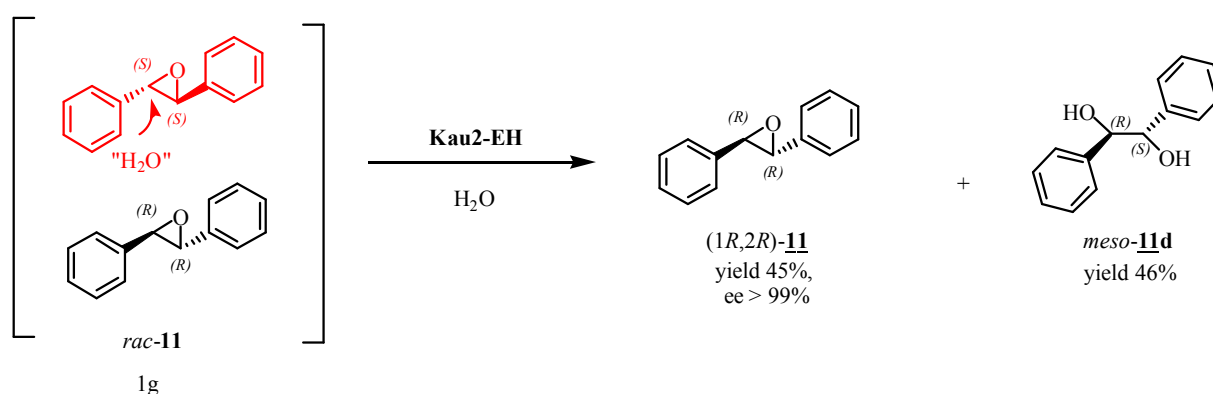


**Figure 99.** Preparative scale (1 g) Kau2-EH catalysed bio-hydrolysis of *rac*-**11**.

It should be noted that the preparative reaction was found to be much quicker than its analytical counterpart (5 h instead of 40 h to reach an ee of the epoxide over 99%). No clear explanation could be given to this fact since the preparative reaction was linearly extrapolated from the analytical one, except a better stirring in the former case.

### III.3.4.6.3 Analytical scale study of Kau2-EH catalysed bio-hydrolysis of *meso*-*cis*-stilbene oxide-**12**

The reaction was then extended to the desymmetrization of the *meso*-epoxide *cis*-stilbene-oxide-**12** using only DMF (5%) as a miscible co-solvent (**Figure 100**). One of the advantage of using *meso*-epoxides is that EH catalysed desymmetrization could theoretically afford the corresponding diol optically pure and in 100% yield to the contrary of kinetic resolutions where the maximum theoretical yield of the diol is only 50%.

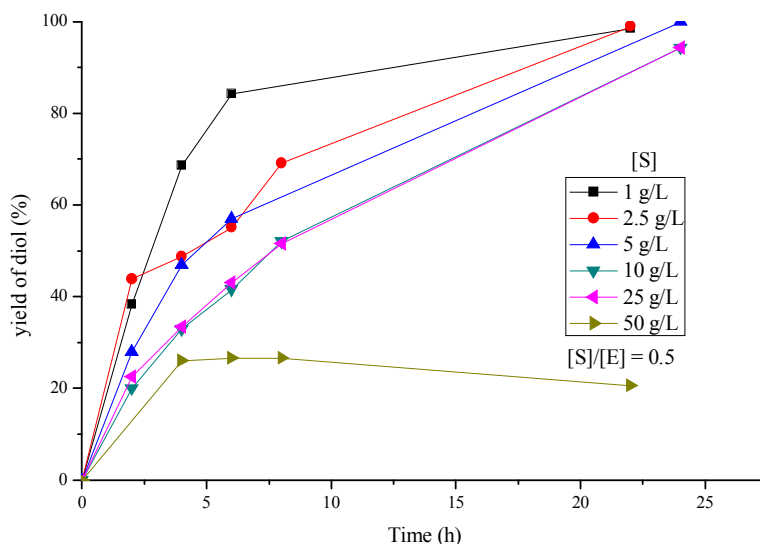


**Figure 100.** Evolution of the yields of the formed diol-**12d** during the desymmetrization of *meso*-**12** at different concentrations (1-50 g/L) using Kau2-EH.

The *cis*-*meso*-epoxide-**12** displayed almost quantitative transformation when used at 1, 2.5, 5, 10 and 25 g/L concentrations of starting material (S/E ratio was 0.5), the formed (1*R*,2*R*)-diol-**12d** being obtained in all cases almost enantiomerically pure ( $ee > 99\%$ ) and in more than 90% analytical yield in 24 h. The reactions were stopped when all the epoxide was consumed and the yield in diol was determined by HPLC with the standard 4-methoxybenzyl alcohol. The absolute configuration have been determined through comparison of available optical rotation found in the literature (for (1*R*,2*R*)-**12d**,  $[\alpha]_D^{28} = +92.7$  ( $c = 1$ , EtOH) (Takenaka *et al.*, 2004)) and the one experimentally determined in this work ( $[\alpha]_D^{28} = +93.8$  ( $c = 1$ , EtOH)). At higher substrate concentration (50 g/L) the yield of formed **12d** dropped considerably being around 20% after 24h reaction.

#### III.3.4.6.4 Preparative kinetic resolution of *meso*-**12** at 25 g·L<sup>-1</sup> on the 1 g scale

Thus a preparative reaction was run on the 1 g scale and 25 g/L concentration of *meso*-**12** (Figure 101).

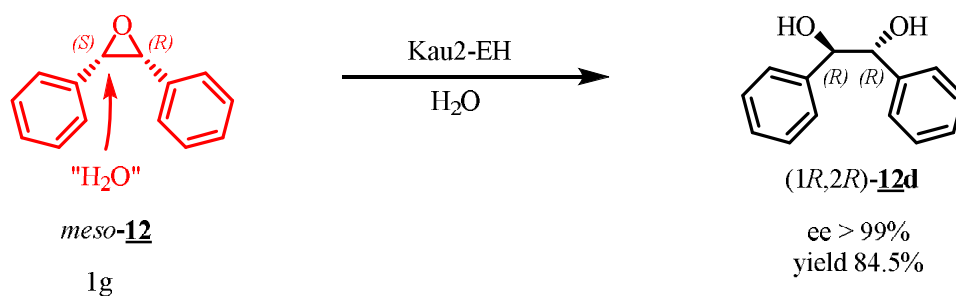


**Figure 101.** Preparative scale (1 g) bio-hydrolysis of *meso-12* using Kau2-EH.

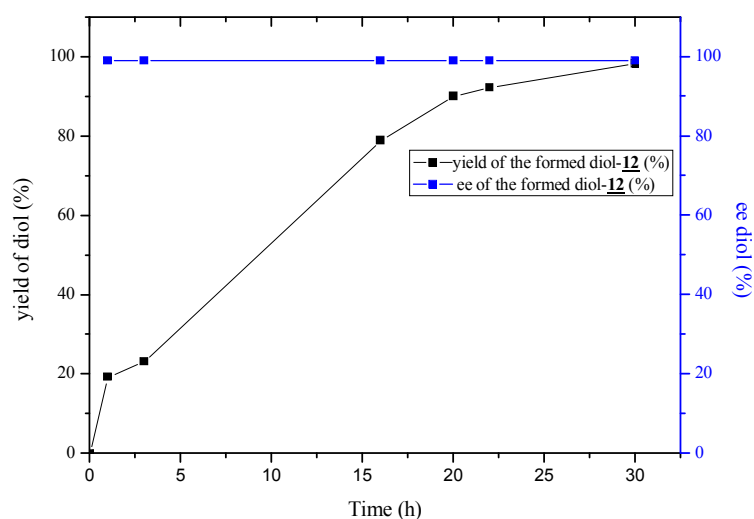


**Figure 102.** Evolution of the yields and ees of the formed diol-12d during the preparative scale (1 g) Kau2-EH catalyzed desymmetrization of 12.

After 30 hours reaction time, the starting epoxide was totally consumed and the formed *1R,2R*-diol-12d (ee 99%) was recovered in 85% (920 mg) isolated yield (**Figure 102**). This result is comparable to those described in a previously reported work dedicated to desymmetrization of *meso*-epoxides using various EHs obtained from a metagenomic library (Zhao *et al.*, 2004). Using cell extracts of 4 different EHs (BD 8877, BD 8676, BD 9300, BD 9883) (*1R,2R*)-diol-12d with ees ranging from 96 to 99.5% was obtained while its antipode (*1S,2S*)-diol-12d was obtained in 99% ee using cell extracts of BD 9196 (Zhao *et al.*, 2004).

### III.3.5 Overall conclusion

From the above reported results it could be put forward that Kau2-EH is a particularly useful enzyme in the kinetic resolution/desymmetrization of 1,2-disubstituted epoxides, one of the substituent being a phenyl ring. Indeed exceptionally high stereoselectivities were demonstrated using this enzyme leading in all but two cases to ees' of at least 99% for both remaining epoxide and formed diol, showing thus a nearly perfect kinetic resolution. Furthermore the Kau2-EH catalyzed hydrolysis could be conducted at very high substrate concentrations (from 25 and up to 75 g/L) and was generally performed within 1h, thus closely approaching industrial needs. The used enzymatic preparation well tolerated the presence of non-water miscible organic solvent such as di-isopropyl ether and methyl-*t*-butyl ether alleviating or diminishing both substrate and product inhibition as well as allowing the dissolution of very high substrate and product quantities. The biocatalyst is also tolerant to pH change (up to 8.5 in the basic range) allowing, when combined with the use of an organic non-water miscible organic solvent, to minimize spontaneous chemical hydrolysis of fairly unstable epoxides. Some of the tested substrates were potential very useful chiral synthons, valuable in the synthesis of numerous biologically active targets. When compared to a recently reported investigations about the *Galactomyces geotrichum* whole cells catalyzed resolution of glycidates **4**, **5** and **6**, Kau2-EH expressed in *E. coli* proved to be an outstanding biocatalyst to get access to optically pure epoxides (Wei *et al.*, 2014). Unfortunately, in all cases the remaining epoxide did not bear the correct configuration in order to be used *directly* as chiral synthon to access Taxol-side chain ((2*R*,3*S*)-**4** and (2*R*,3*S*)-**5**) or Diltiazem (2*R*,3*S*)-**6**. Obtained glycidates (2*S*,3*R*)-**4** and (2*S*,3*R*)-**5** could nevertheless be used in the synthesis of nootropic drug (-)-Clausenamide (Zheng *et al.*, 2006). It has also been shown in this work that bi-functional epoxides could be used without noticeable influence on the stability of the different functionalities such as nitrile, methyl or ethyl esters and bromine. In the latter case a new terminal epoxide is easily accessible from the enzymatically formed diol by simply using basic conditions, the initial enantiopurity being conserved. Even very sterically demanding substrates such as *trans*- and *cis*-stilbene-oxides could be accommodated in the enzyme active site but lower reaction rates than for 1,2-epoxides bearing only one phenyl substituent are observed. Nevertheless even in the worst cases (*trans*-stilbene oxide kinetic resolution and desymmetrization of *cis*-stilbene-oxide), the preparative reaction was conducted to completion within one day. In order to compare the various biocatalytic reactions described above, we present in **Figure 103** the results obtained for all the tested substrates at the same

concentration of 25 g/L under the various reaction conditions described in experimental part for each substrate. Generally speaking the obtained results showed that the smaller the substituent the highest the activity (Br>Cl>CN>COOMe>COOEt>Phe) and that *trans*-configured substrates were hydrolyzed quicker than their *cis*-counterpart.

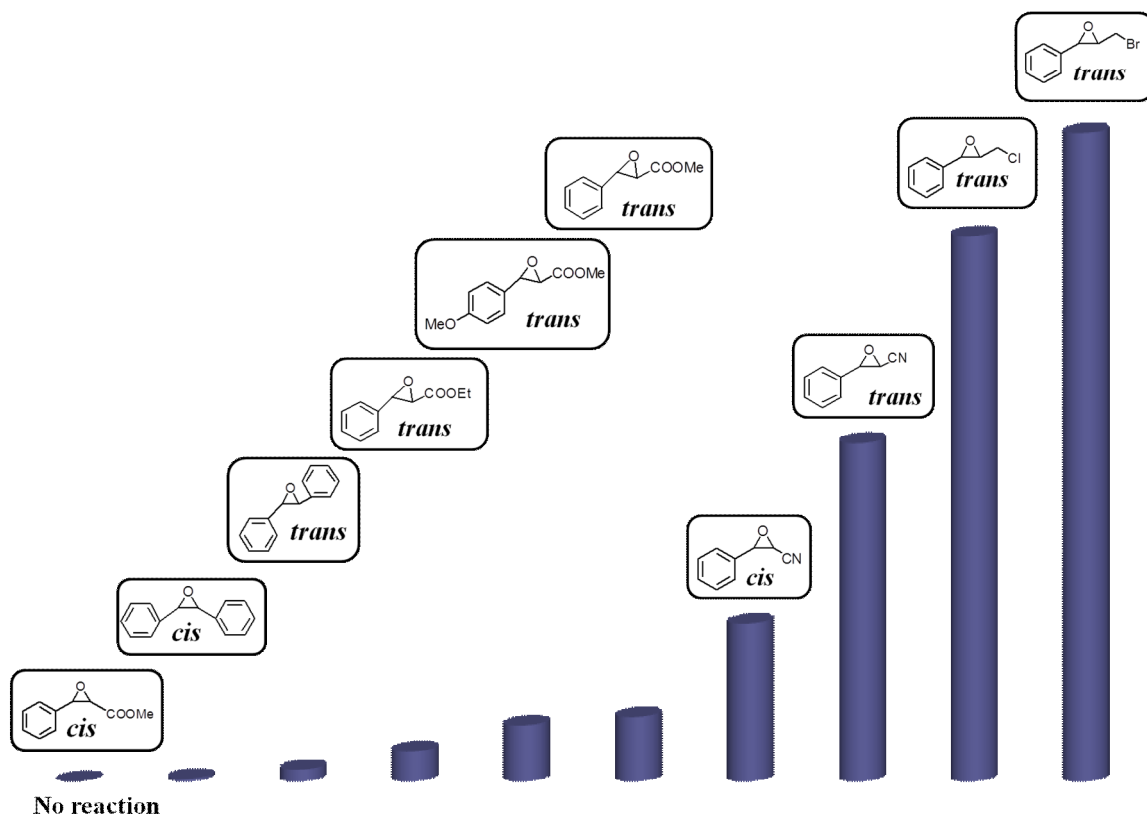


**Figure 103.** Comparison of Kau2-EH activities on different epoxides at the same 25 g/L concentration but under reaction conditions adapted for each substrate.

Astonishingly and when compared for example to *cis*-methyl styrene oxide (Kotik *et al.*, 2010), *cis*-stilbene oxide, *cis*-2,3-epoxy-3-phenyl propano nitrile and *trans*-methyl phenyl glycidate, the *cis*-methyl phenyl glycidate proved to be totally recalcitrant to Kau2-EH catalyzed bio-hydrolysis. No clear explanation of this fact could be given at that time.

In almost every case the biocatalytic reaction was of extremely high enantioselectivity, giving rise to numerous enantiomerically pure epoxides and diols except in two cases. Furthermore the tested reaction could be run on a preparative scale (1 g in each case) and the reaction times rarely exceeded 60-80 minutes (except with *cis*- and *trans*-styrene oxides). In order to conduct the bioconversion reactions with such water-insoluble substrates it has been proved that an organic immiscible phase could be used in order to dissolved the starting

material. A supplementary favorable effect in that case is that water sensitive substrates like *p*-methoxy-phenyl-glycidate are somewhat protected from chemical hydrolysis without affecting too much enzyme activity and furthermore substrate and/or product inhibition, if existing, could be alleviate or at least diminish.

In conclusion we have proved that Kau2-EH is an outstanding catalyst allowing an easy and performing access to numerous potentially useful optically pure diols and epoxides that could be used for example as chiral synthons in the production of some biologically active chemicals.

## III.4 Kinetic Studies

### III.4.1 Introduction

*The work described in this chapter was done in the context of a joint research project between the CNRS and the Academy of Sciences of the Czech Republic entitled: "Kinetic characterization of Kau2-EH and its enantioconvergent/enantioselective variants by steady-state and stopped-flow techniques". The financial support of this joint project allows me to work 4 weeks in the Laboratory of Enzyme Technology (Prague) under the supervision of M. Kotik. This project is always running and complementary studies should be done in the future.*

The aim of this study was to determine the mechanism of action of the wild type Kau2-EH as well as some of its mutants by steady-state and pre-steady-state kinetics measurements (stopped-flow). Kau2-EH whose behavior in some cases do not correlate with Michaelis-Menten law (Kotik *et al.*, 2010) seems to aggregate in solution or to allow different kinetically competent enzyme-substrate complexes to form (hysteretic behavior), leading to complex kinetics. Thanks to steady-state and stopped-flow kinetic measurements we wanted to get access to the true kinetic constants of the various enzyme-substrate complexes in order to establish a robust kinetic model for such an enzyme.

However, this type of study is consuming high quantities of purified protein and cannot be easily realized using wild type enzyme. In order to perform detailed functional studies and site-directed mutagenesis of Kau2-EH, a recombinant expression system enabling DNA manipulations and an efficient purification system must be developed. A widely employed method utilized immobilized metal-affinity chromatography to purify recombinant proteins containing a short affinity-tag consisting of poly-histidine residues. Poly-histidine affinity tags are commonly placed on either the N- or the C-terminus of recombinant proteins.

Using of stopped-flow technology to study enzymatic mechanisms of EHs was previously described in the case of *Agrobacterium radiobacter* EH (Rink and Janssen, 1998), murine EH (Laughlin *et al.*, 1998) and *Solanum tuberosum* EH (StEH or potato EH), (Elfstrom and Widersten, 2005; Elfström and Widersten, 2006; Lindberg *et al.*, 2010; Lindberg *et al.*, 2008). Interestingly, it was shown by Widersten and coworker (Elfstrom and Widersten, 2005) that, in the case of potato EH, the formation of the alkyl-enzyme could be followed by fluorescence decay using stopped-flow measurements. This was proposed to be the result of the fluorescence quenching of a tryptophan residue (Trp106) very close to the nucleophile, Asp105. Analysis of Kau2-EH sequence showed that, as for potato EH, a

tryptophan residue (Trp110) is also located just after the catalytic nucleophile residue, Asp109. The similitude (sequence identity and biocatalysis properties) between these two enzymes led us to use this technique to access the Kau2-EH kinetic constants involved in catalysis.

At first we decided to carry out this kinetic study using *trans*-stilbene oxide (TSO) as substrate mainly for two reasons:

First, the kinetic constants were previously determined for the biohydrolysis of the two enantiomers of TSO catalyzed by potato EH (Lindberg *et al.*, 2008) using the stopped-flow technology allowing thus to compare the data.

Second, despite similitude in the amino-acid sequence with the potato EH the Kau2-EH enzyme proved to be very efficient during kinetic resolution of *trans*-stilbene oxide (TSO) (E value >100, see chapter **III.3**) compared to EH of potato (E value = 2.9) (Lindberg *et al.*, 2008).

This study should thus help us to compare Kau2-EH and potato EHs from a kinetic point of view, in order to understand the difference in behavior of these two enzymes while structurally they are relatively close.

#### III.4.2 Construction of Kau2-HisTag and mutants

In order to purify protein of interest by affinity chromatography, two plasmids were constructed by using the pET100/D-TOPO<sup>®</sup> or pET101/D-TOPO<sup>®</sup> vectors (Invitrogen), allowing an affinity tag composed of six consecutive histidine residues (6×His-tag) to be located respectively on the N- or C-terminus of Kau2-EH. The two new plasmids were transformed into competent *E. coli* BL21 Star (DE3) cells as a host for expression (**Figure 104**).

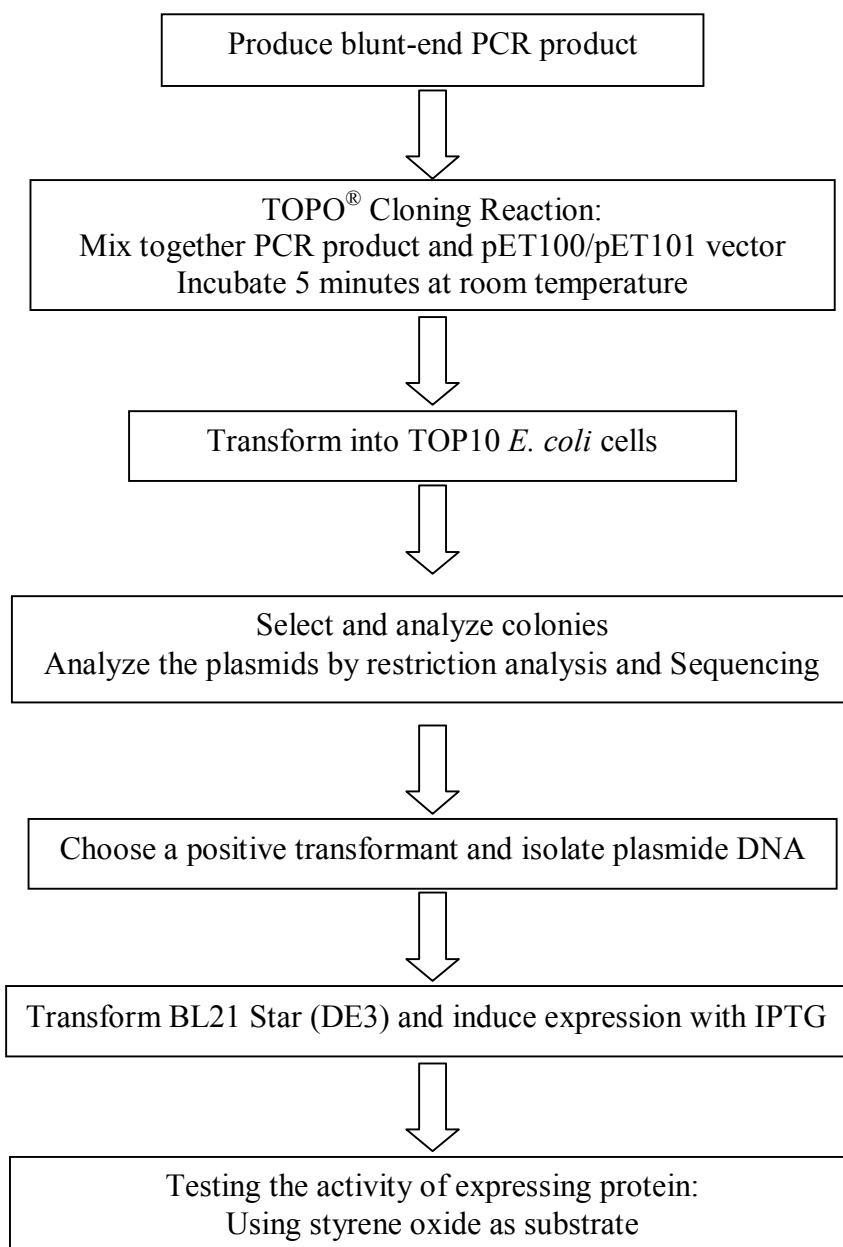


**Figure 104.** Experimental outline of recombinant plasmids construction and expression. Protocol to produce Kau2-His-6 EHs at N and C terminus position.

The activities of expressed enzymes were tested by using styrene oxide as substrate. After GC analysis, the results showed that the expression of the construction pET100+Kau2-EH (6×His-tag located N-terminus) displayed activity while the expression of the construction pET101+Kau2-EH (6×His-tag located C-terminus) displayed no activity at all.

Four mutants were also constructed based on pET100+Kau2 plasmid. D109A, D109N were produced based on the QuikChange Site-Directed Mutagenesis Protocol (Agilent),

H316A and H316Q Mutants were created by using Phusion site-Directed mutagenesis kit (Thermo). For primers used in the mutagenesis PCRs see **Annexe 10**.

After transformation into *E. coli* TOP10, plasmid DNA was isolated from selected colonies, and the EH-encoding inserts were sequenced using the automated DNA sequencer ABI PRISM 3130xl (Applied Biosystems) (see **Annexe 10**). After sequencing, all five pET100-based plasmids containing wild-type or mutant Kau2-encoding genes were transformed into *E. coli* BL21 Star (DE3) as an expression host.

### III.4.3 Heterologous expression of Kau2-His<sub>6</sub> and the corresponding mutants

An optimization of the expression level of the active enzyme in *E. coli* BL21 Star (DE3) cells was carried out. The expressions were done in 250 mL flask containing 100 mL of medium and several experimental conditions were studied:

- nature of the medium: LB or TB medium
- cell concentration before induction with IPTG (1 mM)
- time of expression after induction
- temperature of expression.

The results of this study are reported in **Table 28**

**Table 28.** Expression level of Kau2-HisTag using *E. coli* BL21 Star (DE3) as a host for expression under various conditions.

Medium	Cultivation temperature with IPTG	OD <sup>IPTG</sup>	OD <sup>H</sup>	Cultivation time with IPTG (h)	Total cultivation time (h)	Specific activity (U/mg)	Total Activity (U/flask)
TB	16 °C	1.06	3.2	19	23	1785	183097
	23 °C	1.01	4.5	4	7	1843	<b>265875</b>
		1.06	10.5	19	23	731	246009
	37 °C	1.01	5.4	4	7	161	27848
		1.06	14.5	19	23	17	7900
LB	16 °C	0.70	1.5	19	23	<b>2037</b>	97951
	23 °C	0.71	2.2	4	7	1055	74398
		0.70	2.3	19	23	1807	133215
	37 °C	0.71	3.2	4	7	120.6	12369
		0.70	2.5	19	23	61.6	4935

OD<sup>IPTG</sup>: Optical Density (OD600) at time of IPTG induction.

OD<sup>H</sup>: Optical Density (OD600) at time of harvest.

Activity (U/mg): Specific activity of Kau2-EH determined using (*S*)-*para*-chlorostyrene oxide as substrate and based on cell dry mass at time of harvest.

Total activity: total activity of EH Kau2-EH produced per flask (100 mL of medium).

From the results reported in **Table 28** it appears that the highest specific activity (2037 U/mg) was obtained using LB medium at the lowest temperature of induction (16 °C). However, it is also clear that utilization of TB medium with an induction at high cell concentration (OD 1.0 at 23 °C during 4 hours corresponded to the best conditions to obtain the highest level of enzyme quantity per flask (100 mL of medium). Based on these results the preparative expression of Kau2-EH-His-Tag and its corresponding mutants were carried out in 3L flasks containing 500 mL of TB medium with an induction at 23 °C during 4 h. After centrifugation the cells were kept at -80 °C.

#### III.4.4 Purification of Kau2-His<sub>6</sub> and the corresponding mutants

The frozen cells were thawed and directly suspended in the binding buffer, then broken using a disrupter apparatus (Constant System, one shot and 1.3 kbar). After

centrifugation the supernatant was loaded on HisTrap HP column (5mL) and the Kau2-EH protein was eluted using a linear gradient for the elution-buffer containing imidazole (500 mM). The protein started to be eluted when the imidazole concentration reached about 20%. (Figure 105)

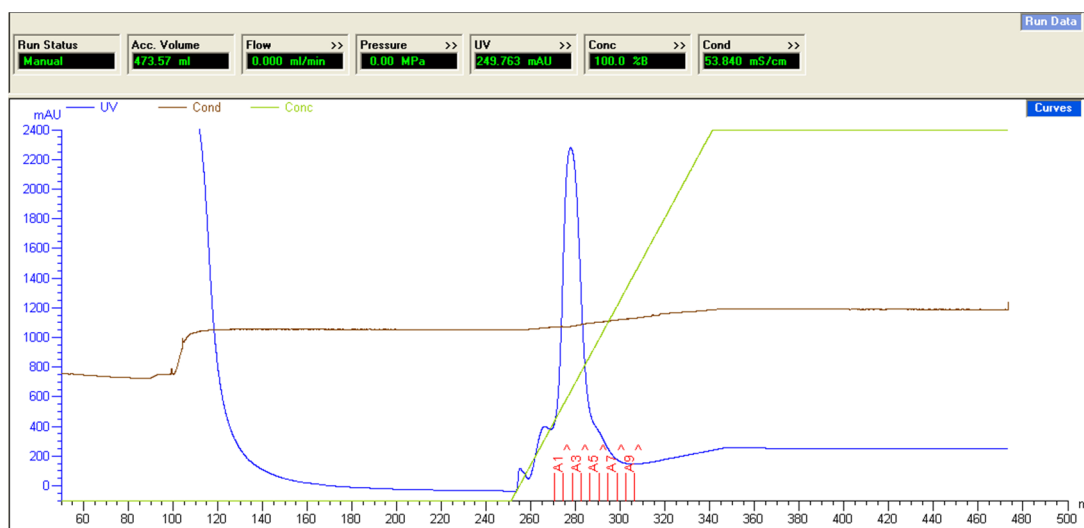


**Figure 105.** Protein purification process by FPLC using a HisTrap HP column (5mL).

The protein concentrations of collected fractions were determined using a Nanodrop 2000c apparatus (Thermo fisher) by measuring their intrinsic UV absorbance at 280 nm and applying a calculated molar extinction coefficient of  $58900 \text{ M}^{-1}\text{cm}^{-1}$ . About 22 mg of pure protein were obtained from 1 L of culture medium (TB medium using the optimized conditions described above). The purified protein had the expected molecular mass (38.2 kDa) and a specific activity of 9.13 U/mg using (*S,S*) *trans*-stilbene oxide as substrate. The purified Kau2-His<sub>6</sub> were analyzed by SDS-PAGE (Figure 106)

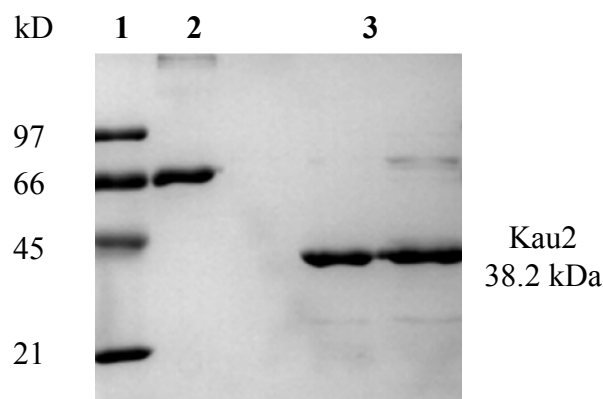


**Figure 106.** SDS-PAGE analysis of Kau2-His<sub>6</sub> lane 1: molecular weight marker (97.4 kD, 66.2 kD, 45.0 kD, 31.0 kD, 21.5 kD); lane 2: Bovine Serum Albumin (BSA); lane 3: purified Kau2-EH (1st isolation); lane 4: purified Kau2-EH (2nd isolation).

The four mutants were then also over-expressed and purified by the procedure used for the native-HisTag enzyme without modification (**Table 29**).

**Table 29.** Overexpression of the four mutants and the obtained mass of purified protein from 1L of medium culture.

Mutants	Wet biomass	Total mass of purified protein	Activity
H316Q	5.4 g	5.8 mg	0 U/mg
H316A	6.5 g	7.5 mg	0 U/mg
D109N	5.5 g	15.6 mg	0 U/mg
D109A	5.7 g	16.8 mg	0 U/mg

### III.4.5 Preparation of (*SS*)- and (*RR*)-TSO

To get access to the kinetic constants of TSO, pure (*S,S*)- and (*R,R*)- enantiomers of TSO must be in hand. Use of Kau2-EH as biocatalyst could be interest to prepare pure (*R,R*)-TSO as the residual enantiomer (see chapter **III.3**) however it was not possible to get access to its antipode, no enantiocomplementary EH being available in our laboratory. Fortunately, these two enantiomers can be separated using chiral HPLC column and this work was kindly done by Nicolas Vanthuyne (Chiral Analysis Platform of iSm2) using a preparative chiral

HPLC column (Chiralpak IC). The separation process allowed Nicolas Vanthuyne to isolate 1.2 g of each enantiomer in optically pure form starting for 2.5 g of *rac*-TSO (**Figure 107**).

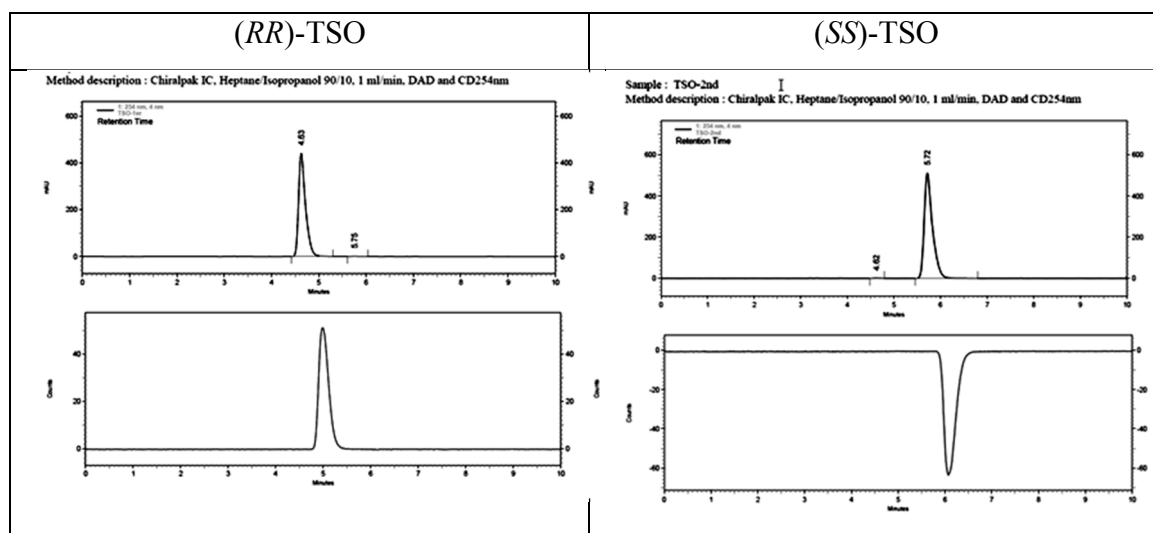


**Figure 107.** Results of the separation of the two enantiomers of TSO using a preparative chiral HPLC column (Chiralpak IC). The upper traces correspond to the UV (254 nm) analysis and the lower traces to the optical rotation associated to each enantiomers.

### III.4.6 Kinetic study

As mentioned in the introduction part of this chapter we wished to compare the results obtained previously by Widersten and coworkers (Lindberg *et al.*, 2008) using potato EH and the results obtained during the present study. Also we first used the same experimental conditions: temperature (30 °C), buffer (Phosphate buffer 100 mM, pH 8), organic co-solvent added to dissolve the substrate (acetonitrile, 1-2 % (v/v) and studied substrate concentrations range (12 to 130  $\mu$ M)). Unfortunately, we have observed that using these experimental conditions, the solubility of TSO in the reaction medium is very low and that a white emulsion occurred for the highest concentrations. We have thus carried out a complete study using these parameters but the obtained results were not satisfying for the substrate concentration was higher than 70-80  $\mu$ M (results not shown). In order to increase the substrate concentration in the reaction medium we decided to increase the acetonitrile concentration up to 4% (instead of 2%). In these conditions, the substrate solubility reached about 90-100  $\mu$ M and the residual activity of Kau2-EH was about 75%. To compensate a possible deleterious

effect of CH<sub>3</sub>CN onto the enzyme we have also decreased the reaction temperature from 30 to 23 °C.

### III.4.6.1 Steady-state kinetics

#### III.4.6.1.1 Steady-state kinetics of Kau2-EH catalyzed (*S,S*)-TSO hydrolysis

The activity during the steady-state was determined using a spectrophotometric test previously described by Hammock and coworkers (Hasegawa and Hammock, 1982). It is a continuous assay based on the differences in the UV spectra of TSO and its reaction product 1,2-diphenyl-1,2-ethanediol. Epoxide hydrolysis was followed by recording the decrease in absorbance at 229nm ( $\Delta\epsilon = 16140 \text{ M}^{-1}\text{cm}^{-1}$ ). Kinetic parameters were calculated using the Lineweaver-Burk plots (**Figure 108**).

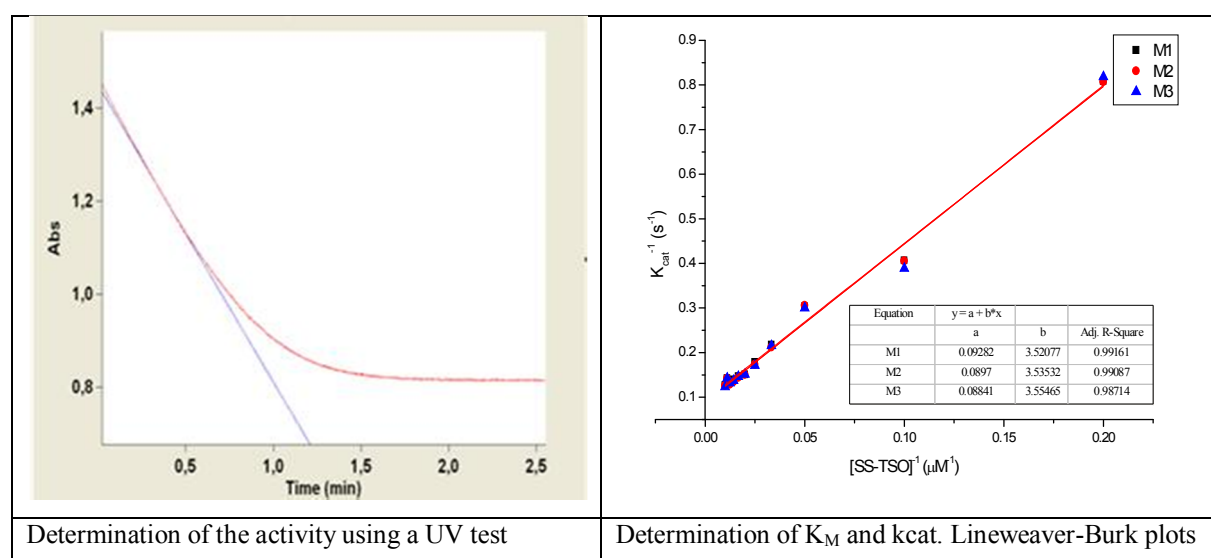


**Figure 108.** Determination of steady-state kinetic parameters for Kau2-His<sub>6</sub>-catalyzed hydrolysis of (*S,S*)-TSO. Experimental conditions: 23 °C, 4% CH<sub>3</sub>CN.

According to **Figure 108**, the Michaelis constants have been determined as:

$$K_M = 39 \mu\text{M} \text{ and } k_{\text{cat}} = 11 \text{ s}^{-1}.$$

#### III.4.6.1.2 Steady-state kinetics of (*R,R*)-TSO hydrolysis

No activity was detected when (*R,R*)-TSO was used as substrate. This result confirms the high level of enantioselectivity of Kau2-EH observed during the preparative biocatalysis

of the *rac*-TSO (see chapter III.3). Indeed, only the (*S,S*)-TSO was hydrolysed by Kau2-EH leaving its antipode unchanged.

Finally, we have controlled that the rate of the hydrolysis of the (*S,S*)-TSO was not affected by the presence of its antipode in the reaction medium (data not shown).

### III.4.6.2 Presteady-state kinetics of TSO conversion

#### III.4.6.2.1 Presteady-state kinetics of TSO hydrolysis using native Kau2-His<sub>6</sub>

When an enzyme is mixed with a substrate there is a transient phase called “presteady-state” during which free enzyme binds substrate, converts it to product at the active site and begins to release product to solution as the system approaches the steady-state. Under conditions in which product release is rate-limiting, there will be an initial “burst” of accumulation of product at the active site of the enzyme prior to the steady-state phase. In the case of some epoxide hydrolases it was shown that the presteady-state phase can be visualized by the decay of intrinsic fluorescence of the protein. This decay would correspond to the formation and the accumulation of the alkyl-enzyme (hydroxy-ester) intermediate in the active site and should be a function of the substrate concentration (**Figure 109 and 110**).

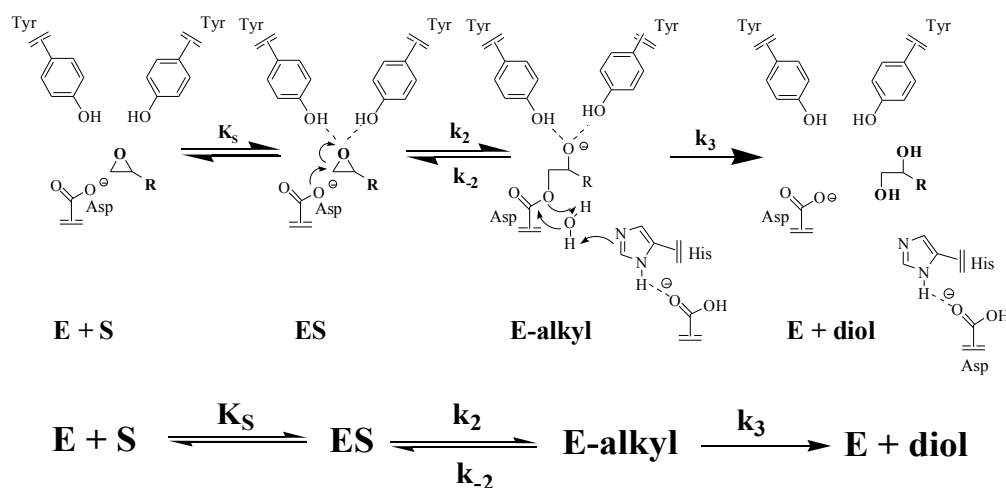


**Figure 109.** Kinetic mechanism of epoxide hydrolases ( $\alpha/\beta$ -hydrolase). This mechanism includes the Michaelis complex formation followed by the formation of a covalent alkyl-enzyme with a rate  $k_2$ . The alkyl-enzyme is subsequently hydrolyzed with rate  $k_3$ , to restore the enzyme.  $K_s$ , the equilibrium constant of the dissociation of the Michaelis complex ( $k_{-1}/k_1$ ).

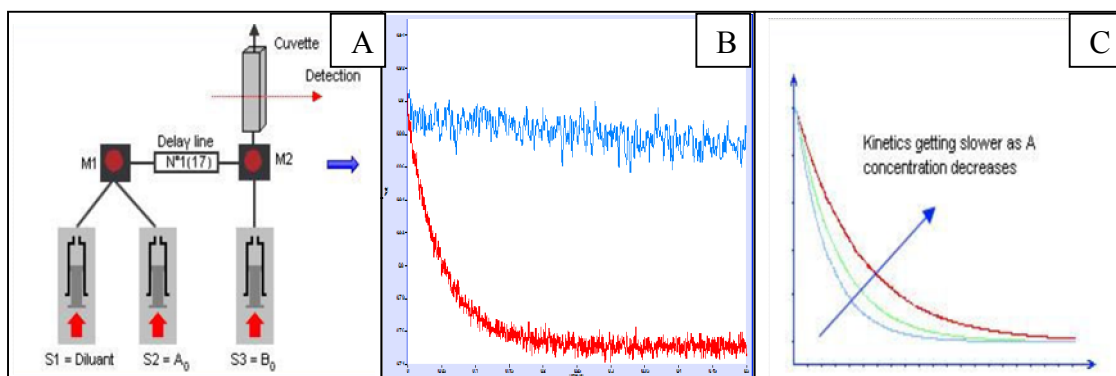


**Figure 110.** A- Schematic diagram of a stop-flow apparatus. In the case of an enzymatic study the syringe S3 is filled by enzyme solution and syringes S1 & S2 are respectively filled with pure buffer and substrate diluted in buffer. M1 and M2 are the mixing chambers. B - Fluorescence traces, without substrate (blue), immediately after the mixing of substrate and enzyme (red). C- Fluorescence traces for different substrate concentrations.

From the kinetic model described in **Figure 109** it was demonstrated (Lindberg *et al.*, 2008) that the corresponding steady-state law was described by Eqn (1). In this equation  $k_{cat}$  corresponds to the first term in numerator (Eqn (2)) and  $K_M$  the first factor in the denominator (Eqn (3)). It was demonstrated that the relation between the observed kinetic constant ( $k_{obs}$ ) obtained from the stopped-flow experiment (presteady-state) and the substrate concentration can be described by Eqn (4). Eqn (5) and Eqn (6) correspond to a simplification of the Eqn (4) an Eqn (2) respectively.

Eqn (1)	Eqn (2)	Eqn (3)
$v = \frac{\frac{k_2 * k_3}{(k_2 + k_{-2} + k_3)} [E]_0 * [S]}{\frac{K_S * (k_2 + k_3)}{(k_2 + k_{-2} + k_3)} + [S]}$	$k_{cat} = \frac{k_2 * k_3}{(k_2 + k_{-2} + k_3)}$	$K_M = \frac{K_S * (k_{-2} + k_3)}{(k_2 + k_{-2} + k_3)}$
Eqn (4)	Eqn (5) if $K_S \gg S$	Eqn (6) if $k_2 \gg k_{-2} + k_3$
$k_{obs} = \frac{k_2 * [S]}{K_S + [S]} + k_{-2} + k_3$	$k_{obs} = \frac{k_2 * [S]}{K_S} + k_{-2} + k_3$	$k_{cat} = k_3$

The presteady-state kinetic experiments were conducted on a Biologic SFM 300 stopped-flow spectrometer mode. The tryptophane residues were excited at 290 nm and the total protein fluorescence was recorded after passage through a 320 nm cutoff filter. All the

reactions were performed in 100 mM Phosphate buffer (pH 8.0) containing 4% CH<sub>3</sub>CN at 23 °C. The concentration of (*S,S*)-TSO was varied between 5 and 90 μM. Each concentration was prepared, just before utilization, by mixing the substrate dissolved in CH<sub>3</sub>CN (5 mM) with the phosphate buffer in order to get a final CH<sub>3</sub>CN concentration of 4% (v/v) in the measurement cell. Kau2-EH was dissolved in phosphate buffer (100 mM, pH 8.0) to a final concentration of 1.2 μM.

Using these experimental conditions, rapid mixing of Kau2-His<sub>6</sub> and (*S,S*)-TSO resulted in fast-transient decreases in intrinsic Trp-fluorescence following a single exponential curve (**Figure 111-A**) until a steady-state level is reached. The observed first-order rate constant ( $k_{\text{obs}}$ ) for the fluorescence decrease was dependent on the substrate concentration, the higher  $k_{\text{obs}}$  being obtained with increasing substrate concentrations (**Figure 111-B**). In addition, observed rates ( $k_{\text{obs}}$ ) showed linear substrate dependence indicating that the enzyme is far from substrate saturation concentration. Unfortunately, in these conditions it is not possible to access all the kinetic constants, however, this observation leads to a simplification of the Eqn (4) into the Eqn (5) ( $K_s \gg [S]$ ). The intercept with the abscissa yields the sum  $k_{-2} + k_3$  ( $13.1 \text{ s}^{-1}$ ) and from the slope, the ratio of the  $k_2/K_s$  value ( $0.29 \mu\text{M}^{-1} \cdot \text{s}^{-1}$ ) can be obtained. In these conditions the value of  $k_{\text{cat}}$  should be dictated by the rate of  $k_3$  (Eqn (6)) and  $k_3$  should correspond to the value of  $k_{\text{cat}}$  ( $11 \text{ s}^{-1}$ ) determined in the steady state study (see **Figure 108**). Finally, using this  $k_3$  value an estimation of  $k_{-2}$  ( $k_{-2} = 13.1 - 11 = 2.1 \text{ s}^{-1}$ ) can be done from the  $k_{\text{obs}}$ -intercept value (**Table 30**).

The same protocol was applied to the study of the (*R,R*)-TSO but no change of the intrinsic protein fluorescence could be observed. This last result is an agreement with the absence of activity previously observed ( $k_{\text{cat}} = 0$ ) in the steady-state study. In addition it would seem to indicate that no alkyl-enzyme was formed in the active site, this observation is also in agreement with the fact that the (*R,R*)-TSO is not an inhibitor of the biohydrolysis of its antipode (data not shown).

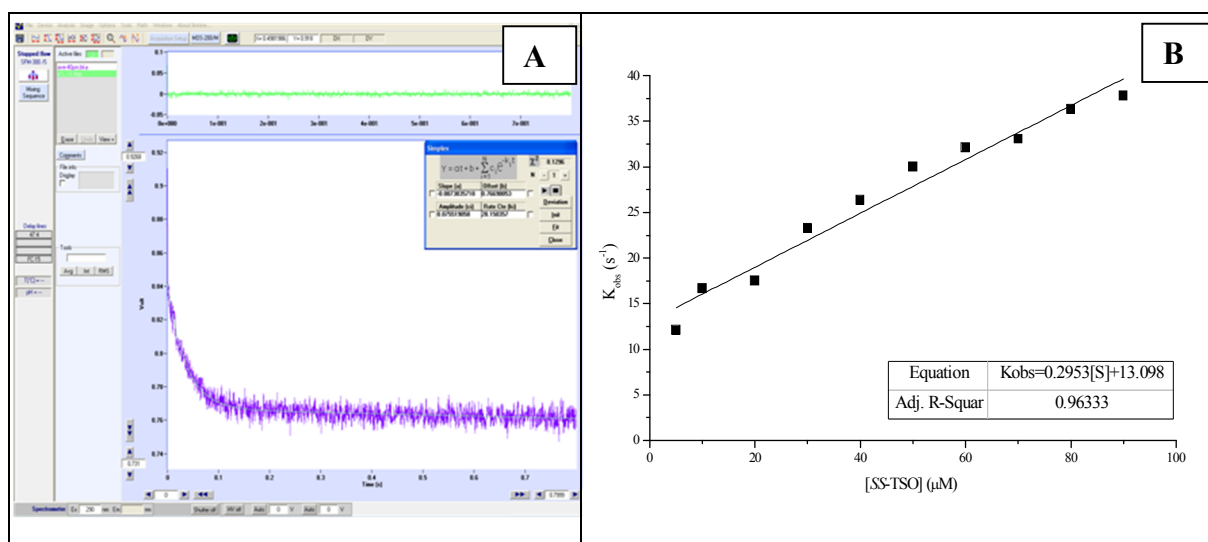


**Figure 11.** **A-** Tryptophane fluorescence trace of 1.2  $\mu\text{M}$  Kau2-His<sub>6</sub> and 40  $\mu\text{M}$  (S,S)-TSO. For the determination of the corresponding  $k_{\text{obs}}$  a fit with a single exponential curve [ $F = A \exp(-k_{\text{obs}}t) + C$ ] in which A is the amplitude of fluorescence change,  $k_{\text{obs}}$  the observed rate constant and C the floating end point of the progression curve (average of 5 traces). **B-** Observed rates,  $k_{\text{obs}}$ , plotted versus (S,S)-TSO concentration. The solid line corresponds to the linear fit of Eqn 5 to the substrate dependence (Lindberg *et al.*, 2008).

**Table 30.** Presteady-state and steady-state kinetic constants for the Kau2-EH catalyzed hydrolysis of (S,S)- and (R,R)-TSO and the kinetic constants previously described by Widersten and coworker (Lindberg *et al.*, 2008) using StEH.

	$k_{\text{cat}}$ ( $\text{s}^{-1}$ ) <sup>a</sup>	$K_M$ ( $\mu\text{M}$ ) <sup>a</sup>	$K_s$ ( $\mu\text{M}$ )	$k_2$ ( $\text{s}^{-1}$ )	$k_2$ ( $\text{s}^{-1}$ )	$k_3$ ( $\text{s}^{-1}$ )	$k_{\text{cat}}/K_M$ ( $\text{s}^{-1} \cdot \mu\text{M}^{-1}$ ) <sup>a</sup>	$k_2/K_s$ ( $\text{s}^{-1} \cdot \mu\text{M}^{-1}$ )
Kau2-EH/S,S-TSO	11	39	>1000 <sup>c</sup>	>290 <sup>c</sup>	2.1	11	0.3	0.29
Kau2-EH/R,R-TSO	0	-	-	-	-	-	-	-
StEH/S,S-TSO <sup>b</sup>	0.9	0.31	14	29	14	1.4	2.9	3.3
StEH/R,R-TSO <sup>b</sup>	15	16	42	51	26	32	1	2.6

<sup>a</sup> Determined by the steady-state experiments.

<sup>b</sup> Determined by Widersten and coworker using 2% acetonitrile and 30 °C (Lindberg *et al.*, 2008).

<sup>c</sup> Estimated value considering that  $K_s + [S] \approx K_s$  if  $K_s > 20*[S]$  (Rink *et al.*, 1998).

In a first time, we wanted to compare the kinetic results previously described for the potato EH (see **Table 30**) and our Kau2-EH. However, we were not able to use the same experimental conditions (% of cosolvent and temperature) also a comparison of our results to those described by Widersten and coworkers is not really possible. In addition, we have some

doubts about the accuracy of the Widersten's results when "high TSO concentrations" were used in the stopped-flow apparatus due in our hands to solubility problems.

The formation of a "burst" confirms accumulation of an alkyl-enzyme intermediate, and thus, that the limiting step for Kau2-EH would be the hydrolysis of the covalent alkyl-enzyme intermediate. The steady state value of  $K_M$  (39  $\mu\text{M}$ ) is much smaller than the estimated apparent dissociation constant of the substrate ( $K_s > 1 \text{ mM}$ ) due to extensive accumulation of the alkyl-enzyme intermediate in the steady state. The above presteady-state analysis is consistent with the steady-state kinetic measurements. Indeed, a calculation of the  $K_M$  after simplification of the Eqn (3) [ $K_M = (K_s/k_2) \cdot (k_{-2} + k_3)$ ] leads to a value of 44  $\mu\text{M}$  that is in perfect agreement with the value of 39  $\mu\text{M}$  determined in the steady-state study.

In conclusion, the experimental results verified the proposed catalytic mechanism of Kau2-EH, as illustrated in **Figure 109**. The Michaelis complex is formed with a high  $K_s$  (*i.e.* low ES stabilization), followed by the fast and almost irreversible ( $k_{-2} = 2.1 \text{ s}^{-1}$ ) formation of the alkyl-enzyme intermediate (high  $k_2$  value). The subsequent hydrolytic step is rate limiting ( $k_3 = 11 \text{ s}^{-1}$ ) occurring as a steady-state reaction producing the *meso*-diol.

#### **III.4.6.2.2 Presteady-state kinetics of (*S,S*)-TSO hydrolysis using Kau2-His<sub>6</sub> mutants**

As expected mixing of the Asp109Ala or Asp109Asn mutant enzymes with (*S,S*)-TSO did not result in any change of the intrinsic protein fluorescence, indicating that formation of the Michaelis complex (ES) did not affect the fluorescence signal.

Astonishingly, mixing of His316Ala or His316Gln mutants with (*S,S*)-TSO did not result in any change of the intrinsic protein fluorescence as expected. Two possible reasons may be proposed to explain these results. First, the mutant enzyme is not alkylated, the mutation of the His316 residue prevent using the nucleophilic attack of the Asp109 onto the epoxide ring of the substrate. Second, the mutant enzyme may be alkylated but with no concomitant change in the intrinsic protein fluorescence for any reaction.

Some others mutants should be built and tested to clarify this point, in particular it would be very interesting to test a mutant in which the Trp110 would be replaced by an Alanine for example.

#### **III.4.6.2.3 Presteady-state kinetics of various epoxides hydrolysis using native enzyme**

The following substrates were tested: (*S*)- and (*R*)-SO; (*S*) and (*R*)-*p*ClSO, (*R,R*)- and (*S,S*)-*trans*-Methyl-styrene oxide, *cis*-Stilbene oxide all known to be substrates of Kau2-EH as well as the inhibitors N-cyclohexyl-N'-decylurea (CDU) and N-cyclohexyl-N'-(4-iodophenyl) urea (CIU).

No “burst” was observed when CDU and CIU inhibitors were mixed with Kau2-EH. This result seems to confirm that the variation of fluorescence is not connected to the formation of the ES complex. Very curiously no “burst” was observed when all the above known epoxide substrates of Kau2-EH were tested. It should be noticed that important changes of the intrinsic protein fluorescence were reported using potato EH as enzyme and the enantiomers of styrene oxide or *trans*-methyl-styrene oxide as substrate (Lindberg *et al.*, 2010). An explanation of these facts could be that, as for His316, mutants, the alkylation of the enzyme occurred but with no concomitant change in the intrinsic protein fluorescence, the fluorescence of the Trp110 being not modified by these epoxides. The other explanation would be that the alkylation reaction is much slower than the hydrolytic half-reaction so that the ester intermediate does not accumulate to an appreciable extent in the steady state ( $k_3 > k_2$ ).

### III.4.7 Conclusion

The determination of the kinetic constants of an enzyme reaction represents a huge work and it would be necessary in our case to carry out some more experiments to clarify the somewhat curious results we have obtained in this preliminary study. In particular, it would be of interest to carry out experiments called “Single-turnover” in which the enzyme concentration must be high and higher than the substrate concentration, for which a great quantity of pure enzyme must be available. Nevertheless, these preliminary results allowed us to get some interesting information on the Kau2-EH mechanism and open the way to further experiments.

## References:

- Adger, B., Barkley, J., Cappi, M., Flowerdew, B., Jackson, M., Nugent, T. and Roberts, S. (1997) Improved procedure for Juliß–Colonna asymmetric epoxidation of  $\alpha$ ,  $\beta$ -unsaturated ketones: total synthesis of diltiazem and Taxol TM side-chain. *J. Chem. Soc., Perkin Trans. 1*, 3501-3508.
- Afon'kin, A., Kostrikin, L., Shumeiko, A., Popov, A., Matveev, A., Matvienko, V. and Zabudkin, A. (2012) Regio- and stereoselective methods for the conversion of (2*S*,3*R*)- $\beta$ -phenylglycidic acid esters to taxoids and other enantiopure (2*R*,3*S*)-phenylisoserine esters. *Russ. Chem. Bull.*, **61**, 2149-2162.
- Archelas, A. and Furstoss, R. (1997) Synthesis of enantiopure epoxides through biocatalytic approaches. *Annu. Rev. Microbiol.*, **51**, 491-525.
- Archelas, A. and Furstoss, R. (1998) Epoxide hydrolases: new tools for the synthesis of fine organic chemicals. *Trends Biotechnol.*, **16**, 108-116.
- Argiriadi, M.A., Morisseau, C., Goodrow, M.H., Dowdy, D.L., Hammock, B.D. and Christianson, D.W. (2000) Binding of alkylurea inhibitors to epoxide hydrolase implicates active site tyrosines in substrate activation. *J. Biol. Chem.*, **275**, 15265-15270.
- Argiriadi, M.A., Morisseau, C., Hammock, B.D. and Christianson, D.W. (1999) Detoxification of environmental mutagens and carcinogens: structure, mechanism, and evolution of liver epoxide hydrolase. *Proc. Natl. Acad. Sci.*, **96**, 10637-10642.
- Barth, S., Fischer, M., Schmid, R.D. and Pleiss, J. (2004) Sequence and structure of epoxide hydrolases: a systematic analysis. *Proteins: Struct., Funct., Bioinf.*, **55**, 846-855.
- Bershtein, S. and Tawfik, D.S. (2008) Advances in laboratory evolution of enzymes. *Curr. Opin. Chem. Biol.*, **12**, 151-158.
- Berti, G., Bottari, F., Ferrarini, P.L. and Macchia, B. (1965) Stereochemistry of the Additions of Acids to Stilbene and Styrene Oxides. *J. Org. Chem.*, **30**, 4091-4096.
- Cabon, O., Buisson, D., Larcheveque, M. and Azerad, R. (1995) Stereospecific preparation of glycidic esters from 2-chloro-3-hydroxyesters. Application to the synthesis of (2*R*,3*S*)-3-phenylisoserine. *Tetrahedron: Asymmetry*, **6**, 2211-2218.
- Cornish-Bowden, A. (1974) A simple graphical method for determining the inhibition constants of mixed, uncompetitive and non-competitive inhibitors. *Biochem. J.*, **137**, 143-144.
- Cortes, A., Cascante, M., Cardenas, M. and Cornish-Bowden, A. (2001) Relationships between inhibition constants, inhibitor concentrations for 50% inhibition and types of inhibition: new ways of analysing data. *Biochem. J.*, **357**, 263-268.
- Dehli, J.R. and Gotor, V. (2002) Parallel kinetic resolution of racemic mixtures: a new strategy for the preparation of enantiopure compounds? *Chem. Soc. Rev.*, **31**, 365-370.
- Devi, A.V., Lahari, C., Swarnalatha, L. and Fadnavis, N. (2008) Gelozymes in organic synthesis. Part IV: Resolution of glycidate esters with crude Mung bean (*Phaseolus radiatus*) epoxide hydrolase immobilized in gelatin matrix. *Tetrahedron: Asymmetry*, **19**, 1139-1144.
- Effenberger, F., Hopf, M., Ziegler, T. and Hudelmayer, J. (1991) Darstellung O-geschützter (*R*)-2-Hydroxyaldehyde und ihre Hydrocyanierung. *Chem Ber*, **124**, 1651-1659.
- Elfstrom, L. and Widersten, M. (2005) Catalysis of potato epoxide hydrolase, StEH1. *Biochem. J.*, **390**, 633-640.
- Elfström, L.T. and Widersten, M. (2006) Implications for an ionized alkyl-enzyme intermediate during StEH1-catalyzed trans-stilbene oxide hydrolysis. *Biochemistry*, **45**, 205-212.
- Gentile, A., Giordano, C., Fuganti, C., Ghirotto, L. and Servi, S. (1992) The enzymic preparation of (2*R*,3*S*)-phenyl glycidic acid esters. *J. Org. Chem.*, **57**, 6635-6637.
- Gomez, G.A., Morisseau, C., Hammock, B.D. and Christianson, D.W. (2004) Structure of human epoxide hydrolase reveals mechanistic inferences on bifunctional catalysis in epoxide and phosphate ester hydrolysis. *Biochemistry*, **43**, 4716-4723.
- Grulich, M., Maršálek, J., Kyslík, P., Štěpánek, V. and Kotík, M. (2011) Production, enrichment and immobilization of a metagenome-derived epoxide hydrolase. *Process Biochem.*, **46**, 526-532.
- Hamamoto, H., Mamedov, V.A., Kitamoto, M., Hayashi, N. and Tsuboi, S. (2000) Chemoenzymatic synthesis of the C-13 side chain of paclitaxel (Taxol) and docetaxel (Taxotere). *Tetrahedron: Asymmetry*, **11**, 4485-4497.
- Hameršák, Z., Šepac, D., Žiher, D. and Šunjić, V. (2003) Synthesis of all stereoisomers and some congeners of isocytosazone. *Synthesis*, **2003**, 375-382.
- Hasegawa, L.S. and Hammock, B.D. (1982) Spectrophotometric assay for mammalian cytosolic epoxide hydrolase using trans-stilbene oxide as the substrate. *Biochem Pharmacol*, **31**, 1979-1984.
- Hoover, T.R., Groeper, J.A., Parrott II, R.W., Chandrashekar, S.P., Finefield, J.M., Dominguez, A. and Hitchcock, S.R. (2006) Towards the development of oxadiazinanones as chiral auxiliaries: synthesis and application of *N*<sub>3</sub>-haloacetyloxadiazinanones. *Tetrahedron: Asymmetry*, **17**, 1831-1841.

Imashiro, R. and Seki, M. (2004) A catalytic asymmetric synthesis of chiral glycidic acid derivatives through chiral dioxirane-mediated catalytic asymmetric epoxidation of cinnamic acid derivatives. *J. Org. Chem.*, **69**, 4216-4226.

Jobson, N.K., Crawford, A.R., Dewar, D., Pimlott, S.L. and Sutherland, A. (2009) Design and synthesis of (2*R*, 3*S*)-iodoreboxetine analogues for SPECT imaging of the noradrenaline transporter. *Bioorg. Med. Chem. Lett.*, **19**, 4996-4998.

Kotik, M. (2009) Novel genes retrieved from environmental DNA by polymerase chain reaction: current genome-walking techniques for future metagenome applications. *J. Biotechnol.*, **144**, 75-82.

Kotik, M., Štěpánek, V., Grulich, M., Kyslík, P. and Archelas, A. (2010) Access to enantiopure aromatic epoxides and diols using epoxide hydrolases derived from total biofilter DNA. *J. Mol. Catal. B: Enzym.*, **65**, 41-48.

Kotik, M., Štěpánek, V., Marešová, H., Kyslík, P. and Archelas, A. (2009) Environmental DNA as a source of a novel epoxide hydrolase reacting with aliphatic terminal epoxides. *J. Mol. Catal. B: Enzym.*, **56**, 288-293.

Kotik, M., Zhao, W., Iacazio, G. and Archelas, A. (2013) Directed evolution of metagenome-derived epoxide hydrolase for improved enantioselectivity and enantioconvergence. *J. Mol. Catal. B: Enzym.*, **91**, 44-51.

Kumar, P., Dubey, A. and Harbindu, A. (2012) Enantio- and diastereocontrolled conversion of chiral epoxides to trans-cyclopropane carboxylates: application to the synthesis of cascarillic acid, grenadamide and L-(-)-CCG-II. *Org. Biomol. Chem.*, **10**, 6987-6994.

Laughlin, L.T., Tzeng, H.-F., Lin, S. and Armstrong, R.N. (1998) Mechanism of microsomal epoxide hydrolase. Semifunctional site-specific mutants affecting the alkylation half-reaction. *Biochemistry*, **37**, 2897-2904.

Lindberg, D., de la Fuente Revenga, M. and Widersten, M. (2010) Temperature and pH dependence of enzyme-catalyzed hydrolysis of trans-methylstyrene oxide. A unifying kinetic model for observed hysteresis, cooperativity, and regioselectivity. *Biochemistry*, **49**, 2297-2304.

Lindberg, D., Gogoll, A. and Widersten, M. (2008) Substrate - dependent hysteretic behavior in StEH1 - catalyzed hydrolysis of styrene oxide derivatives. *FEBS journal*, **275**, 6309-6320.

Matthews, B., Jackson, W., Jacobs, H. and Watson, K. (1990) Synthesis of Aryl Carbohydrate Synthons and 2, 3-Dihydroxypropanoic Acid-Derivatives of High Optical Purity. *Aust. J. Chem.*, **43**, 1195-1214.

McGuire, W.P., Rowinsky, E.K., Rosenshein, N.B., Grumbine, F.C., Ettinger, D.S., Armstrong, D.K. and Donehower, R.C. (1989) Taxol: a unique antineoplastic agent with significant activity in advanced ovarian epithelial neoplasms. *Ann. Intern. Med.*, **111**, 273-279.

Mhamdi, L., Bohli, H., Moussaoui, Y. and ben Salem, R. (2011) Phase Transfer Catalysis of Henry and Darzens Reactions. *Int. J. Org. Chem.*, **1**, 119-123.

Mowbray, S.L., Elfström, L.T., Ahlgren, K.M., Andersson, C.E. and Widersten, M. (2006) X - ray structure of potato epoxide hydrolase sheds light on substrate specificity in plant enzymes. *Protein Sci*, **15**, 1628-1637.

Otten, L.G. and Quax, W.J. (2005) Directed evolution: selecting today's biocatalysts. *Biomol. Eng.*, **22**, 1-9.

Palazón, J., Añorbe, B. and Martín, V. (1986) General method to transform chiral 2, 3-epoxyalcohols into erythro or threo 1, 2-epoxyalcohols with total stereochemical control. *Tetrahedron Lett.*, **27**, 4987-4990.

Palin, R., Barn, D.R., Clark, J.K., Cottney, J.E., Cowley, P.M., Crockatt, M., Evans, L., Feilden, H., Goodwin, R.R., Griekspoor, F., Grove, S.J., Houghton, A.K., Jones, P.S., Morphy, R.J., Smith, A.R., Sundaram, H., Vrolijk, D., Weston, M.A., Wishart, G. and Wren, P. (2005) Synthesis and SAR studies of 3-phenoxypropyl piperidine analogues as ORL1 (NOP) receptor agonists. *Bioorg. Med. Chem. Lett.*, **15**, 589-593.

Pavlova, M., Klvana, M., Prokop, Z., Chaloupkova, R., Banas, P., Otyepka, M., Wade, R.C., Tsuda, M., Nagata, Y. and Damborsky, J. (2009) Redesigning dehalogenase access tunnels as a strategy for degrading an anthropogenic substrate. *Nat. Chem. Biol.*, **5**, 727-733.

Reetz, M.T. (2004) Controlling the enantioselectivity of enzymes by directed evolution: practical and theoretical ramifications. *Proc. Nat. Acad. Sci. U.S.A.*, **101**, 5716-5722.

Rink, R. and Janssen, D.B. (1998) Kinetic mechanism of the enantioselective conversion of styrene oxide by epoxide hydrolase from *Agrobacterium radiobacter* AD1. *Biochemistry*, **37**, 18119-18127.

Rowinsky, E.K., Cazenave, L.A. and Donehower, R.C. (1990) Taxol: a novel investigational antimicrotubule agent. *J. Natl. Cancer. Inst.*, **82**, 1247-1259.

Saikia, I., Kashyap, B. and Phukan, P. (2010) Efficient Protocol for Stereoselective Epoxidation of Cinnamic Esters Using TsNBr<sub>2</sub>. *Synth. Commun.*, **40**, 2647-2652.

Seki, M., Furutani, T., Imashiro, R., Kuroda, T., Yamanaka, T., Harada, N., Arakawa, H., Kusama, M. and Hashiyama, T. (2001) A novel synthesis of a key intermediate for diltiazem. *Tetrahedron Lett.*, **42**, 8201-8205.

Steinreiber, A. and Faber, K. (2001) Microbial epoxide hydrolases for preparative biotransformations. *Curr. Opin. Biotechnol.*, **12**, 552-558.

Svoboda, J., Kocfeldová, Z. and Paleček, J. (1988) Reaction of 4-substituted benzaldehydes and acetophenones with chloroacetonitrile. *Collect. Czech. Chem. Commun.*, **53**, 822-832.

Takenaka, N., Xia, G. and Yamamoto, H. (2004) Catalytic, highly enantio- and diastereoselective pinacol coupling reaction with a new tethered bis (8-quinolinolato) ligand. *J. Am. Chem. Soc.*, **126**, 13198-13199.

- Van Loo, B., Kingma, J., Arand, M., Wubbolts, M.G. and Janssen, D.B. (2006) Diversity and biocatalytic potential of epoxide hydrolases identified by genome analysis. *Appl. Environ. Microbiol.*, **72**, 2905-2917.
- Wang, Z.-X. and Shi, Y. (1997) A new type of ketone catalyst for asymmetric epoxidation. *J. Org. Chem.*, **62**, 8622-8623.
- Wei, C., Ling, J., Shen, H. and Zhu, Q. (2014) Bioresolution Production of (2*R*,3*S*)-Ethyl-3-phenylglycidate for Chemoenzymatic Synthesis of the Taxol C-13 Side Chain by *Galactomyces geotrichum* ZJUTZQ200, a New Epoxide-Hydrolase-Producing Strain. *Molecules*, **19**, 8067-8079.
- Wubbolts, M.G., Favre - Bulle, O. and Witholt, B. (1996) Biosynthesis of synthons in two - liquid - phase media. *Biotechnol. Bioeng.*, **52**, 301-308.
- Yadav, J.S., Premalatha, K., Harshavardhan, S.J. and Subba Reddy, B.V. (2008) The first stereoselective and the total synthesis of Leiocarpin C and total synthesis of (+)-Goniodiol. *Tetrahedron Lett.*, **49**, 6765-6767.
- Yang, M.-H., Cao, Y.-H., Li, W.-X., Yang, Y.-Q., Chen, Y.-Y. and Huang, L. (1987) Isolation and structural elucidation of clausenamides from the leaves of *Clausena lansium* (Lour.) Skeels. *Acta Pharm Sin*, **22**, 33-40.
- Yudin, A.K. (2006) *Aziridines and epoxides in organic synthesis*. John Wiley & Sons.
- Zagozda, M. and Plenkiewicz, J. (2008) Biotransformations of 2, 3-epoxy-3-arylpropanenitriles by *Debaryomyces hansenii* and *Mortierella isabellina* cells. *Tetrahedron: Asymmetry*, **19**, 1455-1460.
- Zheng, G., Yuan, Q., Yang, L., Zhang, X., Wang, J. and Sun, W. (2006) Preparation of (2*S*,3*R*)-methyl-3-phenylglycidate using whole cells of *Pseudomonas putida*. *J. Mol. Catal. B: Enzym.*, **43**, 133-136.
- Zhu, X.Z., Li, X.Y. and Liu, J. (2004) Recent pharmacological studies on natural products in China. *Eur. J. Pharmacol.*, **500**, 221-230.

## Chapter IV. Conclusion

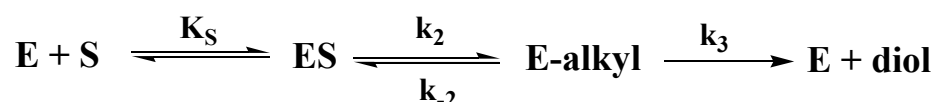
The work described in this manuscript was conducted in order to get valuable information about the metagenome derived Kau2-EH from both structural, mechanistic and biocatalytic point of view.

In a first chapter and following amino acid alignment comparison with other EHs of known 3D structure, Kau2-EH sequence proved to be most closely related to the potato, human and murine EHs with sequence identities of 32, 35 and 37%, respectively. Three structural homology models were then constructed using as template these three 3D structures. To determine which model is the best, inhibition studies were conducted with CDU and CIU as inhibitors of potato and Kau2 EHs. Both CDU and CIU inhibitors were previously shown to act as potent competitive inhibitors of murine sEH (Argiriadi *et al.*, 2000). Conducted inhibition studies allowed to determine that the found competitive inhibition constants ( $K_i$ ) for Kau2-EH are more closely related to the ones found for murine EH than to the ones determined for potato EH. We thus decided to use homology model derived from murine EH 3D structure to model Kau2-EH. From this model M. Kotik in Prague has conducted saturation mutagenesis experiments, targeted at specific residues within the large substrate binding pocket of Kau2-EH, in order to generate mutants with improved properties. Five amino acid substitutions (W110L, F113L, F161Y, P193G and V290W) were sufficient to increase the degree of enantioconvergence from 84.2% for the wild-type Kau2-EH enzyme to 93.0% for the final evolved EH variant, enabling the production of the chiral building block (*R*)-*para*-chlorophenylethane-1,2-diol with an enantiomeric excess of 93.0% in a complete conversion of the starting epoxide *rac*-*p*CISO.

In a second chapter the biocatalytic potential of Kau2-EH was assessed. A series of 10 aromatic epoxides were tested and nine of them proved to be substrates of Kau2-EH except *cis*-methyl glycidate that was not substrate at all. Of these nine compounds, eight were racemic mixtures that presented kinetic resolution when submitted to Kau2-EH catalysed hydrolysis and for six of them the kinetic resolution was nearly perfect (ees of more than 99% for both remaining substrate and formed product). The last substrate (*cis*-stilbene oxide was prochiral and found to undergo a nearly perfect desymmetrization when submitted to Kau2-EH catalysis. Furthermore the reactions could be conducted at high substrate concentrations (up to 75 g/L) in short times (usually 1h) and have been all easily conducted on the 1g scale. Since all these nine substrates possessed at least one phenyl ring and according to previously reported results (Kotik *et al.*, 2010), it is concluded that Kau2-EH is a particularly useful biocatalysts in the kinetic resolution/desymmetrization of such racemate/prochiral epoxides. It

should be noted that numerous of the tested epoxides/formed diols are of high synthetic relevance.

Finally, a study dedicated to the better understanding of the mechanism of action of Kau2-EH was conducted using stopped-flow techniques. Also this work has not yet been completed, access to various kinetic constants of Kau2-EH catalysis were gained through the use of (*S,S*)-*trans*-stilbene oxide as substrate. The obtained results are consistent with the following proposed mechanism of action:



The Michaelis complex is formed with a high  $K_s$  (*i.e.* low ES stabilization), followed by the fast and almost irreversible ( $k_{-2} = 2.1 \text{ s}^{-1}$ ) formation of the alkyl-enzyme intermediate E-alkyl (high  $k_2$  value), the subsequent hydrolytic step being rate limiting ( $k_3 = 11 \text{ s}^{-1}$ ).

This Kau2-EH dedicated work has enhanced our understanding of this enzyme. It proved to be an extremely performant enantioselective biocatalyst that could probably be used in industrial applications as long as intracellular overexpression could be enhanced in order to use less biomass to perform bio-hydrolysis of (mainly) aromatic epoxides. Furthermore evolutionary techniques leave space to improve Kau2-EH properties based on homology model and mechanism of action described in this work.

## Reference

- Argiriadi, M.A., Morisseau, C., Goodrow, M.H., Dowdy, D.L., Hammock, B.D. and Christianson, D.W. (2000) Binding of alkylurea inhibitors to epoxide hydrolase implicates active site tyrosines in substrate activation. *J. Biol. Chem.*, **275**, 15265-15270.
- Kotik, M., Štěpánek, V., Grulich, M., Kyslík, P. and Archelas, A. (2010) Access to enantiopure aromatic epoxides and diols using epoxide hydrolases derived from total biofilter DNA. *J. Mol. Catal. B: Enzym.*, **65**, 41-48.

# Chapter V. Material and Methods

## LIST OF ABBREVIATIONS

<b>EHs:</b>	Epoxide Hydrolases
<b>CDU:</b>	<i>N</i> -Cyclohexyl- <i>N'</i> -DecylUrea
<b>CIU:</b>	<i>N</i> -Cyclohexyl- <i>N'</i> -(4-Iodophenyl)Urea
<b>DMF:</b>	DiMethylFormamide
<b>DMSO:</b>	DiMethylSulfOxyde
<b>MTBE:</b>	Methyl <i>Tert</i> -Butyl Ether
<b>THF:</b>	TetraHydroFuran
<b>GC:</b>	Gas Chromatography
<b>HPLC:</b>	High Pressure Liquid Chromatography
<b>LB:</b>	Luria Bertani
<b>TB:</b>	Terrific Broth
<b>FPLC:</b>	Fast Protein Liquid Chromatography
<b>NMR:</b>	Nuclear Magnetic Resonance
<b>TLC:</b>	Thin Layer Chromatography

## V.1 General

### V.1.1 Reagents, solvents and chromatography

All reagents were used as received from Sigma-Aldrich, Acros or Fluka. Dimethylformamide (DMF), tetrahydrofuran (THF), and dimethyl sulfoxide (DMSO) were of analytical grade. *n*-Hexane, *n*-pentane and diethyl ether were chemically pure from commercial. The epoxides *rac*-methyl *trans*-3-(4-methoxyphenyl) glycidate-**6**, *rac-trans*-stilbene oxide-**11** and *meso-cis*-stilbene oxide-**12** were from Sigma-Aldrich.

### V.1.2 Buffer and culture media

#### V.1.2.1 Buffer for enzyme assay:

##### **Buffer A-50 mM Na-phosphate buffer pH 7.0 (for 1L)**

5.13 g Na<sub>2</sub>HPO<sub>4</sub>·2H<sub>2</sub>O

2.92 g NaH<sub>2</sub>PO<sub>4</sub>·H<sub>2</sub>O

Complete to 1.0 L with deionized water

##### **Buffer B-50 mM Na-phosphate buffer pH 8.5 (for 1L)**

8.70 g Na<sub>2</sub>HPO<sub>4</sub>·2H<sub>2</sub>O

0.16 g NaH<sub>2</sub>PO<sub>4</sub>·H<sub>2</sub>O

Complete to 1.0 L with deionized water

##### **Binding buffer -20 mM Na-phosphate buffer pH 7.4 (for 1L)**

2.75 g Na<sub>2</sub>HPO<sub>4</sub>·2H<sub>2</sub>O

0.62 g NaH<sub>2</sub>PO<sub>4</sub>·H<sub>2</sub>O

29.22 g NaCl (500 mM)

1.36 g Imidazole (20 mM)

Complete to 1.0 L with deionized water

##### **Elution buffer -20 mM Na-phosphate buffer pH 7.4 (for 1L)**

2.75 g Na<sub>2</sub>HPO<sub>4</sub>·2H<sub>2</sub>O

0.62 g NaH<sub>2</sub>PO<sub>4</sub>·H<sub>2</sub>O

29.22 g NaCl (500 mM)

34.4 g Imidazole (500 mM)

Complete to 1.0 L with deionized water

### V.1.2.2 Culture media

#### **Luria Bertani (LB) medium:**

10 g Peptone, 5 g yeast extract and 5 g NaCl were dissolved in 950 mL of deionized water. The pH of the medium was adjusted to 7.5 using 1M NaOH. Medium volume was brought up to 1 liter and autoclaved on liquid cycle for 20 min at 115 °C and stored at room temperature.

#### **Luria Bertani (LB) Agar medium:**

10 g Peptone, 5 g yeast extract 5 g NaCl and 15 g Agar were added to 950 mL of deionized water. The pH of the medium was adjusted to 7.5 using 1M NaOH. Medium volume was brought up to 1 litre and autoclaved on liquid cycle for 20 min at 115 °C and stored at room temperature.

#### **Terrific Broth (TB) medium:**

12 g Peptone, 24 g yeast extract and 5 g Glycerol were dissolved in 900 mL of deionized water. Medium volume was brought up to 1 liter with 100 mL buffer containing  $K_2HPO_4$  (15 g) and  $KH_2PO_4$  (2.3 g) and autoclaved on liquid cycle for 20 min at 115 °C and stored at room temperature.

#### **Minimal medium**

Sucrose 10 g·L<sup>-1</sup>

$KH_2PO_4$  13.6 g·L<sup>-1</sup>

$(NH_4)_2SO_4$  4 g·L<sup>-1</sup>

NaOH 3 g·L<sup>-1</sup>

$MgSO_4 \cdot 7H_2O$  2 g·L<sup>-1</sup>

$CaCl_2$  0.377 g·L<sup>-1</sup>

$FeSO_4 \cdot 7H_2O$  0.01 g·L<sup>-1</sup>

The pH was not adjusted for culture medium in flask but adjusted for fermentation.

## V.2 Instruments

### V.2.1 Nuclear Magnetic Resonance (NMR)

$^1\text{H}$  and  $^{13}\text{C}$  Nuclear Magnetic Resonance (NMR) spectra were recorded on a Bruker Avance 300 Ultrashield NMR spectrometer. Chemical shifts are given in ppm relative to residual peaks of chloroform- $d_3$  ( $\delta = 7.28$  ppm), THF- $d_8$  ( $\delta = 1.73$  and  $3.58$  ppm), benzene ( $\delta = 7.16$  ppm), acetone- $d_6$  ( $\delta = 7.22$ ,  $7.58$  and  $8.74$  ppm) or DMSO- $d_6$  ( $\delta = 2.50$  ppm). The constants of coupling are given in Hertz (Hz). The abbreviations of brs, s, d, t, dt, q, tt and m correspond respectively to a broad signal, a singlet, a doublet, a triplet, a doublet of triplet, a quadruplet, a triplet of triplet and a multiplet.

### V.2.2 Gas chromatography (GC)

For GC analysis, a Shimadzu GC2010 chromatograph was equipped with a Shimadzu auto injector AOC-20i. Injector and detector temperature were set at  $250\text{ }^\circ\text{C}$  and  $300\text{ }^\circ\text{C}$ . Hydrogen was used as carrier gas.

Columns: Lipodex-G column ( $0.25\mu\text{m}$ ,  $25\text{ m}\times 0.25\text{ mm}$ , Macherey-nagel) used for chiral analysis of epoxide **4** and diols **4d**.

Cyclosil B ( $0.25\mu\text{m}$ ,  $60\text{m}\times 0.25\text{ mm}$ , Agilent, USA) used for chiral analysis of epoxide **5** and diols **5d**.

### V.2.3 High Pressure Liquid Chromatography (HPLC)

Two HPLC systems were used:

For quantitative analysis of epoxide **1** and diol **1-d**

**a) Reversed phase** (water/acetonitrile)

Pump: Agilent 1100 Series G1311A Quat Pump

Detector: Agilent 1100 Series G1315A DAD

Degasser: Agilent 1100 Series G1322A Degasser

Injector: Agilent 1100 Series G1313A Standard Autosampler

Column: NUCLEOSIL<sup>®</sup> C<sub>18</sub>, ( $250\times 4.60\text{ mm}$ , Macherey-nagel)

For chiral analysis of the epoxides **6~11** and diols **6d~11d**

**b) Chiral phase** (hexane/isopropanol)

Controller: SCL-10A System Controller

Pump: LC-10AD Liquid Chromatograph  
Detector: Shimadzu SPD-10A UV-Vis detector  
Degasser: Degasys DG-1310  
Injector: Auto Injector SIL-10A  
Chiral column: Lux-4 (250×4.60 mm, Phenomenex)  
Lux-3 (250×4.60 mm, Phenomenex)  
Chiralcel OD-H (0.4 cm×1.0 cm, Daicel)  
Chiralpak AD-H column (250 × 4.60 mm, Daicel)

#### V.2.4 5 L Fermentor

Two fermentor systems were used:

**Fermentor I:** BioBundle system was from *Applikon Biotechnology* including BioController ADI-1030, BioConsole ADI-1035 and 10 L fermentor.

**Fermentor II:** Fermentation system (7 L) was made by *Setric Genie Industriel*.

#### V.2.5 Chromatography

The chemical reactions were followed by thin layer chromatography (TLC) (Merck 60 F254) and revealed by a UV lamp ( $\lambda = 254$  nm). Flash column chromatography was performed on silica gel 60 (230-400 mesh). All the retention factors are noted  $R_f$ .

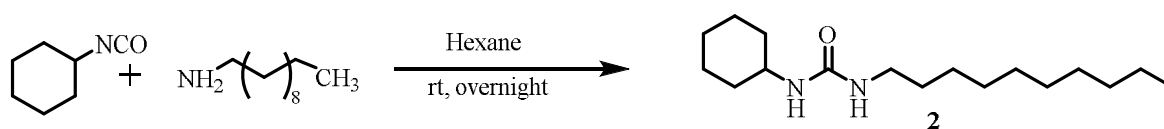
#### V.2.6 Others

Polarimeter: Perkin Elmer 241 Polarimeter (589 nm, 18-28 °C)  
Bulb-to-bulb distillation: Büchi GKR-50  
Centrifuges: Sigma 6K15, Eppendorf Minispin®  
Freeze drying machine: LSL Secfroid Lyolab A (Biolaffitte SA.)  
Incubator: Infors Multitron  
FPLC: Amersham Biosciences Akta FPLC system  
UPC-900, P-920, INV-907, M-925, FRAC-900

## V.3 Chemical Synthesis

The synthesis of CDU and CIU were carried out as described previously (Argiriadi *et al.*, 2000).

### V.3.1 Synthesis of *N*-cyclohexyl-*N'*-decylurea (CDU)-2



To a stirred solution of 0.60 ml (0.47 g, 3.0 mmol) of decylamine in hexane was added 0.38 ml (0.37 g, 3.0 mmol) of cyclohexylisocyanate, leading to a white crystalline solid. After standing overnight the mixture was cooled and the solid product was collected, washed with cold hexane, and dried to obtain 0.658 g (2.75 mmol, yield 78%) of CDU-2 as a white powder. M.p: 90-91 °C. <sup>1</sup>H NMR (DMSO-d<sub>6</sub>, 300 MHz) δ=4.2 (m, 2H, 2NH), 3.51 (m, 1H, CH), 3.13 (t, J = 7.0 Hz 2 H, CH<sub>2</sub>), 1.96 (m, 2H), 1.1-1.8 (m, 24H), 1.8 (m, 2H), 0.89 (t, J = 6.3 Hz, 3H, CH<sub>3</sub>). <sup>13</sup>C NMR (DMSO-d<sub>6</sub>, 75 MHz) δ=157.7, 49.3, 40.7, 33.8, 31.8, 30.1, 29.5, 29.3, 29.2, 26.9, 22.5, 24.8, 22.6.

### V.3.2 Synthesis of *N*-cyclohexyl-*N'*-(4-iodophenyl) urea (CIU)-3



A solution of 1.10 g (5.0 mmol) of 4-iodoaniline and 0.688 g (5.5 mmol) of cyclohexylisocyanate in 25 mL of diethyl ether was kept in the dark at room temperature for one week, 1.253 g of CIU-3 was obtained after filtration (yield 72.6%). M.p: 256-257 °C, <sup>1</sup>H NMR (DMSO-*d*<sub>6</sub>, 300 MHz) δ=8.39 (s, 1H, ArNH), 7.50 (d, J = 8.0 Hz, 2H), 7.21 (d, J = 8.7

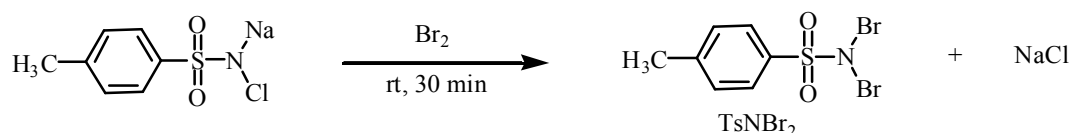
Hz, 2H), 6.08 (d,  $J = 7.6$  Hz, 1H), 3.38 (m, 1H), 1.8 (m, 2H), 1.6 (m, 2H), 1.5 (m, 1H), 1.2 (m, 5H).  $^{13}\text{C}$  NMR (DMSO- $d_6$ , 75 MHz)  $\delta = 154.1, 140.4, 137.2, 119.7, 83.3, 47.5, 32.8, 25.2, 24.3$ .

### V.3.3 Synthesis of *rac-trans*-methyl phenylglycidate **4**

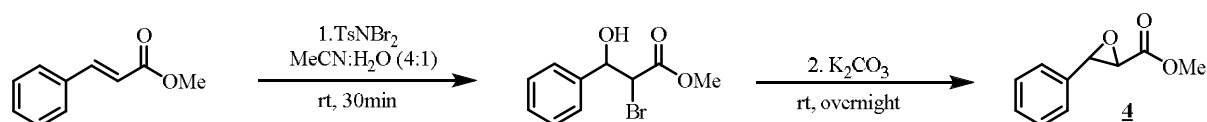
The synthesis of *rac*-**4** and *rac*-**5** were carried out as described previously (Saikia *et al.*, 2010)

#### V.3.3.1 Synthesis of dibromoamine-T

10 g chloroamine-T were weighed and added to a 250 mL round bottom flask filled with 200 mL distilled water under magnetic stirring. When chloroamine-T was dissolved, 2 mL of bromine were added dropwise. A yellow precipitate formed and the mixture was stirred at room temperature for 30 min. The mixture was filtered under vacuum and the yellow solid washed with water and dried for one hour under vacuum. The solid was placed in a desiccator overnight. 10.54 g dibromoamine-T was obtained as a yellow solid (yield 91%).



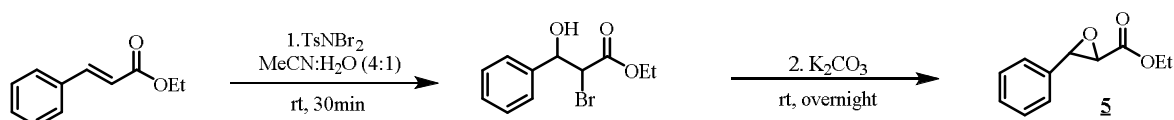
#### V.3.3.2 Synthesis of *rac-trans*-methyl phenylglycidate-**4**



In a 100 mL round bottom flask were weighed 0.896 g (5.5 mmol) of *trans*-methyl cinnamate followed by the addition of 20 mL of acetonitrile and 5 mL distilled water. Then 1.87 g of dibromoamine-T was added and the mixture was stirred at room temperature for 30 minutes. The formed bromohydrine was cyclized by adding 5.2 g of  $\text{K}_2\text{CO}_3$  and leaving the reaction under stirring at room temperature overnight. The reaction was stopped by addition of 1.0 g of  $\text{Na}_2\text{S}_2\text{O}_3$ . The mixture was poured into a separatory funnel, extracted 3 times with 50 mL of diethyl ether, the organic phases were collected, dried over  $\text{MgSO}_4$ , filtered and

evaporated under vacuum. The product was purified by flash chromatography on silica gel using an 8/2 mixture of pentane and diethyl ether as eluent, affording 0.81 g of *rac-trans*-methyl phenylglycidate-**4** as a colourless liquid (82% yield). <sup>1</sup>H NMR (CDCl<sub>3</sub>, 300 MHz): δ = 7.2-7.3 (brs, 5H), 4.1 (d, *J* = 1.8 Hz, 1H), 3.8 (s, 3H), 3.5 (d, *J* = 1.7 Hz, 1H); <sup>13</sup>C NMR (CDCl<sub>3</sub>, 75 MHz): δ = 168.6, 135.0, 128.9, 128.6, 125.8, 57.9, 56.6, 52.5.

### V.3.4 Synthesis of *rac-trans*-ethyl-3-phenylglycidate-**5**



In a 100 mL round bottom flask were weighed 0.979 g (5.5 mmol) of *trans*-ethyl cinnamate followed by the addition of 20 mL of acetonitrile and 5 mL distilled water. Then 3.949 g of dibromoamine-T were added and the mixture was stirred at room temperature for 30 minutes. The formed bromohydrine was cyclized by adding 5.2 g of K<sub>2</sub>CO<sub>3</sub> and leaving the reaction under stirring at room temperature overnight. The reaction was stopped by addition of 1.0 g of Na<sub>2</sub>S<sub>2</sub>O<sub>3</sub>. The mixture was poured into a separatory funnel, extracted 3 times with 50 mL of diethyl ether, the organic phases were collected, dried over MgSO<sub>4</sub>, filtered and evaporated under vacuum. The product was purified by flash chromatography on silica gel using an 8/2 mixture of pentane and diethyl ether as eluent affording 0.82 g of *rac-trans*-ethyl phenylglycidate-**5** as a colourless liquid (78% yield). <sup>1</sup>H NMR (CDCl<sub>3</sub>, 300 MHz): δ = 7.2-7.3 (brs, 5H), 4.3 (m, 2H), 4.1 (d, *J* = 1.7 Hz, 1H), 3.5 (d, *J* = 1.8 Hz, 1H), 1.3 (t, 3H); <sup>13</sup>C NMR (CDCl<sub>3</sub>, 75 MHz): δ = 168.1, 135.0, 128.9, 128.6, 125.8, 61, 57.9, 56.7, 14.1.

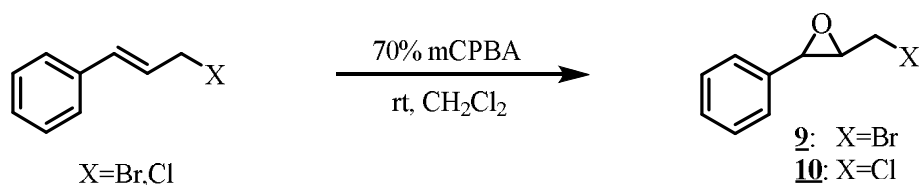
### V.3.5 Synthesis of *cis* and *trans*-2, 3-epoxy-3-phenylpropanenitrile **7** and **8**



The synthesis of *rac*-**7** and **-8** was carried out as described previously (Mhamdi *et al.*, 2011). To a solution of benzaldehyde (380 mg, 3.0 mmol), chloroacetonitrile (450 mg, 6.0 mmol) and tetrahexylammonium bromide (154 mg, 0.36 mmol) in THF (15.0 mL) was added KOH (400 mg, 7.2 mmol) at room temperature. After 22 h under stirring, NaBH<sub>4</sub> (200 mg)

was added to the mixture in order to remove the remaining benzaldehyde. After 5 minutes the reaction was quenched with water and the mixture extracted 3 times with 15 mL of ethyl acetate. The combined organic layers were washed with brine and water, dried over MgSO<sub>4</sub>, filtrated and finally concentrated under vacuum. The crude mixture was purified by flash chromatography on silica gel using a 9/1 mixture of pentane and diethyl ether as eluent, affording 0.09 g of *trans*-**7** as a colourless liquid (22.5% yield) and 0.16 g of *cis*-**8** as a white solid (40% yield.). **7**: <sup>1</sup>H NMR (CDCl<sub>3</sub>, 300 MHz): δ = 7.40 (m,3H), 7.28 (m,2H), 4.28 (d, *J* = 1.8 Hz, 1H), 3.42 (d, *J* = 1.8 Hz, 1H); <sup>13</sup>C NMR (CDCl<sub>3</sub>, 75 MHz): δ = 132.6, 129.7, 128.9, 125.7, 116.1, 58.4, 44.6; **8**: m. p: 54-55 °C, <sup>1</sup>H NMR (CDCl<sub>3</sub>, 300 MHz): δ = 7.42 (m, 5H), 4.25 (d, *J* = 3.8 Hz, 1H), 3.79 (d, *J* = 1.8 Hz, 1H); <sup>13</sup>C NMR (CDCl<sub>3</sub>, 75 MHz): δ = 131.3, 129.7, 128.6, 126.3, 114.9, 57.7, 45.0.

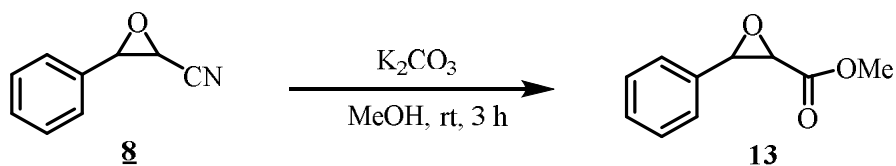
### V.3.6 Synthesis of *rac-trans*-2,3-epoxy-3-phenyl-1-bromo propane-**9** and *rac-trans*-2,3-epoxy-3-phenyl-1-chloro propane-**10**



To a solution of 70% *m*-chloroperoxybenzoic acid (*m*CPBA) (8.5 mmol) in 20 mL of CH<sub>2</sub>Cl<sub>2</sub> was added a 30 mL cinnamyl bromide (571 mg, 2.9 mmol) solution in CH<sub>2</sub>Cl<sub>2</sub>. Then 20 mL of 0.5 M NaHCO<sub>3</sub> were added and the heterogeneous mixture was stirred at 25 °C for 17 h. The resulting mixture was washed 3 times with 10% sodium bicarbonate and the combined aqueous phases were extracted 3 times with 30mL of diethyl ether. The combined organic layers were finally washed with brine then water, dried over MgSO<sub>4</sub>, filtrated and then concentrated under vacuum. The crude product was first purified by flash chromatography on silica gel using a 9/1 mixture of pentane and diethyl ether as eluent and then by bulb-to-bulb distillation at 200 °C under vacuum (0.4 mbar) affording 0.302 g of *rac-trans*-2-bromomethyl-3-phenyloxirane-**9** as a slightly yellow liquid (yield 49%). <sup>1</sup>H NMR (CDCl<sub>3</sub>, 300 MHz): δ = 7.2-7.3 (brs, 5H), 3.7 (d, *J* = 1.8 Hz, 1H), 3.4 (d, *J* = 5.7 Hz, 1H), 3.2 (dt, 2H); <sup>13</sup>C NMR (CDCl<sub>3</sub>, 75 MHz): δ = 135.8, 128.6, 128.6, 125.6, 60.9, 60.3, 31.9.

To a solution of 70% *m*-chloroperoxybenzoic acid (*m*CPBA) (8.5 mmol) in 20 mL of CH<sub>2</sub>Cl<sub>2</sub> was added a 30 mL cinnamyl chloride (497 mg, 2.9 mmol) solution in CH<sub>2</sub>Cl<sub>2</sub>. Then 20 mL of 0.5 M NaHCO<sub>3</sub> were added and the heterogeneous mixture was stirred at 25 °C for 17 h. The resulting mixture was washed 3 times with 10% sodium bicarbonate and the combined aqueous phases were extracted 3 times with 30 mL of diethyl ether. The combined organic layers were finally washed with brine then water, dried over MgSO<sub>4</sub>, filtrated and then concentrated under vacuum. The crude product was first purified by flash chromatography on silica gel using a 9/1 mixture of pentane and diethyl ether as eluent and then by bulb-to-bulb distillation at 200 °C under vacuum (0.4 mbar) affording 0.275 g of *rac*-*trans*-2-bromomethyl-3-phenyloxirane-**10** as a colourless liquid (yield 52.1%). <sup>1</sup>H NMR (CDCl<sub>3</sub>, 300 MHz): δ = 7.2-7.3 (brs, 5H), 3.7 (d, J = 1.8 Hz, 1H), 3.5 (d, J = 5.7 Hz, 1H), 3.2 (dt, 2H); <sup>13</sup>C NMR (CDCl<sub>3</sub>, 75 MHz): δ = 135.8, 128.6, 125.7, 61.0, 58.6, 44.4.

### V.3.7 Synthesis of *rac*-*cis*-methyl phenylglycidate-**13**



The synthesis of *rac*-**13** was carried out as already described (Svoboda *et al.*, 1988) and is based on the easy transformation of *cis*-2,3-epoxy-3-phenylpropanenitrile-**8** into the corresponding methyl ester.

A mixture of *cis*-2,3-epoxy-3-phenylpropanenitrile-**8** (0.302 g, 2 mmol), dry potassium carbonate (0.289 g, 2.0 mmol) and dry methanol (10 mL) was stirred at room temperature for 3 hours and then acidified with diluted HCl for 2 hours at 4 °C. The reaction solution was then extracted 3 times by ethyl acetate (30 mL), the combine organic layers were washed with brine then water, dried over MgSO<sub>4</sub>, filtrated and finally concentrated under vacuum. The crude product was purified by flash chromatography on silica gel (230-400 mesh) using a 70/30 mixture of pentane and diethyl ether as eluent affording 0.287 g of *rac*-*cis*-methyl phenylglycidate-**13** as a colourless liquid (80% yield). <sup>1</sup>H NMR (CDCl<sub>3</sub>, 300 MHz): δ = 7.2-7.3 (brs, 5H), 4.2 (d, J = 4.7 Hz, 1H), 3.7 (d, J = 4.6 Hz, 1H), 3.5 (s, 3H); <sup>13</sup>C NMR (CDCl<sub>3</sub>, 75 MHz): δ = 166.1, 133.0, 128.2, 128.2, 126.2, 58.2, 55.9, 53.2.

### V.3.8 Chemical hydrolysis of *rac-trans*-methyl phenylglycidate-**4**

In order to get access to racemic forms of the various diol products, acidic opening of the corresponding epoxides was carried out as exemplified for *rac-4*. In a 100 mL round bottomed flask was added 100 mg of *rac-4*, 20mL of water and two drops of H<sub>2</sub>SO<sub>4</sub> (98%). The reactions were run overnight at room temperature under magnetic stirring (800 rpm). The reaction mixture was then extracted with 20 mL of ethyl acetate and the formed couple of *rac*-diols analysed by chiral GC or HPLC. The chemical hydrolysis of *rac-5*, **6**, **7**, **8**, **9**, **10**, **11**, **12** and **13** were carried out using the same protocol leading to diastereoisomeric mixtures of corresponding diols.

## V.4 Kau2-EH Production

### V.4.1 Cells expressing Kau2-EH production in flask

Frozen glycerol stock suspensions of Kau2-EH expressing *Escherichia coli* cells provided by Dr. Michael Kotik were spread on a Petri dish filled by LB agar containing 100 µg·mL<sup>-1</sup> of Ampicillin. After 24 h at 28 °C, fresh *E. coli* cells were removed and used to inoculate a culture tube containing 5 mL of LB medium. The culture tube was placed under 200 rpm stirring at 28 °C for 24 h. The whole tube was used to inoculate 50 mL of minimal medium contained in a 250 mL Erlenmeyer flask at 28 °C with 200 rpm stirring for 24 h. After 24 h of cultivation, the whole 50 mL culture was used to inoculate 400 mL of minimal medium contained in a 2 L Erlenmeyer flask and placed at 28 °C with 200 rpm stirring for 24 h. The culture was induced with IPTG (final concentration 0.45 mM), and placed at 23 °C with stirring (200 rpm) overnight. The cells were harvested by centrifugation at 9600 rpm, the cells were frozen in liquid nitrogen and then lyophilized for 48 hours affording 933 mg of dry cells as biocatalyst with a specific activity of 780 U·mg<sup>-1</sup>.

### V.4.2 Cells production in fermentor

Frozen glycerol stock suspensions of Kau2-EH expressing *E. coli* cells were spread on a Petri dish filled with LB agar at 28 °C containing 100 µg·mL<sup>-1</sup> of Ampicillin for 24h. One colony of *E. coli* expressing Kau2-EH was used to inoculate one Erlenmeyer flask filled with 30 mL of pre-culture medium containing 100 µg·mL<sup>-1</sup> of Ampicillin. The flask was cultured at 31 °C for 24 h. The whole flask was used to inoculate a fermentor filled with 3 L of

minimal medium and run at 28 °C while pO<sub>2</sub> was maintained above 20% with stirring speed set at 300 rpm. After few hours (see below), the cultivation temperature was reduced from 28 °C to 25 °C and then stock solution of IPTG (1M) was added for a final concentration of 0.45 mM. After cultivation at 25 °C (15-18 h, see below), the cells were harvested by centrifugation at 9600 rpm, the cells were frozen in liquid nitrogen and then lyophilized for 48 hours affording 1.4-2.9 g of dry cells as biocatalyst with a specific activity ranging from 1667 to 2757 U·mg<sup>-1</sup> (Grulich *et al.*, 2011).

Fermentor	Equipment	Pre culture medium	Total cultivation time (h)	Cultivation time with IPTG (h)	Air flow rate (v.v.m)	X <sup>IPTG</sup> (g·L <sup>-1</sup> ) <sup>d</sup>	X (g·L <sup>-1</sup> ) <sup>e</sup>	A (U·mg <sup>-1</sup> ) <sup>f</sup>
1	Fermentor I <sup>a</sup>	Mm <sup>c</sup>	24	15	1.0	1.4	2.9	1667
2	Fermentor I	LB	27	18	1.0	0.2	1.4	2757
3	Fermentor II <sup>b</sup>	LB	23	15	1.0	1.5	2.9	2743

<sup>a</sup> Fermentor I: See V. 2. 4.

<sup>b</sup> Fermentor II: See V. 2. 4.

<sup>c</sup> Minimal medium : see V. 1. 2. 2.

<sup>d</sup> Biomass concentration (dry mass) at time of induction.

<sup>e</sup> Biomass concentration (dry mass) at time of harvest.

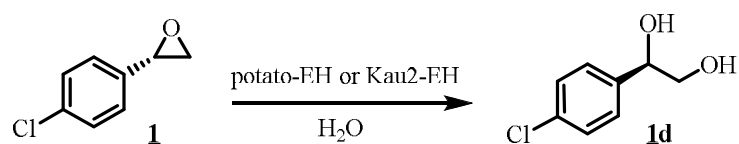
<sup>f</sup> Specific activity of Kau2-EH, based on cell dry mass at time of harvest.

### V.4.3 Determination of EH activity

EH activities were determined using (*S*)-*para* chlorostyrene oxide ((*S*)-*p*ClISO) as substrate. Aliquots of 15 µL of a stock solution of 400 mM of (*S*-*p*ClISO) in acetonitrile (final concentration: 3.0 mM) and lyophilized cells expressing Kau2-EH (0.1 g·L<sup>-1</sup>) were added to 2 mL of buffer A into a 10 mL round bottom flask and enzymatic reactions incubated at 27 °C. Samples (200 µL) were withdrawn time to time and mixed with 200 µL acetonitrile. After 3 min centrifugation (13400 rpm), the supernatant (200 µL) was filtered by 0.45 µm syringe filter and analysed by HPLC (see V. 2.3-a). Mobile phase was 55% acetonitrile in deionized water; Flow rate was set at 0.7 mL·min<sup>-1</sup>; Detection wavelength was set at 220 nm. Retention times of the epoxide and the diol were 15.5 min. and 5.5 min respectively.

## V.5 Modelisation Study of Kau2-EH

### V.5.1 Determination of EH activities and kinetic parameters ( $K_m$ , $V_{max}$ )



The EH activities were determined using (*S*)-*p*ClISO as substrate. Aliquots of a stock solution (400 mM) in acetonitrile (0.1~8.0 mM) and lyophilized cells expressing Kau2-EH were added to 2 mL of buffer A into a 10 mL round bottom flask. The concentration of cells was diluted to ensure a liner relationship between EH activities and amount of sample. Enzymatic reactions were incubated at 27 °C and run and analysed as described above.

### V.5.2 Determination of $K_i$ and type of inhibition using CDU and Kau2-EH

EH activity was determined using (*S*)-*p*ClISO as substrate. Enzymatic reactions were incubated at 27 °C of buffer A (2 mL) in 10mL round bottom flask, which containing 0.5 mM, 1.0 mM, 2.0 mM, 4.0 mM of (*S*)-*p*ClISO. For each substrate concentration, EH activities with CDU inhibitor (range concentration 30~120 nM) were determined. For the detailed protocol of sample making and HPLC analysis conditions see **V. 4. 3**.

### V.5.3 Determination of $K_i$ and type of inhibition using CIU and Kau2-EH

EH activity was determined using (*S*)-*p*ClISO as substrate. Enzymatic reactions were incubated at 27 °C of buffer A (2 mL) in 10mL round bottom flask, which containing 0.5 mM, 1.0 mM, 2.0 mM, 4.0 mM of (*S*)-*p*ClISO. For each substrate concentration, EH activities with CIU inhibitor (concentration range 120~360 nM) were determined. For the detailed protocol of sample making and HPLC analysis conditions see **V. 4. 3**.

### V.5.4 Determination of $K_i$ and type of inhibition using CDU and Potato-EH

EH activity was determined using (*S*)-*p*ClISO as substrate. Enzymatic reactions were incubated at 27 °C of buffer A (2 mL) in 10mL round bottom flask, which containing 0.5 mM, 1.0 mM, 2.0 mM, 4.0 mM of (*S*)-*p*ClISO. The concentration of lyophilized enzymatic extract of potato-EH (available in the lab) was diluted to ensure a liner relationship between EH

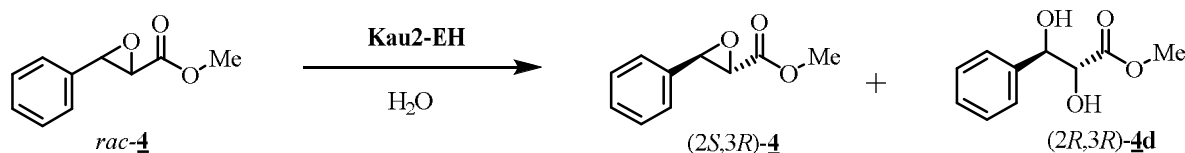
activities and amount of sample. For each substrate concentration, EH activities with CDU inhibitor (concentration range 1000~1500 nM) were determined. For the detailed protocol of sample making and HPLC analysis conditions see **V. 4. 3**.

### V.5.5 Determination of $K_i$ and the type of inhibitor of CIU with Potato EHs

EH activity was determined using (*S*)-*p*ClISO as substrate. Enzymatic reactions were incubated at 27 °C of buffer A (2 mL) in 10mL round bottom flask, which containing 0.5 mM, 1.0 mM, 2.0 mM, 4.0 mM of (*S*)-*p*ClISO. For each substrate concentration, EH activities with CIU inhibitor (concentration range 1500~3000 nM) were determined. For the detailed protocol of sample making and HPLC analysis conditions see **V. 4. 3**.

## V.6 Bioconversions

### V.6.1 Bioconversion of *rac-trans*-methyl-phenylglycidate-**4**



#### V.6.1.1 Analytical scale

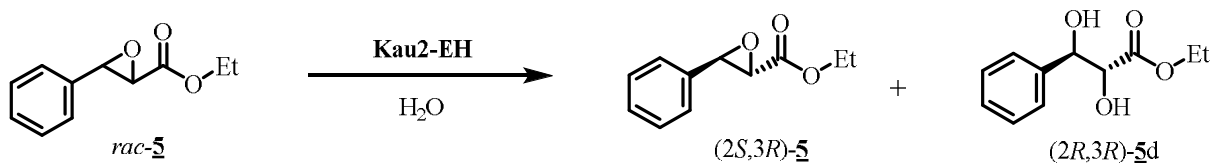
A specific volume of a stock solution of 2.8 M of *rac-trans*-methyl-3-phenylglycidate-**4** (final concentration 1~100 g/L) in DMF (final concentration of DMF adjusted at 5%) and cells expressing Kau2-EH (1667 U/mg, final concentration 2~200 g/L) were added to 0.4 mL of buffer A and 50 L of di-isopropyl ether in a 10 mL round bottom flask (final reaction volume 0.5 mL). Enzymatic reactions were incubated at 27 °C under magnetic stirring (1200 rpm). Regularly withdrawn aliquots were extracted with ethyl acetate and analysed by chiral GC in order to determine ees of both residual substrate and formed diol, 4-bromoacetophenon being used as an internal standard. A Lipodex-G column (0.25  $\mu$ m, 25 m $\times$ 0.25 mm, Macherey-Nagel) was used, the flow rate of carrier gas ( $H_2$ ) was set at 2.96 mL $\cdot$ min $^{-1}$ . The column temperature was set at 110 °C and kept at this temperature for 20 minutes and then increased to 140 °C at a rate of 10 °C/min. The retention times were as follow: *(2R,3S)*-**4**:

17.5 min, (2*S*,3*R*)-**4**: 17.9 min, (2*R*,3*R*)-**4d**: 38.2 min, (2*S*,3*S*)-**4d**: 38.6 min and for the 2 *syn*-diols-**4d**: 39.1 min and 40.1 min (**Annexe 2**).

### V.6.1.2 Preparative scale at 50 g·L<sup>-1</sup>

In a 100 mL round bottomed flask was added 1.0 g of *rac*-**4** dissolved in 1 mL of DMF, 17 mL of buffer A and 2 mL of di-isopropyl ether. The biocatalytic reaction was initiated by the addition of 1.5 g of lyophilized cells expressing Kau2-EH (1667 U/mg) and run at 27 °C under magnetic stirring (1200 rpm). After 60 min, the reaction mixture was extracted 3 times with 40 mL ethyl acetate. The combined organic phases were dried over MgSO<sub>4</sub>, filtered and then evaporated under reduced pressure. The products were purified by flash chromatography (pentane/diethyl ether, 7/3) affording 0.49 g of (2*S*,3*R*)-**4** (ee 99%, [α]<sup>15</sup><sub>D</sub> = +171.9 (c = 1.0, CHCl<sub>3</sub>), yield 49%) as a colourless liquid and 0.52 g of (2*R*,3*R*)-**4d** (ee 99%, [α]<sup>22</sup><sub>D</sub> = -44 (c = 0.5, CHCl<sub>3</sub>), yield 47 %) as a white solid (**Annexe 2**). (2*R*,3*R*)-**4d**: m. p: 77-78 °C; <sup>1</sup>H NMR (CDCl<sub>3</sub>, 300 MHz): δ = 7.2-7.3 (brs, 5H), 4.9 (s, 1H), 4.4 (s, 1H), 3.6 (s, 3H), 2.9 (s, 1H); <sup>13</sup>C NMR (CDCl<sub>3</sub>, 75 MHz): δ = 172.4, 138.5, 128.4, 126.3, 75.0, 74.8, 52.4.

### V.6.2 Bioconversion of *rac*-*trans*-ethyl-3-phenylglycidate-**5**



#### V.6.2.1 Analytical scale

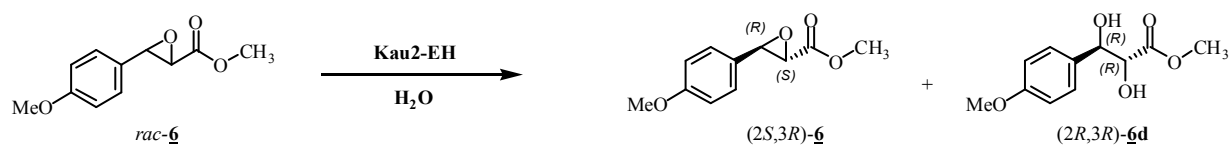
The same protocol as described above was used. The samples were analysed by chiral GC with a Cyclosil B column (60 m, 0.25 μm×0.25 mm, Agilent, USA), the flow rate of the carrier gas (H<sub>2</sub>) was set at 2.67 mL/min. The column temperature was set at 150 °C and kept at this temperature for 20 minutes and then increased to 180 °C at a rate of 10 °C/min. The retention times were as follow: (2*R*,3*S*)-**5**: 22.7 min, (2*S*,3*R*)-**5**: 23.0 min. The formed diols were analysed at 180 °C directly, the retention times were as follow: (2*R*,3*R*)-**5d**: 17.7 min, (2*S*,3*S*)-**5d**: 18.0 min and for the 2 *syn*-diols-**5d**: 18.5 min and 18.8 min (**Annexe 3**). For (2*R*,3*R*)-**5d** a Chiralpak AD-H column (250 × 4.60 mm) was used for the determination of its absolute configuration using an isocratic mode (85/15) mixture of hexane/isopropanol

delivered at a flow rate of 0.7 mL/min. UV detection was set at 230 nm. The retention times were as follow: (2*S*,3*S*)-**5d**: 15.5 min, (2*R*,3*R*)-**5d**: 16.5 min and for the 2 *syn*-diols-**5**: 18.4 min and 20.3 min (**Annexe 3**). For the detailed of GC analysis conditions see **V. 2. 2**.

### V.6.2.2 Preparative scale at 25 g·L<sup>-1</sup>

In a 100 mL round bottomed flask was added 1.0 g of *rac*-**5** dissolved in 2 mL of DMF, 34 mL of buffer A and 4 mL of di-isopropyl ether. The biocatalytic reaction was initiated by the addition of 2.0 g of lyophilized cells expressing Kau2-EH (1667 U/mg) and run at 27 °C under magnetic stirring (1200 rpm). After 60 min, the reaction mixture was extracted 3 times with 40 mL ethyl acetate. The combined organic phases were dried over MgSO<sub>4</sub>, filtered and then evaporated under reduced pressure. The products were purified by flash chromatography (pentane/diethyl ether, 7/3) affording 0.46 g of (2*S*,3*R*)-**5** as a colourless liquid (ee 99%,  $[\alpha]_D^{25} = + 154.7$  (c = 1.0, CHCl<sub>3</sub>), yield 46.8%) and 0.49 g of (2*R*,3*R*)-**5d** as a colourless liquid (ee 94%,  $[\alpha]_D^{25} = - 37.5$  (c = 1.0, CHCl<sub>3</sub>), yield 47%)(**Annexe 3**). (2*R*,3*R*)-**5d**: <sup>1</sup>H NMR (CDCl<sub>3</sub>, 300 MHz): δ = 7.2-7.3 (brs, 5H), 4.9 (d, *J* = 3.6 Hz, 1H), 4.3 (s, 1H), 4.0 (m, 2H), 3.0 (s, 1H), 1.1 (t, 3H); <sup>13</sup>C NMR (CDCl<sub>3</sub>, 75 MHz): δ = 171.4, 138.5, 128.1, 126.4, 74.9, 74.7, 61.1, 13.9.

### V.6.3 Bioconversion of *rac*-methyl-*trans*-3-(4-methoxyphenyl)-glycidate-**6**



#### V.6.3.1 Analytical scale

A specific volume of a stock solution of 100 g/L of *rac*-methyl-*trans*-3-(4-methoxyphenyl)-glycidate-**6** (final concentration 1~50 g/L) in MTBE (final concentration of MTBE 40%) and cells expressing Kau2-EH (1667 U/mg, final concentration 2~100 g/L) were added to 0.3 mL of buffer B in a 10 mL round bottom flask (final reaction volume 0.5 mL). Enzymatic reactions were incubated at 17 °C under magnetic stirring (800 rpm). Regularly withdrawn aliquots were saturated with NaCl and extracted with ethyl acetate (200

$\mu\text{L}$ ). Then 100  $\mu\text{L}$  of the organic phase were evaporated under reduced pressure and filled back with 100  $\mu\text{L}$  of isopropyl alcohol. Then 20  $\mu\text{L}$  of this solution were analysed by HPLC to determine the ees of both remaining epoxide and formed diol. A Lux-4 chiral column (250 $\times$ 4.60 mm, Phenomenex) was used in the isocratic mode with an 8/2 mixture of hexane/isopropanol delivered at a flow rate of 1.2 mL/min. UV detection was set at 230 nm. The retention times were as follow: (2*S*,3*R*)-**6**: 8.4 min, (2*R*,3*S*)-**6**: 8.8 min, (2*S*,3*S*)-**6d**: 17.7 min, (2*R*,3*R*)-**6d**: 19.8 min and for the 2 *syn*-diols-**6d**: 21.7 min and 27.4 min (**Annexe 4**).

### V.6.3.2 Preparative scale at 40 g·L<sup>-1</sup>

In a 100 mL round bottomed flask was added 1.0 g of *rac*-**6** dissolved in 10 mL of MTBE and 15 mL of buffer B. The biocatalytic reaction was initiated by addition of 1.75 g of lyophilized cells expressing Kau2-EH (1667 U/mg) and run at 17 °C under magnetic stirring (800 rpm). After 60 min, the reaction mixture was extracted 3 times with 40 mL ethyl acetate. The combined organic phases were dried over MgSO<sub>4</sub>, filtered and then evaporated under reduced pressure. The products were purified by flash chromatography (pentane/diethyl ether, 7/3) affording 0.40 g of (2*S*,3*R*)-**6** as a colourless liquid (ee 99%,  $[\alpha]_{\text{D}}^{24} = +190.7$  (c = 1.0, MeOH), yield 40%) and 0.51 g of (2*R*,3*R*)-**6d** as a white solid (ee 88%,  $[\alpha]_{\text{D}}^{18} = -39.2$  (c = 1.0, CHCl<sub>3</sub>), yield 46 %)(**Annexe 4**). (2*R*,3*R*)-**6d**: melting point: 105-106 °C; <sup>1</sup>H NMR (CDCl<sub>3</sub>, 300 MHz):  $\delta = 7.1$ -7.2 (brs, 2H), 6.8 (d, *J* = 8.7 Hz, 2H), 4.8 (d, *J* = 4.4 Hz, 1H), 4.4 (s, 1H), 3.72 (s, 3H), 3.67 (s, 3H), 1.9 (s, 1H). <sup>13</sup>C NMR (CDCl<sub>3</sub>, 75 MHz):  $\delta = 171.1$ , 159.5, 130.1, 127.5, 113.8, 74.7, 60.3, 55.2, 52.4.

### V.6.4 Bioconversion of *rac-trans*-2,3-epoxy-3-phenylpropanenitrile-**7**



#### V.6.4.1 Analytical scale

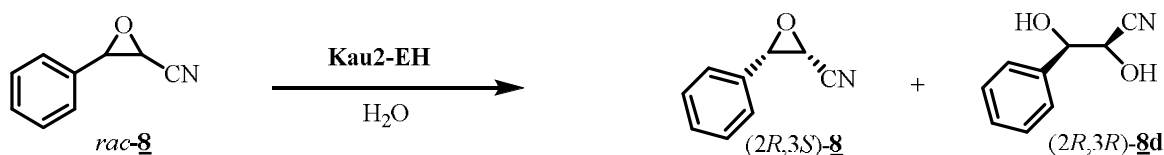
A specific volume of a stock solution of 200 g/L of *rac-trans*-2,3-epoxy-3-phenylpropanenitrile-**7** (final concentration 1~100 g/L) in MTBE (final concentration of MTBE 20%) and cells expressing Kau2-EH (2757 U/mg, final concentration 0.75~75 g/L)

were added to 0.8 mL of buffer A in a 10 mL round bottom flask (final volume of reaction 1 mL). Enzymatic reactions were incubated at 27 °C under magnetic stirring (800 rpm). Regularly withdrawn aliquots were saturated with NaCl and extracted with ethyl acetate (200  $\mu$ L). Then 100  $\mu$ L of the organic phase were evaporated under reduced pressure and filled back with 100  $\mu$ L of isopropyl alcohol. Then 20  $\mu$ L of this solution were analysed by HPLC to determine the enantiomeric excesses of both remaining epoxide and formed diol. A Chiralcel OD-H column (250 $\times$ 4.60 mm) was used in the isocratic mode with an 8/2 mixture of hexane/isopropanol delivered at a flow rate of 1.2 mL/min. UV detection was set at 215 nm. The retention times were as follow: (2*R*,3*R*)-**7**: 10.2 min, (2*S*,3*S*)-**7**: 11.2 min, (2*R*,3*S*)-**7d**: 6.7 min, (2*S*,3*R*)-**7d**: 7.4 min (**Annexe 5**).

#### V.6.4.2 Preparative scale at 50 g·L<sup>-1</sup>

In a 100 mL round bottomed flask was added 1.0 g of *rac*-**7** dissolved in 4 mL of MTBE and 16 mL of buffer A. The biocatalytic reaction was initiated by addition of 0.75 g of lyophilized cells expressing Kau2-EH (2757 U/mg) and run at 27 °C under magnetic stirring (800 rpm). After 60 min, the reaction mixture was extracted 3 times with 40 mL ethyl acetate. The combined organic phases were dried over MgSO<sub>4</sub>, filtered and then evaporated under reduced pressure. The products were purified by flash chromatography (pentane/diethyl ether, 7/3) affording 0.45 g of (2*R*,3*R*)-**7** as a slightly yellow liquid (ee 99%, [ $\alpha$ ]<sub>D</sub><sup>22</sup> = + 150.8 (c = 1.1, EtOH), yield 45%) and 0.52 g of (2*S*,3*R*)-**7d** as a white solid (ee 99%, [ $\alpha$ ]<sub>D</sub><sup>22</sup> = - 44.3 (c = 1.0, EtOH), yield 46 %)(**Annexe 5**). (2*S*,3*R*)-**7d**: m. p: 83-84 °C; <sup>1</sup>H NMR (CDCl<sub>3</sub>, 300 MHz):  $\delta$  = 7.2-7.3 (brs, 5H), 4.9 (d, *J* = 1.6 Hz, 1H), 4.6 (d, *J* = 1.5 Hz, 1H), 2.1(s, 2H); <sup>13</sup>C NMR (CDCl<sub>3</sub>, 75 MHz):  $\delta$  = 136.6, 129.0, 128.8, 126.3, 117.7, 74.4, 67.2.

#### V.6.5 Bioconversion of *rac*-*cis*-2,3-epoxy-3-phenylpropanenitrile-**8**



##### V.6.5.1 Analytical scale

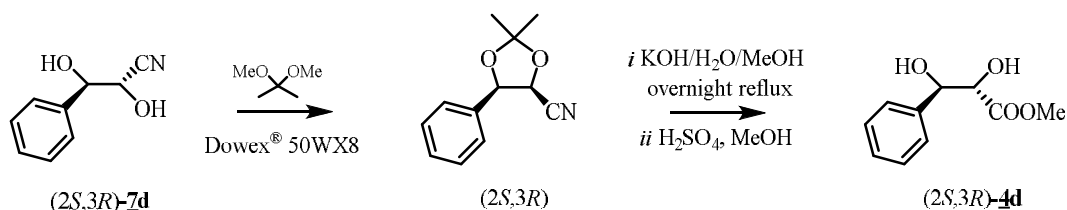
A specific volume of a stock solution of 100 g/L of *rac*-*cis*-2,3-epoxy-3-phenylpropanenitrile-**8** (final concentration 1 ~ 50 g/L) in MTBE (final concentration of

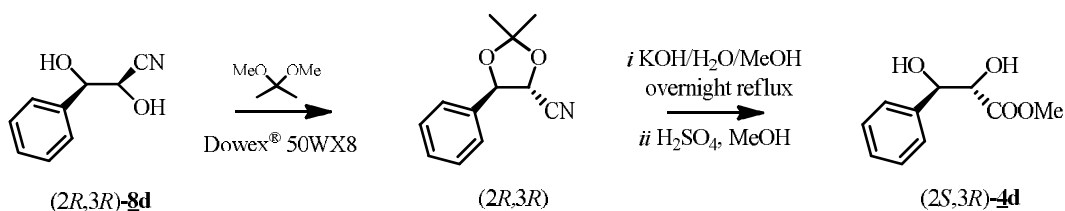
MTBE 20%) and cells expressing Kau2-EH (2757 U/mg, final concentration 1~50 g/L) were added to 0.8 mL of buffer A in a 10 mL round bottom flask (final volume of reaction 1 mL). Enzymatic reactions were incubated at 27 °C under magnetic stirring (800 rpm). Regularly withdrawn aliquots were saturated with NaCl and extracted with ethyl acetate (200  $\mu$ L). Then 100  $\mu$ L of the organic phase were evaporated under reduced pressure and filled back with 100  $\mu$ L of isopropyl alcohol. Then 20  $\mu$ L of this solution were analysed by HPLC to determine the enantiomeric excesses of both remaining epoxide and formed diol. A Chiralcel OD-H column (250 $\times$ 4.60 mm) was used in the isocratic mode with a 92.5/7.5 mixture of hexane/isopropanol delivered at a flow rate of 1.2 mL/min. UV detection was set at 215 nm. The retention times were as follow: (2*S*,3*R*)-**8**: 11.2 min, (2*R*,3*S*)-**8**: 12.0 min, (2*R*,3*R*)-**8d**: 20.6 min, (2*S*,3*S*)-**8d**: 23.9 min (**Annexe 6**).

### V.6.5.2 Preparative scale at 25 g·L<sup>-1</sup>

In a 100 mL round bottomed flask was added 1.0 g of *rac*-**8** dissolved in 8 mL of MTBE and 32 mL of buffer A. The biocatalytic reaction was initiated by addition of 1 g of lyophilized cells expressing Kau2-EH (2757 U/mg) and run at 27 °C under magnetic stirring (800 rpm). After 60 min, the reaction mixture was extracted 3 times with 40 mL ethyl acetate. The combined organic phases were dried over MgSO<sub>4</sub>, filtered and then evaporated under reduced pressure. The products were purified by flash chromatography (pentane/diethyl ether, 7/3) affording 436 mg of (2*S*,3*R*)-**8** as a white solid, m. p: 54-55 °C; (ee 99%, [ $\alpha$ ]<sub>D</sub><sup>25</sup> = + 109.8 (c = 0.86, EtOH), yield 43.6%) and 510 mg of (2*R*,3*R*)-**8d** as a slightly yellow liquid (ee 99%, [ $\alpha$ ]<sub>D</sub><sup>25</sup> = - 32.1 (c = 1.0, EtOH), yield 45.2 %)(**Annexe 6**). (2*R*,3*R*)-**8d**: <sup>1</sup>H NMR (CDCl<sub>3</sub>, 300 MHz):  $\delta$  = 7.2-7.3 (brs, 5H), 4.8 (d, *J* = 3.9 Hz, 1H), 4.5 (d, *J* = 3.8 Hz, 1H), 2.0 (s, 2H); <sup>13</sup>C NMR (CDCl<sub>3</sub>, 75 MHz):  $\delta$  = 136.6, 129.0, 128.8, 126.3, 117.7, 74.4, 67.2.

### V.6.5.3 Synthesis of (2*S*,3*R*)-**4d** from diols (2*S*,3*R*)-**7d** and (2*R*,3*R*)-**8d** formed in bioconversions of *rac*-**7** and *rac*-**8**

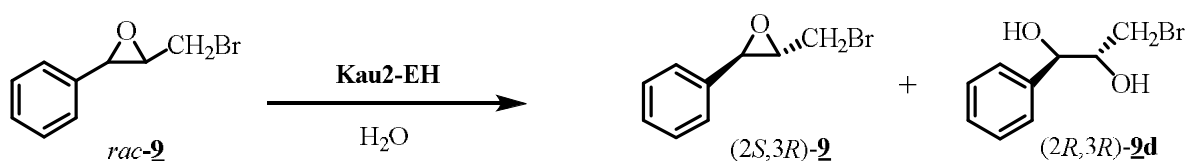




$(2S,3R)$ -**7d** from bioconversion of *rac*-**7** (400 mg, 2.45 mmol) was dissolved in acetone dimethyl acetal (40 mL) and then Dowex<sup>®</sup> 50WX8 (4 g) was added to the solution. The reaction was monitored by TLC for 1 h 30 min and then it was filtered and evaporated under reduced pressure. The residue was dissolved in a mixture of methanol and water (2:1) and KOH (0.59 g) was added to the solution. Then the reaction solution was refluxed overnight at 75°C. The reaction was stopped by adding HCl (20%) and adjusted pH to 2, the mixture was extracted 3 times with 40 mL diethyl ether, and then dried over MgSO<sub>4</sub>. The diethyl ether was removed by rotary evaporation, the crude product was dissolved in methanol and a few drops of H<sub>2</sub>SO<sub>4</sub> (98%) were added to the solution. The mixture was stirred at room temperature for 1 h 30 min and it was quenched with a saturated aqueous solution of sodium bicarbonate (20 mL). The mixture was extracted 3 times with 40 mL diethyl ether, dried over MgSO<sub>4</sub> and evaporated under vacuum. The product was purified by flash chromatography on silica gel (230-400 mesh) using an 50/50 mixture of pentane and diethyl ether as eluent, affording 85 mg  $(2S,3R)$ -**4d**. HPLC analysis: Lux-4 (250×4.60 mm, Phenomenex), Hexane/Isopropanol 90/0, 1.0 ml/min, UV 215nm, retention time was 57.1 min. Absolute configuration for  $(2S,3R)$ -**4d** have been determined through comparison of available optical rotation found in the literature ( $[\alpha]_{\text{D}}^{20} = -16.2$  ( $c = 0.692$ , CH<sub>2</sub>Cl<sub>2</sub> (Effenberger *et al.*, 1991)) and the one experimentally determined in this work ( $[\alpha]_{\text{D}}^{20} = -12.7$  ( $c = 0.71$ , CH<sub>2</sub>Cl<sub>2</sub>)).

The same protocol was used for  $(2R,3R)$ -**8d** leading to  $(2S,3R)$ -**4d**.

#### V.6.6 Bioconversion of *rac-trans*-2,3-epoxy-3-phenylpropyl bromide **9**



### V.6.6.1 Analytical scale

A specific volume of a stock solution of 100 g/L of *rac-trans*-2,3-epoxy-3-phenyl propylbromide-**9** (final concentration 1~100 g/L) in MTBE (final concentration of MTBE 20%) and cells expressing Kau2-EH (2743 U/mg, varying concentrations: see text) were added to 0.8 mL of buffer A in a 10 mL round bottom flask (final volume of reaction 1 mL). Enzymatic reactions were incubated at 27 °C under magnetic stirring (800 rpm). Regularly withdrawn aliquots were saturated with NaCl and extracted with ethyl acetate (200  $\mu$ L). Then 100  $\mu$ L of the organic phase were evaporated under reduced pressure and filled back with 100  $\mu$ L of isopropyl alcohol. Then 20  $\mu$ L of this solution were analysed by HPLC to determine the enantiomeric excesses of both remaining epoxide and formed diol. A Lux-4 chiral column (250 $\times$ 4.60 mm, Phenomenex) was used in the isocratic mode with a 92.5/7.5 mixture of hexane/isopropanol delivered at a flow rate of 1 mL/min. UV detection was set at 215 nm. The retention times were as follow: (2*S*,3*R*)-**9**: 8.5 min, (2*R*,3*S*)-**9**: 10.2 min, (2*R*,3*R*)-**9d**: 20.6 min, (2*S*,3*S*)-**9d**: 22.6 min and for the 2 *syn*-diols-**9d**: 25.6 min and 26.7 min (**Annexe 7**).

### V.6.6.2 Preparative scale 75 g·L<sup>-1</sup>

In a 100 mL round bottomed flask was added 1.0 g of *rac*-**9** dissolved in 2.6 mL of MTBE and 10.7 mL of buffer A. The biocatalytic reaction was initiated by addition of 0.8 g of lyophilized cells expressing Kau2-EH (2743 U/mg) and run at 27 °C under magnetic stirring (800 rpm). After 60 min, the reaction mixture was extracted 3 times with 40 mL ethyl acetate. The combined organic phases were dried over MgSO<sub>4</sub>, filtered and then evaporated under reduced pressure. The products were purified by flash chromatography (pentane/diethyl ether, 7/3) affording 0.44 g of (2*S*,3*R*)-**9** as a colourless liquid (ee 99%,  $[\alpha]_D^{24} = + 11.3$  (c = 1, CHCl<sub>3</sub>), yield 44%) and 0.53 g of (2*R*,3*R*)-**9d** as a colourless liquid (ee 99%,  $[\alpha]_D^{24} = - 8.5$  (c = 1, CHCl<sub>3</sub>), yield 48 %)(**Annexe 7**). <sup>1</sup>H NMR (CDCl<sub>3</sub>, 300 MHz):  $\delta = 7.2-7.3$  (brs, 5H), 4.8 (d, *J* = 5.3 Hz, 1H), 3.9 (m, 1H), 3.4 (m, 1H), 1.2 (t, 2H); <sup>13</sup>C NMR (CDCl<sub>3</sub>, 75 MHz):  $\delta = 139.8, 128.6, 128.2, 126.8, 75.0, 74.7, 35.8$ .

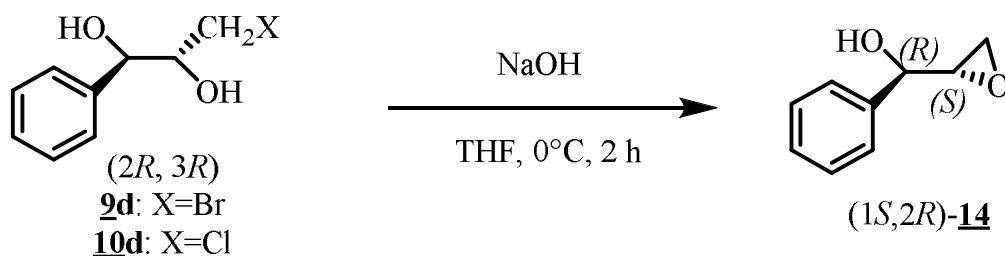
### V.6.7 Bioconversion of *rac-trans*-2,3-epoxy-3-phenylpropyl-chloride **10**



### V.6.7.1 Preparative scale 50 g·L<sup>-1</sup>

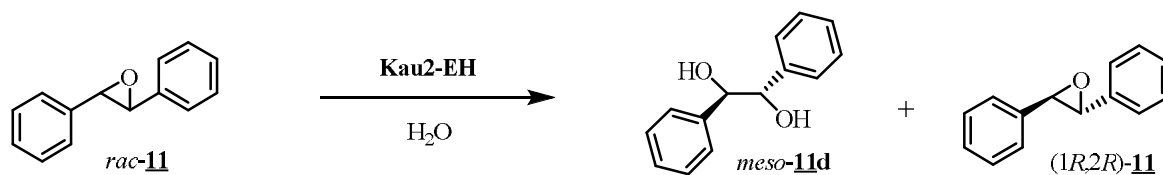
1.0 g of *rac-trans*-2,3-epoxy-3-phenylpropyl-chloride was added in 16 mL buffer A with 4 mL MTBE to a final concentration of 20% MTBE. 0.5 g of lyophilized cells expressing Kau2-EH was suspended in the solution to initiate the reaction. This resulted in a substrate concentration of 50g·L<sup>-1</sup> and a cell concentration of 25 g·L<sup>-1</sup>. Biotransformation was carried out at 27 °C for 40 min. The same protocol was used as described in chapter V. 6. 6. 2. Drying with MgSO<sub>4</sub> and removing the solvent, afforded 0.43 g epoxide (*2S,3R*)-**10** as a colourless liquid (ee 99%, yield 43%) and 0.49 g diol (*2R,3R*)-**10d** as a yellow liquid (ee 99%, yield 44.5%)(Annexe 7). (*2R,3R*)-**10d** <sup>1</sup>H NMR (CDCl<sub>3</sub>, 300 MHz): δ = 7.2-7.3 (brs, 5H), 4.8 (d, *J* = 5.3 Hz, 1H), 3.9 (m, 1H), 3.5 (m, 1H), 3.1 (t, OH); <sup>13</sup>C NMR (CDCl<sub>3</sub>, 75 MHz): δ = 139.5, 128.6, 128.2, 126.6, 74.9.0, 74.5, 46.0.

### V.6.7.2 Synthesis of (*1S,2R*)-phenyl-glycidol-**14**



In a 25 mL round bottom flask were weighed 123.5 mg (7.0 mmol) of (*2R,3R*)-**9d** followed by the addition of 3 mL of THF. Then 56 mg (14.0 mmol) of NaOH was added and the mixture was stirred at 0 °C for 2 hours. The mixture was poured into a separatory funnel, extracted 3 times with 15 mL of ethyl acetate, the organic phases were collected, dried over MgSO<sub>4</sub>, filtered and evaporated under vacuum. The product was purified by flash chromatography on silica gel (230-400 mesh) using an 7/3 mixture of pentane and diethyl ether as eluent affording 57 mg of (*1S,2R*)-phenyl-glycidol-**14** as a colourless liquid (59% yield). (*1S,2R*)-**14**: <sup>1</sup>H NMR (CDCl<sub>3</sub>, 300 MHz): δ = 7.2-7.3 (brs, 5H), 4.9 (d, *J* = 1.7 Hz, 1H), 3.2 (m, 1H), 2.9 (m, 1H), 2.7 (m, 1H), 3.1 (s, OH); <sup>13</sup>C NMR (CDCl<sub>3</sub>, 75 MHz): δ = 139.4, 128.6, 128.2, 126.4, 70.9, 55.1, 43.6.

## V.6.8 Bioconversion of *rac-trans*-stilbene oxide-**11**



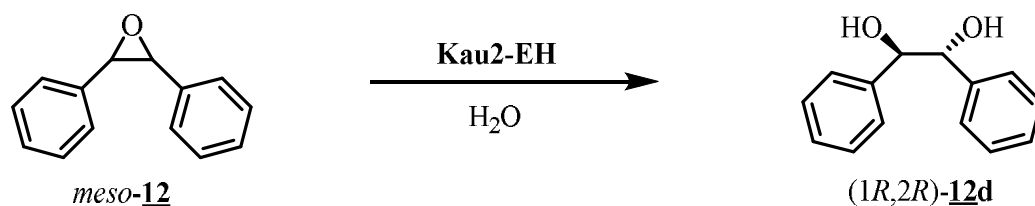
### V.6.8.1 Analytical scale

In all experiments 100 mg of *rac-trans*-stilbene oxide-**11** were dissolved in MTBE (from 20 mL to 0.4 mL) and buffer A added to reach a final 20% MTBE concentration and a final total concentration of **11** in the range 1~50 g·L<sup>-1</sup>. The reaction was initiated by the addition of 200 mg of lyophilized cells expressing Kau2-EH (2757 U/mg). Biotransformation was carried out at 27 °C, under stirring (1200 rpm). Regularly withdrawn aliquots were saturated with NaCl and extracted with ethyl acetate (200 μL). Then 100 μL of the organic phase were evaporated under reduced pressure and filled back with 100 μL of isopropyl alcohol. Then 20 μL of this solution were analysed by HPLC to determine the ees of both remaining epoxide and formed diol. A Lux-4 chiral column (250×4.60 mm, Phenomenex) was used in the isocratic mode with a 9/1 mixture of hexane/isopropanol delivered at a flow rate of 1 mL/min. UV detection was set at 215 nm. The retention times were as follow: (1*R*,2*R*)-**11**: 4.9 min, (1*S*,2*S*)-**11**: 8.0 min, *meso*-diol-**11d**: 17.3 min (**Annexe 8**).

### V.6.8.2 Preparative scale at 50 g·L<sup>-1</sup>

In a 100 mL round bottomed flask was added 1.0 g of *rac*-**11** dissolved in 4 mL of MTBE and 16 mL of buffer A. The biocatalytic reaction was initiated by addition of 2 g of lyophilized cells expressing Kau2-EH (2757 U/mg) and run at 27 °C under magnetic stirring (800 rpm). After 5 h, the reaction mixture was extracted 3 times with 40 mL ethyl acetate. The combined organic phases were dried over MgSO<sub>4</sub>, filtered and then evaporated under reduced pressure. The products were purified by flash chromatography (pentane/diethyl ether, 1/1) affording 0.45 g of a slightly yellow solid (1*R*,2*R*)-**11**, m. p: 65-66 °C; (ee% 99%, [α]<sub>D</sub><sup>20</sup> = + 348 (c = 0.59, benzene), yield 44.5%)(**Annexe 8**) and 0.51 g of *meso*-**11d** as a white solid (yield 46 %). M. p: 122-124 °C; <sup>1</sup>H NMR (CDCl<sub>3</sub>, 300 MHz): δ = 7.2-7.3 (brs, 5H), 4.7 (s, 1H), 3.3 (s, 1H); <sup>13</sup>C NMR (CDCl<sub>3</sub>, 75 MHz) δ = 142.0, 127.4, 127.3, 126.8, 77.7.

## V.6.9 Bioconversion of *cis*-stilbene oxide-**12**



### V.6.9.1 Analytical scale

A specific volume of a stock solution of 100 g/L of *meso*-*cis*-stilbene oxide-**12** (final concentration 1~50 g/L) in DMF (final concentration of DMF 5%) and cells expressing Kau2-EH (2743 U/mg, final concentration 2~100 g/L) were added to 1.9 mL of buffer A in a 25 mL round bottom flask (final reaction volume: 2 mL). Enzymatic reactions were incubated at 27 °C under magnetic stirring (1200 rpm). Regularly withdrawn aliquots were saturated with NaCl and extracted with ethyl acetate (200  $\mu$ L). Then 100  $\mu$ L of the organic phase were evaporated under reduced pressure and filled back with 100  $\mu$ L of isopropyl alcohol. Then 20  $\mu$ L of this solution were analysed by HPLC to determine the enantiomeric excesses of both remaining epoxide and formed diol. A Lux-4 chiral column (250 $\times$ 4.60 mm, Phenomenex) was used in the isocratic mode with a 9/1 mixture of hexane/isopropanol delivered at a flow rate of 1 mL/min. UV detection was set at 215 nm. The retention times were as follow: *meso*-**12**: 5.3 min, (1*R*,2*R*)-**12d**: 26.9 min and (1*S*,2*S*)-**12d**: 23.9 min (**Annexe 9**).

### V.6.9.2 Preparative scale at 25 g $\cdot$ L<sup>-1</sup>

In a 100 mL round bottomed flask was added 1.0 g of *rac*-**12** dissolved in 2 mL of DMF and 38 mL of buffer A. The biocatalytic reaction was initiated by the addition of 2 g of lyophilized cells expressing Kau2-EH (2743 U/mg) and run at 27 °C under magnetic stirring (800 rpm). After 22 h, the reaction mixture was extracted 3 times with 40 mL ethyl acetate. The combined organic phases were dried over MgSO<sub>4</sub>, filtered and then evaporated under reduced pressure. The products were purified by flash chromatography (pentane/diethyl ether, 1/1) affording 0.92 g of a slightly yellow solid (1*R*,2*R*)-**12d** (ee% 99%,  $[\alpha]_D^{28} = +93.8$  (c = 1, EtOH), yield 84.5%)(**Annexe 9**). M. p: 136-138 °C; <sup>1</sup>H NMR (CDCl<sub>3</sub>, 300 MHz) :  $\delta = 7.2$ -7.3

(brs, 5H), 4.5 (s, 1H), 4.4 (s, 1H);  $^{13}\text{C}$  NMR ( $\text{CDCl}_3$ , 75 MHz)  $\delta$  = 141.6, 127.5, 127.2, 127.0, 78.8.

## V.7 Kinetic Studies

### V.7.1 Protein purification

#### V.7.1.1 Recombinant plasmid construction and expression

In order to purify the Kau2 protein, the new plasmid was constructed by using the pET100/D-TOPO<sup>®</sup> or pET101/D-TOPO<sup>®</sup> vector (Invitrogen), which have an affinity tag composed of six consecutive histidine residues (6×His-tag) located at the N- or C-terminus, respectively. The Kau2-EH gene was cloned into these vectors using a topoisomerase-mediated cloning strategy, following the manufacturer's instructions in the Champion<sup>™</sup> pET Directional TOPO expression kit (Invitrogen).

The insert of the Kau2 gene was prepared by PCR using primers described (**Annexe 10**). The PCR product and the TOPO<sup>®</sup> vector (pET100/pET101) (see **Table 31**) were mixed gently and incubated for 5 minutes at room temperature (22–23 °C). The topoisomerase-mediated reaction was placed on ice and subsequently transformed into chemically competent *E. coli*. TOP10 cells.

After transformation, the bacterial solution was spread on a selective plate and incubated overnight at 34 °C. Some colonies were picked and cultured overnight at 28 °C in 3 mL LB medium containing 100  $\mu\text{g}\cdot\text{mL}^{-1}$  of ampicillin. The plasmid DNA was isolated using the High Pure Plasmid Isolation Kit (Roche).

Restriction analysis and sequencing were used to confirm the presence and correct orientation of the insert in the newly constructed plasmid. For restriction analysis *HincII* was used as the restriction enzyme. Correct orientation of the Kau2 gene in the TOPO<sup>®</sup> vector (pET100/pET101) was confirmed by the presence of four fragments (1487, 348, 1419, and 3530 bp for pET100+Kau2) (**Figure 112**). In conclusion, the restriction analysis confirmed the successful insertion of the Kau2 gene into the TOPO<sup>®</sup> vectors pET100 or pET101 for most of the analysed clones. The two new plasmids were transformed into competent cells *E. coli* BL21 Star (DE3) as a host for expression. The activities of expressed enzymes were tested by using styrene oxide as substrate. After GC analysis, we concluded that the Kau2-EH

containing the N-terminal His-tag (pET100+Kau2) had activity, whereas the Kau2-EH with the C-terminal His-tag (pET101+Kau2) exhibited no activity at all (see **Figure 113**).

**Table 31.** The fusion tag, cleavage site, and selection marker for each vector.

Vector	Fusion Peptide	Fusion Tag	Cleavage Site	Selection Marker
pET100/D-TOPO	N-terminal	6xHis	EK <sup>a</sup>	Ampicillin
pET101/D-TOPO	C-terminal	6xHis	-	Ampicillin

<sup>a</sup> EK = enterokinase.

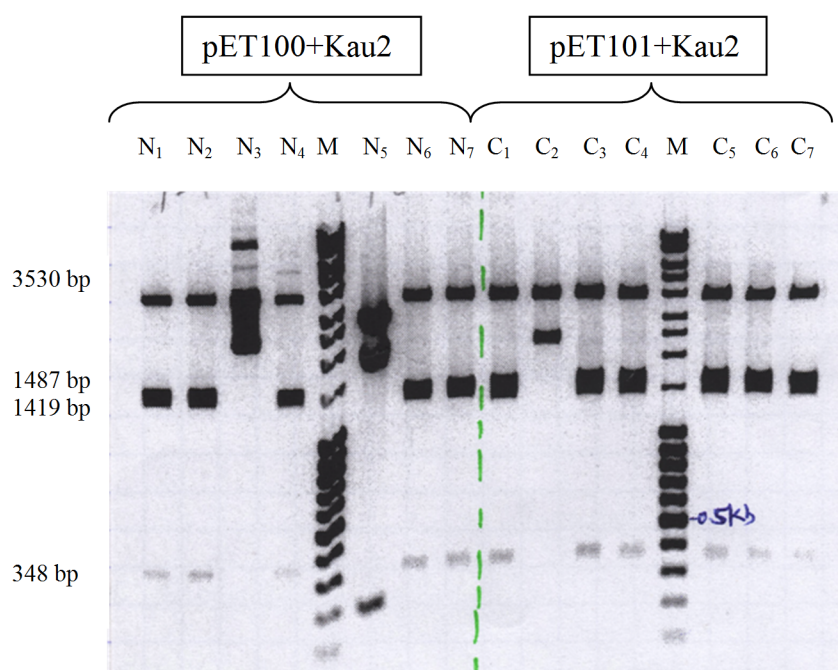


**Figure 112.** Result of restriction digest with *HincII* (1% agarose gel, 90 V, 90 mA, 60 min).

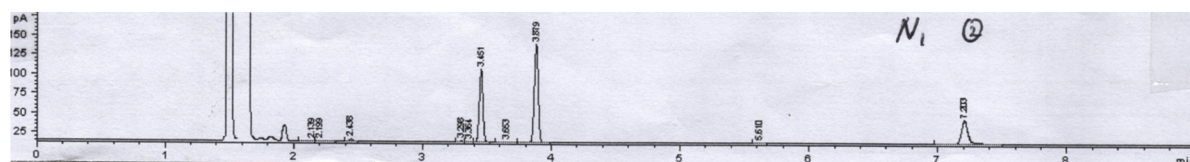


**Figure 113.** A chiral GC analysis after 30 min reaction with 50 mM styrene oxide as substrate and suspended cells harbouring the pET100+Kau2 plasmid (N-terminal). 1, 3.8, and 7.2 min, respectively.

Four Kau2 mutants were constructed based on the pET100+Kau2 plasmid. The exchanges D109A and D109N were produced using the QuikChange Site-Directed

Mutagenesis kit (Agilent), the H316A and H316Q mutants were created using the Phusion site-Directed mutagenesis kit (Thermo). For primers used in the mutagenesis PCRs see **Annexe 10**.

After transformation into *E. coli* TOP10, plasmid DNA was isolated from selected colonies, and the EH-encoding inserts were sequenced using the automated DNA sequencer ABI PRISM 3130xl (Applied Biosystems) (see **Annexe 10** for the pET100+Kau2-based nucleotide sequence of the Kau2-encoding insert). After sequencing, all five pET100-based plasmids containing wild-type or mutant Kau2-encoding genes were transformed into *E. coli* BL21 Star (DE3) as an expression host.

### **V.7.1.2 Enzyme preparation**

Frozen glycerol stock suspensions of *E. coli* cells harbouring one of the above-mentioned Kau2-containing pET100-based plasmids were spread on LB-agar with 200  $\mu\text{g}\cdot\text{mL}^{-1}$  of Ampicillin. After 24 h at 27 °C, fresh *E. coli* cells were removed and inoculated to a culture tube containing 5 mL of LB medium with 200  $\mu\text{g}\cdot\text{mL}^{-1}$  of Ampicillin. The culture tube was placed under 200 rpm stirring at 28 °C for 24 h. These cells were used to inoculate a 500 mL of TB medium contained in a 3 L Erlenmeyer flask under 200 rpm stirring at 37 °C. The culture was induced with IPTG (final concentration 1.0 mM) when the OD (600) reached a value around 1 then stirred at 23 °C for 4 h. The cells were harvested by centrifugation at 9600 rpm, then frozen in liquid nitrogen and placed at -80 °C.

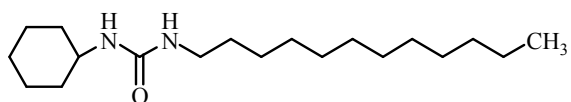
### **V.7.1.3 Protein purification**

After thawing the cells were resuspended in the binding buffer which containing protease inhibitor cocktail (SIGMA S8830-20TAB) then broken using a disrupter apparatus (one shot and 1.3 kbar). After disrupting cells, the solution was centrifuged (25000 rpm, 30 min). After centrifugation the supernatant was loaded on HisTrap HP column (5mL) and the Kau2-EH protein was eluted using a linear gradient for the elution-buffer containing imidazole (500 mM). The protein started to be eluted when the imidazole concentration reached about 20%.

The protein concentrations of collected fractions were determined using a Nanodrop 2000c apparatus (Thermo fisher) by measuring their intrinsic UV absorbance at 280 nm and applying a calculated molar extinction coefficient of 58900  $\text{M}^{-1}\text{cm}^{-1}$ . About 22 mg of pure protein were obtained from 1 L of culture medium (TB medium using the optimized

conditions described above). The purified protein had the molecular mass expected (38.2 kDa) and a specific activity of 9.13 U/mg with oxide of (*S,S*) *trans*- stilbene as substrate.

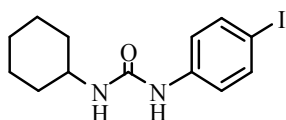
## Analytical data



**2**

$^1\text{H}$  NMR (DMSO- $d_6$ , 300 MHz)  $\delta$ =4.2 (m, 2H, 2NH), 3.51 (m, 1H, CH), 3.13 (t,  $J$  = 7.0 Hz 2 H, CH<sub>2</sub>), 1.96 (m, 2H), 1.1-1.8 (m, 24H), 1.8 (m, 2H), 0.89 (t,  $J$  = 6.3 Hz, 3H, CH<sub>3</sub>).

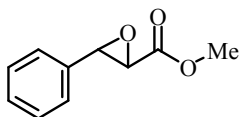
$^{13}\text{C}$  NMR (DMSO- $d_6$ , 75 MHz)  $\delta$ =157.7, 49.3, 40.7, 33.8, 31.8, 30.1, 29.5, 29.3, 29.2, 26.9, 22.5, 24.8, 22.6.



**3**

$^1\text{H}$  NMR (DMSO- $d_6$ , 300 MHz)  $\delta$ =8.39 (s, 1H, ArNH), 7.50 (d,  $J$  = 8.0 Hz, 2H), 7.21 (d,  $J$  = 8.7 Hz, 2H), 6.08 (d,  $J$  = 7.6 Hz, 1H), 3.38 (m, 1H), 1.8 (m, 2H), 1.6 (m, 2H), 1.5 (m, 1H), 1.2 (m, 5H).

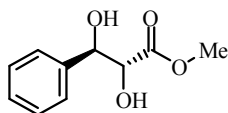
$^{13}\text{C}$  NMR (DMSO- $d_6$ , 75 MHz)  $\delta$ =154.1, 140.4, 137.2, 119.7, 83.3, 47.5, 32.8, 25.2, 24.3.



**4**

$^1\text{H}$  NMR (CDCl<sub>3</sub>, 300 MHz):  $\delta$  = 7.2-7.3 (brs, 5H), 4.1 (d,  $J$  = 1.8 Hz, 1H), 3.8 (s, 3H), 3.5 (d,  $J$  = 1.7 Hz, 1H).

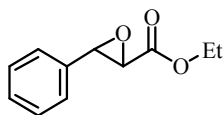
$^{13}\text{C}$  NMR (CDCl<sub>3</sub>, 75 MHz):  $\delta$  = 168.6, 135.0, 128.9, 128.6, 125.8, 57.9, 56.6, 52.5.



(2*R*,3*R*)-4d

$^1\text{H}$  NMR (CDCl<sub>3</sub>, 300 MHz):  $\delta$  = 7.2-7.3 (brs, 5H), 4.9 (s, 1H), 4.4 (s, 1H), 3.6 (s, 3H), 2.9 (s, 1H).

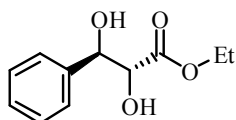
$^{13}\text{C}$  NMR (CDCl<sub>3</sub>, 75 MHz):  $\delta$  = 172.4, 138.5, 128.4, 126.3, 75.0, 74.8, 52.4.



5

$^1\text{H NMR}$  ( $\text{CDCl}_3$ , 300 MHz):  $\delta$ =7.2-7.3 (brs, 5H), 4.3(m, 2H), 4.1 (d,  $J$ = 1.7 Hz, 1H), 3.5 (d,  $J$ = 1.8 Hz, 1H), 1.3(t, 3H).

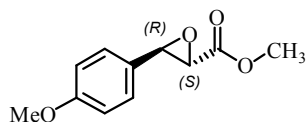
$^{13}\text{C NMR}$  ( $\text{CDCl}_3$ , 75 MHz):  $\delta$ =168.1, 135.0, 128.9, 128.6, 125.8, 61, 57.9, 56.7, 14.1.



(2*R*,3*R*)-5d

$^1\text{H NMR}$  ( $\text{CDCl}_3$ , 300 MHz):  $\delta$  = 7.2-7.3 (brs, 5H), 4.9 (d,  $J$  = 3.6 Hz, 1H), 4.3 (s, 1H), 4.0 (m, 2H), 3.0 (s, 1H), 1.1 (t, 3H).

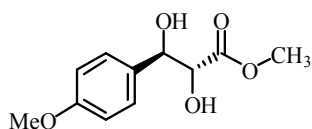
$^{13}\text{C NMR}$  ( $\text{CDCl}_3$ , 75 MHz):  $\delta$  = 171.4, 138.5, 128.1, 126.4, 74.9, 74.7, 61.1, 13.9.



(2*S*,3*R*)-6

$^1\text{H NMR}$  ( $\text{CDCl}_3$ , 300 MHz):  $\delta$  = 7.1-7.2 (brs, 2H), 6.8 (d,  $J$  = 8.7 Hz, 2H), 3.95 (d,  $J$  = 1.4 Hz, 1H), 3.72 (s, 3H), 3.7 (s, 3H), 3.51 (d,  $J$  = 1.7 Hz, 1H).

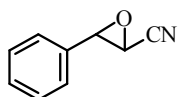
$^{13}\text{C NMR}$  ( $\text{CDCl}_3$ , 75 MHz):  $\delta$  = 168.7, 160.3, 127.2, 126.7, 57.6, 56.5, 55.3, 52.5.



(2*R*,3*R*)-6d

$^1\text{H NMR}$  ( $\text{CDCl}_3$ , 300 MHz):  $\delta$  = 7.1-7.2 (brs, 2H), 6.8 (d,  $J$  = 8.7 Hz, 2H), 4.8 (d,  $J$  = 4.4 Hz, 1H), 4.4 (s, 1H), 3.72 (s, 3H), 3.67 (s, 3H), 1.9 (s, 1H).

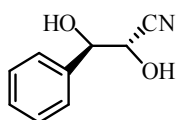
$^{13}\text{C NMR}$  ( $\text{CDCl}_3$ , 75 MHz):  $\delta$  = 171.1, 159.5, 130.1, 127.5, 113.8, 74.7, 60.3, 55.2, 52.4.



7

$^1\text{H NMR}$  ( $\text{CDCl}_3$ , 300 MHz):  $\delta$ =7.40 (m, 3H), 7.28 (m, 2H), 4.28 (d,  $J$ = 1.8 Hz, 1H), 3.42 (d,  $J$ = 1.8 Hz, 1H).

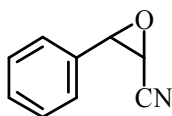
$^{13}\text{C NMR}$  ( $\text{CDCl}_3$ , 75 MHz):  $\delta$ =132.6, 129.7, 128.9, 125.7, 116.1, 58.4, 44.6.



(2*S*,3*R*)-**7d**

$^1\text{H}$  NMR ( $\text{CDCl}_3$ , 300 MHz):  $\delta$  = 7.2-7.3 (brs, 5H), 4.9 (d,  $J$  = 1.6 Hz, 1H), 4.6 (d,  $J$  = 1.5 Hz, 1H), 2.1 (s, 2H).

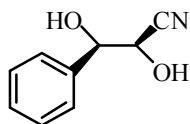
$^{13}\text{C}$  NMR ( $\text{CDCl}_3$ , 75 MHz):  $\delta$  = 136.6, 129.0, 128.8, 126.3, 117.7, 74.4, 67.2.



**8**

$^1\text{H}$  NMR ( $\text{CDCl}_3$ , 300 MHz):  $\delta$  = 7.42 (m, 5 H), 4.25 (d,  $J$  = 3.8 Hz, 1H), 3.79 (d,  $J$  = 1.8 Hz, 1H).

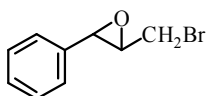
$^{13}\text{C}$  NMR ( $\text{CDCl}_3$ , 75 MHz):  $\delta$  = 131.3, 129.7, 128.6, 126.3, 114.9, 57.7, 45.0.



(2*R*,3*R*)-**8d**

$^1\text{H}$  NMR ( $\text{CDCl}_3$ , 300 MHz):  $\delta$  = 7.2-7.3 (brs, 5H), 4.8 (d,  $J$  = 3.9 Hz, 1H), 4.5 (d,  $J$  = 3.8 Hz, 1H), 2.0 (s, 2H).

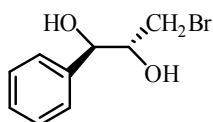
$^{13}\text{C}$  NMR ( $\text{CDCl}_3$ , 75 MHz):  $\delta$  = 136.6, 129.0, 128.8, 126.3, 117.7, 74.4, 67.2.



**9**

$^1\text{H}$  NMR ( $\text{CDCl}_3$ , 300 MHz):  $\delta$  = 7.2-7.3 (brs, 5H), 3.7 (d,  $J$  = 1.8 Hz, 1H), 3.4 (d,  $J$  = 5.7 Hz, 1H), 3.2 (dt, 2H).

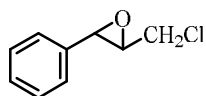
$^{13}\text{C}$  NMR ( $\text{CDCl}_3$ , 75 MHz):  $\delta$  = 135.8, 128.6, 128.6, 125.6, 60.9, 60.3, 31.9.



(2*R*,3*R*)-**9d**

$^1\text{H}$  NMR ( $\text{CDCl}_3$ , 300 MHz):  $\delta$  = 7.2-7.3 (brs, 5H), 4.8 (d,  $J$  = 5.3 Hz, 1H), 3.9 (m, 1H), 3.4 (m, 1H), 1.2 (t, 2H).

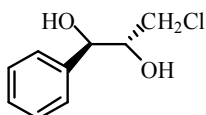
$^{13}\text{C}$  NMR ( $\text{CDCl}_3$ , 75 MHz):  $\delta$  = 139.8, 128.6, 128.2, 126.8, 75.0, 74.7, 35.8.



**10**

$^1\text{H NMR}$  ( $\text{CDCl}_3$ , 300 MHz):  $\delta = 7.2-7.3$  (brs, 5H), 3.7 (d,  $J = 1.8$  Hz, 1H), 3.5 (d,  $J = 5.7$  Hz, 1H), 3.2 (dt, 2H).

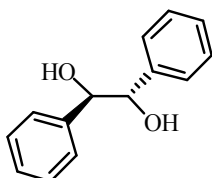
$^{13}\text{C NMR}$  ( $\text{CDCl}_3$ , 75 MHz):  $\delta = 135.8, 128.6, 125.7, 61.0, 58.6, 44.4$ .



(2*R*,3*R*)-**10d**

$^1\text{H NMR}$  ( $\text{CDCl}_3$ , 300 MHz):  $\delta = 7.2-7.3$  (brs, 5H), 4.8 (d,  $J = 5.3$  Hz, 1H), 3.9 (m, 1H), 3.5 (m, 2H), 3.1 (t, OH).

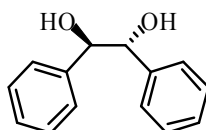
$^{13}\text{C NMR}$  ( $\text{CDCl}_3$ , 75 MHz):  $\delta = 139.5, 128.6, 128.2, 126.6, 74.9.0, 74.5, 46.0$ .



*meso*-**11d**

$^1\text{H NMR}$  ( $\text{CDCl}_3$ , 300 MHz):  $\delta = 7.2-7.3$  (brs, 5H), 4.7 (s, 1H), 3.3 (s, 1H).

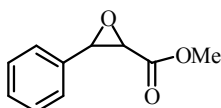
$^{13}\text{C NMR}$  ( $\text{CDCl}_3$ , 75 MHz)  $\delta = 142.0, 127.4, 127.3, 126.8, 77.7$ .



(1*R*,2*R*)-**12d**

$^1\text{H NMR}$  ( $\text{CDCl}_3$ , 300 MHz):  $\delta = 7.2-7.3$  (brs, 5H), 4.5 (s, 1H), 4.4 (s, 1H).

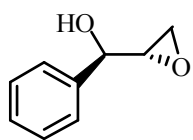
$^{13}\text{C NMR}$  ( $\text{CDCl}_3$ , 75 MHz):  $\delta = 141.6, 127.5, 127.2, 127.0, 78.8$ .



**13**

$^1\text{H NMR}$  ( $\text{CDCl}_3$ , 300 MHz):  $\delta = 7.2-7.3$  (brs, 5H), 4.2 (d,  $J = 4.7$  Hz, 1H), 3.7 (d,  $J = 4.6$  Hz, 1H), 3.5 (s, 3H).

$^{13}\text{C NMR}$  ( $\text{CDCl}_3$ , 75 MHz):  $\delta = 166.1, 133.0, 128.2, 128.2, 126.2, 58.2, 55.9, 53.2$ .



**14**

$^1\text{H}$  NMR ( $\text{CDCl}_3$ , 300 MHz):  $\delta$  = 7.2-7.3 (brs, 5H), 4.9 (d,  $J$  = 1.7 Hz, 1H), 3.2 (m, 1H), 2.9 (m, 1H), 2.7 (m, 1H), 3.1 (s, OH).

$^{13}\text{C}$  NMR ( $\text{CDCl}_3$ , 75 MHz):  $\delta$  = 139.4, 128.6, 128.2, 126.4, 70.9, 55.1, 43.6.

**Table 32.** Physical characterizations of various biosynthesized compounds

Compound	Appearance	Melting point (°C)	Absol. conf./ee/[ $\alpha$ ] <sub>D</sub> <sup>T</sup> <sup>a</sup>
(2 <i>S</i> ,3 <i>R</i> )- <b>4</b>	colourless liquid		(2 <i>S</i> ,3 <i>R</i> )/99% [ $\alpha$ ] <sub>D</sub> <sup>15</sup> = + 171.9° (c=1.0, CHCl <sub>3</sub> )
<b>4d</b>	white solid	77-78	(2 <i>R</i> ,3 <i>R</i> )/99% [ $\alpha$ ] <sub>D</sub> <sup>22</sup> = - 44° (c=0.5, CHCl <sub>3</sub> )
(2 <i>S</i> ,3 <i>R</i> )- <b>5</b>	colourless liquid		(2 <i>S</i> ,3 <i>R</i> )/99% [ $\alpha$ ] <sub>D</sub> <sup>25</sup> = + 154.7° (c=1.0, CHCl <sub>3</sub> )
<b>5d</b>	colourless liquid		(2 <i>R</i> ,3 <i>R</i> )/94%/ [ $\alpha$ ] <sub>D</sub> <sup>25</sup> = - 37.5° (c=1.0, CHCl <sub>3</sub> )
(2 <i>S</i> ,3 <i>R</i> )- <b>6</b>	colourless liquid		(2 <i>S</i> ,3 <i>R</i> )/99% [ $\alpha$ ] <sub>D</sub> <sup>24</sup> = + 190.7° (c=1.0, Methanol)
<b>6d</b>	white solid	105-106	(2 <i>R</i> ,3 <i>R</i> )/84% [ $\alpha$ ] <sub>D</sub> <sup>18</sup> = - 39.2° (c=1.0, CHCl <sub>3</sub> )
(2 <i>R</i> ,3 <i>R</i> )- <b>7</b>	yellow liquid		(2 <i>R</i> ,3 <i>R</i> )/99% [ $\alpha$ ] <sub>D</sub> <sup>22</sup> = + 150.8° (c=1.1, Ethanol)
<b>7d</b>	white solid	83-84	(2 <i>S</i> ,3 <i>R</i> )/99% [ $\alpha$ ] <sub>D</sub> <sup>22</sup> = - 44.3° (c=1.0, Ethanol)
(2 <i>R</i> ,3 <i>S</i> )- <b>8</b>	white solid	54-55	(2 <i>R</i> ,3 <i>S</i> )/99%/ [ $\alpha$ ] <sub>D</sub> <sup>25</sup> = + 109.8° (c=0.86, Ethanol)
<b>8d</b>	yellow liquid		(2 <i>R</i> ,3 <i>R</i> )/99% [ $\alpha$ ] <sub>D</sub> <sup>25</sup> = - 32.1° (c=1.0, Ethanol)
(2 <i>S</i> ,3 <i>R</i> )- <b>9</b>	colourless liquid		(2 <i>S</i> ,3 <i>R</i> )/99% [ $\alpha$ ] <sub>D</sub> <sup>24</sup> = + 11.3° (c=1.0, CHCl <sub>3</sub> )
<b>9d</b>	colourless liquid		(2 <i>R</i> ,3 <i>R</i> )/99% [ $\alpha$ ] <sub>D</sub> <sup>24</sup> = - 8.5° (c=1.0, CHCl <sub>3</sub> )
(2 <i>S</i> ,3 <i>R</i> )- <b>10</b>	colourless liquid		(2 <i>S</i> ,3 <i>R</i> )/99% [ $\alpha$ ] <sub>D</sub> <sup>25</sup> = + 20° (c=0.6, CHCl <sub>3</sub> )
<b>10d</b>	yellow liquid		(2 <i>S</i> ,3 <i>R</i> )/99% [ $\alpha$ ] <sub>D</sub> <sup>25</sup> = - 4.6° (c=1.0, Ethanol)
(1 <i>S</i> ,2 <i>R</i> )- <b>14</b>	colourless liquid		(1 <i>S</i> ,2 <i>R</i> )/99% [ $\alpha$ ] <sub>D</sub> <sup>25</sup> = - 104° (c=2.74, CHCl <sub>3</sub> )
(1 <i>R</i> ,2 <i>R</i> )- <b>11</b>	yellow solid	65-66	(1 <i>R</i> ,2 <i>R</i> )/99% [ $\alpha$ ] <sub>D</sub> <sup>20</sup> = + 348 (c = 0.59, benzene)
<i>meso</i> - <b>11d</b>	white solid	122-124	-
(1 <i>R</i> ,2 <i>R</i> )- <b>12d</b>	yellow solid	136-138	(1 <i>R</i> ,2 <i>R</i> )/99% [ $\alpha$ ] <sub>D</sub> <sup>28</sup> = + 93.8 (c = 1, EtOH)

<sup>a</sup> Absolute configuration of compounds obtained from bioconversion using Kau2-EH.

**Table 33.** Results for preparative scale bioconversion of the various tested substrates.

Substrates	[S] <sup>a</sup> (g·L <sup>-1</sup> )	[cells] <sup>b</sup> (g·L <sup>-1</sup> )	Temp (°C)	Reaction time	Ee <sub>s</sub> <sup>c</sup> remaining epoxide	Abs. conf. remaining epoxide	Yield of epoxide	Ee <sub>p</sub> <sup>d</sup> of formed diol	Abs. conf. formed diol	Yield of diol
<b><u>4</u></b>	50	75	27	60 min	99%	(2 <i>S</i> ,3 <i>R</i> )	48%	99%	(2 <i>R</i> ,3 <i>R</i> )	46.8%
<b><u>5</u></b>	25	50	27	100 min	99%	(2 <i>S</i> ,3 <i>R</i> )	46%	94%	(2 <i>R</i> ,3 <i>R</i> )	46.8%
<b><u>6</u></b>	40	70	17	60 min	99%	(2 <i>S</i> ,3 <i>R</i> )	40%	88%	(2 <i>R</i> ,3 <i>R</i> )	46.2%
<b><u>7</u></b>	50	37.5	27	60 min	99%	(2 <i>R</i> ,3 <i>R</i> )	45.3%	99%	(2 <i>S</i> ,3 <i>R</i> )	46.1%
<b><u>8</u></b>	25	25	27	60 min	99%	(2 <i>R</i> ,3 <i>S</i> )	43.6%	99%	(2 <i>R</i> ,3 <i>R</i> )	45.2%
<b><u>9</u></b>	75	60	27	60 min	99%	(2 <i>S</i> ,3 <i>R</i> )	44.1%	99%	(2 <i>R</i> ,3 <i>R</i> )	48.8%
<b><u>10</u></b>	50	25	27	40 min	99%	(2 <i>S</i> ,3 <i>R</i> )	42.9%	99%	(2 <i>R</i> ,3 <i>R</i> )	44.5%
<b><u>11</u></b>	50	100	27	5 h	99%	(1 <i>R</i> ,2 <i>R</i> )	44.5%	-	meso	46.2%
<b><u>12</u></b>	25	50	27	22 h	-	meso	-	99%	(1 <i>R</i> ,2 <i>R</i> )	84.5%

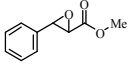
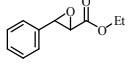
<sup>a</sup> [S]: substrate concentration (g·L<sup>-1</sup>). For each of substrate, the starting quantity of racemic epoxide was 1.0 g in reaction.

<sup>b</sup> [cells]: cells expressing Kau2-EH concentration (g·L<sup>-1</sup>).

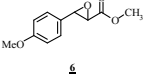
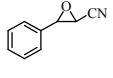
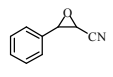
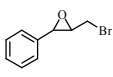
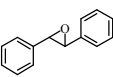
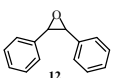
<sup>c</sup> ee<sub>s</sub>: enantiomeric excess of remaining epoxide (%).

<sup>d</sup> ee<sub>p</sub>: enantiomeric excess of formed diol (%).

**Table 34.** Conditions for chiral GC analysis

Compound	Type analysis	Type column	Retention time epoxid		Retention time diol	Temperature programming	
 4	GC	Lipodex-G	(2 <i>R</i> ,3 <i>S</i> )	(2 <i>S</i> ,3 <i>R</i> )	(2 <i>R</i> ,3 <i>R</i> )	110 °C	140 °C
			17.5 min	17.9 min	38.2 min	20 min	30 min
 5	GC	Cyclosil-B	(2 <i>R</i> ,3 <i>S</i> )	(2 <i>S</i> ,3 <i>R</i> )	(2 <i>R</i> ,3 <i>R</i> )	150 °C	180 °C
			22.7 min	23.0 min	17.7 min	20 min	30 min

**Table 35.** Conditions for HPLC analysis.

Compound	Type of analysis	Type of column	Retention times for epoxides		Retention time for diols	Mobile phase	Detector wavelength (nm)	Flow rate (mL·min <sup>-1</sup> )
 6	HPLC	Lux-4	(2 <i>S</i> ,3 <i>R</i> )	(2 <i>R</i> ,3 <i>S</i> )	(2 <i>R</i> ,3 <i>R</i> )	20% Isopropyl alcohol 80% Hexane	230	1.2
			8.4 min	8.8 min	19.8 min			
 7	HPLC	OD-H	(2 <i>R</i> ,3 <i>R</i> )	(2 <i>S</i> ,3 <i>S</i> )	(2 <i>S</i> ,3 <i>R</i> )	20% Isopropyl alcohol 80% Hexane	215	1.2
			10.2 min	11.2 min	7.4 min			
 8	HPLC	OD-H	(2 <i>S</i> ,3 <i>R</i> )	(2 <i>R</i> ,3 <i>S</i> )	(2 <i>R</i> ,3 <i>R</i> )	7.5% Isopropyl alcohol 92.5% Hexane	215	1.2
			11.2 min	12.0 min	20.6 min			
 9	HPLC	Lux-4	(2 <i>R</i> ,3 <i>S</i> )	(2 <i>S</i> ,3 <i>R</i> )	(2 <i>R</i> ,3 <i>R</i> )	7.5% Isopropyl alcohol 92.5% Hexane	215	1.0
			10.2 min	8.5 min	20.6 min			
 10	HPLC	Lux-4	(1 <i>R</i> ,2 <i>R</i> )	(1 <i>S</i> ,2 <i>S</i> )	<i>meso</i>	10% Isopropyl alcohol 90% Hexane	215	1.0
			4.9 min	8.0 min	17.3 min			
 11	HPLC	Lux-4	<i>meso</i>		(1 <i>R</i> ,2 <i>R</i> )	10% Isopropyl alcohol 90% Hexane	215	1.0
			5.3 min	26.9 min				

# Annexe 1

```

AAA81892 Solanum tuberosum (potato) -----
ACO95125 Kau2 -----
AAA37555 Mus musculus (Murine) MALRVAAPFDLDGVLALPSIAGAFRRSEEALALPRDFLLGAYQTEFFPEGPTQLMKGKITF
AAA02756 Homo sapiens MTLRGAVFDLDGVLALPAVFGVLGRTEEALALPRGLLNDAFQKGGPEGATTRLMKGEITL

AAA81892 Solanum tuberosum (potato) -----
ACO95125 Kau2 -----
AAA37555 Mus musculus (Murine) SQWVPLMDESIRKSSKACGANLPENFSISQIFSQAMAARSINRPMQAALALKKKGTTTC
AAA02756 Homo sapiens SQWVPLMEENCRKCSETAKVCLPKNFSIKEIFDKAISARKINRPMQAALMLRKKGFTTA

AAA81892 Solanum tuberosum (potato) -----
ACO95125 Kau2 -----
AAA37555 Mus musculus (Murine) IVTNNWLDGDKRDSLAQMMCELSQHFDPLIESCQVGMKPEPQIYNFLDITLAKAPNEV
AAA02756 Homo sapiens ILTNTWLDRAERDGLAQLMCELMKHFDFPLIESCQVGMKPEPQIYKFLDITLAKAPSEV

AAA81892 Solanum tuberosum (potato) -----MEKIEH
ACO95125 Kau2 -----MAPAM-----DMPPL
AAA37555 Mus musculus (Murine) VFLDDFGSNLKPARDLGMVTLLVHNTASALRELEKVTGTQFPPE--APLPVPCNPNDVSHG
AAA02756 Homo sapiens VFLDDIGANLKPARDLGMVTLLVQDITDALKLEKVTGTQQLLNTAPLPPTSNCNPSDMSHG
:

AAA81892 Solanum tuberosum (potato) KMVAVNGLNMHLAELG---EGPTILFIHGFPPELWYSWRHQMVYLAERGYRAVAPDLRGGY
ACO95125 Kau2 QYANVNGIRMGFYEAGPKTDTPTPLVLCHGWPEIAFWSRHWIKALSETGLRVIAPDQQRGGY
AAA37555 Mus musculus (Murine) YVTVKPGIRLHFVEMG---SGPALCLCHGFPESWFSWRYQIPALAQAGFRVLAIDMKGGY
AAA02756 Homo sapiens YVTVKPRVRLHFVDELG---W-PAVCLCHGFPESWFSWRYQIPALAQAGYRVLAMDMKGGY
.: * * * * : * * * * : * * * * : * * * * : * * * * : * * * * : * * * *

AAA81892 Solanum tuberosum (potato) DTTGAPLNDPSKFSILHLVGDVVALLEAIAPNEEKVFFVAHDWGALIAWHLCFLFRPKVK
ACO95125 Kau2 ATDRPEFVE--AYDIENLTADLVGLDLHLN--IDKAI FVGHDWGGFIVWQMPILRHPERVA
AAA37555 Mus musculus (Murine) DSSSPPEIE--EYAMELLCKEMVTFDLKLG--IPQAVFIGHDWAGVVMVMALFYPERVR
AAA02756 Homo sapiens ESSAPPEIE--EYCMEVLCHEMVTFLDKLG--LSQAVFIGHDWGGMVLVVMALFYPERVR
: : : * : * : * : : : * * * * : * * * * : * * * *

AAA81892 Solanum tuberosum (potato) ALVNLVSHVFSKRNPKMNVVEGLKAIYGEDHYISRFPQVPEI-EAEFAPIGAKSVLKKILT
ACO95125 Kau2 GVIQVNTPHTPRTAT-DPIELLRQRYGDHLYIAQFQHPSPREPDRI FADNVE-KTFDFE--
AAA37555 Mus musculus (Murine) AVASLNTPFMPDPDPVSPMKVIRSI-PVFNYQLYFQEPGVA-EAELEKNMS-RTFKSF--
AAA02756 Homo sapiens AVASLNTPFIPANPNMSPLESIKAN-PVPDYQLYFQEPGVA-EAELEQNLS-RTFKSL--
.: : . . . : : : * * * * : : : : : :

AAA81892 Solanum tuberosum (potato) YRDPAPFFYP-----KKGLEAI-----PDAPVALSSWLSEEELDY
ACO95125 Kau2 MRKMPQKQPSAADANAGPPAAGLGSPLNMAFPQMVAGYDGKLDPREKILSPEEMKVF
AAA37555 Mus musculus (Murine) FRASDETGFIAVH---KATEIGGILV-----NTPEDPNLSKITTEEEIEFY
AAA02756 Homo sapiens FRASDES-VLSMH---KVCEAGGLFV-----NSPEEPSLSRMVTEEEIQFY
* * : . : * * : :

AAA81892 Solanum tuberosum (potato) ANKFEQTGTFGAVNYRALPINWELTAPWTGAQVKVPTKFI VGEFDLVYHIPGAKEYIHN
ACO95125 Kau2 VDTFRGSGFTGGINWYRNMTNRNWEA-HIDHTVRVPSLMIMAE SDSVLPSSAC-----
AAA37555 Mus musculus (Murine) IQQFKKTGFRGFLNWRNTERNWKWSCGLGRKILV PALMVTAEKDIVLRPEMS-----
AAA02756 Homo sapiens VQQFKKSGFRGFLNWRNTERNWKWACKSLGRKILIPALMVTAEKDFVLVPQMS-----
: * : * * * : * * * * : * * : : : * * * *

AAA81892 Solanum tuberosum (potato) GGFKKDVPLLEEVVLEGAHFVSQERPHEISKHIYDFIQKF-----
ACO95125 Kau2 DGMEQIVPDLEK-YLVRNSGHWTQQEQPDEVS AKILEWRRRRFG-----
AAA37555 Mus musculus (Murine) KNMEKIWIPFLKR-GHIEDCGHWTQIEKPTEVNQILIKWLQTEVQNPSVTSKI
AAA02756 Homo sapiens QHMEDWIWPHLKR-GHIEDCGHWTQMDKPTEVNQILIKWLDSDARNPFPVVS KM
.: : * * : . : . . * : : * * : : :

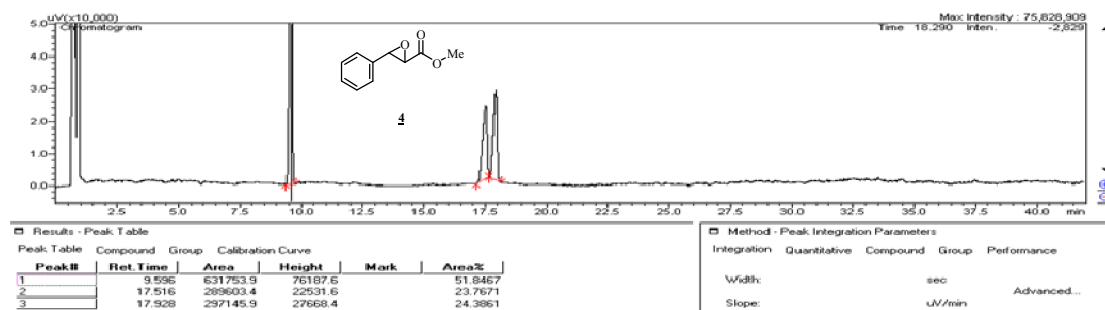
```

## Annexe 2

### Chiral GC analysis of *rac*-**4**, *syn*- and *anti*-*rac*-**4d** and Kau2-EH catalyzed bio-hydrolysis of *rac*-**4**

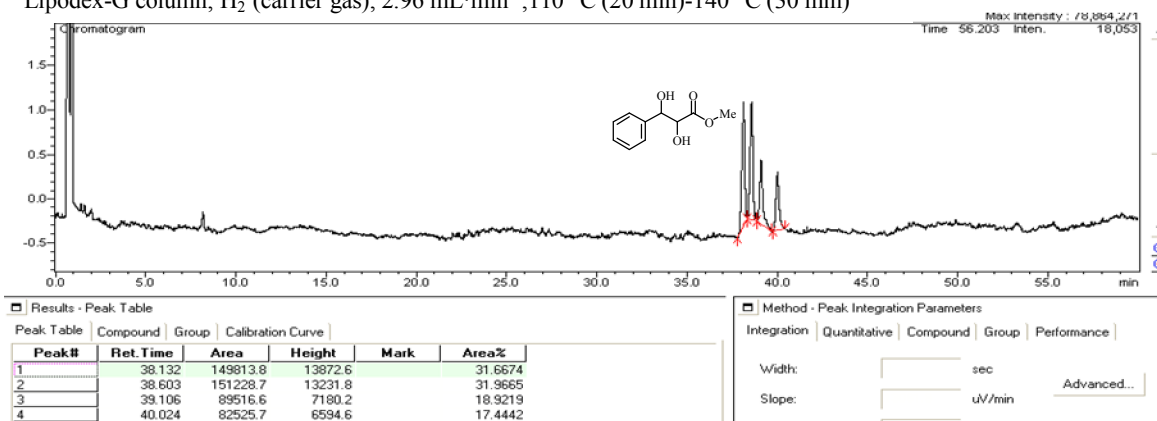
#### *rac*-**4**

Lipodex-G column, H<sub>2</sub> (carrier gas), 2.96 mL·min<sup>-1</sup>, 110 °C (20 min)-140 °C (30 min)



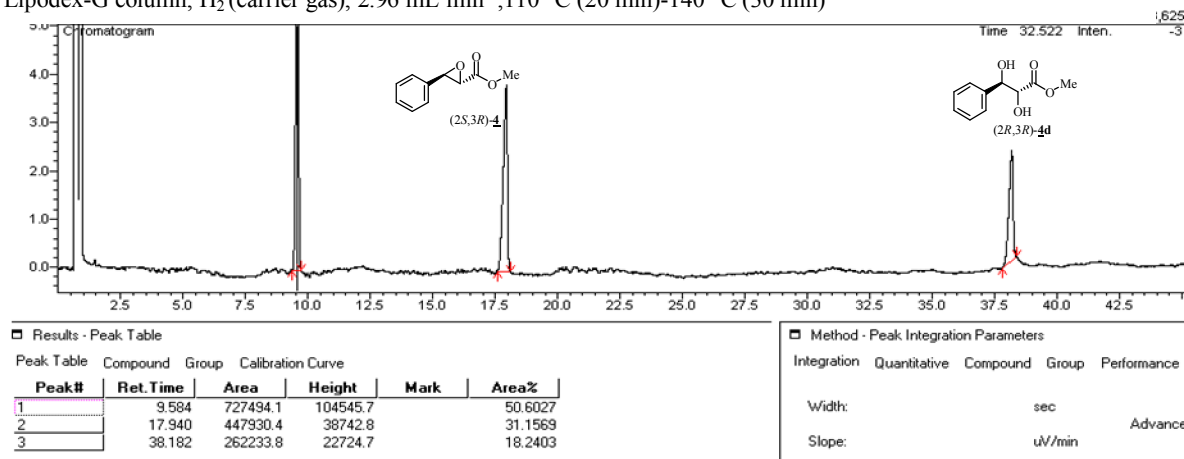
#### *syn*- and *anti*-*rac*-**4d**

Lipodex-G column, H<sub>2</sub> (carrier gas), 2.96 mL·min<sup>-1</sup>, 110 °C (20 min)-140 °C (30 min)



Ees determination of (*2S,3R*)-**4** and (*2R,3R*)-**4d** obtained from Kau2-EH catalyzed bio-hydrolysis of *rac*-**4** at 60min

Lipodex-G column, H<sub>2</sub> (carrier gas), 2.96 mL·min<sup>-1</sup>, 110 °C (20 min)-140 °C (30 min)

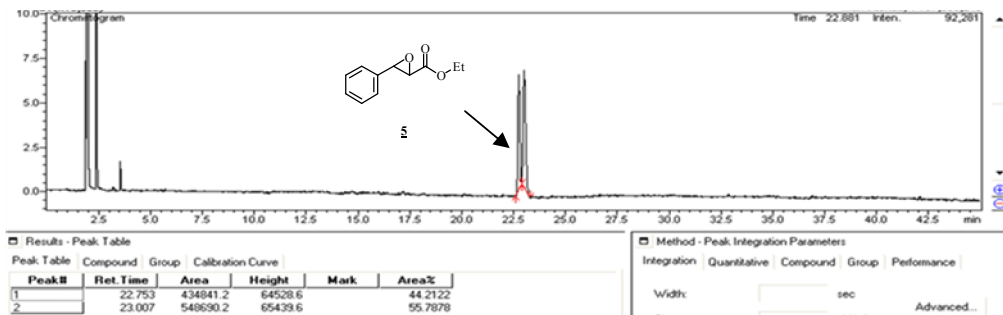


## Annexe 3

### Chiral GC analysis of *rac-5*, *syn-* and *anti-rac-5d* and Kau2-EH catalyzed bio-hydrolysis of *rac-5*

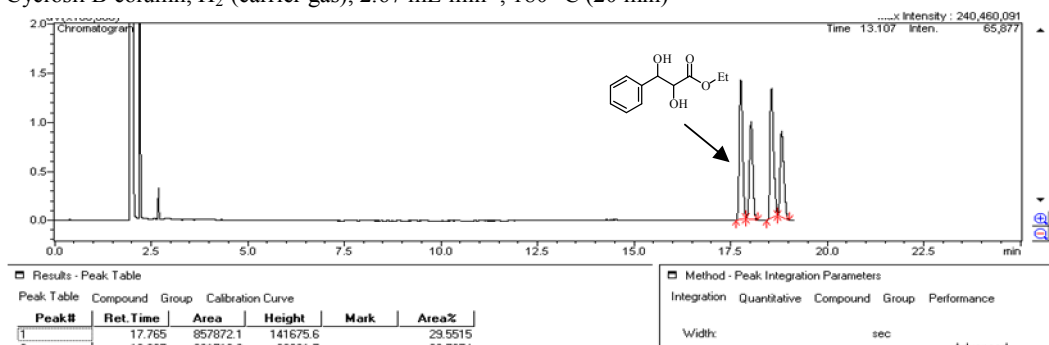
#### *rac-5*

Cyclosil B column, H<sub>2</sub> (carrier gas), 2.67 mL·min<sup>-1</sup>, 150 °C (20 min)-180 °C (20 min)



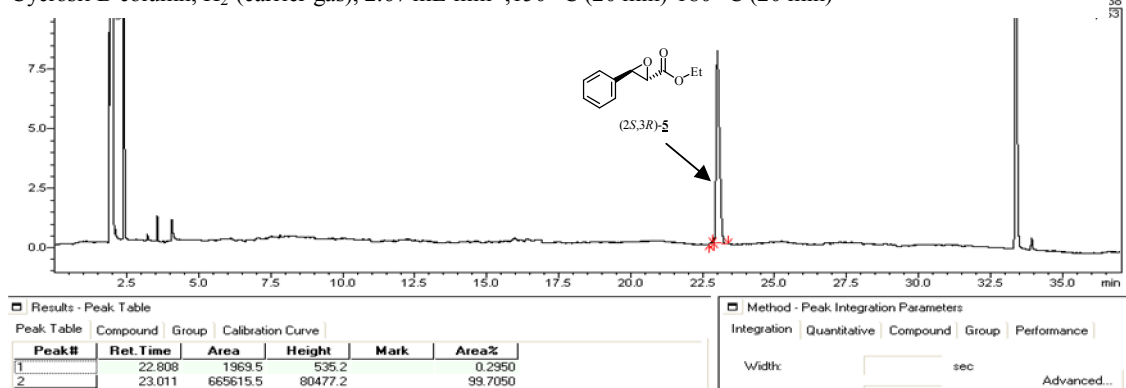
#### *syn-* and *anti-rac-5d*

Cyclosil B column, H<sub>2</sub> (carrier gas), 2.67 mL·min<sup>-1</sup>, 180 °C (20 min)



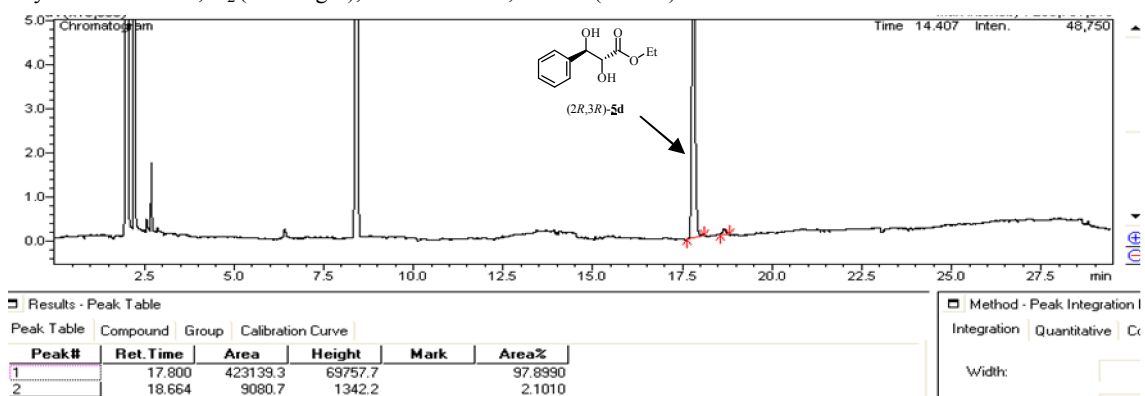
Ee determination of (*2S,3R*)-**5** obtained from Kau2-EH catalyzed bio-hydrolysis of *rac-5* at 60min

Cyclosil B column, H<sub>2</sub> (carrier gas), 2.67 mL·min<sup>-1</sup>, 150 °C (20 min)-180 °C (20 min)



Ee determination of (*2R,3R*)-**5d** obtained from Kau2-EH catalyzed bio-hydrolysis of *rac-5* at 60min

Cyclosil B column, H<sub>2</sub> (carrier gas), 2.67 mL·min<sup>-1</sup>, 180 °C (20 min)

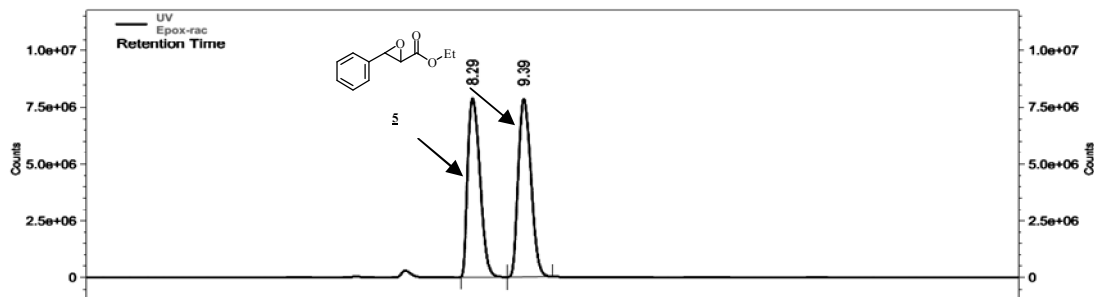


### Annexe 3

Chiral HPLC determination of 5 and 5d absolute configuration obtained from Kau2-EH catalyzed bio-hydrolysis of *rac*-5.

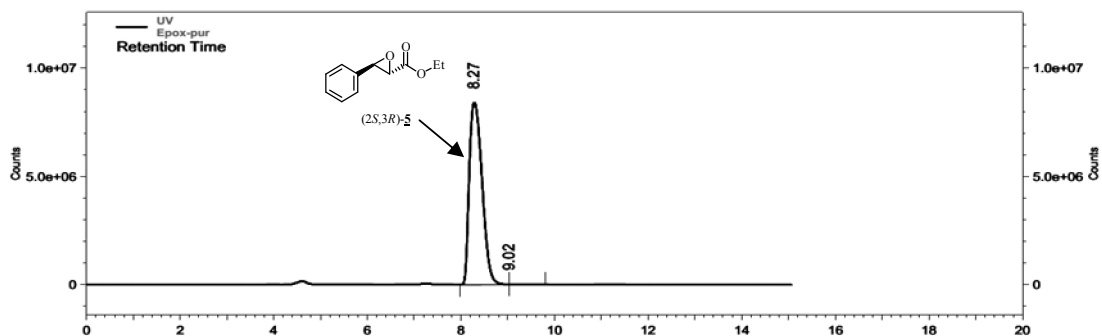
*rac*-5

Method description : Chiralpak AD-H, Hexane/isopropanol 85/15, 0.7 ml/min, UV 230 nm et CD 254nm



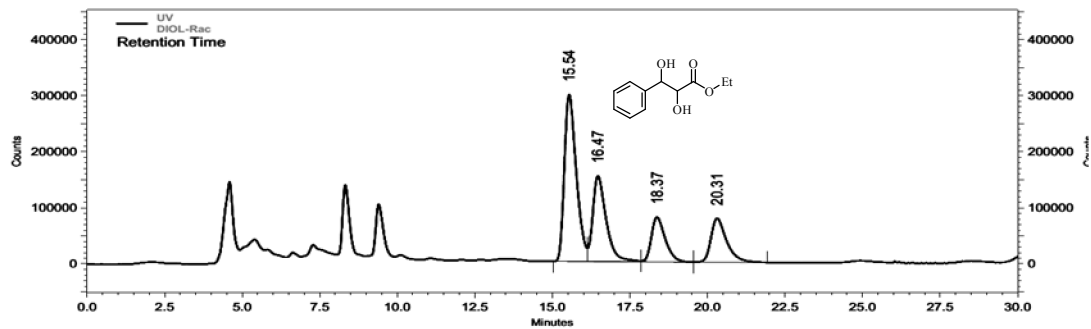
(2*S*,3*R*)-5 obtained from Kau2-EH catalyzed bio-hydrolysis of *rac*-5 at 80 min

Method description : Chiralpak AD-H, Hexane/isopropanol 85/15, 0.7 ml/min, UV 230 nm et CD 254nm



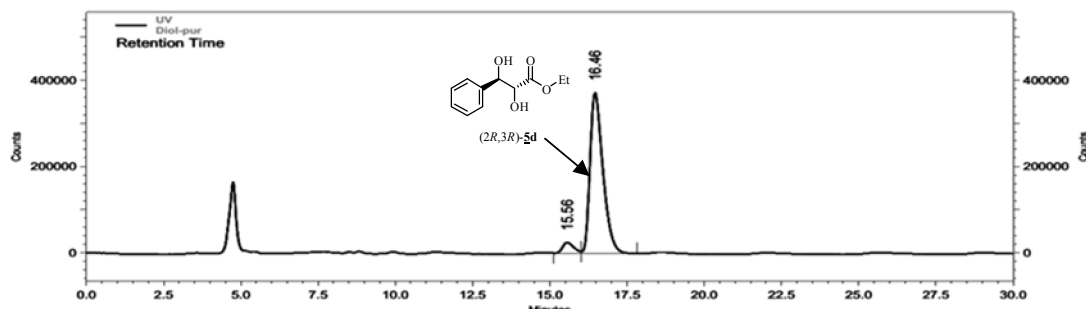
Diols from chemical hydrolysis of *rac*-5

Method description : Chiralpak AD-H, Hexane/isopropanol 85/15, 0.7 ml/min, UV 230 nm et CD 254nm



(2*R*,3*R*)-5d obtained from Kau2-EH catalyzed bio-hydrolysis of *rac*-5 at 80 min

Method description : Chiralpak AD-H, Hexane/isopropanol 85/15, 0.7 ml/min, UV 230 nm et CD 254nm

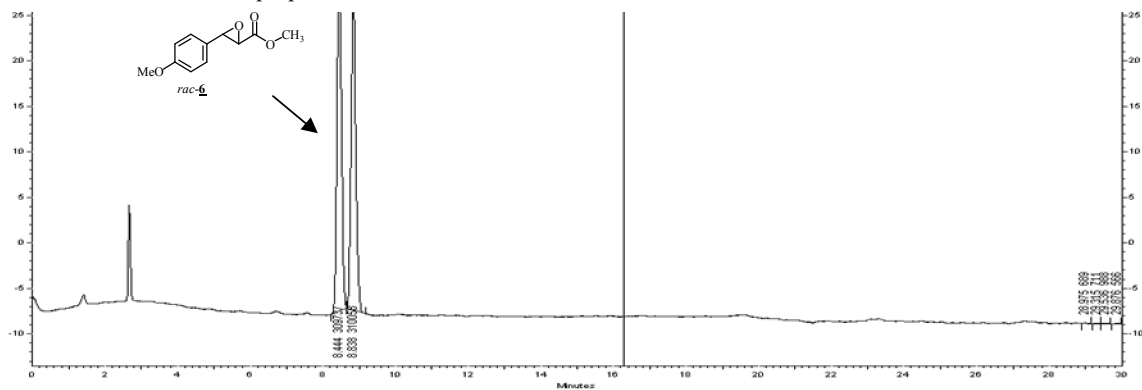


## Annexe 4

### Chiral HPLC analysis of *rac*-**6**, *syn*- and *anti*-*rac*-**6d** and Kau2-EH catalyzed bio-hydrolysis of *rac*-**6**

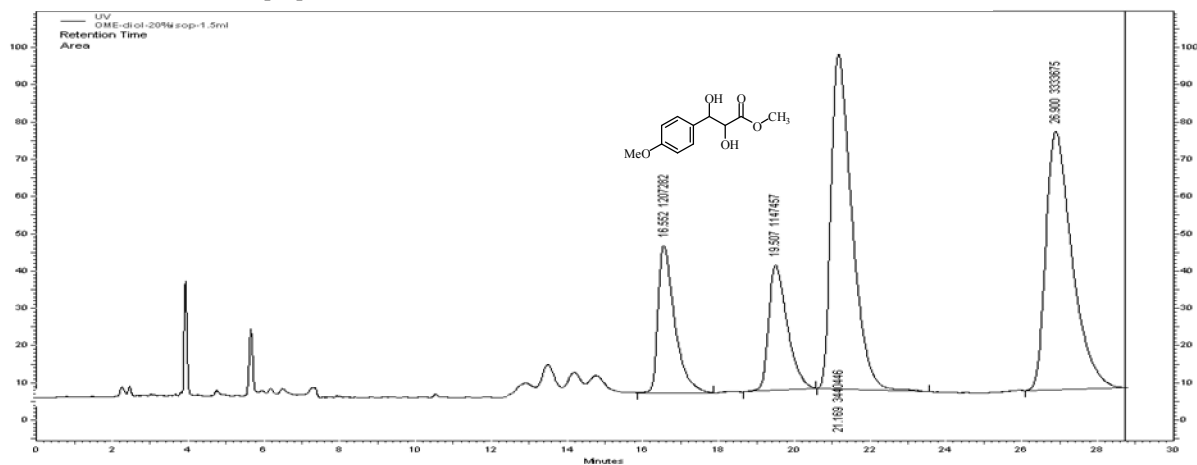
#### *rac*-**6**

Lux-4 column, hexane/isopropanol 8/2, 1.2 mL·min<sup>-1</sup>, UV 230 nm ;

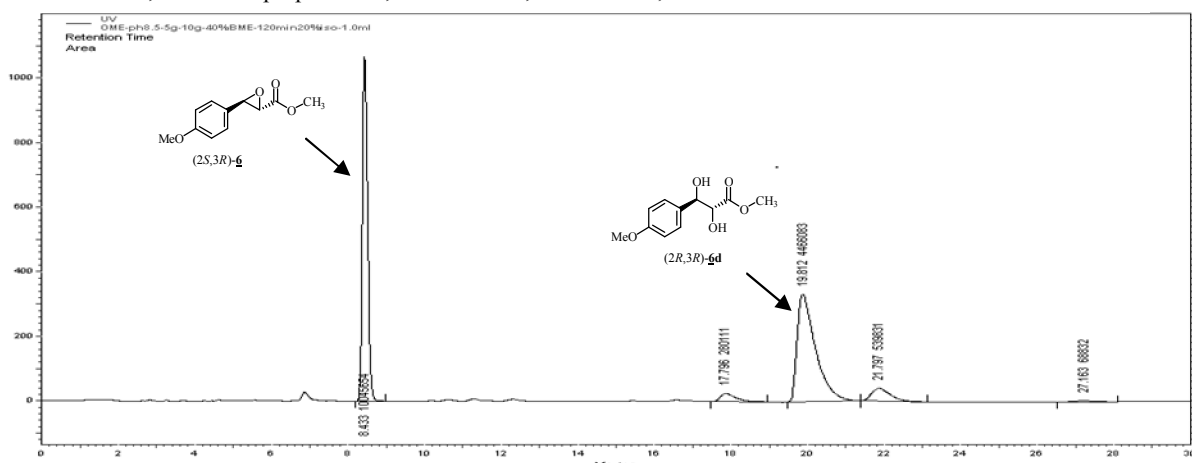


#### *syn*- and *anti*-*rac*-**6d**

Lux-4 column, hexane/isopropanol 8/2, 1.2 mL·min<sup>-1</sup>, UV 230 nm ;



Ees determination of (*2S,3R*)-**6** and (*2R,3R*)-**6d** obtained from Kau2-EH catalyzed bio-hydrolysis of *rac*-**4** at 60min  
Lux-4 column, hexane/isopropanol 8/2, 1.2 mL·min<sup>-1</sup>, UV 230 nm ;



## Annexe 5

Chiral HPLC analysis of *rac-7*, *syn-rac-4d* arising from chemical transformation *syn-rac-7d* and of Kau2-EH catalyzed bio-hydrolysis of *rac-7*

*rac-7*

Chiralcel OD-H column, hexane/isopropanol 8/2, 1.2 mL·min<sup>-1</sup>, UV 215 nm ;



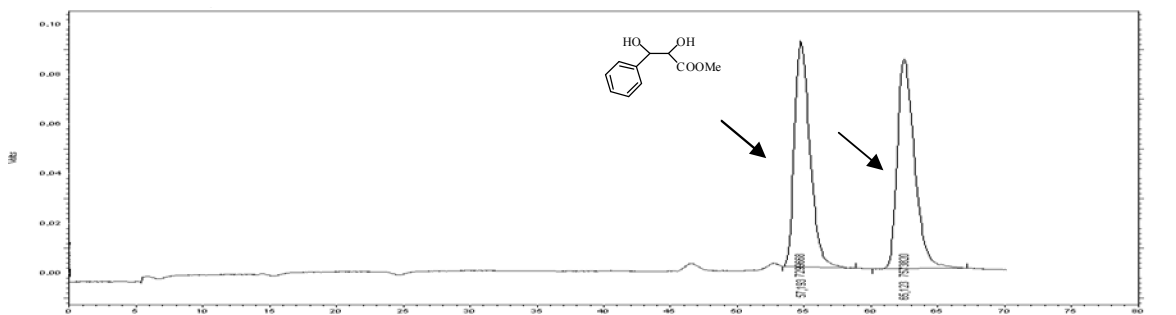
Ee determination of (2*R*,3*R*)-**7** obtained from Kau2-EH catalyzed bio-hydrolysis of *rac-7* at 60min

Chiralcel OD-H column, hexane/isopropanol 8/2, 1.2 mL·min<sup>-1</sup>, UV 215 nm ;



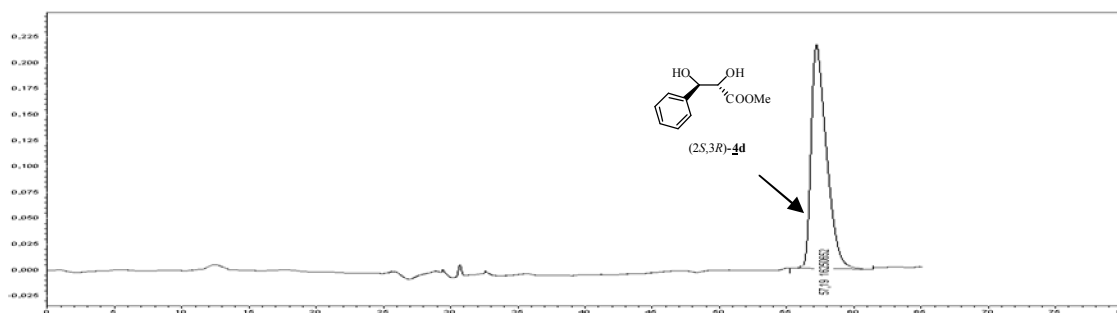
*syn-rac-4d* arising from chemical transformation *syn-rac-7d*

Lux-4 column, hexane/isopropanol 9/1, 1.0 ml/min, UV 215nm ;



(2*S*,3*R*)-**4d** arising from chemical transformation of (2*R*,3*R*)-*syn-7d* obtained from Kau2-EH catalyzed bio-hydrolysis of *rac-7*

Lux-4 column, hexane/isopropanol, 9/1, 1.0 ml/min, UV 215nm ;

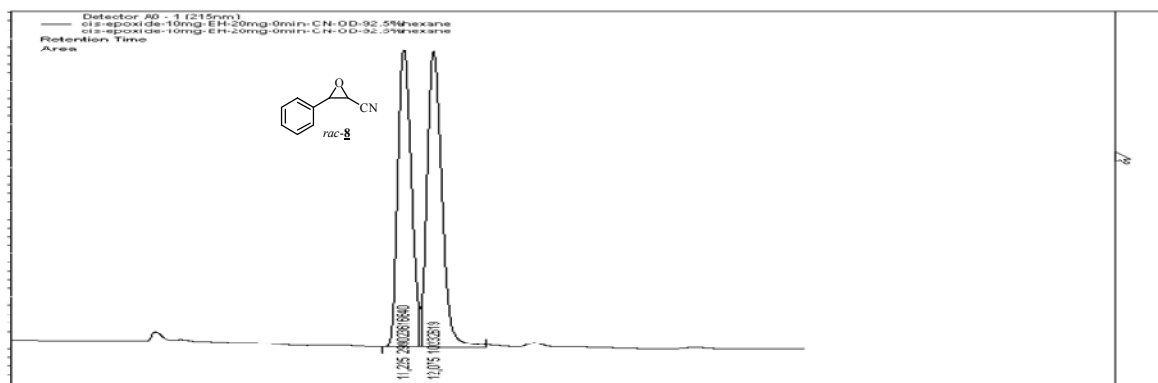


## Annexe 6

Chiral HPLC analysis of *rac-8*, *anti-rac-8d* and Kau2-EH catalyzed bio-hydrolysis of *rac-8*

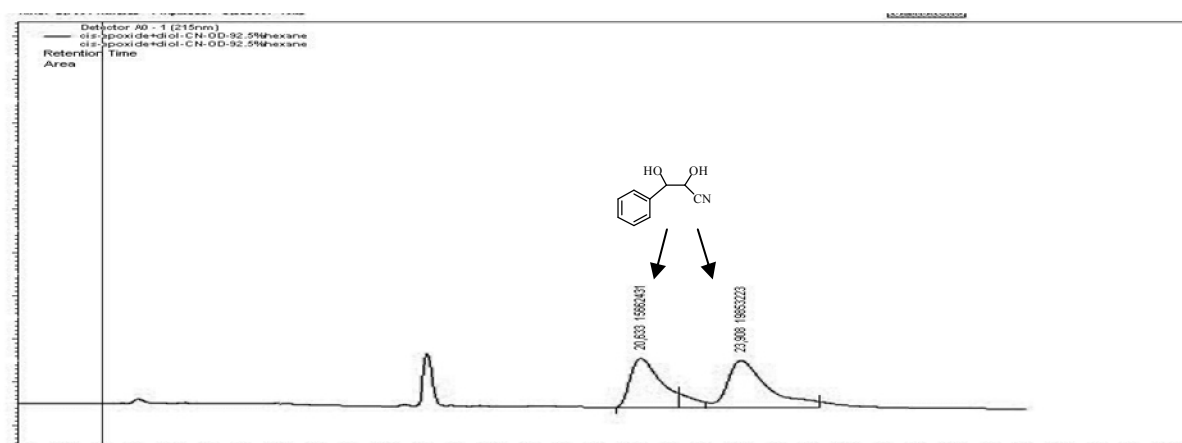
*rac-8*

Chiralcel OD-H column, hexane/isopropanol, 92.5/7.5, 1.2 mL·min<sup>-1</sup>, UV 215 nm ;

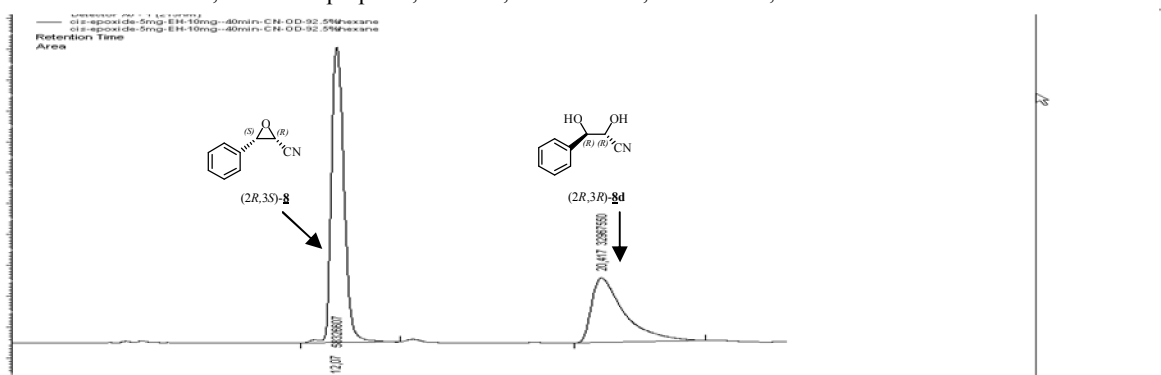


*anti-rac-8d*

Chiralcel OD-H column, hexane/isopropanol, 92.5/7.5, 1.2 mL·min<sup>-1</sup>, UV 215 nm ;



Ees determination of (2*R*,3*S*)-**8** and (2*R*,3*R*)-**8d** obtained from Kau2-EH catalyzed bio-hydrolysis of *rac-8* at 60 min  
Chiralcel OD-H column, hexane/isopropanol, 92.5/7.5, 1.2 mL·min<sup>-1</sup>, UV 215 nm;

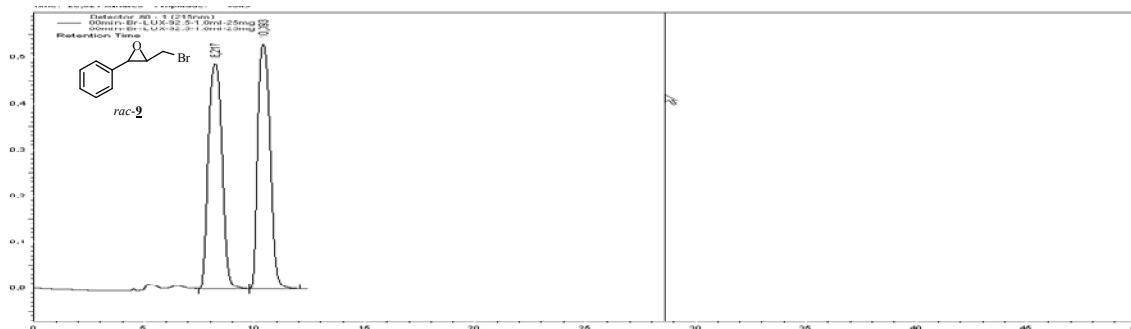


## Annexe 7

### Chiral HPLC analysis of *rac-2*, *syn-* and *anti-rac-2d* and Kau2-EH catalyzed bio-hydrolysis of *rac-2*

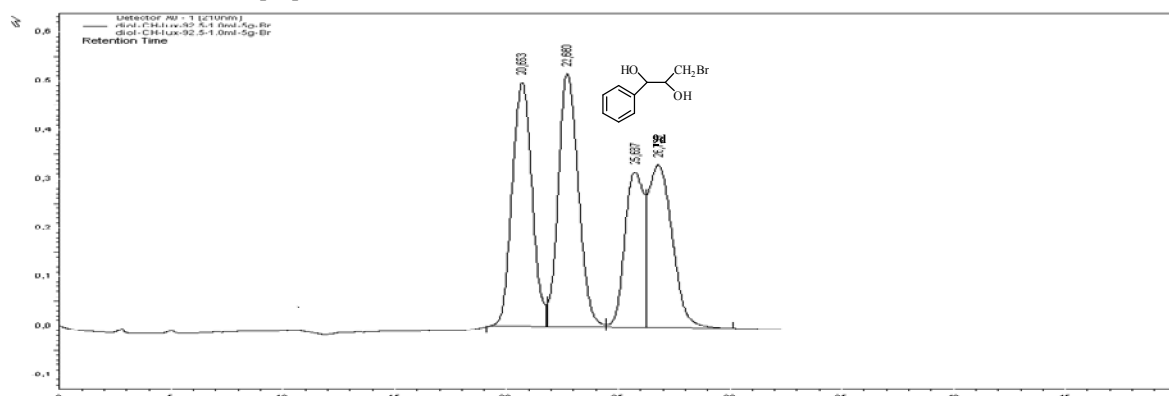
#### *rac-2*

Lux-4 column, hexane/isopropanol 92.5/7.5, 1.0 mL·min<sup>-1</sup>, UV 215 nm ;

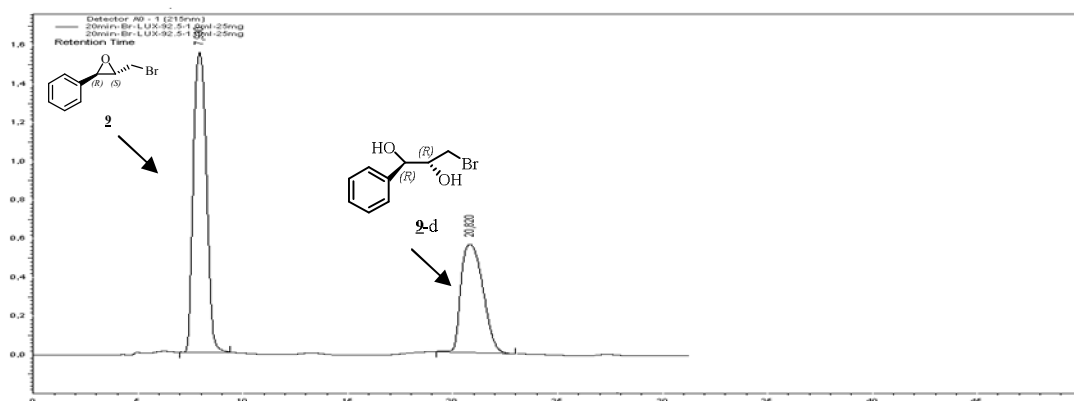


#### *syn-* and *anti-rac-2d*

Lux-4 column, hexane/isopropanol 92.5/7.5, 1.0 mL·min<sup>-1</sup>, UV 215 nm ;



Ees determination of (2*S*,3*R*)-**2** and (2*R*,3*R*)-**2d** obtained from Kau2-EH catalyzed bio-hydrolysis of *rac-2* at 60 min  
 Lux-4 column, hexane/isopropanol 92.5/7.5, 1.0 mL·min<sup>-1</sup>, UV 215 nm ;

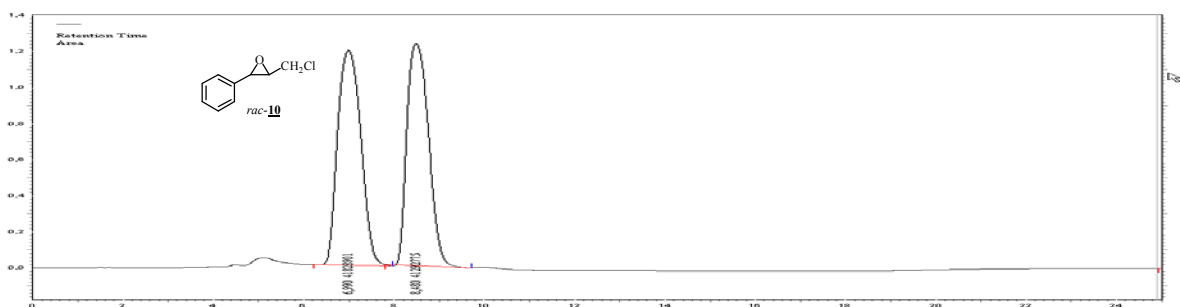


## Annexe 7

### Chiral HPLC analysis of *rac*-**10**, *syn*- and *anti*-*rac*-**10d** and Kau2-EH catalyzed bio-hydrolysis of *rac*-**10**

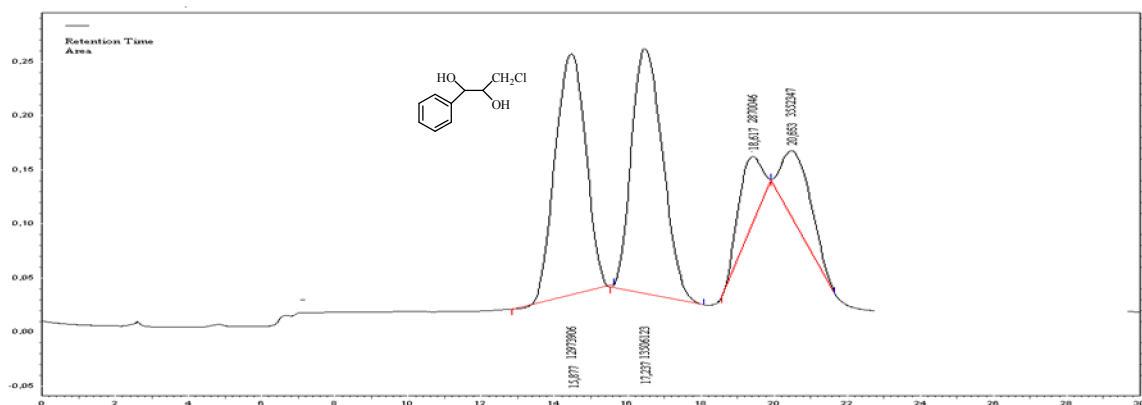
#### *rac*-**10**

Lux-4 column, hexane/isopropanol 92.5/7.5, 1.0 mL·min<sup>-1</sup>, UV 215 nm ;

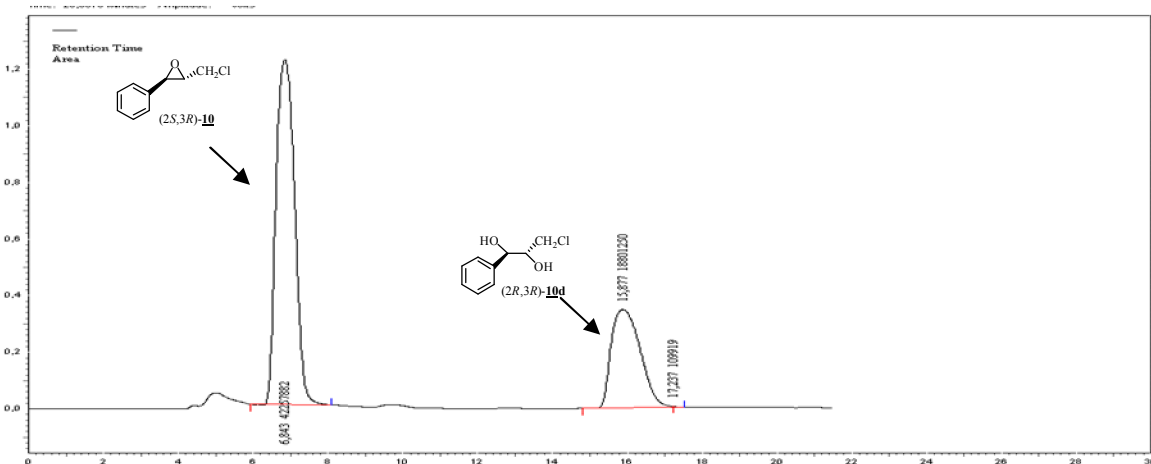


#### *syn*- and *anti*-*rac*-**10d**

Lux-4 column, hexane/isopropanol 92.5/7.5, 1.0 mL·min<sup>-1</sup>, UV 215 nm ;



Ees determination of (*2S,3R*)-**10** and *anti*-(*2R,3R*)-**10d** obtained from Kau2-EH catalyzed bio-hydrolysis of *rac*-**10** at 60 min  
Lux-4 column, hexane/isopropanol 92.5/7.5, 1.0 mL·min<sup>-1</sup>, UV 215 nm ;

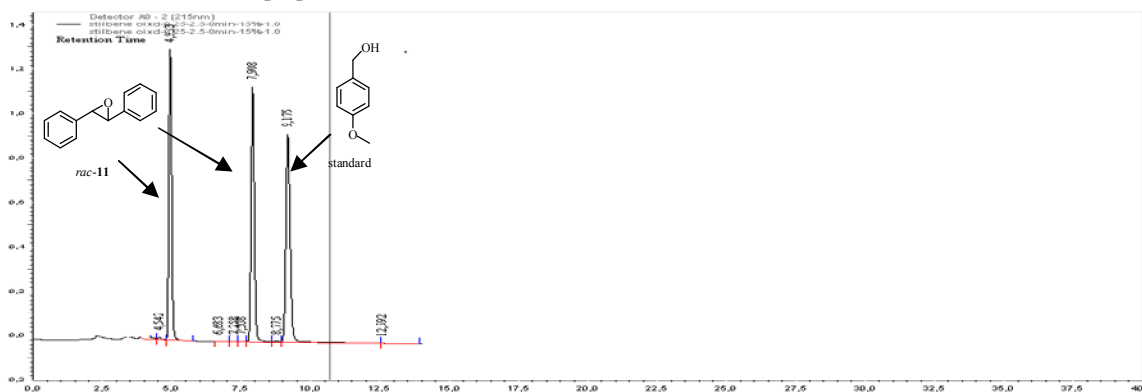


## Annexe 8

### Chiral HPLC analysis of *rac*-**11**, *meso*-**11d** and Kau2-EH catalyzed bio-hydrolysis of *rac*-**11**

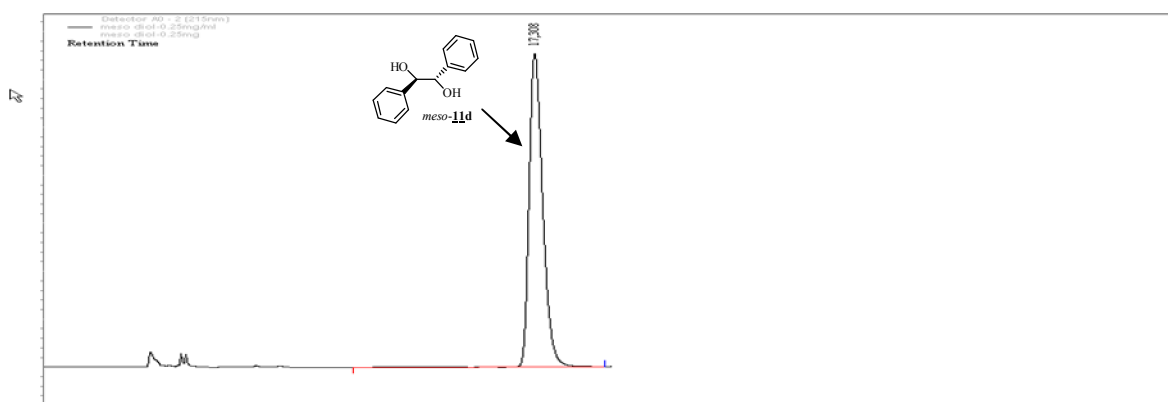
#### *rac*-**11**

Lux-4 column, hexane/isopropanol 9/1, 1.0 mL·min<sup>-1</sup>, UV 215 nm ;

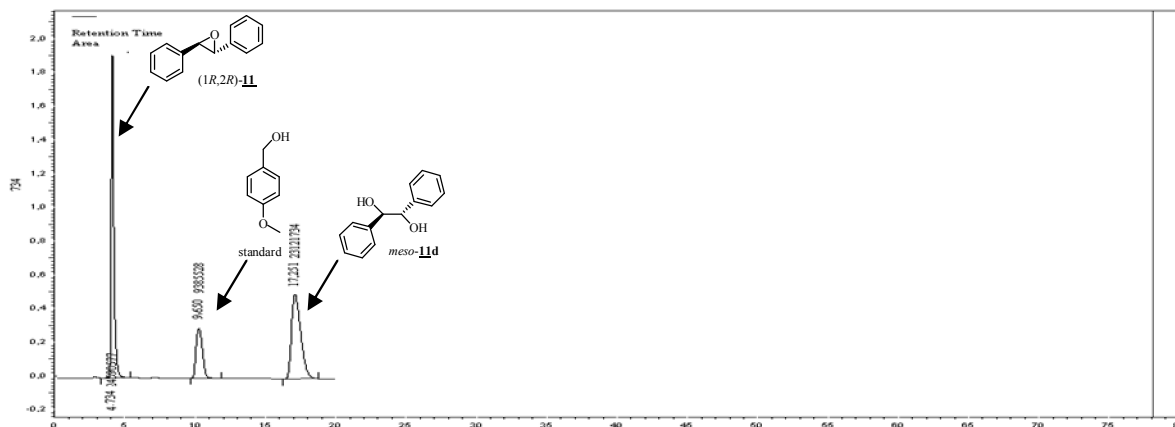


#### *meso*-**11d**

Lux-4 column, hexane/isopropanol 9/1, 1.0 mL·min<sup>-1</sup>, UV 215 nm ;



Ees determination of (1*R*,2*R*)-**11** obtained from Kau2-EH catalyzed bio-hydrolysis of *rac*-**11** at 5 hours  
Lux-4 column, hexane/isopropanol 9/1, 1.0 mL·min<sup>-1</sup>, UV 215 nm ;

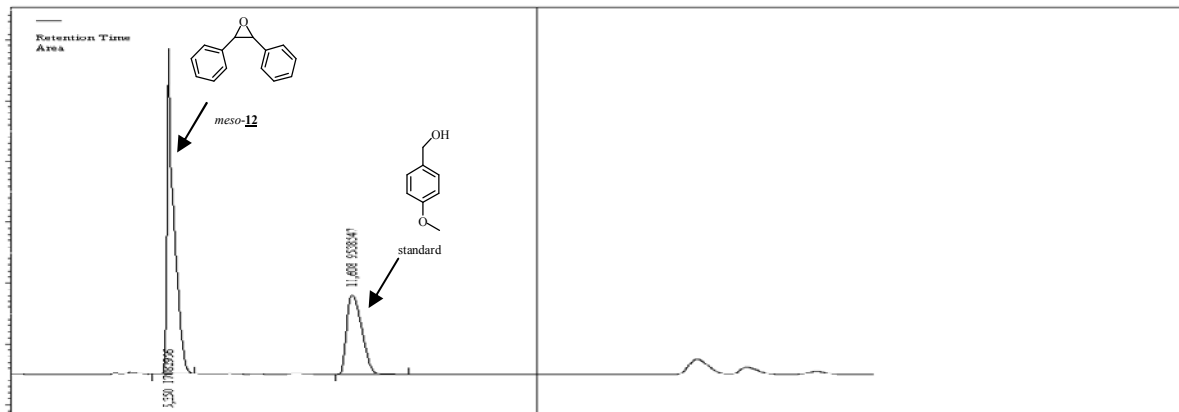


## Annexe 9

### Chiral HPLC analysis of *meso*-**12**, *rac*-**12d** and Kau2-EH catalyzed bio-hydrolysis of *meso*-**12**

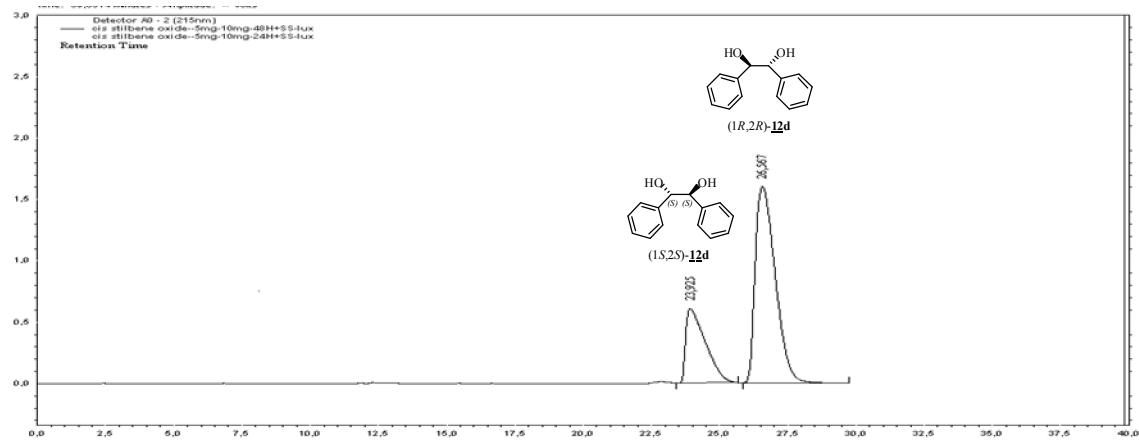
#### *meso*-**12**

Lux-4 column, hexane/isopropanol 9/1, 1.0 mL·min<sup>-1</sup>, UV 215 nm ;



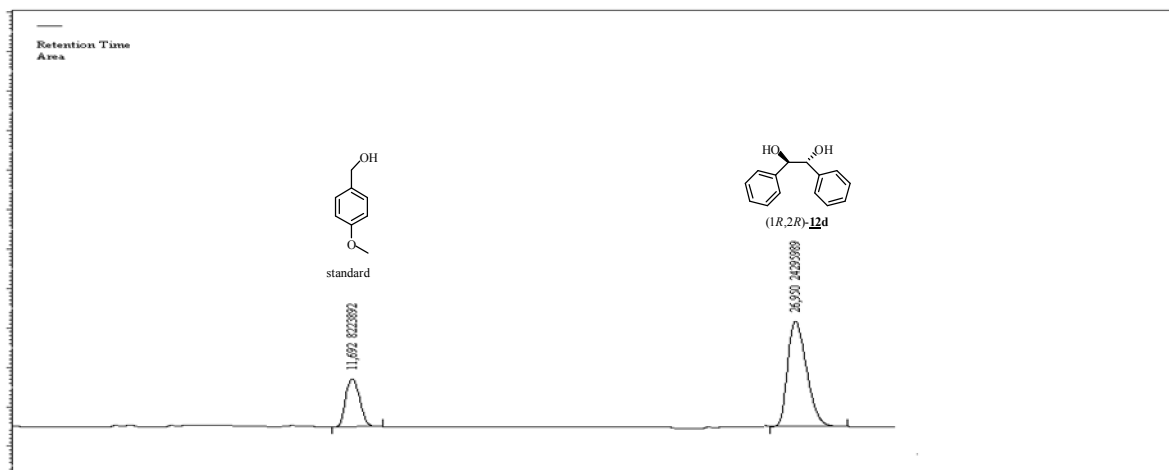
#### Commercial mixture of (1*R*,2*R*)- and (1*S*,2*S*)- **12d**

Lux-4 column, hexane/isopropanol 9/1, 1.0 mL·min<sup>-1</sup>, UV 215 nm ;



#### Ees determination of (1*R*,2*R*)-**12d** obtained from Kau2-EH catalyzed bio-hydrolysis of *meso*-**12** at 30 hours

Lux-4 column, hexane/isopropanol 9/1, 1.0 mL·min<sup>-1</sup>, UV 215 nm ;



### Annexe 10

PCR primers used for cloning the Kau2-encoding gene into pET100/D-TOPO and pET101/D-TOPO, and for mutagenesis at the sites 109 and 316

Primer name	Sequence	pET100/D-TOPO cloning	pET101/D-TOPO cloning	Quick Change	Phusion Site-Directed Mutagenesis
Kau2_Histag_N_F	CACCGCGCCTGCAATGATGGAC ATGCCGCCGCTTCAGTATG	X			
Kau2_Histag_N_R	TCAGCCGAACCGCCGCTGCGC CACTC	X			
Kau2_Histag_C_F	CACCATGGCGCCTGCAATGATG GACATGCCGC		X		
Kau2_Histag_C_R	GCCGAACCGCCGCTGCGCCAC TCCAG		X		
K2_109A_F	TCTTCGTTGGCCACGCNTGGGG CGGGTTCATC			X	
K2_109A_R	GATGAACCCGCCCCANGCGTGG CCAACGAAGA			X	
K2_109N_F	GATCTTCGTTGGCCACAAATGG GGCGGGTTCATCG			X	
K2_109N_R	CGATGAACCCGCCCCARTTGTG GCCAACGAAGATC			X	
K2_H316A_F	ATAGCGGCGCNTGGACCCA				X
K2_H316A_R	TCCTGACCAGATATTTCTCAAG GTCC				X
K2_H316Q_F	GAATAGCGGCCARTGGACCCAG				X
K2_H316Q_R	TCCTGACCAGATATTTCTCAAG GTCC				X

>Wild-type Kau2\_His-tag\_N-terminal

1	ATG CGG GGT TCT CAT CAT CAT CAT CAT CAT GGT ATG GCT AGC ATG	45
1	Met Arg Gly Ser His His His His His His Gly Met Ala Ser Met	15
46	ACT GGT GGA CAG CAA ATG GGT CGG GAT CTG TAC GAC GAT GAC GAT	90
16	Thr Gly Gly Gln Gln Met Gly Arg Asp Leu Tyr Asp Asp Asp Asp	30
91	AAG GAT CAT CCC TTC ACC GCG CCT GCA ATG ATG GAC ATG CCG CCG	135
31	Lys Asp His Pro Phe Thr Ala Pro Ala Met Met Asp Met Pro Pro	45
136	CTT CAG TAT GCC AAT GTC AAC GGC ATA CGC ATG GGC TTC TAC GAG	180
46	Leu Gln Tyr Ala Asn Val Asn Gly Ile Arg Met Gly Phe Tyr Glu	60
181	GCC GGT CCT AAA ACC GAC ACG CCG CCG CTG GTG CTG TGT CAC GGC	225
61	Ala Gly Pro Lys Thr Asp Thr Pro Pro Leu Val Leu Cys His Gly	75
226	TGG CCG GAG ATT GCG TTT TCA TGG CGG CAC CAG ATC AAG GCG CTG	270
76	Trp Pro Glu Ile Ala Phe Ser Trp Arg His Gln Ile Lys Ala Leu	90
271	AGC GAG ACA GGT CTT CGC GTG ATC GCG CCG GAC CAG CGC GGC TAT	315
91	Ser Glu Thr Gly Leu Arg Val Ile Ala Pro Asp Gln Arg Gly Tyr	105
316	GGC GCG ACG GAC CGG CCC GAG CCT GTC GAA GCC TAT GAC ATC GAG	360
106	Gly Ala Thr Asp Arg Pro Glu Pro Val Glu Ala Tyr Asp Ile Glu	120
361	AAC CTG ACG GCC GAT CTG GTC GGG CTA CTC GAT CAC CTG AAC ATC	405
121	Asn Leu Thr Ala Asp Leu Val Gly Leu Leu Asp His Leu Asn Ile	135
406	GAC AAG GCG ATC TTC GTT GGC CAC GAC TGG GGC GGG TTC ATC GTC	450
136	Asp Lys Ala Ile Phe Val Gly His Asp Trp Gly Gly Phe Ile Val	150
451	TGG CAG ATG CCG CTG CGT CAT CCG TCG CGT GTC GCA GGC GTC ATC	495
151	Trp Gln Met Pro Leu Arg His Pro Ser Arg Val Ala Gly Val Ile	165
496	GGT GTC AAC ACG CCG CAC ACG CCG CGC ACG GCG ACC GAT CCG ATT	540
166	Gly Val Asn Thr Pro His Thr Pro Arg Thr Ala Thr Asp Pro Ile	180
541	GAA TTG CTG CGC CAG CGC TAT GGC GAT CAT CTT TAC ATC GCG CAG	585
181	Glu Leu Leu Arg Gln Arg Tyr Gly Asp His Leu Tyr Ile Ala Gln	195
586	TTT CAG CAT CCG TCG CGG GAG CCT GAC AGG ATT TTC GCC GAC AAT	630
196	Phe Gln His Pro Ser Arg Glu Pro Asp Arg Ile Phe Ala Asp Asn	210
631	GTC GAA AAG ACG TTC GAC TTC TTC ATG CGC AAA CCG ATG CCG CAG	675
211	Val Glu Lys Thr Phe Asp Phe Phe Met Arg Lys Pro Met Pro Gln	225
676	AAG CAG CCA TCG GCA GCG GAT GCC AAT GCG GGG CCA CCC GCG GCG	720
226	Lys Gln Pro Ser Ala Ala Asp Ala Asn Ala Gly Pro Pro Ala Ala	240
721	GGT CTC GGT GCC TCG CCA AAG TTG AAC ATG GCC TTT CCG CAG ATG	765
241	Gly Leu Gly Ala Ser Pro Lys Leu Asn Met Ala Phe Pro Gln Met	255
766	GTC GCG GGC TAT GAC GGC AAG CTC GAT CCG CGG GAG AAG ATA TTG	810
256	Val Ala Gly Tyr Asp Gly Lys Leu Asp Pro Arg Glu Lys Ile Leu	270
811	TCG CCC GAG GAA ATG AAG GTT TTC GTC GAT ACG TTC AGG GGG TCG	855
271	Ser Pro Glu Glu Met Lys Val Phe Val Asp Thr Phe Arg Gly Ser	285
856	GGC TTC ACC GGC GGG ATC AAC TGG TAT CGC AAC ATG ACC CGC AAC	900
286	Gly Phe Thr Gly Gly Ile Asn Trp Tyr Arg Asn Met Thr Arg Asn	300
901	TGG GAA CGC TCG GCG CAT ATC GAT CAC ACC GTG CGC GTA CCA TCG	945
301	Trp Glu Arg Ser Ala His Ile Asp His Thr Val Arg Val Pro Ser	315
946	CTG ATG ATC ATG GCC GAG AGC GAT TCG GTG CTG CCG CCT TCG GCC	990
316	Leu Met Ile Met Ala Glu Ser Asp Ser Val Leu Pro Pro Ser Ala	330

991	TGC	GAC	GGG	ATG	GAG	CAG	ATT	GTG	CCG	GAC	CTT	GAG	AAA	TAT	CTG	1035
331	Cys	Asp	Gly	Met	Glu	Gln	Ile	Val	Pro	Asp	Leu	Glu	Lys	Tyr	Leu	345
1036	GTC	AGG	AAT	AGC	GGC	CAC	TGG	ACC	CAG	CAG	GAG	CAG	CCT	GAC	GAG	1080
346	Val	Arg	Asn	Ser	Gly	His	Trp	Thr	Gln	Gln	Glu	Gln	Pro	Asp	Glu	360
1081	GTC	AGC	GCC	AAA	ATT	CTG	GAG	TGG	CGC	AGG	CGG	CGG	TTC	GGC	TGA	1125
361	Val	Ser	Ala	Lys	Ile	Leu	Glu	Trp	Arg	Arg	Arg	Arg	Phe	Gly	End	375

## References:

- Argiriadi, M.A., Morisseau, C., Goodrow, M.H., Dowdy, D.L., Hammock, B.D. and Christianson, D.W. (2000) Binding of alkylurea inhibitors to epoxide hydrolase implicates active site tyrosines in substrate activation. *J. Biol. Chem.*, **275**, 15265-15270.
- Grulich, M., Maršálek, J., Kyslík, P., Štěpánek, V. and Kotik, M. (2011) Production, enrichment and immobilization of a metagenome-derived epoxide hydrolase. *Process Biochem.*, **46**, 526-532.
- Mhamdi, L., Bohli, H., Moussaoui, Y. and ben Salem, R. (2011) Phase Transfer Catalysis of Henry and Darzens Reactions. *Int. J. Org. Chem.*, **1**, 119-123.
- Saikia, I., Kashyap, B. and Phukan, P. (2010) Efficient Protocol for Stereoselective Epoxidation of Cinnamic Esters Using TsNBr<sub>2</sub>. *Synth. Commun.*, **40**, 2647-2652.
- Svoboda, J., Kocfeldová, Z. and Paleček, J. (1988) Reaction of 4-substituted benzaldehydes and acetophenones with chloroacetonitrile. *Collect. Czech. Chem. Commun.*, **53**, 822-832.

## List of figures

- Figure 1.** EH-catalyzed hydrolysis of a racemic epoxide, resulting in the formation of a vicinal diol with an enantiomeric excess of  $100\% \geq ee_p \geq 0\%$  at complete conversion ( $c = 100\%$ ) of the substrate. Depending on the EH-substrate interactions and consequently its substrate-related enantiomeric ratio or E-value (which characterizes the ability of the enzyme to discriminate between the two competing substrate enantiomers, Chen *et al.*, 1982), enantiopure epoxide is obtained at a specific degree of conversion within the range of  $50\% < c < 100\%$ . The kinetics of highly enantioselective EHs is characterized by a rapid hydrolysis of the preferred epoxide enantiomer, followed by a much slower hydrolysis of the remaining epoxide.....10
- Figure 2.** Attack at the oxirane ring can occur at either the terminal carbon atom, which results in a diol product with retained configuration ( $\beta$ -attack), or the carbon atom with the substituent R, resulting in a diol with an inverted configuration ( $\alpha$ -attack). The percentages of epoxide molecules following a particular reaction pathway are represented by the corresponding regioselectivity coefficients; the following relationships between the four regioselectivity coefficients are valid:  $\alpha_R + \beta_R = 100\%$ , and  $\alpha_S + \beta_S = 100\%$ . .....11
- Figure 3.** Phylogenetic relationships among protein sequences encoding EHs with confirmed activities. Each sequence is represented by its GenBank accession number; for sequences and further data regarding EHs with codes starting with BD, see Zhao *et al.*, 2004. The data set includes sequences of mammalian EHs ( $\blacklozenge$ ), plant EHs ( $\blacktriangle$ ), fish EHs ( $\nabla$ ), insect EHs ( $\triangle$ ), yeast EHs ( $\circ$ ), fungal EHs ( $\bullet$ ), bacterial EHs ( $\square$ ), and eDNA-derived EHs ( $\blacksquare$ ). A star represents an EH with a determined X-ray protein structure: human EH (NP\_001970), murine EH (NP\_031966), potato EH (AAA81892), a bacterial EH from *Agrobacterium radiobacter* AD1 (CAA73331), a fungal EH from *Aspergillus niger* LCP 521 (CAB59812), and two bacterial EHs which are not members of the  $\alpha/\beta$ -hydrolase fold superfamily (CAA77012 and O33283). The bootstrap consensus tree was inferred from 1000 replicates. The evolutionary distances were computed using the Poisson correction method. The bar represents 0.2 amino acid substitutions per site.....13
- Figure 4.** Proposed catalytic mechanism of EHs which are members of the  $\alpha/\beta$ -hydrolase fold superfamily.....15
- Figure 5.** Proposed catalytic mechanism of the limonene-1,2-epoxide hydrolase from *Rhodococcus erythropolis* and the EH from *Mycobacterium tuberculosis*. The catalytic water molecule is activated by the formation of hydrogen bonds involving aspartic acid, asparagine and tyrosine residues. At the same time, polarization and activation of the oxirane ring is achieved by hydrogen bonding with the oxirane oxygen involving another aspartic acid residue.....15
- Figure 6.** Biohydrolytic kinetic resolution of racemic styrene oxide (*rac*-SO) catalyzed by *Aspergillus niger* LCP 521 (*AnEH*) and/or *Beauveria sulfurescens* ATCC 7159 (*BsEH*). Using both fungi together led to an enantioconvergent production of (*R*)-phenyl-1,2-ethanediol. ....17
- Figure 7.** Enantioconvergent biohydrolytic transformation of *para*-chlorostyrene oxide using a bi-enzymatic process. The sequential use of *Solanum tuberosum* and *Aspergillus niger* EHs as biocatalysts led to the formation of enantiopure (*R*)-*para*-chlorophenyl-1,2-diol, a chiral building block for the synthesis of (*R*)-Eliprodil. ....19
- Figure 8.** Enantioconvergent synthesis of the  $\beta$ -blocker (*R*)-Nifenalol using a combined chemoenzymatic approach. ....22

<b>Figure 9.</b> Preparative scale synthesis of enantiopure (4-trifluoromethoxyphenyl)-oxirane using a partially purified recombinant EH from <i>Aspergillus niger</i> LCP 521 as a biocatalyst.....	23
<b>Figure 10.</b> Preparative kinetic resolution of 2-pyridyloxirane with EHs from <i>A. niger</i> and <i>A. radiobacter</i> AD1 (mutant Tyr215Phe). .....	24
<b>Figure 11.</b> Kinetic hydrolytic resolution at high substrate concentration of <i>para</i> -bromo- <i>methyl</i> styrene oxide using an enzymatic extract of <i>A. niger</i> LCP 521.....	25
<b>Figure 12.</b> Preparative-scale resolution of <i>rac</i> -4-isobutyl- $\alpha$ -methylstyrene oxide using an enzymatic extract of <i>A. niger</i> LCP 521. A four step enantioconvergent procedure enabled the synthesis of ( <i>S</i> )-Ibuprofen. ....	26
<b>Figure 13.</b> Preparative-scale synthesis of enantiopure <i>para</i> -trifluoromethyl- $\alpha$ -methyl styrene oxide using a partially purified recombinant EH from <i>Aspergillus niger</i> LCP 521 as biocatalyst.....	27
<b>Figure 14.</b> Preparative-scale kinetic resolution of racemic <i>trans</i> - $\beta$ -methylstyrene oxide using the Kau2-EH at high substrate concentration. ....	27
<b>Figure 15.</b> Preparative enantioconvergent biohydrolysis of racemic <i>cis</i> - $\beta$ -methylstyrene oxide using the Kau2-EH.....	28
<b>Figure 16.</b> Biohydrolytic kinetic resolution of racemic indene oxide. Access to (1 <i>S</i> ,2 <i>R</i> )- or (1 <i>R</i> ,2 <i>S</i> )-indene oxide as a function-of the biocatalyst used. ....	29
<b>Figure 17.</b> Kinetic resolution of 1,2-epoxyoctane at high substrate concentration with two yeast EHs.....	30
<b>Figure 18.</b> Biohydrolytic kinetic resolutions of racemic-PGE. Use of enantiocomplementary wild-type and evolved mutant EHs for the preparation of two antipodes of PGE. ....	31
<b>Figure 19.</b> Chemoenzymatic deracemization of <i>rac-gem</i> -disubstituted oxiranes.....	33
<b>Figure 20.</b> Kinetic resolution of O-axial or O-equatorial 4-methyl-1-oxaspiro[2,5]octane by <i>Rhodotorula glutinis</i> EH. ....	33
<b>Figure 21.</b> Preparative hydrolytic resolution of <i>trans</i> -divinyl spiroepoxide using AnEH and LEH as biocatalysts, enabling the synthesis of enantiopure 11-heterosteroids.....	34
<b>Figure 22.</b> Deracemization of <i>rac-cis</i> -2,3-epoxyheptane via enantioconvergent biohydrolysis using <i>Nocardia</i> EH1 leading to the formation of an ( <i>R,R</i> )-diol. ....	35
<b>Figure 23.</b> Synthesis of both enantiomers of Bower's compound using whole cells of <i>A. niger</i> LCP 521 as biocatalyst.....	36
<b>Figure 24.</b> Chemoenzymic resolution and deracemization of <i>rac</i> -1-methyl-1,2-epoxycyclohexane using whole cells of <i>Corynebacterium</i> C12. ....	36
<b>Figure 25.</b> Deracemization of three <i>rac</i> -trialkyl oxiranes via enantioconvergent biohydrolysis using whole cells of <i>Mycobacterium paraffinicum</i> and <i>Rhodococcus ruber</i> . ....	37
<b>Figure 26.</b> Synthesis of the pheromone (2 <i>R</i> ,5 <i>R</i> )-Pityol via a diastereoconvergent biohydrolysis using <i>Rhodococcus ruber</i> DSM 44540 EH as biocatalyst. ....	38
<b>Figure 27.</b> Stereochemical courses of EH-catalyzed hydrolysis/cyclisation cascades of 6,7:9,10-bis(epoxy)pentadecane to yield tetrahydrofurane derivatives. ....	39
<b>Figure 28.</b> Desymmetrization of aryl <i>meso</i> -epoxides with BD887 obtained from DNA libraries of environmental samples. ....	39
<b>Figure 29.</b> Kinetic resolution of racemic epichlorohydrin using purified EH from <i>Agrobacterium radiobacter</i> leading to the formation of enantiomerically pure ( <i>R</i> )-epichlorohydrin.....	41
<b>Figure 30.</b> Kinetic resolution of racemic epichlorohydrin using the purified EH from <i>Agromyces mediolanus</i> leading to the formation of enantiomerically pure ( <i>S</i> )-epichlorohydrin.....	41

<b>Figure 31.</b> Preparative hydrolytic resolution of <i>rac</i> -1-chloro- and 1-triazole-2(2,4-difluorophenyl)-2,3-epoxypropane using <i>AnEH</i> as biocatalyst. The latter compound is a useful building block for the synthesis of enantiopure D0870.....	42
<b>Figure 32.</b> Kinetic resolution of racemic 4-bromo-1,2-epoxybutane using purified Oxy-9 EH and its use in the synthesis of ( <i>S</i> )- <i>N</i> -benzyl-3-hydroxypyrrolidine.....	43
<b>Figure 33.</b> Kinetic resolution of racemic epoxyamide using purified Oxy-10 EH and its application to the synthesis of ( <i>S</i> )- <i>N</i> -benzyl-3-hydroxypyrrolidine en route to (–)-Swainsonine. (i) See Calvez <i>et al.</i> , 1998; (ii) See Haddad <i>et al.</i> , 2001 and Ferreira <i>et al.</i> , 1997.....	43
<b>Figure 34.</b> Chemo-enzymatic access to ( <i>S</i> )-3-hydroxytetrahydrofuran. (i) See Yuasa <i>et al.</i> , 1997; 79% .....	44
<b>Figure 35.</b> Enantioconvergent chemo-enzymatic access to ( <i>R</i> )-3-benzyloxy-2-methylpropane-1,2-diol. ....	45
<b>Figure 36.</b> Kinetic resolution of <i>rac</i> -ethyl-3,4-epoxybutyrate by <i>Acinetobacter baumannii</i> . ....	46
<b>Figure 37.</b> Kinetic resolution of two <i>trans</i> -(+/-)-3-phenyl glycidates by immobilized Mung bean EH. ....	46
<b>Figure 38.</b> Gram scale and high substrate concentration preparation of enantiopure glycidaldehyde 2,2-dimethyltrimethylene acetal using partially purified recombinant EH from <i>Aspergillus niger</i> LCP 521 as biocatalyst.....	47
<b>Figure 39.</b> Synthesis of enantiopure 4-deoxy-D-fructose 6-phosphate using two enzymatic steps.....	47
<b>Figure 40.</b> Various epoxide racemates tested as substrates of Kau2-EH.....	58
<b>Figure 41.</b> Preparative biohydrolysis of <i>trans</i> -methylstyrene oxide-L and <i>cis</i> -methylstyrene oxide-M using Kau2-EH.....	60
<b>Figure 42.</b> Hydrolysis of <i>rac</i> - <i>para</i> -chlorostyrene oxide using wild-type Kau2-EH. ....	62
<b>Figure 43.</b> Three homology models of Kau2-EH based on the crystal structures of the murine (A), potato (B) and human EH (C). The models were built using SWISS-MODEL. ....	64
<b>Figure 44.</b> Structure of CDU and CIU.....	65
<b>Figure 45.</b> Hydrolysis of <i>rac</i> -1 using Kau2-EH.....	66
<b>Figure 46.</b> Relationship between enzyme activity and substrate concentration.....	66
<b>Figure 47.</b> Characteristic plots for the common inhibition types (Cortes <i>et al.</i> , 2001). ....	67
<b>Figure 48.</b> Effect of various concentrations of CDU inhibitor on EH activity at different substrate concentrations. ....	68
<b>Figure 49.</b> Determination of inhibition constant for CDU and type of inhibition using Kau2-EH.....	69
<b>Figure 50.</b> Determination of inhibition constant for CIU and type of inhibition using Kau2-EH.....	70
<b>Figure 51.</b> Determination of inhibition constant for CDU and type of inhibition using potato EH.....	72
<b>Figure 52.</b> Determination of inhibition constant for CIU and type of inhibition using potato EH.....	73
<b>Figure 53.</b> Comparison of CDU inhibition acting on murine, potato and Kau2-EHs. ....	75
<b>Figure 54.</b> Substrate binding pocket of Kau2-EH homology model based on X-ray structure of murine EH. The ( <i>S</i> )- <i>p</i> -chlorostyrene oxide (in yellow) is represented after docking (Autodock 4.0 software) in the active site of Kau2-EH. The catalytic nucleophile Asp-109, the oxirane-polarizing tyrosines Tyr-157 and Tyr-259, and the general base His-316 are depicted in grey stick representation. Important residues of sites that were randomized during the directed evolution are depicted in color. ....	75

<b>Figure 55.</b> Preparative kinetic resolution of <i>trans</i> -methyl styrene oxide and enantioconvergent deracemization of <i>cis</i> -methyl styrene oxide using Kau2-EH as catalyst (Kotik <i>et al.</i> , 2010).	76
<b>Figure 56.</b> Aromatic epoxides tested as potential substrates of Kau2-EH as catalyst.	77
<b>Figure 57.</b> Synthesis of <i>rac</i> -5.	78
<b>Figure 58.</b> Synthesis of <i>rac</i> -4.	79
<b>Figure 59.</b> Synthesis of <i>rac</i> -7 and 8.	80
<b>Figure 60.</b> Synthesis of <i>rac</i> -9 and <i>rac</i> -10.	80
<b>Figure 61.</b> Synthesis of <i>rac</i> -13.	81
<b>Figure 62.</b> Structure of Paclitaxel (Taxol <sup>TM</sup> ) and synthesis of its side chain using <i>trans</i> -2 <i>S</i> ,3 <i>R</i> -methyl phenyl glycidate (Afon'kin <i>et al.</i> , 2012).	82
<b>Figure 63.</b> Synthesis of (-)-Clausenamidine using <i>trans</i> -2 <i>S</i> ,3 <i>R</i> -methyl-phenyl-glycidate-4 (Zheng <i>et al.</i> , 2006).	83
<b>Figure 64.</b> Evolution of the ees of the remaining epoxide-4 during stability test of Kau2-EH.	84
<b>Figure 65.</b> Evolution of the ees of the remaining epoxide-4 as influenced by different types of co-solvent during the Kau2-EH catalyzed kinetic resolution of <i>rac</i> -4.	85
<b>Figure 66.</b> Evolution of the ees of the remaining epoxide-4 as influence by various diisopropyl ether concentrations (10-30%, v/v) during the Kau2-EH catalyzed kinetic resolution of <i>rac</i> -4.	86
<b>Figure 67.</b> Evolution of the ees of the remaining epoxide-4 during the Kau2-EH catalyzed kinetic resolution of <i>rac</i> -4 at different substrate concentration [S] (1-75 g/L), the ratio of [S]/[E] was 0.5.	87
<b>Figure 68.</b> Evolution of the ees of the remaining epoxide-4 during the Kau2-EH catalyzed kinetic resolution of <i>rac</i> -4 (25 g/L) in absence or in presence of diol-4d (25 g/L).	88
<b>Figure 69.</b> Evolution of the ees of the remaining epoxide-4 during the Kau2-EH catalyzed kinetic resolution of <i>rac</i> -4 at a fixed substrate concentration of 50 g/L and varying S/E ratio ranging from 1 to 0.33.	90
<b>Figure 70.</b> Evolution of the ees of the remaining epoxide during the bio-hydrolysis of <i>rac</i> -4 (75 g/L) using Kau2-EH at different substrate-over-enzyme ratio.	91
<b>Figure 71.</b> Preparative scale (1 g) bio-hydrolysis of <i>rac</i> -4 using Kau2-EH.	92
<b>Figure 72.</b> Evolution of the ees of the remaining epoxide during the bio-hydrolysis of <i>rac</i> -5 at different substrate concentrations (1-50 g/L) using Kau2-EH.	94
<b>Figure 73.</b> Evolution of the ees of the remaining epoxide during the Kau2-EH catalyzed bio-hydrolysis of <i>rac</i> -5 (50 g/L) at different substrate-over-enzyme ratio.	95
<b>Figure 74.</b> Preparative scale (1 g) Kau2-EH catalysed bio-hydrolysis of <i>rac</i> -5.	96
<b>Figure 75.</b> Evolution of ees of both remaining epoxide and formed diol during the preparative Kau2-EH (50 g/L) catalyzed bio-hydrolysis of <i>rac</i> -5 (25 g/L) on the 1 g scale.	97
<b>Figure 76.</b> Synthesis of Diltiazem using <i>tert</i> -butyl-(2 <i>R</i> ,3 <i>S</i> )- <i>trans</i> 3-(4-methoxyphenyl)-glycidate-6.	98
<b>Figure 77.</b> Synthesis of isocytosazone using methyl (2 <i>S</i> ,3 <i>R</i> )-3 <i>trans</i> -(4-methoxyphenyl) glycidate-6.	98
<b>Figure 78.</b> Evolution of the ees of the remaining epoxide during Kau2-EH catalyzed bio-hydrolysis of <i>rac</i> -6 at different concentrations (1-40 g/L).	101
<b>Figure 79.</b> Evolution of the ees of the formed diol during Kau2-EH catalyzed bio-hydrolysis of <i>rac</i> -6 at different substrate concentrations (1-40 g/L).	102
<b>Figure 80.</b> Preparative scale (1 g) bio-hydrolysis of <i>rac</i> -6 using Kau2-EH.	104
<b>Figure 81.</b> Evolution of the ees of both remaining epoxide and formed diol during the Kau2-EH (70 g/L) catalyzed preparative bio-hydrolysis of <i>rac</i> -6 (40 g/L) on the 1 g scale.	104

<b>Figure 82.</b> Evolution of the ees of the remaining epoxide during the Kau2-EH catalyzed bio-hydrolysis of <i>rac-7</i> at different concentrations (1-75 g/L).....	106
<b>Figure 83.</b> Preparative scale (1 g) Kau2-EH catalysed bio-hydrolysis of <i>rac-7</i> . ....	107
<b>Figure 84.</b> Absolute configuration determination of the formed diol (2 <i>S</i> ,3 <i>R</i> )- <b>7d</b> .....	107
<b>Figure 85.</b> Evolution of the ees of the remaining epoxide during Kau2-EH catalyzed bio-hydrolysis of <i>rac-8</i> at different concentrations (1-50 g/L).....	108
<b>Figure 86.</b> Biohydrolysis of <i>rac-8</i> (50 g/L) catalyzed by Kau2-EH at different substrate-over-enzyme ratio. ....	109
<b>Figure 87.</b> Preparative scale (1 g) bio-hydrolysis of <i>rac-8</i> using Kau2-EH. ....	110
<b>Figure 88.</b> Chemical transformation of (2 <i>R</i> ,3 <i>S</i> )- <b>8</b> into (2 <i>S</i> ,3 <i>S</i> )- <b>13</b> (Svoboda <i>et al.</i> , 1988). ..	110
<b>Figure 89.</b> Absolute configuration determination of the formed diol (2 <i>R</i> ,3 <i>R</i> )- <b>8d</b> . ....	111
<b>Figure 90.</b> The four possible combination of remaining epoxides and formed products arising from Kau2-EH catalyzed bio-hydrolysis of <i>rac-8</i> . ....	111
<b>Figure 91.</b> Synthesis of Leiocarpin C and (+)-Goniodiol using (2 <i>S</i> ,3 <i>R</i> )- <b>10</b> . ....	112
<b>Figure 92.</b> Synthesis of 1-Phenyl-glycidol- <b>14</b> using diol- <b>9d</b> and - <b>10d</b> . ....	113
<b>Figure 93.</b> Synthesis of L-(-)-CCG-II using terminal epoxide- <b>14</b> (Kumar <i>et al.</i> , 2012). ....	113
<b>Figure 94.</b> Evolution of the ees of the remaining epoxide during Kau2-EH catalyzed bio-hydrolysis of <i>rac-9</i> at different concentrations (1-75 g/L).....	114
<b>Figure 95.</b> Preparative scale (1 g) Kau2-EH catalysed bio-hydrolysis of <i>rac-9</i> . ....	115
<b>Figure 96.</b> Preparative scale (1 g) Kau2-EH catalysed bio-hydrolysis of <i>rac-10</i> . ....	116
<b>Figure 97.</b> Cyclisation of formed diols <b>9d</b> and <b>10d</b> to epoxy-alcohol <b>14</b> . ....	117
<b>Figure 98.</b> Evolution of the ees of the remaining epoxide during Kau2-EH bio-hydrolysis of <i>rac-11</i> at different concentrations (1-50 g/L).....	118
<b>Figure 99.</b> Preparative scale (1 g) Kau2-EH catalysed bio-hydrolysis of <i>rac-11</i> . ....	119
<b>Figure 100.</b> Evolution of the yields of the formed diol- <b>12d</b> during the desymmetrization of <i>meso-12</i> at different concentrations (1-50 g/L) using Kau2-EH. ....	120
<b>Figure 101.</b> Preparative scale (1 g) bio-hydrolysis of <i>meso-12</i> using Kau2-EH.....	121
<b>Figure 102.</b> Evolution of the yields and ees of the formed diol- <b>12d</b> during the preparative scale (1 g) Kau2-EH catalyzed desymmetrization of <b>12</b> . ....	121
<b>Figure 103.</b> Comparison of Kau2-EH activities on different epoxides at the same 25 g/L concentration but under reaction conditions adapted for each substrate. ....	123
<b>Figure 104.</b> Experimental outline of recombinant plasmids construction and expression. Protocol to produce Kau2-His-6 EHs at N and C terminus position. ....	127
<b>Figure 105.</b> Protein purification process by FPLC using a HisTrap HP column (5mL). ....	130
<b>Figure 106.</b> SDS-PAGE analysis of Kau2-His <sub>6</sub> lane 1: molecular weight marker (97.4 kD, 66.2 kD, 45.0 kD, 31.0 kD, 21.5 kD); lane 2: Bovine Serum Albumin (BSA); lane 3: purified Kau2-EH (1st isolation; lane 4: purified Kau2-EH (2nd isolation). ....	131
<b>Figure 107.</b> Results of the separation of the two enantiomers of TSO using a preparative chiral HPLC column (Chiralpak IC). The upper traces correspond to the UV (254 nm) analysis and the lower traces to the optical rotation associated to each enantiomers.....	132
<b>Figure 108.</b> Determination of steady-state kinetic parameters for Kau2-His <sub>6</sub> -catalyzed hydrolysis of ( <i>S,S</i> )-TSO. Experimental conditions: 23 °C, 4% CH <sub>3</sub> CN.....	133
<b>Figure 109.</b> Kinetic mechanism of epoxide hydrolases ( $\alpha/\beta$ -hydrolase). This mechanism includes the Michaelis complex formation followed by the formation of a covalent alkyl-enzyme with a rate $k_2$ . The alkyl-enzyme is subsequently hydrolyzed with rate $k_3$ , to restore the enzyme. $K_s$ , the equilibrium constant of the dissociation of the Michaelis complex ( $k_{-1}/k_1$ ). ....	134
<b>Figure 110.</b> A- Schematic diagram of a stop-flow apparatus. In the case of an enzymatic study the syringe S3 is filled by enzyme solution and syringes S1 & S2 are respectively filled with pure buffer and substrate diluted in buffer. M1 and M2 are the mixing	

chambers. B - Fluorescence traces, without substrate (blue), immediately after the mixing of substrate and enzyme (red). C- Fluorescence traces for different substrate concentrations.....135

**Figure 111.** A- Tryptophane fluorescence trace of 1.2  $\mu\text{M}$  Kau2-His<sub>6</sub> and 40  $\mu\text{M}$  (*S,S*)-TSO. For the determination of the corresponding  $k_{\text{obs}}$  a fit with a single exponential curve [ $F = A \exp(-k_{\text{obs}}t) + C$ ] in which A is the amplitude of fluorescence change,  $k_{\text{obs}}$  the observed rate constant and C the floating end point of the progression curve (average of 5 traces)]. B- Observed rates,  $k_{\text{obs}}$ , plotted versus (*S,S*)-TSO concentration. The solid line corresponds to the linear fit of Eqn 5 to the substrate dependence (Lindberg *et al.*, 2008).

.....137

**Figure 112.** Result of restriction digest with *HincII* (1% agarose gel, 90 V, 90 mA, 60 min).

.....173

**Figure 113.** A chiral GC analysis after 30 min reaction with 50 mM styrene oxide as substrate and suspended cells harbouring the pET100+Kau2 plasmid (N-terminal). 1, 3.8, and 7.2 min, respectively.....173

## List of tables

<b>Table 1.</b> Selected kinetic resolutions of <i>rac-p</i> -nitrostyrene oxide.....	21
<b>Table 2.</b> Selected kinetic resolutions of some <i>gem</i> -disubstituted alkyl epoxides.....	32
<b>Table 3.</b> Biohydrolytic reactions catalyzed by Kau2-EH using substrates <b>A-M</b> . ....	59
<b>Table 4.</b> FASTA sequence of Kau2-EH.....	63
<b>Table 5.</b> Sequences identity between Kau2-EH and the other three EHs. ....	63
<b>Table 6.</b> Comparison between the three Kau2-EH homology models, which were generated using the crystal structures of the murine, potato or human EH as a template; indicated are the r.m.s. deviations for the C $\alpha$ atoms of the residues 12–335 and the segments with the most significant spatial differences between the model tertiary structures.....	64
<b>Table 7.</b> Inhibition of CDU and CIU with murine EH. ....	65
<b>Table 8.</b> Values of $V^{-1}$ and $S \cdot V^{-1}$ determined for various CDU inhibitor concentrations at different substrate concentrations during Kau2-EH catalyzed biohydrolysis of ( <i>S</i> )- <i>p</i> ClISO. ....	69
<b>Table 9.</b> Values of $V^{-1}$ and $S \cdot V^{-1}$ determined for various CIU inhibitor concentrations at different substrate concentrations during Kau2-EH catalyzed biohydrolysis of ( <i>S</i> )- <i>p</i> ClISO. ....	70
<b>Table 10.</b> Values of $V^{-1}$ and $S \cdot V^{-1}$ determined for various CDU inhibitor concentrations at different substrate concentrations during potato EH catalyzed biohydrolysis of ( <i>S</i> )- <i>p</i> ClISO. ....	71
<b>Table 11.</b> Values of $V^{-1}$ and $S \cdot V^{-1}$ determined for various CIU inhibitor concentrations at different substrate concentrations during potato EH catalyzed biohydrolysis of ( <i>S</i> )- <i>p</i> ClISO. ....	72
<b>Table 12.</b> Inhibitions of CDU and CIU with murine, Kau2 and potato EHs. ....	73
<b>Table 13.</b> Comparison of the different conditions used for the synthesis of <i>rac-5</i> . ....	79
<b>Table 14.</b> Kau2-EH bio-hydrolysis of <i>rac-4</i> at two substrate concentrations (5 and 25 g/L) in absence or presence of 25 g/L diol- <b>4d</b> . ....	89
<b>Table 15.</b> Biohydrolysis of <i>rac-4</i> (50 g/L) with Kau2-EH at different S/E ratio. ....	90
<b>Table 16.</b> Kau2-EH catalyzed biohydrolysis of <i>rac-4</i> (70 g/L) at different S/E ratio.....	91
<b>Table 17.</b> Optical rotations and absolute configurations of isolated products obtained from preparative scale bio-hydrolysis of <i>rac-4</i> . ....	93
<b>Table 18.</b> Kau2-EH catalyzed biohydrolysis of <i>rac-5</i> at different substrate-over-enzyme ratio. ....	95
<b>Table 19.</b> Optical rotations and absolute configurations of isolated products from preparative scale bio-hydrolysis of <i>rac-5</i> . ....	97
<b>Table 20.</b> Stability of <i>rac-6</i> at different Na-Phosphate buffer pHs. ....	99
<b>Table 21.</b> Stability of <i>rac-6</i> at different reaction temperatures. ....	100
<b>Table 22.</b> Stability of <i>rac-6</i> under different MTBE concentrations. ....	100
<b>Table 23.</b> Biohydrolysis of <i>rac-6</i> with Kau2-EH at different substrate-over-enzyme ratio. ....	103
<b>Table 24.</b> Optical rotations and absolute configurations of isolated products obtained from preparative scale bio-hydrolysis of <i>rac-6</i> . ....	104
<b>Table 25.</b> Bio-hydrolysis of <i>rac-8</i> with Kau2-EH at different substrate-over-enzyme ratio. ....	109
<b>Table 26.</b> Kau2-EH catalyzed bio-hydrolysis of <i>rac-9</i> at different substrate-over-enzyme ratio. ....	115
<b>Table 27.</b> Optical rotations and absolute configurations of isolated products from the preparative scale bio-hydrolysis of <i>rac-9</i> and <b>10</b> . ....	117
<b>Table 28.</b> Expression level of Kau2-HisTag using <i>E. coli</i> BL21 Star (DE3) as a host for expression under various conditions. ....	129

<b>Table 29.</b> Overexpression of the four mutants and the obtained mass of purified protein from 1L of medium culture.....	131
<b>Table 30.</b> Presteady-state and steady-state kinetic constants for the Kau2-EH catalyzed hydrolysis of ( <i>S,S</i> )-and ( <i>R,R</i> )-TSO and the kinetic constants previously described by Widersten and coworker (Lindberg <i>et al.</i> , 2008) using <i>StEH</i> . .....	137
<b>Table 31.</b> The fusion tag, cleavage site, and selection marker for each vector. ....	173
<b>Table 32.</b> Physical characterizations of various biosynthesized compounds.....	181
<b>Table 33.</b> Results for preparative scale bioconversion of the various tested substrates. ....	182
<b>Table 34.</b> Conditions for chiral GC analysis .....	183
<b>Table 35.</b> Conditions for HPLC analysis. ....	184